Human cohesin dynamics and their regulation in M and S phase

DISSERTATION

zur Erlangung des akademischen Grades

– Doktor der Naturwissenschaften (Dr. rer. nat.) –

an der Bayreuther Graduiertenschule für Mathematik
und Naturwissenschaften (BayNAT) der Universität Bayreuth

Vorgelegt von

Johannes Buheitel, M.Sc.

aus Erlangen

Bayreuth, Juni 2015

Die vorliegende Arbeit wurde in der Zeit von Oktober 2009 bis Juni 2015 in Bayreuth am Lehrstuhl für Genetik unter der Betreuung von Herrn Prof. Dr. Olaf Stemmann angefertigt.

Vollständiger Abdruck der von der Bayreuther Graduiertenschule für Mathematik und Naturwissenschaften (BayNAT) der Universität Bayreuth genehmigten Dissertation zur Erlangung des akademischen Grades eines Doktors der Naturwissenschaften (Dr. rer. nat.).

Dissertation eingereicht am: 29.06.2015

Zulassung durch das Leitungsgremium: 07.07.2015

Wissenschaftliches Kolloquium: 14.10.2015

Amtierender Direktor: Prof. Dr. Stephan Kümmel

Prüfungsausschuss:

Prof. Dr. Olaf Stemmann	(Erstgutachter)
Prof. Dr. Benedikt Westermann	(Zweitgutachter)
PD Dr. Stefan Geimer	(Vorsitz)
Prof. Dr. Gerrit Begemann	

Table of contents

Summary

Cohesin is a multimeric ring complex, which associates with DNA throughout most of the eukaryotic cell cycle. Its canonical role is to hold the two copies (sister chromatids) of each chromosome together from the time of their generation in S phase until their separation in M phase, thus ensuring the fidelity of mitosis. The complex mediates this so-called cohesion by topologically embracing the sister chromatids inside its ring structure composed of the three subunits Scc1, Smc1 and Smc3. For this thesis, I have studied cohesin's dynamic association with chromatin in M and S phase as well as its role at the mitotic centrosome, the main microtubule-organizing center of most eukaryotic cells.

In order to separate sister chromatids in mitosis, cohesin must be removed from chromosomes. This is ultimately achieved by the action of the cystein protease separase, which cleaves cohesin at the centromeres (the primary constriction site of mitotic chromosomes) to release DNA. In vertebrates, however, the bulk of cohesin molecules, which is located on chromosome arms, is already removed from DNA in the first stage of mitosis, prophase, by a non-proteolytic mechanism called the prophase pathway. Since cohesin embraces the sister chromatids, prophase pathway signaling requires the ring to open up at at least one of its three subunit interaction sites ("gates"). However, which gate opens up for DNA exit has remained enigmatic. The same is true (at least in humans) for cohesin's DNA entry gate, which would be required to open up to topologically reload the ring complex after chromatid separation in telophase. For my thesis, I set out to identify cohesin's DNA exit (prophase) and entry (telophase) gates by employing the so-called FRB/FKBP system, allowing me to artificially close each of cohesin's gates individually in a conditional manner. I found that cohesin's DNA exit gate during prophase is composed of Smc3 and Scc1. To load the complex onto DNA, however, the gate situated between Smc1-Smc3 needs to open up. Utilizing different gates allows for more precise control over cohesin dynamics by maintaing the delicate balance between DNA entry and exit.

Cohesin's association with chromatin remains very dynamic during G1 phase, but has to be stabilized as soon as the second sister chromatid is synthesized in S phase. Today, we know that this so-called cohesion establishment and DNA replication are two tightly co-regulated processes. However, how the replication machinery achieves DNA duplication, while simultaneously depositing the nascent chromatid inside the ring's lumen

is still an unsolved problem. Using the aforementioned FRB/FKBP system in combination with an assay allowing me to assess DNA synthesis on a single replication fork level, I set out to determine whether the replisome might be able to pass through the closed ring or whether cohesin has to open up one of its three gates. These experiments revealed that cohesin gate opening unlikely to be required during replication but impaired dynamics of the complex in the preceeding G1 phase causes a dramatic reduction of replication fork velocities in the following S phase, likely by altering cohesin levels on chromatin. While these results confirm a strong correlation between cohesin dynamics and replication, they also argue for a model in which pre-S phase-loaded cohesin complexes represent the future cohesive fraction and, moreover, that during co-replicative cohesion establishment the replisome may pass through the closed cohesin ring.

Finally, we and other groups have shown that cohesin plays a functional role at the centrosomes. Each centrosomes comprises two centrioles, which are rigidly coordinated ("engaged") in a perpendicular fashion. Separase-mediated proteolysis of centrosome-associated cohesin causes centriole disengagement, a prerequisite for centrosome duplication in the following S phase. In a collaboration with Lisa Mohr (University of Bayreuth, Germany), we found that the same factor, which protects centromeric cohesin from prophase pathway signaling until its proteolysis at the metaphase-to-anaphase transition, namely Sgo1, is also required to maintain centriole engagement. More specifically, human cells express a set of Sgo1 splice variants, which exclusively localize and function either at the centromere or the centrosome. Further studies revealed that Sgo1's determinant for centrosomal function lies in its C-terminal 40 amino acids, an area, which we therefore named the "centrosomal targeting signal of Sgo1" or CTS. Nonetheless, Sgo1's centromeric function is conserved at the centrosome, since my results demonstrate that CTS-containing Sgo1 variants protect centrosomal cohesin from the action of the prophase pathway by recruiting protein phosphatase 2 A (PP2A). Our results provide compelling evidence that the cell coordinates chromosome and centrosome cycles by multiple use of proteins like cohesin and its regulatory framework. However, employing specific Sgo1 splice variants allows these two processes to be precisely and individually controlled or maybe even uncoupled under certain circumstances as, for example, during spermatogenesis.

Zusammenfassung

Cohesin ist ein multimerer Ring-Komplex, welcher während des größten Teils des eukaryontischen Zellzyklus mit DNA assoziiert. Seine kanonische Funktion besteht darin, die zwei Kopien (Schwester-Chromatide) jedes Chromosoms von der Zeit ihrer Entstehung in der S Phase bis zu ihrer Trennung in der M Phase zusammenzuhalten, um einen korrekten Ablauf der Mitose zu garantieren. Der Komplex vermittelt diese sogenannte Kohäsion durch topologisches Umfassen der Schwester-Chromatide mithilfe seiner Ring-Struktur, welche sich aus den drei Untereinheiten Scc1, Smc1 und Smc3 zusammensetzt. Für diese Arbeit habe ich die dynamische Assoziation Cohesins mit Chromatin in M und S Phase, sowie seine Rolle am mitotischen Zentrosom, dem Haupt-Mikrotubuli-organisierenden Zentrum der meisten eukaryontischen Zellen, untersucht.

Um Schwester-Chromatide in Mitose zu trennen, muss Cohesin von den Chromosomen entfernt werden. Dies wird schlussendlich durch die Aktivität der Cystein-Protease Separase erreicht, welche Cohesin an den Zentromeren (der primären Einschnürung mitotischer Chromosomen) schneidet, um DNA aus dem Ring zu entlassen. In Vertebraten jedoch, wird das Gros der Cohesin-Moleküle, welche an den Chromosomen-Armen lokalisiert, bereits in der ersten Phase der Mitose, der Prophase, durch einen nicht-proteolytischen Mechanismus namens Prophase-Weg entfernt. Da Cohesin die Schwester-Chromatide umschließt, muss der Prophase-Weg ein Öffnen des Rings an mindestens einer der Interaktionsstellen ("*gates*") zwischen seinen drei Untereinheiten bewirken. Welches *gate* sich jedoch öffnet, um DNA zu entlassen, verblieb bis heute unklar. Dasselbe lässt sich auch über Cohesins DNA-Eintritts*gate* aussagen (zumindest im Menschen), welches sich öffnen müsste, um den Ring-Komplex nach Chromatid-Trennung in Telophase wieder topologisch auf DNA zu laden. Für meine Arbeit plante ich sowohl Cohesins DNA-Austritts- (Prophase) als auch dessen -Eintritts*gate* (Telophase) zu identifizieren. Hierfür entschied ich mich für die Verwendung des sogenannten FRB/FKBP-Systems, welches mir erlaubte künstlich jedes Cohesin-*gate* einzelnd und in konditionaler Weise zu schließen. Ich fand heraus, dass Cohesins DNA-Austritts*gate* zwischen Smc3 und Scc1 liegt. Um den Komplex allerdings auf DNA zu laden, muss sich das Smc1-Smc3-*gate* öffnen. Die Verwendung verschiedener *gates* erlaubt der Zelle eine exakte Kontrolle der Cohesin-Dynamik durch das Einstellen eines präzisen Gleichgewichts zwischen DNA-Ein- und -Austritt.

Cohesins Chromatin-Assoziation gestaltet sich sehr dynamisch während der G1 phase, muss jedoch stabilisiert werden sobald das zweite Schwester-Chromatid in S Phase synthetisiert wird. Heute wissen wir, dass diese sogenannte Kohäsionsetablierung und DNA-Replikation zwei streng ko-regulierte Prozesse darstellen. Wie jedoch die Replikations-Maschinerie DNA verdoppelt und dabei gleichzeitig das naszierende Chromatid im Ring-Lumen ablegt, stellt immer noch ein ungelöstes Problem dar. Unter Verwendung des zuvor genannten FRB/FKBP-Systems in Kombination mit einem Versuchsaufbau, welcher mir erlaubt DNA-Synthese auf der Ebene einzelner Replikationsgabeln zu untersuchen, plante ich herauszufinden, ob das Replisom durch den geschlossenen Ring hindurchpassieren könnte oder ob Cohesin hierzu eines seiner drei *gates* öffnen müsste. Diese Experimente zeigten, dass das Öffnen von Cohesin-*gates* während der Replikation wahrscheinlich nicht notwendig ist, aber auch, dass die Beeinträchtigung der Dynamik des Komplexes in der vorherigen G1 Phase eine dramatische Reduktion der Geschwindigkeit von Replikationsgabeln in der folgenden S Phase, wahrscheinlich aufgrund veränderter Cohesin-Mengen an Chromatin, zur Folge hat. Während diese Ergebnisse eine starke Korrelation zwischen Cohesin-Dynamik und Replikation bestätigen, sprechen sie weiterhin auch für ein Modell, nach welchem vor der S Phase geladene Cohesin-Komplexe bereits die zukünftige kohäsive Fraktion darstellen. Darüber hinaus zeigen sie, dass das Replisom während der ko-replikativen Kohäsionsetablierung durch den geschlossen Cohesin-Ring hindurchpassiert.

Schlussendlich haben wir und andere Gruppen bereits zeigen können, das Cohesin eine funktionale Rolle an den Zentrosomen spielt. Jedes Zentrosom besteht aus zwei Zentriolen, welche fest in einem rechten Winkel zueinander stehend koordiniert ("gekoppelt") sind. Separase-abhängige Proteolyse von zentrosomen-assoziiertem Cohesin verursacht Entkopplung von Zentriolen, was eine Voraussetzung für Zentrosomen-Duplikation in der folgenden S Phase darstellt. In Kollaboration mit Lisa Mohr (Universität Bayreuth) haben wir festgestellt, dass derselbe Faktor, welcher zentromerisches Cohesin bis zu seiner Proteolyse am Metaphase-zu-Anaphase-Übergang vor der Aktivität des Prophase-Wegs schützt, Sgo1, auch benötigt wird, um Zentriolen-Kopplung aufrechtzuerhalten. Genauer gesagt, menschliche Zellen exprimieren eine Reihe von Sgo1-Spleiß-Varianten, welche exklusiv entweder ans Zentromer oder ans Zentrosom lokalisieren und dann auch nur dort wirken. Weitere Versuche zeigten, dass der bestimmende Faktor für die zentrosomale Funktion von Sgo1 in seinen C-terminalen 40 Aminosäuren liegt, welche wir aufgrund dieser Eigenschaft "*centrosomal targeting*

signal of Sgo1" bzw. CTS genannt haben. Trotzdem bleibt die zentromerische Funktion von Sgo1 konserviert, da meine Ergebnisse zeigen können, dass CTS-enthaltende Sgo1-Varianten zentrosomales Cohesin durch Rekrutierung von Protein Phosphatase 2 A (PP2A) vor der Aktivität des Prophase-Wegs schützen. Unsere Ergebnisse liefern überzeugende Beweise dafür, dass die Zelle Chromosomen- und Zentrosomen-Zyklen durch die mehrfache Verwendung von Proteinen wie Cohesin und dessen regulatorischen Umfeld, koordiniert. Jedoch erlaubt der Einsatz spezifischer Sgo1-Spleiß-Varianten die präzise und individuelle Kontrolle dieser zwei Prozesse und unter Umständen sogar ihre Entkopplung in Fällen, wie z.B. der Spermatogenese.

1. Introduction

1.1 The cell cycle

The purpose of the (somatic) eukaryotic cell cycle is to generate two identical daughter cells from one mother cell by means of cell division. Therefore, each one-chromatid-chromosome (a chromatid comprises one DNA double strand and associated proteins) of the mother cell has to be replicated accurately in S phase to generate two-chromatid chromosomes, which remain in close contact ("cohesion"). In the following mitosis, the two sister chromatids are ultimately separated and equally distributed into the newly forming cells (mitosis/cytokinesis or M phase). DNA synthesis and mitosis are typically separated

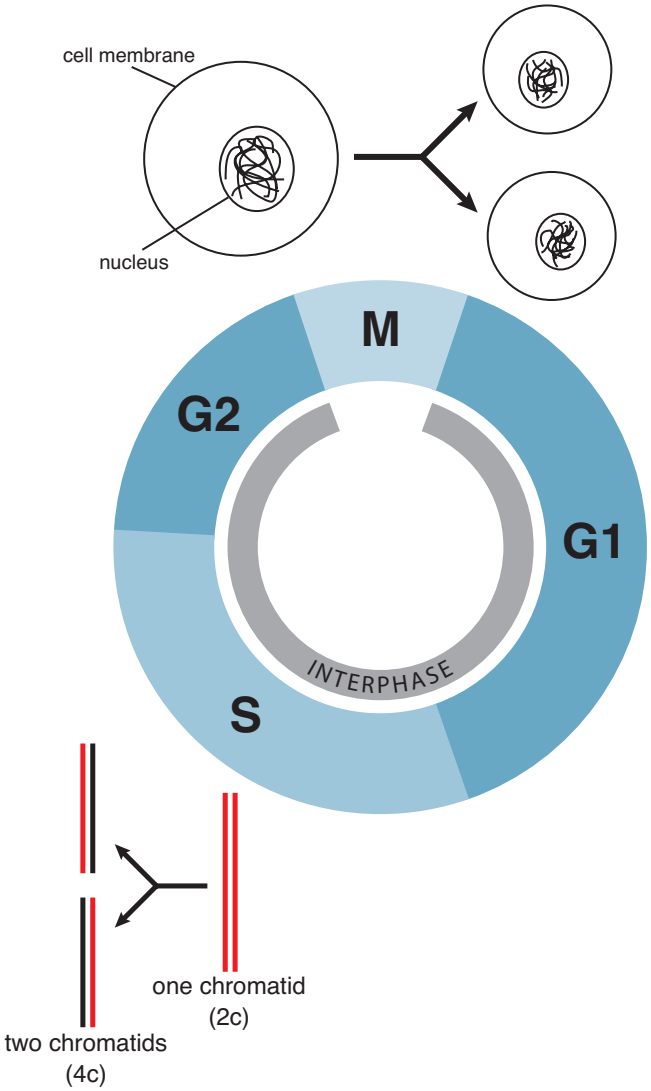

Figure 1 | **The eukaryotic cell cycle.** For details see text. Mitotic cell division and semi-conservative DNA replication are depicted in more detail. M: M phase, S: S phase, G1/2: gap phase 1/2, 2c/4c: chromosome copy number

by two gap phases (G1 and G2 phase), which allow cell growth and integration of environmental cues (Figure 1). The cell cycle is driven by the periodic generation/ activation and degradation/inactivation of regulators and has a clear direction governed by irreversible switch-like events guarded by "checkpoints". A major force behind the cell cycle progression are cyclin-dependent kinases (Cdks), whose activity is regulated by cell-cycle-specific activators, called cyclins.

1.2 DNA replication (S phase)

DNA replication during S phase is the first major chromosomal event of the cell cycle. After the preceding cytokinesis the cell contains a full set of chromosomes, each of which comprises one DNA double strand (a "chromatid") associated with histones and other proteins. During S phase, each DNA double strand becomes locally denatured to generate small stretches of single strand DNA (ssDNA), which are used as templates to generate new strings of complementary nucleotides by the action of specialized DNA polymerases. Since DNA can only be synthesized in a 5' to 3' direction but both antiparallel DNA strands are simultaneously duplicated from the same replisome (the large multimeric replication machinery), only one strand, the so-called "leading strand", can be replicated continuously. The other so-called "lagging strand", however, is replicated in a discontinuous fashion, yielding short 100-200 nucleotide-stretches of new DNA (Okazaki fragments), which have to be processed ("matured") and ultimately ligated to create a continuous complementary DNA strand (Okazaki *et al*, 1968; Waga & Stillman, 1994). This semi-conservative mode of DNA replication ultimately generates two identical DNA double strands or sister chromatids, each containing one original DNA single strand from the mother cell. During replication, cohesion between the two sister chromatids is continuously established, generating two-chromatid chromosomes which remain closely associated until their separation in the following mitosis. This mechanism ultimately ensures the correct distribution of genomic material into the newly generated daughter cells.

1.2.1 Origin licensing and assembly of the pre-replicative complex

In all organisms, DNA replication is initiated from specific starting points, called "origins". While bacterial and archeal replication origins are determined by specific DNA sequences, eukaryotic origins are typically defined by many and also varying factors such as promotor

distances and nucleosome occupancy (reviewed in Costa *et al*, 2013). A prominent exception from this rule is budding yeast, whose autonomous replicating sequences (ARS) determine replication factor recruitment (Stinchcomb *et al*, 1979). In both, bacteria and eukaryotes, loading of their respective DNA-unwinding helicase marks the initial step of replisome assembly. Only in eukaryotes however, helicase loading ("licensing") and activation are divided into two temporally distinctive steps, which ensures that replication can take place exactly once per cell cycle. Origins already become licensed in late mitosis and early G1 phase by recruiting various proteins forming the so-called pre-replication complex (pre-RC), a barrel-like structure encompassing double-strand DNA (dsDNA; Speck *et al*, 2005; Evrin *et al*, 2009; Remus *et al*, 2009). Pre-RC assembly is initiated by consecutive loading of the origin recognition complex (ORC), consisting of Orc1-6, and Cdc6 (cell division cycle) onto replication origins (Liang *et al*, 1995; Cocker *et al*, 1996; Seki & Diffley, 2000). ORC-Cdc6 then recruits the hexameric helicase complex consisting of MCM2-7 (minichromosome maintenance) bound to Cdt1 (Cdc10-dependent transcript) yielding the ORC-Cdc6-Cdt1-MCM2-7 complex (OCCM), which is still only loosely associated with DNA (Seki & Diffley, 2000; Tanaka & Diffley, 2002; Evrin *et al*, 2009; Remus *et al*, 2009; Coster *et al*, 2014). ORC, Cdc6 and MCM2-7 are members of the AAA (ATPases associated with diverse cellular activities) family of ATPases and, while binding of various ATP molecules suffices to form the OCCM (Bell & Stillman, 1992; Coster *et al*, 2014), hydrolysis of the nucleotide by MCM2-7 is required to convert the OCCM to the OCM by release of Cdt1 (Coster *et al*, 2014). To ultimately conclude origin licensing by formation of a stably DNA-bound replication initiation-proficient pre-RC, a second MCM2-7 hexamer is recruited to the OCM by a still unknown mechanism and Cdc6 is released by self-hydrolyzing ATP (Evrin *et al*, 2009; Remus *et al*, 2009; Fernández-Cid *et al*, 2013; Yardimci & Walter, 2014; Coster *et al*, 2014).

1.2.2 Assembly of the pre-initiation complex/CMG and components of the replisome

Before replication can be initiated, the pre-RC must recruit additional factors to form the pre-initiation complex (pre-IC). Therefore, the S phase-specific Dbf4-dependent kinase (DDK) phosphorylates the MCM complex, which in turn recruits Cdc45 (Zou & Stillman, 2000; Sheu & Stillman, 2006; Masai *et al*, 2006). Another essential pre-IC component is the GINS (go ichi nii san; japanese for 5, 1, 2, 3) complex, consisting of Sld5 (synthetic lethality with Dpb11-1) and Psf1-3 (partner of Sld five), whose loading requires additional

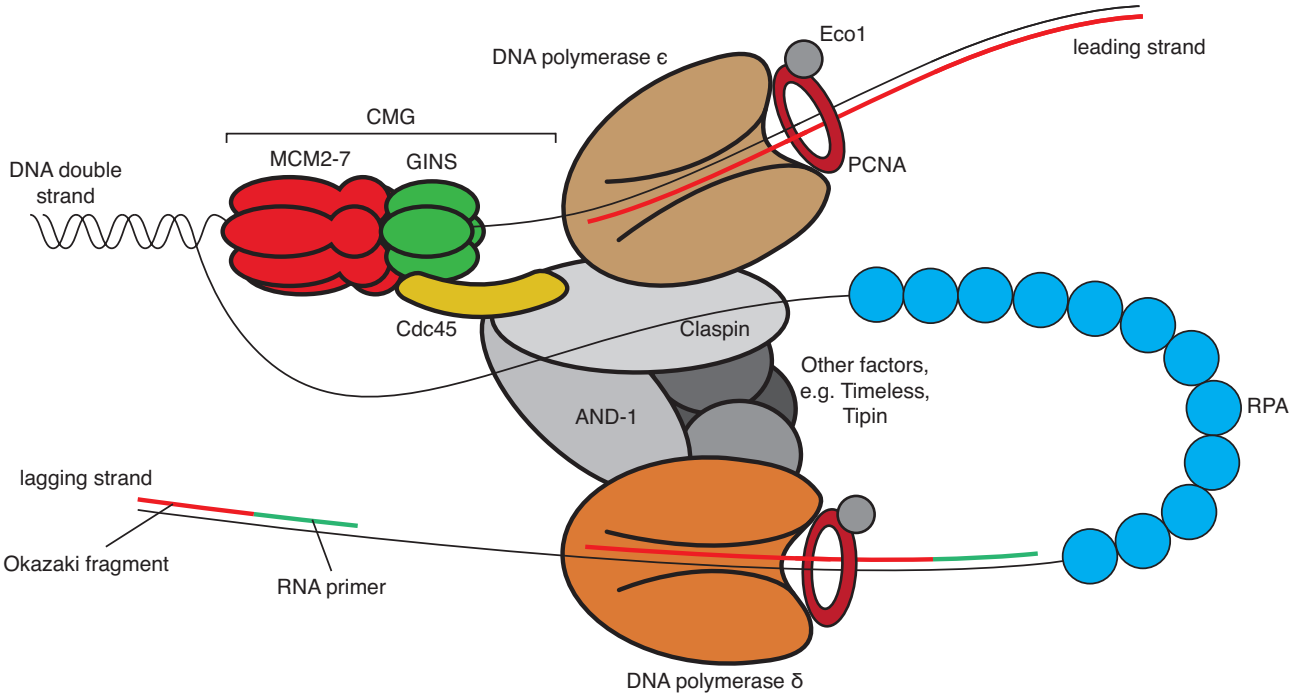

Figure 2 | **The eukaryotic replisome.** The replicative helicase complex CMG, consisting of MCM2-7, Cdc45 and GINS, denatures the DNA double strand. Single strand DNA is stabilized by associating with RPA proteins. Several factors couple the helicase with DNA polymerases ϵ (leading strand) and δ (lagging strand), whose processivity depends on PCNA clamps. PCNA acts as binding platform for several proteins including the cohesion establishment factor Eco1 (ESCO1/2 in humans). Some replisomal proteins have been ommitted for clarity. For more details see text.

factors such as Ctf4/And-1 (chromosome transmission fidelity/acidic nucleoplasmic DNA-binding protein 1; Im *et al*, 2009). While the catalytic core of the helicase might be the MCM complex, proper DNA unwinding and replication fork progression requires the supercomplex of Cdc45, MCM and GINS (also called "CMG", see Figure 2; Pacek & Walter, 2004; Gambus *et al*, 2006; Kanemaki & Labib, 2006; Ilves *et al*, 2010). The CMG links the DNA helicase with the remaining replication machinery functionally and physically. So has it been shown that Ctf4/And-1 not only recruits DNA polymerase α (Pol α) but also stimulate its activity *in vitro* (Zhu *et al*, 2007; Bermudez *et al*, 2010). As Pol α is the priming polymerase (see chapter 1.2.3), its activity is continuously required on the lagging strand (reviewed in Waga & Stillman, 1998). Therefore Ctf4/And-1 is believed to be the main link coupling DNA helicase activity with lagging strand synthesis, which is supported by the fact that Ctf4/And-1-depletion completely abrogates DNA replication *in vivo* (Bermudez *et al*, 2010). Leading strand synthesis on the other hand is most probably linked to the CMG via Mrc1/Claspin (mediator of replication checkpoint), as this protein is not only required for normal replication in yeast and human but also physically interacts with DNA polymerase ϵ (Pol ϵ) and Cdc45 (Szyjka *et al*, 2005; Lou *et al*, 2008; Petermann *et al*, 2008). The exact

composition of the eukaryotic replisome remains subject of extensive research as more and more factors such as nucleosome chaperones (e.g. FACT) and replisome stability factors (e.g. Timeless, Tipin) are found to be associated with the replication machinery (reviewed in Leman & Noguchi, 2013).

1.2.3 Replication initiation, eukaryotic DNA polymerases and PCNA

Once the replisome is assembled, the helicase begins to denature the DNA double strand, creating two single strands, of which one (the leading strand) remains inside the lumen of the CMG while the other (the lagging strand) becomes coated with RPA (replication protein A), which stabilizes ssDNA (Waga & Stillman, 1998). Since most polymerases usually require a short double-stranded DNA (or an RNA-DNA duplex) section as a primer for elongation, the only eukaryotic DNA polymerase that can initiate DNA replication is Pol α. Pol α is associated with a primase, which *de novo*-synthesizes a short RNA primer of 40 nucleotides (nt) using ssDNA as template, allowing the polymerase to initiate duplication (Nethanel *et al*, 1988; Waga & Stillman, 1994). However, since Pol α is not very processive and hence loses its DNA association shortly after priming (Murakami & Hurwitz, 1993), other polymerases have to take over elongation of the RNA primer (Waga & Stillman, 1994). According to the current model, leading strand synthesis is executed by Pol ϵ, while lagging strand synthesis requires reiterative loading of DNA polymerase δ (Pol δ, Figure 2; Pursell *et al*, 2007; Nick McElhinny *et al*, 2008). Structurally similar to Pol α, Pol ϵ and δ require an additional factor to strengthen their interaction with DNA and thereby dramatically increase their replicative processivity: the DNA sliding clamp PCNA (proliferative cellular nuclear antigen, Figure 2; Bravo *et al*, 1987; Prelich *et al*, 1987). PCNA belongs the family of β-clamps, which are structurally highly conserved as they form distinctive ring-shaped complexes (Krishna *et al*, 1994; Schurtenberger *et al*, 1998; Moldovan *et al*, 2007). Eukaryotic PCNA forms a homotrimeric ring with a positively charged inner surface allowing entrapment of a primed DNA-RNA template. The outer surface binds to the polymerase and consequently tethers the enzyme to DNA. Apart from this canonical function, PCNA has been implicated in various processes that require to be coupled with replication. For this, the complex seems to act as a binding platform for a vast variety of proteins involved in DNA ligation, repair, chromatin remodeling or even apoptosis, amongst others (reviewed in Moldovan *et al*, 2007). PCNA is loaded onto chromatin by its specific clamp loader RFC (replication factor C), a multimeric protein

complex comprised of five AAA ATPases. It is able to form a supercomplex with PCNA, open up the latter's ring structure and ultimately load it onto primer/template duplexes (Tsurimoto & Stillman, 1991a; Cai *et al*, 1998). Since repetitive PCNA loading is a prerequisite for the polymerase switch after template priming, it is essential for continuous replication fork processivity (Tsurimoto & Stillman, 1991b; Hedglin *et al*, 2013). Additionally, RFC can also unload the sliding clamp and has therefore been implicated in replication termination and PCNA recycling during S phase (Hedglin *et al*, 2013).

1.2.4 Regulation of replication licensing and initiation

DNA replication has to be limited to occur exactly once per cell cycle as re-replication could cause various kinds of genomic instabilities (e.g. increased gene copy number, polyploidy), which are a hallmark of cancer (Hanahan & Weinberg, 2011). Therefore, eukaryotes employ various and partially redundant mechanisms to prevent overreplication. Eukaryotic replication origins can only be licensed in late mitosis/G1 phase as pre-RC assembly requires absence of Cdk activity. When at the G1-S transition Cdk2 activity rises, pre-RC reassembly is blocked by phosphorylation of multiple of its components (Nguyen *et al*, 2001; Chen & Bell, 2011; Lee *et al*, 2012). Some of these subunits are not only prevented from rebinding to DNA but also actively degraded or exported from the nucleus (Drury *et al*, 1997; Saha *et al*, 1998; Nguyen *et al*, 2001; Tanaka & Diffley, 2002; Méndez *et al*, 2002).

Higher eukaryotes have been shown to attribute particular attention to the regulation of the essential pre-RC component Cdt1 (see chapter 1.2.1). At the onset of S phase Cdt1 is marked for proteasomal degradation by phosphorylation-dependent ubiquitylation (Li *et al*, 2003; Liu *et al*, 2004). Strikingly, ubiquitylation is mediated by two redundant E3 ubiquitin ligases (SCF^{Skp2} and DDB4-Cul4), both of which are individually able to sufficiently promote degradation (Takeda *et al*, 2005; Nishitani *et al*, 2006; Senga *et al*, 2006). On top of that, Cdt1 is negatively regulated in S phase by a specific inhibitor, called geminin, which binds to Cdt1 and blocks its association with the MCM2-7 complex (Wohlschlegel *et al*, 2000; Cook *et al*, 2004; Lee *et al*, 2004). In fact, Cdt1 regulation by geminin seems to be critical, as depletion of the inhibitor alone sufficiently causes re-replication (Mihaylov *et al*, 2002; Zhu *et al*, 2004). To allow efficient replication licensing, geminin itself is tightly controlled by APC/C^{Cdc20}- and APC/C^{Cdh1}-dependent (also E3 ubiquitin ligases, for details see chapter 1.3.3) degradation in late mitosis and G1 phase,

respectively, which suppress geminin levels until the G1-S transition (McGarry & Kirschner, 1998; Wohlschlegel *et al*, 2000; Rape *et al*, 2006). Geminin might also be exported from the nucleus during G1 phase to further secure proper licensing (Dimaki *et al*, 2013). Despite being a negative regulator of DNA re-replication, geminin also seems to have a positive influence on pre-RC assembly as the protein has been shown to promote Cdt1 accumulation during mitosis by inhibiting its ubiquitylation (Ballabeni *et al*, 2004; Tsunematsu *et al*, 2013).

Initiation of replication is dependent on S phase kinases, in humans namely DDK and Cdk2 (reviewed in Labib, 2010), regulating various steps of CMG helicase assembly. It has been shown early that proper origin firing in yeast requires DDK-dependent phosphorylation of the MCM2-7 complex (Lei *et al*, 1997; Weinreich & Stillman, 1999) and later studies then suggested this phosphorylation to facilitate Cdc45-binding to the helicase (Zou & Stillman, 2000; Sheu & Stillman, 2006). Similar observations have been made in human cells, implicating DDK activity in CMG complex formation via MCM2-7 phosphorylation (Masai *et al*, 2000; 2006; Im *et al*, 2009). Although Cdc45 and the priming DNA polymerase Pol α have also been characterized as DDK-targets (Weinreich & Stillman, 1999; Nougarède *et al*, 2000), it remains generally believed that the kinase regulates origin firing mainly via the MCM2-7 complex (Yeeles *et al*, 2015). Cdk2 influences CMG assembly more indirectly via phosphorylation of assembly regulators: the yeast proteins Dpb11 (DNA polymerase B11), Sld2 and Sld3 form a ternary complex, which is believed to act as a chaperone for CMG helicase assembly (Araki *et al*, 1995; Kamimura *et al*, 1998; 2001; Zegerman & Diffley, 2007; Tanaka *et al*, 2007). It has not only been shown that the interaction of Sld2 and -3 with Dbp11 is dependent on S phase Cdk activity but even more strikingly, that Sld2/-3 are the minimum set of S phase Cdk targets required for proper replication (Masumoto *et al*, 2002; Tak *et al*, 2006; Zegerman & Diffley, 2007; Tanaka *et al*, 2007; Yeeles *et al*, 2015). While it has been known for quite some time that Dpb11 is conserved across various species (Mäkiniemi *et al*, 2001), it was demonstrated only recently that the (strikingly also Cdk dependent) formation of a ternary complex consisting of the human Dpb11 ortholog TopBP1 (Topoisomerase IIβ binding protein), the Sld3 equivalent Treslin/TICRR (TopBP1-interacting, replication stimulating protein/TopBP1-interacting, checkpoint, and replication regulator) and the newly found interactor MTBP (MDM two binding protein) is required for efficient CMG assembly and replication in human cells (Kumagai *et al*, 2011; Boos *et al*, 2011; 2013).

1.3 Mitosis (M phase)

The aim of mitosis is to equally divide the previously duplicated genetic material in order to generate two identical daughter cells. Mitosis is subdivided into five phases: prophase, prometaphase, metaphase, anaphase and telophase (Figure 3). The highly ordered sequence of events is initiated in prophase by compaction of chromosomes (consisting of two sister chromatids), while the nuclear envelope disintegrates and the future spindle poles begin (consisting of centrosomes, see also chapter 1.5) to separate, nucleating microtubules and eventually forming the mitotic spindle. Chromosomes can bind to the spindle microtubules via motor proteins, and during prometaphase start to congress and co-align. Metaphase marks the time, at which the chromosomes are correctly aligned at the so-called metaphase plate, a narrow region perpendicular to and amidst the two spindle poles. Only when all chromosomes are properly attached to the spindle, i.e. the two sister chromatids of each chromosome are attached to microtubules emenating from opposite spindle poles, transition into anaphase takes place. The tight interaction between sister chromatids is lost and by being transported towards each spindle pole, the cell's

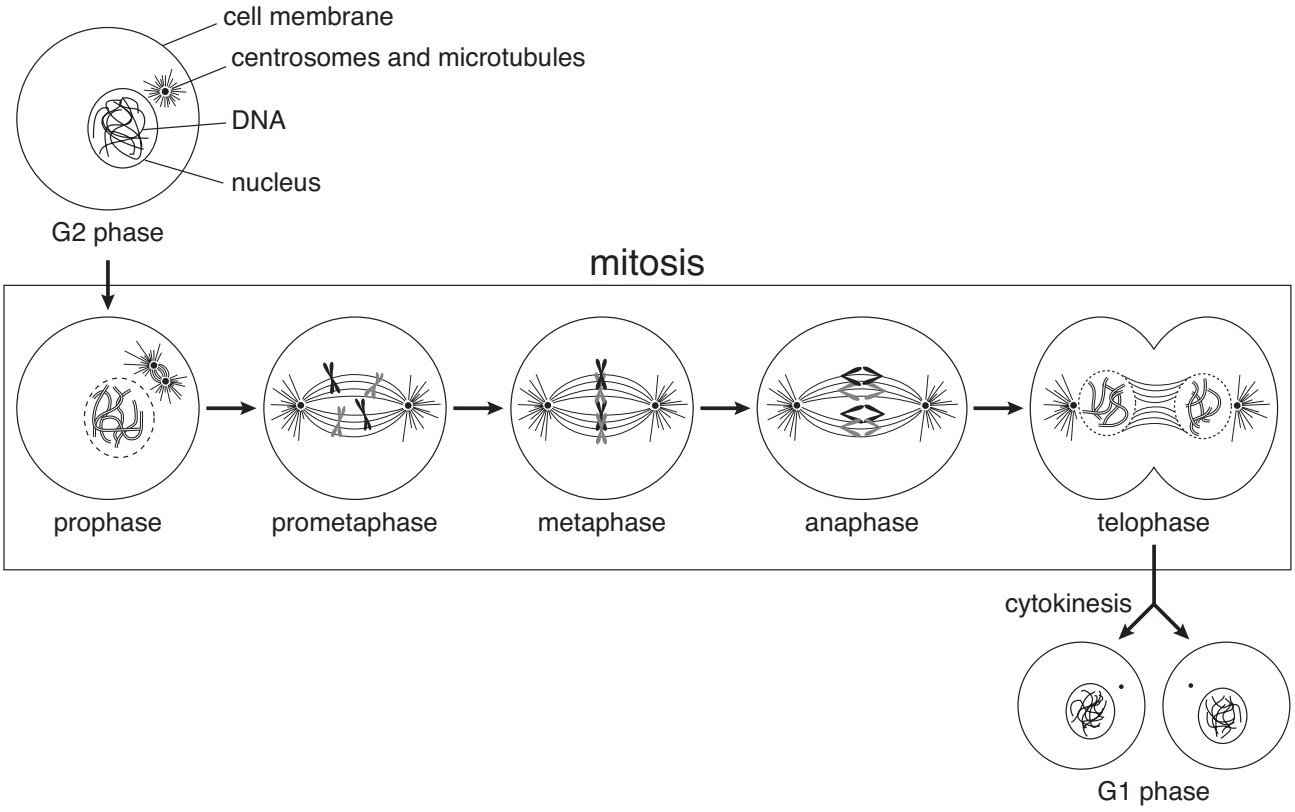

Figure 3 | **Overview over eukaryotic mitosis.** Cartoon depicts transition into mitosis, as well as nuclear envelope breakdown, chromosome condensation, centrosome splitting, and spindle formation in pro- and prometaphase. Chromosomes congress and align at the metaphase plate before sister chromatids are separated at the metaphase-to-anaphase transition. Chromosomes decondense and nuclear envelope reforms in telophase prior to cytokinesis. For more details see text.

genetic material becomes separated. Beginning chromosome decondensation and reformation of the nuclear envelope are hallmarks of telophase. The final step of cell division is cytokinesis, in which the cell membrane constricts to ultimately sever all remaining bonds between the two nascent cells.

1.3.1 Mitotic entry

The cyclin-dependent kinase 1 (Cdk1), together with its coactivator cyclin B1, is the main regulator of mitosis. Cdk1-cyclin B1 activity is essential for a plethora of early mitotic events, including chromosome condensation (Hirano, 2005), nuclear envelope breakdown (Ward & Kirschner, 1990; Heald & McKeon, 1990) and spindle formation (Crasta *et al*, 2006). Therefore, entry into mitosis depends on Cdk1 activation, which is controlled via cyclin B1 levels as well as inhibitory phosphorylations on Cdk1. Cyclin B1 levels begin to rise when its transcription is activated via Cdk2-Cyclin A activity, which peaks in late G2 phase (Guadagno & Newport, 1996). Although cyclin B1 is already proficient in binding to Cdk1, the kinase remains inactive due to inhibitory phosphorylations on T14 and Y15 brought about by Wee1 and Myt1 kinases (Parker *et al*, 1992; Mueller *et al*, 1995). Only when in late G2 phase the antagonistic phosphatase Cdc25 (cell division cycle) is activated, the inhibitory phosphorylations can be reversed (Gautier *et al*, 1991; Kumagai & Dunphy, 1992; Qian *et al*, 2001). Partial Cdk1-cyclin B1 activation then triggers a positive feedback loop in which Cdc25 is further activated by the kinase (Hoffmann *et al*, 1993; Izumi & Maller, 1993), while Wee1 and Myt1 are inhibited (McGowan & Russell, 1995; Mueller *et al*, 1995), resulting in a switch-like progression into mitosis. Irreversibility of this switch is further ensured by activating phosphorylations on Cdk1 by the Cdk-activating kinase (CAK, Cdk7 in metazoans; reviewed in Harper & Elledge, 1998; Lindqvist *et al*, 2009).

1.3.2 The mitotic spindle and attachment of chromosomes to spindle microtubules

As cells enter mitosis, their microtubule-organizing centers (MTOC)/centrosomes (see also chapter 1.5) begin wandering to opposite sides of the cell eventually forming the poles of the mitotic spindle (Figure 3). The latter consists of microtubules, long tube-shaped polymers of α- and β-tubulin molecules, which emanate from the spindle poles in a highly dynamic fashion to probe the cytoplasm for chromosomes (and associated motor proteins)

using a biased "search-and-capture" approach (Kirschner & Mitchison, 1986; Wittmann *et al*, 2001; Wollman *et al*, 2005). The ultimate goal is to form a bipolar spindle in which each and every kinetochore is attached to microtubules in a bi-oriented fashion, i.e. the two sister chromatids of each chromosome are attached to microtubules from different spindle poles. Microtubules are directional, consisting of a highly dynamic plus- and a slowly depolymerizing minus-end (Desai & Mitchison, 1997; for more details on the spindle poles and microtubules, see chapter 1.5). We distinguish three types of spindle microtubules: (i) astral microtubules emanate radially from centrosomes and bind to the cell cortex, thereby stabilizing the position of the corresponding spindle pole. (ii) Interpolar microtubules from opposite poles reach deep into the cytoplasm and interact with each other via multivalent motor proteins in an anti-parallel fashion. These interactions in the so-called spindle mid zone ensure the bipolarity of the spindle. (iii) Kinetochore microtubules (also called k-fibers) attach to the chromosomes by plus-end-mediated binding to kinetochores, large proteinaceous structures lying on top of the centromeres (Wittmann *et al*, 2001).

Stable chromosome-association requires microtubules to attach to the conserved Knl1-Mis12-Ndc80 (KMN)-network of the outer kinetochore (Cheeseman *et al*, 2006), but initial attachment is most likely mitigated by other proteins. The motor protein CENP-E (Kinesin-7), which binds to microtubules as well as kinetochores, has been identified early as an essential factor for proper chromosome alignment (Wood *et al*, 1997; Schaar *et al*, 1997). The finding that CENP-E activity can mediate proper chromosome congression to the metaphase plate before bi-orientation implies a role for the motor protein in initial microtubule attachment (Kapoor *et al*, 2006). Recent studies showed that CENP-E's function is facilitated by its ability to bind to microtubules laterally before this association is converted to an end-on binding mode, ensuring not only congression of chromosomes but also maintenance of their alignment at the metaphase plate (Kapoor *et al*, 2006; Shrestha & Draviam, 2013; Gudimchuk *et al*, 2013).

Unfortunately, the aforementioned "search-and-capture" mechanism cannot differentiate between correct and erroneous attachment modes. Therefore, the cell has to employ additional and partly redundant processes to ensure correct binding of microtubules to kinetochores. Besides the desired amphitelic attachment (which produces correctly bi-oriented chromosomes), we distinguish between three erroneous modes of attachment: mono-, syn- and merotelic. Monotelic attachment produces mono-oriented chromosomes in which only one sister kinetochore is attached one spindle pole. This causes activation of the so-called spindle assembly checkpoint (SAC; also simply "mitotic

checkpoint"), which halts mitotic progression until the second sister kinetochore becomes attached (for details on the SAC, see chapter 1.3.3). A mode of attachment is called syntelic, when both sister kinetochores are associated with microtubules emanating from the same spindle pole. As syntelic attachments cannot be directly sensed by the canonical SAC, the cell has to employ a different branch of the mitotic checkpoint, sometimes referred to as the tension checkpoint. This checkpoint percepts the absence of tension, which is normally generated between the two kinetochores of bi-oriented sister chromatids, and remains active until such tension is established (Nezi & Musacchio, 2009; Lampson & Cheeseman, 2011). An integral part of the tension-sensitive branch of the mitotic checkpoint is the Aurora B kinase, which together with the non-enzymatic proteins INCENP, survivin and borealin forms the chromosomal passenger complex (CPC) (Ruchaud *et al*, 2007). Under lack of tension, Aurora B phosphorylates various targets involved in chromosomal spindle attachment such as the KMN network and CENP-E, reducing their affinity towards microtubules, probably by electrostatic repulsion (Welburn *et al*, 2010; Kim *et al*, 2010). In addition, the microtubule-depolymerizing enzyme MCAK (mitotic centromere-associated kinesin), which is intimately regulated by Aurora B, has been implicated to facilitate error correction under lack of tension (Andrews *et al*, 2004; Kline-Smith *et al*, 2004). By creating unattached kinetochores, the tension checkpoint might function as a simple SAC activator (see above and chapter 1.3.3), although there is evidence implying a more direct involvement of the tension checkpoint in causing mitotic arrest (Nezi & Musacchio, 2009; Santaguida *et al*, 2011). Several mechanisms have been suggested as to how successful bi-orientation is actually sensed (reviewed in Lampson & Cheeseman, 2011) but mounting evidence gives credence to a model in which inter-kinetochore tension causes physical separation of the Aurora B kinase and its targets, thus stabilizing microtubule attachments (Liu *et al*, 2009; Keating *et al*, 2009; Welburn *et al*, 2010). At least in yeast, complete inactivation of the tension checkpoint might require additional removal of Aurora B from the centromeres (Peplowska *et al*, 2014; Nerusheva *et al*, 2014). While similar dynamics, i.e. relocalization of the CPC to the spindle mid zone, can be observed in human cells, they occur later and therefore might not have the same function (Mirchenko & Uhlmann, 2010; Vázquez-Novelle & Petronczki, 2010). The last category of erroneous attachment modes is called merotelic. The kinetochores of a chromosome displaying merotelic attachment are both attached to opposite sides of the spindle but at least one kinetochore shows additional syntelic attachment. These situations can be difficult to detect as both the attachment as well as the tension checkpoint should

be satisfied. Yet the empirically observed number of merotelically attached kinetochores is far lower than what would be expected from computational predictions, which is a strong indicator for the existence of a dedicated error correction mechanism (Paul *et al*, 2009). Merotelic attachments might simply be suppressed passively by the structural organization of the chromosomes (reviewed in Gregan *et al*, 2011) but mounting evidence suggests that correction of such attachments does, in fact, require action of components of the tension checkpoint, including Aurora B and MCAK (Knowlton *et al*, 2006; Cimini *et al*, 2006). So has it been proposed that merotely causes intra-kinetochore tension which can be sensed and corrected via Aurora B-dependent disruption of the incorrect kinetochore-microtubule associations (Cimini *et al*, 2006; Courtheoux *et al*, 2009).

1.3.3 Sister chromatid separation and the spindle assembly checkpoint (SAC)

When the kinetochores of all sister chromatids are properly (amphitelically) attached to the spindle, the tight association or cohesion between them is lost, which allows cells to progress from metaphase to anaphase. Sister chromatid cohesion is mediated by the cohesin complex. Cohesin is a centromere-associated multimeric ring complex, which embraces the two sister chromatids inside its lumen from S phase until the metaphase-to-anaphase transition (for more details on cohesin, see chapter 1.4). During this transition, the large cysteine protease separase becomes active and proteolytically cleaves the cohesin ring, allowing the two sister chromatids to separate (Uhlmann *et al*, 1999). It is by this molecular mechanism that anaphase is triggered in all eukaryotic cells.

Because of the irreversible nature of cohesin proteolysis, it is imperative for the cell to tightly control separase activity as premature sister chromatid separation can result in aneuploidies, which have been associated with the formation and progression of cancer (Kops *et al*, 2005; Hanahan & Weinberg, 2011). Canonically, separase is negatively regulated by a specific inhibitor called securin, which associates with the protease until the metaphase-to-anaphase transition (Yamamoto *et al*, 1996; Zou *et al*, 1999). In 2001 however, Stemmann *et al.* found an unexpected role for Cdk1-cyclin B1 as an additional regulator of the protease (Stemmann *et al*, 2001). The kinase not only phosphorylates separase but also stably binds to it, resulting in a securin-independent inhibition of separase (Stemmann *et al*, 2001; Gorr *et al*, 2005; Holland & Taylor, 2006; Boos *et al*, 2008; Hellmuth *et al*, 2014; 2015a). In fact, regulation via Cdk1-cyclin B1 seems to be even more crucial, since *securin*$^{-/-}$ mice are viable and phenotypically normal, while a

knock-in of just one Cdk1 phosphorylation-resistant separase allele causes massive failures in germ line development and embryogenesis, resulting in early embryonic lethality (Mei *et al*, 2001; Huang *et al*, 2008; 2009). Recent advances in the field further highlight the importance of finely tuned separase regulation by revealing various novel mechanisms involving precisely timed securin dephosphorylation and prolyl-isomerization of separase at the end of mitosis (Hellmuth *et al*, 2014; 2015b).

Separase must be kept in check as long as not all chromosomes are properly attached to the spindle. This integration of events is controlled by the spindle assembly checkpoint (SAC). As long as the SAC is not satisfied, it produces a "wait anaphase" signal, which results in a (pro)metaphase arrest. The SAC depends on a variety of (mostly) kinetochore-associated proteins including Mad2 (mitotic arrest deficient). According to the Mad2 template model, unattached kinetochores trigger Mad2 and kinetochore-bound Mad1 to form a complex, which subsequently acts as a platform licensing further soluble Mad2 molecules to bind and sequester Cdc20, an integral co-activator of the anaphase-promoting complex/cyclosome (APC/C; Luo *et al*, 2002; Sironi *et al*, 2002; Luo *et al*, 2004; de Antoni *et al*, 2005; Vink *et al*, 2006). APC/C^{Cdc20} is a large cullin-RING finger E3 ubiquitin ligase consisting of at least 12 subunits in mammals, which targets securin as well as cyclin B1 for ubiquitylation, resulting in their proteasomal degradation and subsequent activation of separase (Funabiki *et al*, 1996; Zou *et al*, 1999; Peters, 2006).

Various mechanisms have been proposed as to how the checkpoint is actually shut down when all requirements have been met including, but not limited to, stripping of SAC components from the kinetochores (Howell *et al*, 2001), competitive binding of $p31^{comet}$ to sites of Mad2 licensing (Mapelli *et al*, 2006; Vink *et al*, 2006; Yang *et al*, 2007) and APC/C-dependent ubiquitylation of SAC proteins (Palframan *et al*, 2006; Reddy *et al*, 2007). A recent study however, proposed simply the loss of Cdk1-activity at the metaphase-to-anaphase transition to be the main event preventing SAC-reactivation in late mitosis (Vázquez-Novelle *et al*, 2014).

1.4 Cohesin

The notion of faithful chromosome separation in mitosis does not only implicate the separation of intact chromosomes but also the balanced distribution of the correct set of chromosomes in order to create two genetically identical daughter cells. A normal post-replicative human cell contains a total of 46 chromosomes, each consisting of two identical

sister chromatids, which have to be distributed in a highly ordered fashion. This problem is elegantly solved by holding sister chromatids together from the time of their generation in S phase until their separation at the metaphase-to-anaphase transition in M phase. This pairing is called cohesion. One way to confer sister chromatid cohesion is DNA catenation which naturally occurs during DNA replication (Sundin & Varshavsky, 1980). But since most DNA catenations become resolved until mitosis (Koshland & Hartwell, 1987; Porter & Farr, 2004), a different mechanism has to take over. A key player of this mechanism is the cohesin complex.

1.4.1 Composition of the cohesin complex and the ring embrace model

The cohesin complex is a multimeric complex comprising a tripartite ring structure and associated proteins (Figure 4 and Peters *et al*, 2008). The integral ring components are Smc1 (structural maintenance of chromosomes), Smc3 and Scc1 (sister chromatid cohesion). Smc1 and -3 are large proteins forming long intramolecular coiled-coil structures by folding back onto themselves (Melby *et al*, 1998; Haering *et al*, 2002). They interact with each other via their middle regions, forming two halves of a toroid, the so-called "hinge". Their individual C- and N-termini interact to form nucleotide binding domains (NBDs). Moreover Smc1 and -3's NBDs have been shown to interact to form a functional ATPase, whose action might be required for various events in cohesin's cycle. As direct Smc1-Smc3 head interactions cannot form a stable ring complex, an additional factor, the α-kleisin (greek for "bridge") Scc1 is required to form a functional cohesin ring (Haering *et al*, 2002). Apart from its termini, Scc1 is predicted to be a rather unstructured protein, which interacts directly with Smc1's head domain via its C-terminus, and with Smc3's neck region (at the beginning of the coiled coil-stretch) via its N-terminus (Haering *et al*, 2004; Gligoris *et al*, 2014; Huis In 't Veld *et al*, 2014). The unstructured middle region of Scc1 constitutes a binding platform for various associated cohesin subunits like SA1/2 (stromalin antigen) and Pds5A/B (precocious dissociation of sisters), which in turn recruits Wapl (wings apart like) or sororin (Peters *et al*, 2008; Nishiyama *et al*, 2010).

There is extensive evidence for cohesin as an essential mediator of sister chromatid cohesion. Early studies in budding yeast already revealed strong cohesion defects in cells expressing mutated cohesin subunits (Michaelis *et al*, 1997; Guacci *et al*, 1997). Similar results were soon obtained for vertebrate cells (Sonoda *et al*, 2001) and *Drosophila* (Vass *et al*, 2003). How the cohesin complex accomplishes this feat has been and is still subject

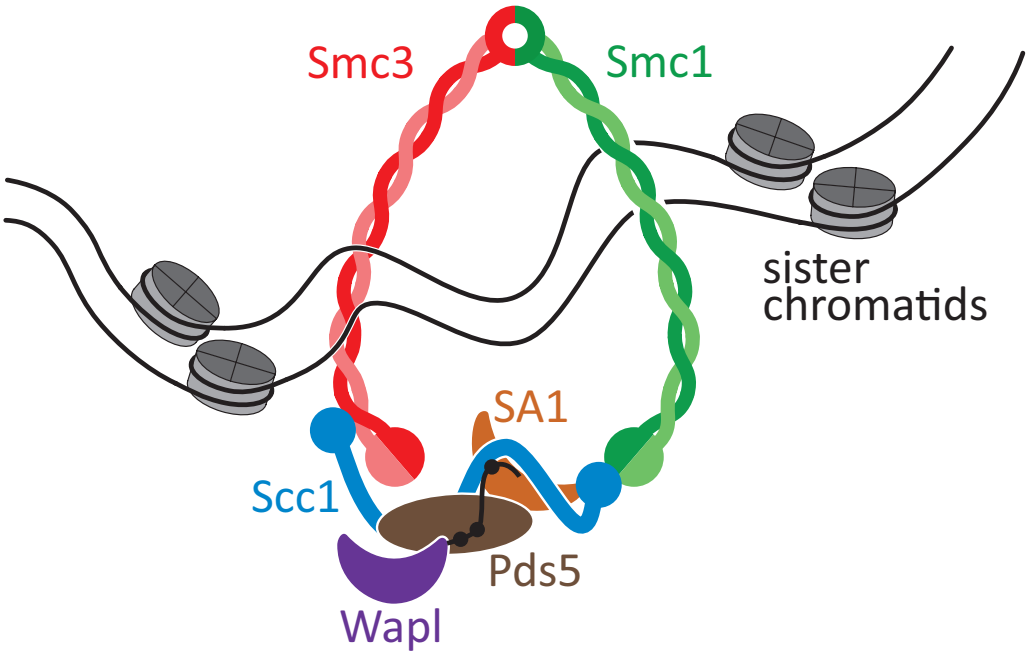

Figure 4 | **The cohesin complex.** The integral ring structure of the multimeric complex is composed of three proteins, Smc1, Smc3 and Scc1. Scc1's unstructured middle region allows association with further cohesin subunits, namely SA1 (or -2) and Pds5A (-or B). Pds5 is the main recruiter for either Wapl (a cohesin destabilizing protein; depicted) or sororin (a cohesin stabilizing protein; not depicted) in a mutually exclusive manner. Wapl's unstructured N-terminus (black line protruding from "Wapl"-marked shape) contains three conserved FGF motifs (black dots on the black line), which interact with Pds5 as well as the Scc1-SA1 subcomplex. The cohesin complex is shown embracing two sister chromatids wrapped around histones. For more details see text.

of many speculations. The finding that the complex forms a ring structure, however, provided the basis for the today widely accepted "ring embrace" model (Haering *et al*, 2002). According to this quite elegant model, the cohesin ring holds sister chromatids together in a topological fashion, embracing the two entities inside its lumen (Figure 4). In support for this theory, it has been shown that natural or artificial cleavage of Scc1 or Smc3 causes sister chromatid separation (Uhlmann *et al*, 1999; 2000; Gruber *et al*, 2003; Schöckel *et al*, 2011). Further studies with circular minichromosomes revealed that cohesin rings dissociate from DNA upon linearization (Ivanov & Nasmyth, 2005) and that this treatment also causes replicated minichromosomes to lose their cohesion (Ivanov & Nasmyth, 2007). Moreover, fusing cohesin subunits to each other via chemical crosslinking makes cohesed minichromosomes resistant to harsh denaturing conditions (Haering *et al*, 2008). Very recently, it has been impressively demonstrated that reconstituted recombinant cohesin complexes can be loaded onto minichromosomes in a topological fashion *in vitro*, which is a strong result in favor of the "ring embrace" model (Murayama & Uhlmann, 2014). Other models that require oligomerization of cohesin molecules (e.g. the "handcuff" model) have been and still are suggested to this day (Huang *et al*, 2005; Eng *et*

al, 2014). While it is very difficult to test for these models on DNA-bound cohesin complexes, multimeric cohesin supercomplexes have never been described in the literature.

1.4.2 An overview of the cohesin cycle

The cohesin cycle commences early after sister chromatid separation with reloading of the complex onto DNA in telophase of the same mitosis (G1 phase in yeast, Figure 5 and chapter 1.4.3; Guacci *et al*, 1997; Michaelis *et al*, 1997; Losada *et al*, 1998; Darwiche *et al*, 1999). Ever since the formulation of the "ring embrace" model (Haering *et al*, 2002), it was widely believed that initial cohesin loading also occurred in a topological fashion. This theory was given further credit, when it was shown that cohesin loading in yeast requires opening the hinge (between Smc1 and Smc3, compare also Figure 4; Gruber *et al*, 2006). Final proof has been provided just recently, as it could be demonstrated that reconstituted recombinant cohesin topologically associated with minichromosomes *in vitro* (Murayama & Uhlmann, 2014). During G1 phase the complex is highly dynamic, being constantly shed from and then reloaded onto chromatin (Gerlich *et al*, 2006; Kueng *et al*, 2006). Actual cohesion is, of course, not established until the second sister chromatid is synthesized in S

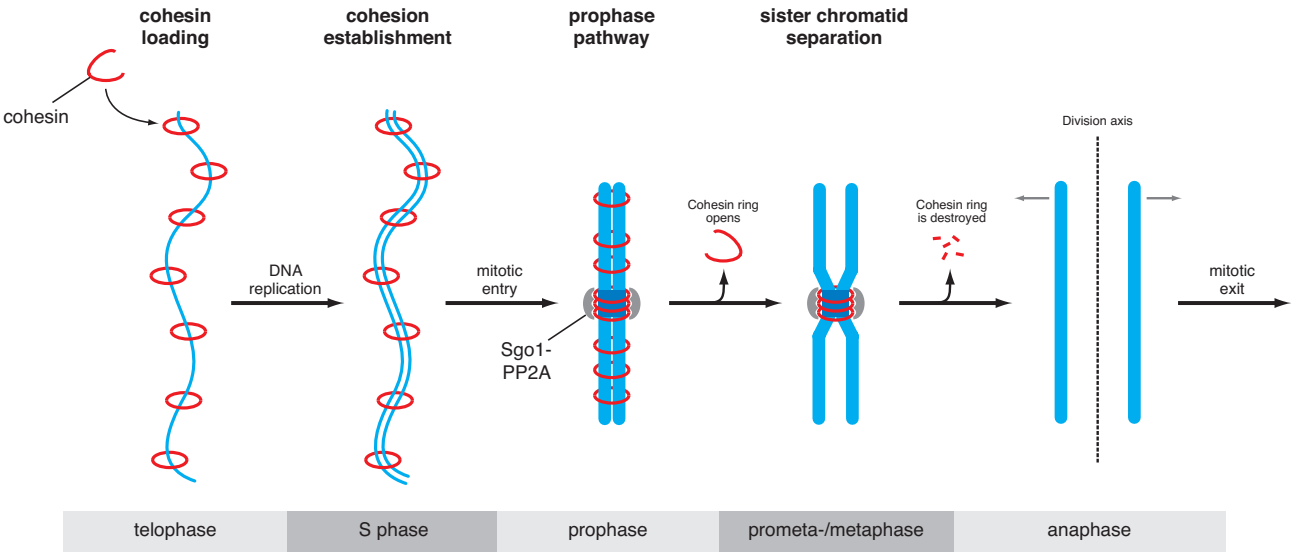

Figure 5 | **The cohesin cycle.** The cohesin ring is topologically loaded onto DNA (blue line) in telophase. Cohesion is established, when the second sister chromatid is synthesized in the following S phase. In prophase, the prophase pathway acts on cohesin molecules associated with chromosome arms and removes them in a non-proteolytic manner. Sister chromatid cohesion is maintained until the metaphase-to-anphase transition by Sgo1-PP2A-mediated protection of centromeric cohesin from prophase pathway signaling. Then, separase proteolytically cleaves cohesin's Scc1 subunit, which leads to separation of sister chromatids in anaphase. For more details see text.

phase, which causes the cohesin complex to stabilize (chapter 1.4.4; Skibbens *et al*, 1999; Tóth *et al*, 1999; Gerlich *et al*, 2006; Rolef Ben-Shahar *et al*, 2008; Lafont *et al*, 2010; Nishiyama *et al*, 2010). To allow final separation of sister chromatids at the metaphase-to-anaphase transition, cohesin must be removed from chromatin (chapter 1.4.5). In vertebrates, this happens in two waves: the bulk of cohesin molecules is removed from chromosome arms already in prophase by the eponymous "prophase pathway" (Figure 5; Waizenegger *et al*, 2000). To ensure sister chromatid cohesion until metaphase, a small amount of cohesin molecules is being protected from the prophase pathway at the centromeric region by the action of shugoshin 1 (japanese for "guardian spirit") in complex with protein phosphatase 2 A (Sgo1-PP2A, see chapter 1.6; McGuinness *et al*, 2005; Kitajima *et al*, 2006). Ultimately, the remaining cohesin complexes are removed from the centromeres, when separase becomes active and cleaves cohesin's Scc1 subunit to open up the ring (Uhlmann *et al*, 1999; see chapter 1.3.3).

1.4.3 Cohesin loading and the kollerin complex

Although it has been suggested that cohesin might directly interact with DNA (Milutinovich *et al*, 2007), its chromosomal association does not seem to be sequence specific. Early yeast studies described chromosomal cohesin-associated regions (CARs) by chromatin immunoprecipitation (ChIP) experiments to reside mostly in intergenic stretches (Blat & Kleckner, 1999; Megee *et al*, 1999). Cohesin was found to be associated with the whole chromosome (average inter-CAR distance: ~10 kb) but was specifically enriched around the centromere (pericentromeric region) to ensure proper resistance against microtubule pulling forces before anaphase (Tanaka *et al*, 1999). As already mentioned, the identified CARs in yeast did not seem to be characterized by specific DNA sequences but have been described as being rich in AT-pairs, which might be coincidental, since most intergenic regions tend to be AT-rich (Laloraya *et al*, 2000). Since then, further studies have revealed that sites of actual cohesin loading and CARs do not overlap and furthermore that CARs seemed to reside in regions of converging transcription suggesting that transcription is the force driving cohesin-association with these intergenic regions (probably simply by pushing cohesin rings to these sites; Ciosk *et al*, 2000; Glynn *et al*, 2004). And indeed, Lengronne and coworkers were able to provide evidence that cohesin deposition at known regions at the 3'-end of specific genes could be abrogated by blocking their transcription (Lengronne *et al*, 2004). Chromosomal cohesin association in mammalian cells differs quite

substantially from the one found in yeast (Parelho *et al*, 2008; Wendt *et al*, 2008). Mammalian CARs were found to be GC- rather than AT-rich and only 13% of cohesin-associated sites were found in intergenic regions between convergent genes but 26% were located at those between divergent genes (compared to 2% in yeast; Parelho *et al*, 2008). Strikingly, a large number of cohesin complexes also bound within introns of actively transcribed genes (Wendt *et al*, 2008).

Stable initial loading of cohesin onto DNA requires a complex consisting of Scc2 and Scc4. Initially, both proteins have individually been described to be essential for proper sister chromatid cohesion in yeast (Michaelis *et al*, 1997; Furuya *et al*, 1998; Tóth *et al*, 1999). In 2000, Ciosk and coworkers found that Scc2 and -4 form a subcomplex, which is required for loading of cohesin onto DNA (Ciosk *et al*, 2000). Today this complex is known as kollerin (from the greek verb "kollao", which means "to attach with glue"; Nasmyth, 2011). The requirement of Scc2 for loading of cohesin in higher eukaryotes has first been described for the *Xenopus* egg system, suggesting conservation of cohesin's loading mechanism (Gillespie & Hirano, 2004; Takahashi *et al*, 2004). For humans, an Scc2 ortholog (NIPBL; Nipped-B like) had already been described at the time (Krantz *et al*, 2004; Tonkin *et al*, 2004), but a respective ortholog of Scc4 and, more importantly, conservation of kollerin function were not reported until two years later (Watrin *et al*, 2006). Interestingly, for *Xenopus*, it was not only found that Scc2/4 physically associates with DDK, which is essential for the formation of pre-replicative complexes (pre-RCs, see also chapters 1.2.1 and 1.2.4; Takahashi *et al*, 2008), but moreover that Scc2-mediated cohesin loading required replication licensing (Gillespie & Hirano, 2004; Takahashi *et al*, 2004). However, despite the fact that human cohesin interacts with the pre-RC complex and, furthermore, that its loading coincides with pre-RC assembly in a timely manner, these two processes appear to be independent (Guillou *et al*, 2010). The same is true for budding yeast, where cohesin loading occurs later (in G1 phase, i.e. after replication licensing): While DDK plays roles in both Scc2/Scc4 recruitment and pre-RC assembly, these two events are not interdependent (Uhlmann & Nasmyth, 1998; Natsume *et al*, 2013). Other than the fact that kollerin can be found to associate with the whole chromosome in humans, yeast and flies, the exact determinants for its DNA association still remain unknown. However, some past studies have suggested sites of active transcription to be a common denominator for kollerin hot-spots on chromatin across various species (Ocampo-Hafalla & Uhlmann, 2011).

Although kollerin-mediated recruitment of cohesin is absolutely required for proper loading, the ring complex only transiently interacts with Scc2/4 (Hu *et al*, 2011; Ladurner *et al*, 2014). A recent study from yeast even suggests that kollerin's main function is merely to maintain nucleosome-free regions, which passively facilitate cohesin loading (Lopez-Serra *et al*, 2014). However, it was shown that after initial recruitment, kollerin stimulates cohesin's ATPase activity (associated with its Smc head domains; see chapter 1.4.1), which is required to load cohesin onto DNA in a topological (DNA-embracing) fashion and to allow its relocation to its final chromosome region (Weitzer *et al*, 2003; Arumugam *et al*, 2003; Hu *et al*, 2011; Ladurner *et al*, 2014). For topological loading, the cohesin ring must transiently open to allow entrance of DNA into its lumen. Data from a yeast study implied that the ring opens at the hinge region, but unfortunately, this has never been shown for other organisms including human (Gruber *et al*, 2006).

1.4.4 Cohesion establishment

Establishment of sister chromatid cohesion is intimately linked to DNA replication. Although cohesin is topologically loaded onto DNA in the preceding telophase, its association with chromatin remains highly dynamic, with the ring complex undergoing constant dissociation from and reloading onto chromosomes during G1 phase (Gerlich *et al*, 2006; Kueng *et al*, 2006). While these dynamics probably serve a purpose beyond cohesin's canonical function (see chapter 1.4.7), they are incompatible with stable sister chromatid cohesion. A corollary of this fact is that cohesin complexes must be stabilized on DNA during S phase.

Eco1 (establishment of cohesion; earlier: Ctf7) was already identified in the early days of cohesin research as an essential cohesion establishment factor in yeast (Skibbens *et al*, 1999; Tóth *et al*, 1999). Eco1 is an acetyl transferase that has been shown to be able to acetylate cohesin subunits *in vitro* (Ivanov *et al*, 2002). *In vivo*, yeast Eco1 as well as its human ortholog ESCO1 (humans have two ESCO variants, ESCO1 and -2) have been shown to co-replicatively acetylate Smc3 at two adjacent lysine residues (K105/106 in humans), which is necessary for proper sister chromatid cohesion (Zhang *et al*, 2008; Ünal *et al*, 2008; Rolef Ben-Shahar *et al*, 2008). More specifically, Smc3 acetylation was described to counteract an "antiestablishment activity" mainly associated with the cohesin subunit Rad61/Wapl (budding yeast: radiation sensitive/humans: wings apart-like), a

known cohesin destabilizer (Rolef Ben-Shahar *et al*, 2008; Sutani *et al*, 2009; Rowland *et al*, 2009; see also chapter 1.4.5).

Humans employ another factor for the establishment of sister chromatid cohesion, called sororin. Interestingly, the functions of sororin and ESCO/Eco1 have always been described as similar or even complementary (Rankin *et al*, 2005; Lafont *et al*, 2010) until it was found that both proteins likely belong to the same pathway and that sororin is, in fact, a direct antagonizer of Wapl. Current data suggests that ESCO-dependent Smc3 acetylation facilitates recruitment of sororin, which competitively displaces Wapl from its binding site on cohesin, thereby stabilizing the ring complex (Nishiyama *et al*, 2010).

1.4.5 Cohesin release in mitosis and the prophase pathway

In order to separate sister chromatids at the metaphase-to-anaphase transition, cohesin must be removed from chromosomes. As described earlier (chapter 1.3.3), the ultimate trigger for sister chromatid separation and, thus, anaphase onset is separase-mediated endoproteolytic cleavage of cohesin's Scc1 subunit. Interestingly, the bulk of cohesin rings, which is mainly associated with chromosome arms, is already removed early in mitosis during prophase by a non-proteolytic mechanism (Waizenegger *et al*, 2000). This mechanism is called the prophase pathway. The key mediator of this pathway is the cohesin subunit Wapl, which, together with Pds5, forms a subcomplex called releasin (Kueng *et al*, 2006; Gandhi *et al*, 2006; Nasmyth, 2011). Releasin is a stoichiometric component of cohesin, which interacts directly with the Scc1/SA1 subcomplex (see Figure 4; Kueng *et al*, 2006; Shintomi & Hirano, 2009). Human Wapl consists of a well-conserved globular C-terminus and an unstructured and flexible N-terminus (Ouyang *et al*, 2013). The latter contains three conserved FGF motifs, which have been shown to be required for the interaction of Wapl with Pds5 and the Scc1-SA1 subcomplex (Shintomi & Hirano, 2009). While Wapl can bind to Scc1 independently of Pds5, it always requires the presence of SA1/2 (Shintomi & Hirano, 2009; Ouyang *et al*, 2013). Although Wapl's C-terminus cannot bind to Scc1 on its own, it seems to facilitate stable binding of the full-length protein (Ouyang *et al*, 2013).

As mammalian cells enter mitosis, the cohesin stabilizer sororin (which competitively binds to Pds5 via its own FGF motif) becomes phosphorylated by Aurora B and Cdk1, causing its dissociation from Pds5 (Nishiyama *et al*, 2010; Dreier *et al*, 2011; Nishiyama *et al*, 2013). This allows Wapl-binding to Pds5 and subsequent cohesin removal

by an as yet unknown mechanism (Gandhi *et al*, 2006; Nishiyama *et al*, 2010). It should be mentioned that, while cohesin stabilization demands Eco1/ESCO1/-2-dependent acetylation of Smc3 (see chapter 1.4.4), early mitotic removal of cohesin from chromatin in does not require the reverse reaction. Nonetheless, Smc3 is actively deacetylated in anaphase (by deacetylases Hos1 in yeast and HDAC8 in humans), which sets back the acetylation cycle, allowing cohesin molecules to re-establish cohesion in the following S phase (Beckouët *et al*, 2010; Borges *et al*, 2010; Xiong *et al*, 2010; Deardorff *et al*, 2012a). In addition to Wapl, the prophase pathway is dependent on Aurora B and Plk1 activities (Sumara *et al*, 2002; Giménez-Abián *et al*, 2004). More specifically, Plk1-dependent phosphorylation of SA2 has been shown to be essential for cohesin-removal from chromosomes during prophase (Hauf *et al*, 2005).

In order to maintain sister chromatid cohesion until metaphase, some cohesin molecules must be protected from the action of the prophase pathway. This feat is mediated by the complex comprising shugoshin 1 (japanese for "guardian spirit") and protein phosphatase 2 A (Sgo1-PP2A; Kitajima *et al*, 2004; Rabitsch *et al*, 2004; Katis *et al*, 2004; Salic *et al*, 2004; Tang *et al*, 2006; Kitajima *et al*, 2006; Riedel *et al*, 2006). Sgo1-PP2A localizes to centromeric cohesin and keeps its SA2 subunit as well as sororin dephosphorylated, thereby antagonizing the prophase pathway in a locally distinct fashion (McGuinness *et al*, 2005; Kitajima *et al*, 2006; Shintomi & Hirano, 2009; Nishiyama *et al*, 2010; Liu *et al*, 2013b). Very recent data suggest an even more direct mechanism in which Sgo1 antagonizes Wapl-association with cohesin by competitive binding (Hara *et al*, 2014). For more details on shugoshin see chapter 1.6.

1.4.6 Meiotic cohesin

In meiosis, one round of DNA replication is followed by two consecutive cell divisions, leading to the formation of haploid gametes, a prerequisite for sexual reproduction. In the first meiotic division (meiosis I; "reductional division"), homologous chromosomes (each consisting of two sister chromatids) are paired and undergo recombination during prophase I. Homologs align at the metaphase I plate and mono-orient, which means that in marked contrast to mitosis, the two sister chromatids of one chromosome attach to the same pole of the meiosis I spindle. In anaphase I the two homologous chromosomes are separated, which leads to a reduction in ploidy (from 2n to 1n). The second meiotic

division (meiosis II; "equatorial division") resembles mitosis, in that the two sister chromatids of each chromosome bi-orient in metaphase II and separate in anaphase II.

As in mitosis, sister chromatid cohesion must be maintained throughout the meiotic divisions until their separation in anaphase II. Failure to do so has been associated with age-related aneuploidies in humans (reviewed in Jones, 2008) and studies in mice suggest that cohesion-loss might even be their leading cause (Chiang *et al*, 2010). Meiotic cohesion depends on a specific form of cohesin, in which Smc1, SA1/2 and Scc1 are (at least partly) replaced by Smc1β, STAG3 and Rec8, respectively (Peters *et al*, 2008). In addition to maintaining sister chromatid cohesion, meiotic cohesin is essential for various processes during early meiosis including homolog pairing, synaptonemal complex formation and recombination (Klein *et al*, 1999; Watanabe & Nurse, 1999; Revenkova *et al*, 2004; Murdoch *et al*, 2013; Winters *et al*, 2014; Fukuda *et al*, 2014). Moreover, meiotic cohesin might also have a role in promoting mono-orientation of homologous chromosomes in meiosis I of fission yeast and mammals, while this function requires a specialized complex in budding yeast, called monopolin (Klein *et al*, 1999; Tóth *et al*, 2000; Yokobayashi & Watanabe, 2005; Petronczki *et al*, 2006; Sakuno *et al*, 2009; Corbett *et al*, 2010; Tachibana-Konwalski *et al*, 2013). More recently, a second meiotic form of Scc1, called Rad21L, has been described, which might contribute to homolog pairing and/or synaptonemal complex formation (Lee & Hirano, 2011; Ishiguro *et al*, 2011; Gutiérrez-Caballero *et al*, 2011; Ishiguro *et al*, 2014).

Both meiotic divisions require separase activation and subsequent cleavage of the kleisin Rec8 to allow separation of homologous chromosomes (meiosis I) or sister chromatids (meiosis II), respectively (Salah & Nasmyth, 2000; Buonomo *et al*, 2000; Kitajima *et al*, 2003). Rec8 cleavage requires its prior phosphorylation by casein kinase 1 (CK1) and DDK, which is counteracted at the centromeres by the meiosis-specific shugoshin variant Sgo2 in complex with PP2A, ensuring sister chromatid cohesion until metaphase II (Katis *et al*, 2004; Riedel *et al*, 2006; Katis *et al*, 2010; Ishiguro *et al*, 2010). Because of the unique requirement of meiotic cohesin during prophase I, the existence of a prophase pathway, at least in a canonical sense, seems unlikely. Nonetheless, studies in mouse spermatocytes demonstrated that synaptonemal complex disassembly coincides with loss of meiotic cohesin from chromosomes in late prophase I (Ishiguro *et al*, 2011). Strikingly similar to the mitotic prophase pathway, this process seems to be dependent on Plk1 activity.

1.4.7 Non-canonical cohesin functions

Over the years, mounting evidence has been put forth, which suggested that cohesin might provide functions beyond sister chromatid cohesion. As already outlined in the previous chapter, non-canonical functions of the complex during meiosis have been observed quite early. So has meiotic cohesin function been associated with the repair of double strand breaks (DSBs), which occur naturally during recombination in prophase I (Klein *et al*, 1999). In later studies, it was shown that this function is not exclusive to meiosis and thus, meiosis-specific cohesin: Upon replicative DNA damage, the mitotic cohesin complex is recruited to DSBs during G2 phase, where it is essentially required for DNA repair (Kim *et al*, 2002; Ünal *et al*, 2004; Ström *et al*, 2004; Bauerschmidt *et al*, 2010). This recruitment depends on DNA damage factors like ATM/ATR as well as cohesin loading and stability factors like kollerin and Eco1 (Ünal *et al*, 2004; Ström *et al*, 2004; 2007; Ünal *et al*, 2007). DSB-associated cohesin is thought to promote DNA repair via homologous recombination between sister chromatids by ensuring their proper cohesion (Sjögren & Nasmyth, 2001; Potts *et al*, 2006; Ström *et al*, 2007; Ünal *et al*, 2007).

Another well-established non-canonical function of cohesin lies in transcriptional regulation. Early yeast studies demonstrated a dependence of *S. cerevisiae* mating type locus silencing on cohesin cleavage (Lau *et al*, 2002). Data from *Drosophila* first implicated cohesin as an insulation factor, blocking long-distance promoter-enhancer association (Rollins *et al*, 2004). Further analysis of mammalian chromosomes revealed a strong correlation between regions associated with cohesin and those associated with the CCCTC-binding protein CTCF, a known transcriptional regulator that binds to insulator elements to promote enhancer-blocking (Parelho *et al*, 2008; Wendt *et al*, 2008; Rubio *et al*, 2008). The studies additionally demonstrated that cohesin's typical chromosomal distribution requires the presence of CTCF, while cohesin loading as well as sister chromatid cohesion do not (Parelho *et al*, 2008; Wendt *et al*, 2008). Strikingly, the ring complex was shown to mediate promoter-enhancer insulation in general (Parelho *et al*, 2008) and, more specifically, at the known CTCF-imprinted *H19*/*IGF2* locus, blocking transcription of *IGF2* (Wendt *et al*, 2008; Rubio *et al*, 2008). Since then, a staggering amount of evidence has been produced demonstrating that cohesin's association with DNA negatively as well as positively controls transcription in a wide variety of human genes/loci (reviewed in Ball *et al*, 2014). It had been speculated previously that CTCF's function might lie in mediating higher order chromatin organization, thereby either allowing or blocking long-range promoter-enhancer interactions (Murrell *et al*, 2004; Mishiro *et al*,

2009). This hypothesis has been validated by many publications in the recent years but it has come to light that the actual effector for the organization of higher order chromatin structure is not CTCF but associated cohesin (Hadjur *et al*, 2009; Nativio *et al*, 2009; Hou *et al*, 2010; Kagey *et al*, 2010; Seitan *et al*, 2011; 2013; Sofueva *et al*, 2013; Gosalia *et al*, 2014). This means that cohesin is able to promote cohesion not only between sister chromatids *in trans* but also between regions on the same chromatid *in cis* to allow for transcriptional regulation.

1.4.8 Clinical relevance of cohesin

Besides its involvement in age-related aneuploidies in human oocytes (see chapter 1.4.6), cohesin also has a well-established role in cancer. While in some cancer types (particularly oral squamous cell carcinoma and myeloid leukemia) cohesin subunits have been found to be downregulated or non-functional, most other studies found elevated levels of cohesin subunits in human cancers (Rhodes *et al*, 2011). Particularly in breast cancer, overexpression of Scc1 is often observed and associated with poor prognosis and resistance to chemotherapy (Xu *et al*, 2011). Because of this unusual correlation, it is generally believed that cohesin's role in cancer is not defined by its canonical but rather its non-canonical function as a transcriptional regulator. Transformed cells share some properties with stem cells, which has lead to the theory that some cancers might form due to acquired pluripotency (Sengupta & Cancelas, 2010). Interestingly, cohesin has been found to contribute to the maintenance of stem cell identity by associating with pluripotency-related transcription factors (Kagey *et al*, 2010; Nitzsche *et al*, 2011). On top of that, cohesin might stimulate the expression of genes (Liu *et al*, 2009b; Rhodes *et al*, 2011). For further information on cohesin's role in cancer development, please see discussion chapter 3.2.3.

A growing field of research in the recent past devoted itself to congenital cohesin defects, jointly called cohesinopathies. It is quite intuitive that cohesin mutations causing a marked loss of sister chromatid cohesion would not lead to viable progeny. Therefore, all known cohesinopathies are attributed to either mild cohesion defects or compromised non-canonical cohesin functions. The two main diseases classically referred to as cohesinopathies are Roberts and Cornelia de Lange syndrome. Roberts syndrome (RBS) is caused by mutations in ESCO2, one of the two acetyl transferases involved in cohesion establishment (Vega *et al*, 2005; Schüle *et al*, 2005; Gordillo *et al*, 2008). Symptoms of this

rare autosomal recessive cohesinopathy include pre- and postnatal growth retardation, craniofacial, upper limb and ophthalmologic abnormalities as well as mental retardation (Van Den Berg & Franke, 1993). The severity of symptoms varies widely, with the milder forms being typically referred to as SC phocomelia (Schüle *et al*, 2005). As has been shown in mice, loss of ESCO2 causes reduced cohesin acetylation and persistence on chromosomes, which leads to cohesion-loss at pericentromeric DNA (Whelan *et al*, 2011). In accordance with these results, chromosomes of RBS patients display a so-called heterochromatin repulsion phenotype, consistent with partial loss of sister chromatid cohesion (Tomkins *et al*, 1979; Van Den Berg & Franke, 1993). Cornelia de Lange syndrome (CdLS) has been described as a heterogenous multisystem developmental disorder. As with RBS, the severity-spectrum of symptoms is wide; patients typically display craniofacial and upper limb deformities, which are, however, distinct from those associated with RBS and/or observed in a smaller number of cases (Kline *et al*, 2007). Ophthalmological abnormalities, hirsutism and mental retardation are additional common symptoms of CdLS. According to a recent study, over 80% of subjects also exhibit mild to severe autism traits (Srivastava *et al*, 2014). CdLS is inherited dominantly and its prevalence is estimated at 1:10,000 (Kline *et al*, 2007). Gene mutations of multiple cohesin regulators or subunits have been associated with CdLS including the cohesin loader Scc2 (in humans NIPBL; cause in over 50% of cases), the integral cohesin subunits Smc1, Smc3 and Scc1, as well as the cohesin deacetylase HDAC8 (Krantz *et al*, 2004; Deardorff *et al*, 2007; 2012b; 2012a). The disease is most probably a result of transcriptional dysregulation caused by impaired cohesin dynamics and localization on DNA as suggested by data from yeast, zebrafish, mice and humans (Liu *et al*, 2009b; Deardorff *et al*, 2012a; Zuin *et al*, 2014; Lindgren *et al*, 2014). NIPBL might have an additional cohesin-independent role in the generation of CdLS: The kollerin component has been demonstrated to affect gene regulation, which might be explained by its ability to influence chromosome organization (see chapter 1.4.7; Zuin *et al*, 2014; Lopez-Serra *et al*, 2014).

1.5 Centrosomes

Centrosomes as the poles of the mitotic spindle have already been identified at the dawn of modern light microscopy in the late 19th century by pioneering work from van Beneden, Boveri and others. But it was not until in the last decades, that we have come to a deeper understanding of their substructural and molecular composition. Centrosomes are the

main microtubule-organizing center (MTOC) in most eukaryotic organisms (notable exceptions are fungi and higher land plants; Marshall, 2009). That means that they are the principal *de novo* nucleation point for microtubules, the predominant structural component of the mitotic spindle (Wittmann *et al*, 2001; for details on microtubules and the mitotic spindle, see chapter 1.3.2). In addition, they assume essential roles in maintaining the integrity of the cell and serving as an anchor for motor proteins, thereby ensuring cellular dynamics (Desai & Mitchison, 1997).

In humans (and many other metazoans), the centrosome consists of two cylindrical protein structures called centrioles, which are arranged in an orthogonal fashion (Fu *et al*, 2015; Figure 6 A). Centrioles themselves are highly symmetrical assemblies: nine radial spokes emanate from a ring-shaped central hub and attach the latter via "pinhead" structures to individual triplets of microtubules (Figure 6 B). Interlinking these triplets via protein fibers completes the so-called "cartwheel" structure. While the basic assemblies of both centrioles of a centrosome are identical, they are not equal with respect to associated structures; The older of the two centrioles, the "mother" (see chapter 1.5.1) recruits an electron-dense array of proteins, referred to as distal and subdistal appendages (Figure 6 A). Moreover, it recruits the pericentriolar matrix (PCM), which includes many factors essential for proper centrosome function. The PCM was originally believed to be an amorphous network of proteins, but recent advances in the three-dimensional structured illumination microscopy (3D-SIM) technique have allowed a more detailed assessment of its composition (Fu & Glover, 2012; Sonnen *et al*, 2012; Lawo *et al*, 2012; Mennella *et al*,

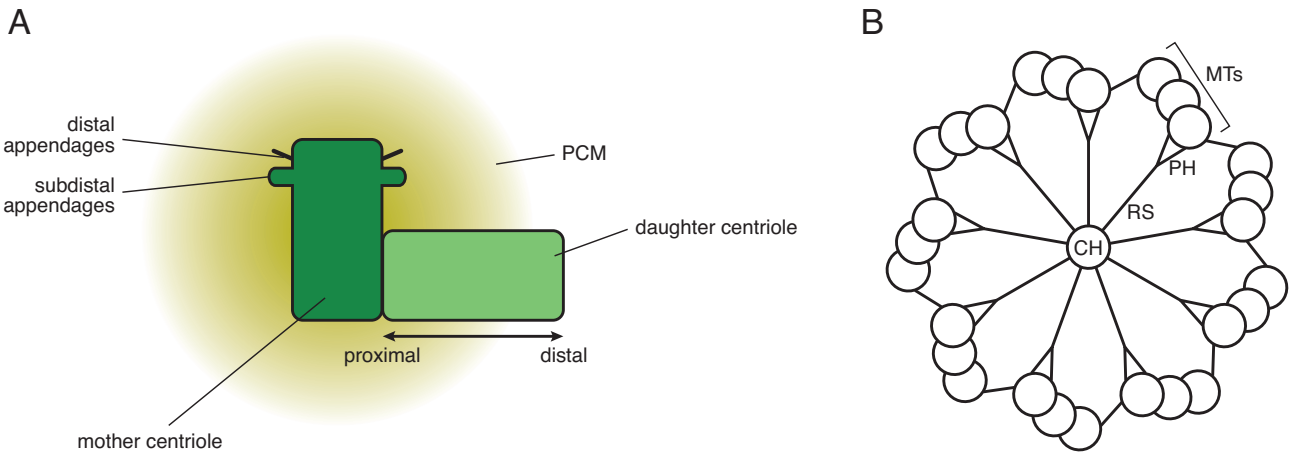

Figure 6 | **The centrosome. (A)** Cartoon depicting a centrosome, consisting of two centrioles (the older "mother" and the younger "daughter") arranged to each other in an orthogonal fashion. The mother centriole associates with additional proteins forming the distal and sub-distal appendages as well as the pericentriolar matrix (PCM), which contains many proteins important for centrosome function. **(B)** Cross-section of a centriole shows its radial "wheelbarrow" structure. CH: central hub, RS: radial spoke, PH: pinhead, MTs: mictrotubules arranged in triplets. For more details see text.

2012). These studies revealed that the proteins of the PCM are, in fact, recruited in a highly ordered fashion, forming distinct layers around the mother centriole. More importantly, the PCM recruits γ-tubulin, an integral component of the γ-tubulin ring complex (γ-TuRC), which acts as the principal assembly platform for microtubules (Moritz *et al*, 1995; Zheng *et al*, 1995).

Another important function of the centrosome is the assembly of cilia. Cilia are long structures protruding from the cell body and consist of a highly organized array of microtubules surrounded by the cell membrane (reviewed in Ishikawa & Marshall, 2011). They can either be motile (then also called flagella; e.g. in spermatocytes) or immotile (then also called primary cilia). Cilia can be found in many human cell types and assume a variety of functions like secreting and directing the flow of mucus and other bodily fluids or as mechanical or biochemical sensors. Their are typically assembled in G1 or G0 phase (quiescent cells) of the cell cycle as an extension of the mother centriole (the centrosome is then called a basal body). Because of cilia's pleiotropic functions, disorders associated with ciliogenesis or cilia function (so-called ciliopathies) have a wide range of phenotypes disrupting proper function of various organs including retinas, kidneys and the respiratory system (reviewed in Bettencourt-Dias *et al*, 2011).

1.5.1 The centrosome cycle and its coordination with the chromosome cycle

After cytokinesis, each daughter cell has inherited one centrosome (consisting of two centrioles) from the mother (Figure 7). In the following S phase, each centriole nucleates a daughter centriole (centrosome duplication; the two older centrioles are called mother centrioles; sometimes the original mother is referred to as grandmother; Robbins *et al*, 1968; Kuriyama & Borisy, 1981). In G2 phase, the new daughter centrioles elongate to full size before the former daughter matures to become a PCM-assembly-proficient mother at the following G2-M transition. At the beginning of mitosis, the centrosomes split and wander to opposite poles of the cell, nucleating microtubules and eventually forming the mitotic spindle. Shortly after sister chromatid separation at the metaphase-to-anaphase transition, the tight association between mother and daughter centrioles of a centrosome ("engagement") is lost and they remain only loosely tethered by proteinaceous fibers (Kuriyama & Borisy, 1981; Mayor *et al*, 2000; Bahe *et al*, 2005; Graser *et al*, 2007; He *et al*, 2013; Fang *et al*, 2014). This centriole disengagement serves as an essential licensing

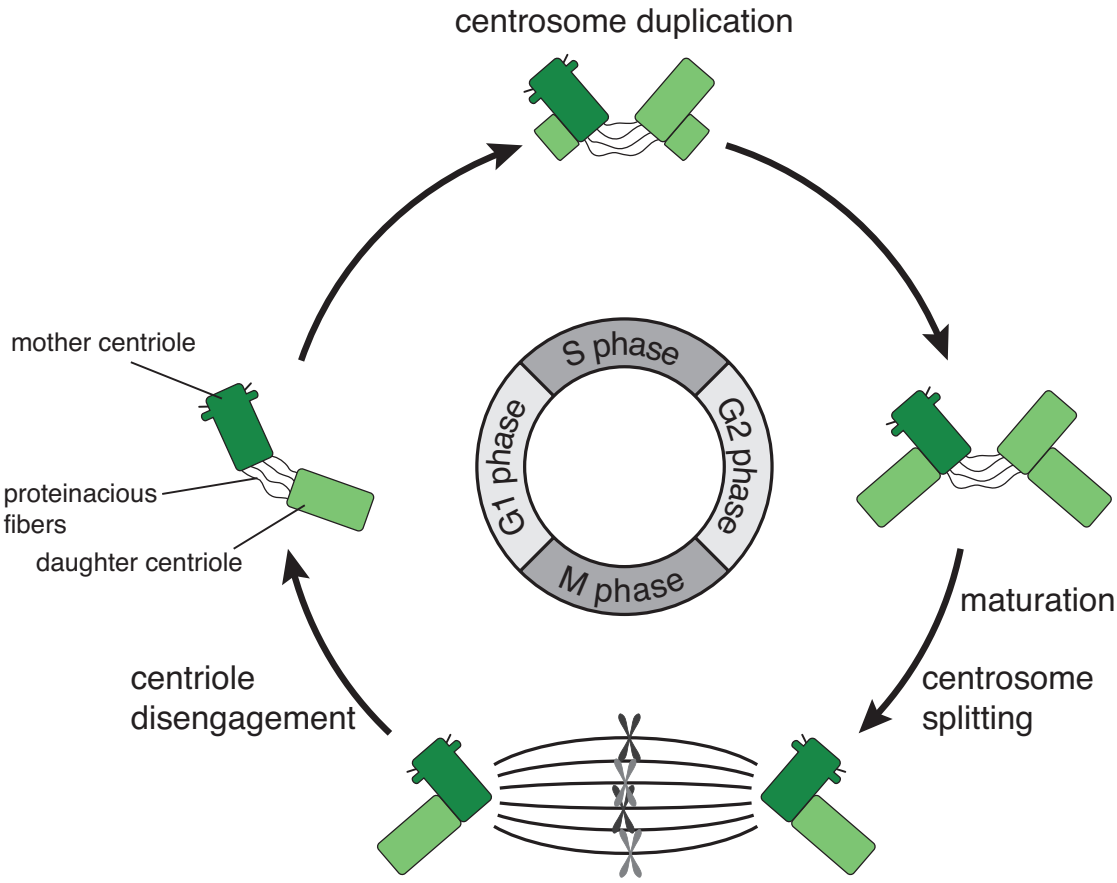

Figure 7 | **The centrosome cycle.** Loosely associated centrioles are duplicated in S phase. The two centrosomes are split to allow for spindle formation when the cells enter mitosis. Shortly after sister chromatid separation, the rigid conformation between the two centrioles of a centrosome is lost, which is an essential prerequisite for centrosome duplication in the following S phase. The centrioles disengage but still remain loosely tethered by proteinacious fibers. Please note that the PCM has been omitted for clarity. For more details see text.

step for centrosome duplication in the following S phase (Tsou & Stearns, 2006; Wang *et al*, 2011).

Intuitively, chromo- and centrosome cycles have to be coordinated at least during mitosis to allow proper spindle formation and chromosome bi-orientation. And in fact, mounting evidence proves the existence of such co-regulation across the cell cycle. So has it been shown that the quintessential S phase kinase Cdk2 is not only required for proper DNA replication (see chapter 1.2.4) but also centrosome duplication (Hinchcliffe *et al*, 1999; Lacey *et al*, 1999; Matsumoto *et al*, 1999; Meraldi *et al*, 1999). Even more strikingly, many pre-RC components including ORC and MCM subunits as well as geminin (see chapters 1.2.1 and 1.2.4), localize at centrosomes to mediate their proper duplication (Prasanth *et al*, 2004; Tachibana *et al*, 2005; Ferguson & Maller, 2008; Hemerly *et al*, 2009; Lu *et al*, 2009). In mitosis, one of the most important factors for the regulation of both chromosome and centrosome cycles is the kinase Plk1 (Polo-like kinase 1). At the

G2-M transition, Plk1-dependent phosphorylation of various early PCM components leads to massive recruitment of additional proteins causing the PCMs of each centrosome to drastically increase in size (Dobbelaere *et al*, 2008; Haren *et al*, 2009; Zhang *et al*, 2009; Lee & Rhee, 2011; Fu & Glover, 2012). This process, referred to as centrosome maturation, is integral for the organelle's proficiency to nucleate spindle microtubules. In early mitosis, Plk1 activity upstream of the Nek2 kinase leads to the phosphorylation of the proteinaceous fibers coordinating the two centrosomes, ultimately causing their dissolution and subsequent centrosome disjunction ("splitting"; Fry *et al*, 1998; Bahe *et al*, 2005; Mardin *et al*, 2011). At the same time on the chromosomal level, Plk1 assumes a role in DNA condensation (St-Pierre *et al*, 2009; Abe *et al*, 2011) and, as part of the prophase pathway, contributes to removal of cohesin complexes from chromosome arms (for details on the prophase pathway, see chapter 1.4.5). Activity of the kinase remains crucial after centrosome maturation, as it targets various spindle/centrosome components as well as centromeric/kintechore-associated proteins and thus helps to maintain spindle integrity and chromosome bi-orientation (Santamaria *et al*, 2011). As the most dramatic step of mitosis, the exquisite regulation of the metaphase-to-anaphase transition is of utmost importance (see also chapter 1.3.3). Only when both sister chromatids and centrosomes are perfectly bi-oriented, the mitotic checkpoint (the SAC) will allow resumption of mitosis, which is initiated by two major events: the separation of sister chromatids and the subsequent disengagement of centrioles. As outlined earlier, sister chromatid separation is brought about by separase-mediated cleavage of centromeric cohesin rings, but the processes leading to centriole disengagement are far less well understood. In recent years, however, increasing evidence has been put forth that suggests that cohesin not only localizes to centrosomes but is even required for proper spindle assembly (Gregson *et al*, 2001; Guan *et al*, 2008; Wong & Blobel, 2008; Kong *et al*, 2009; Giménez-Abián *et al*, 2010). Furthermore, it was shown that, in addition to sister chromatid separation, centriole disengagement is also triggered by separase activity (Tsou & Stearns, 2006; Tsou *et al*, 2009; Nakamura *et al*, 2009). As separase's canonical substrate is cohesin, these results already strongly implied a role for the ring complex in centriole engagement. The dual use of the chromatid separation machinery would also pose a very elegant mechanism for the co-regulation of chromo- and centrosome cycles in anaphase. A first hint towards a role for cohesin in centriole engagement was published in 2005, when Losada and coworkers showed that one of the dominant mitotic phenotypes of Scc1-depletion in HeLa cells was the generation of multipolar spindles (Losada *et al*, 2005). This

result could be further confirmed by various groups (Nakamura *et al*, 2009; Diaz-Martinez *et al*, 2010; Beauchene *et al*, 2010). Finally, our group provided unequivocal proof that human cohesin is not only necessary for proper association of centrioles, but furthermore that cleavage of its Scc1 subunit by separase is sufficient to trigger centriole disengagement in anaphase (Schöckel *et al*, 2011). Extending the parallels between the two cycles, Sgo1 seemed to also protect centrosomal cohesin from the prophase pathway as its depletion caused premature centriole disengagement in addition to sister chromatid separation (for further details on Sgo1, see chapter 1.6).

1.5.2 Centrosomes in human disease

In addition to ciliopathies (see above), centrosome anomalies can be found in a number of diseases. So have some severe brain development disorders been linked to mutations in genes associated with centrosome function (Bettencourt-Dias *et al*, 2011). Defects in neuronal migration, for example, often arise from failure to develop and maintain a proper microtubule cytoskeleton (Friocourt *et al*, 2011). These patients suffer from lissencephaly (also agyria-pachygyria), which is caused by mutations in genes of microtubule components such as *TUBA1A* (α-tubulin gene) or in those of microtubule- and centrosome-associated proteins such as *LIS1*, respectively. Primary microcephaly (autosomal recessive primary microcephaly; MCPH) is another neuronal disease, in which all known causative mutations affect proteins associated with centrosome function, including CENPJ (human SAS-4 ortholog required for centriole assembly in S phase) and CDK5RAP2 (human Cep215 ortholog required for tethering centrosomes until centrosome splitting in early M phase; Thornton & Woods, 2009). Lately, CDK5RAP2 has been found to also function in centriole engagement (Barrera *et al*, 2010; Pagan *et al*, 2015), strongly suggesting a link between the disfunction of centriole engagement and the development of neuronal diseases. This notion is further endorsed by the discovery that mutations in the PCM component pericentrin (PCNT; also kendrin), which have been associated with microcephalic dwarfism (microcephalic osteodysplastic primordial dwarfism type II; MOPD II) in the past, are also implicated with defective centriole engagement (Rauch *et al*, 2008; Matsuo *et al*, 2012; Lee & Rhee, 2012; Pagan *et al*, 2015).

Aside from neuronal disorders, disregulation of the centrosome cycle might also play a role for the development of cancer, as structural and numerical centrosome aberrations can be found in many different human tumors (Nigg, 2002). Whether these

centrosome abnormalities are a cause for or merely a product of tumorigenesis, is still under debate but failure to properly coordinate centrosome and chromosome cycles is easily conceivable to cause abnormal centrosome numbers, ultimately resulting in mitotic catastrophe, which can be a hallmark of cancer (see also discussion chapter 3.3.4).

1.6 Shugoshin, the protector of cohesin

Shugoshins (Sgo; japanese for "guardian spirit") are essential proteins for proper meiotic and mitotic function. As already outlined in chapter 1.4.5, Sgo1's mitotic role is to protect centromeric cohesin from prophase pathway signaling, rendering sister chromatid separation completely dependent on separase-mediated proteolysis of Scc1. However, recent findings suggest that Sgo's role extends to the centrosome, as it seems to also have a function in protecting centriole engagement (see chapter 1.6.1). The dual use of cohesin as well as its regulation machinery poses an attractive mechanism for the co-regulation of chromo- and centrosome cycles.

Shugoshin was originally described as the gene product affected in the meiotic *mei-S332* mutant of *Drosophila melanogaster*, which exhibited precocious sister chromatid separation as its most prominent phenotype (Davis, 1971). Initially, Mei-S332 was believed to have a more direct role in holding sister chromatids together, since it was shown to associate with kinetochores up until sister chromatid separation (Kerrebrock *et al*, 1995). Since in the following years, the actual physical link between sister chromatids was identified to be cohesin (see chapter 1.4), a new role for shugoshin as a general protector of chromatid cohesion was proposed (Kitajima *et al*, 2004; Rabitsch *et al*, 2004). Today, shugoshin orthologs have been found in most eukaryotic model organisms, including humans (reviewed in Marston, 2015). With the exception of *Drosophila* and budding yeast, all investigated organisms possess two shugoshin paralogs. In humans, Sgo1 assumes the role of the mitotic protector of sister chromatid cohesion, while Sgo2 is its meiotic counterpart (Salic *et al*, 2004; Tang *et al*, 2004; Kitajima *et al*, 2005; McGuinness *et al*, 2005; Lee *et al*, 2008).

1.6.1 Sgo1 function during mitosis

As I have already established (above and chapter 1.4.5), Sgo1 function is required to locally counteract the prophase pathway and thereby maintain a centromeric cohesin

population, which ensures sister chromatid cohesion until metaphase (Katis *et al*, 2004; Kitajima *et al*, 2005; McGuinness *et al*, 2005). Sgo1's recruitment to the centromere depends on the kinetochore-associated kinase Bub1 (Kitajima *et al*, 2004; Tang *et al*, 2004; Kitajima *et al*, 2005). For this, Bub1 phosphorylates centromeric histone 2 A (H2A) at serine 120, which allows recruitment of Sgo1 to the kinetochore via direct association with Sgo1's C-terminal C-box (for Sgo1's domain structure see Figure 8; Kawashima *et al*, 2010). However, according to recent findings, Bub1-dependent Sgo1-recruitment only serves as an initial step, after which Sgo1 is handed over to cohesin at the inner centromere, with which it associates depending on phosphorylation of Sgo1 at threonine 346 by Cdk1 (Liu *et al*, 2013b). In accordance with this result, inactivation of Bub1 does not abrogate Sgo1 function but causes the protein to spread to chromosome arms due to its association with cohesin (see also discussion chapter 3.3.1).

As first direct evidence supporting Sgo1 as a counteractor of the prophase pathway, it was shown that a phosphorylation site mutant of SA2 (whose phosphorylation by Plk1 is essential for prophase pathway signaling; see also chapter 1.4.5) rendered human cells immune to RNAi-mediated Sgo1 depletion (McGuinness *et al*, 2005). Since shugoshins do not have an inherent phosphatase activity, this function must ultimately be exerted by a different protein. And indeed, Sgo1 was soon shown to recruit protein phosphatase 2 A (PP2A), and furthermore, that this Sgo1-PP2A complex is the actual effector of SA2 dephosphorylation (Kitajima *et al*, 2006; Riedel *et al*, 2006; Xu *et al*, 2009). Recently, sororin was identified as a second target of Sgo1-PP2A (Liu *et al*, 2013b); counteracting Cdk1-dependent sororin-phosphorylation maintains its association with cohesin, which competitively inhibits Wapl-mediated cohesin destabilization during early mitosis (for details see chapter 1.4.5). Structural investigation of an SA2-Scc1 subcomplex of cohesin has revealed yet another, more direct mode of cohesin protection by Sgo1, as the data suggests that Sgo1 is able to physically shield cohesin from association with Wapl (Hara *et al*, 2014).

Apart from its canonical role, Sgo1 is also required to promote proper chromosome bi-orientation in mitosis (Indjeian *et al*, 2005). As already outlined in chapter 1.3.2, one of the key players in the correction of erroneous kinetochore-microtubule attachments is the CPC. While in budding yeast, shugoshin is merely required to maintain pericentromeric CPC levels (Verzijlbergen *et al*, 2014; Peplowska *et al*, 2014; Nerusheva *et al*, 2014), it is essential for CPC's initial recruitment in fission yeast and humans (Kawashima *et al*, 2007; Vanoosthuyse *et al*, 2007; Tsukahara *et al*, 2010). Proper chromosome-spindle

attachments are stabilized when pulling forces ("tension") physically separate Aurora B/ CPC from its targets at the outer kinetochore (Liu *et al*, 2009a; Welburn *et al*, 2010). Yeast might employ an additional mechanism to switch off the error correction machinery: Sgo1 is redistributed to the outer kinetochore in response to kinetochore tension, which causes loss of CPC from the inner centromere (Peplowska *et al*, 2014; Nerusheva *et al*, 2014). While Sgo1 redistribution can also be observed in humans cells (Liu *et al*, 2013a), the CPC does not relocalize until the metaphase-to-anaphase transition (Ruchaud *et al*, 2007). Recent data also suggest a function for Sgo1 at the centrosome as Sgo1-depletion causes premature centriole disengagement (Wang *et al*, 2008; Schöckel *et al*, 2011). Due to cohesin's role in centriole engagement (see chapter 1.5.1), it seems quite intuitive to assume conservation of Sgo1 as a protector of cohesin at the centrosome, but this has never been proven directly.

1.6.2 Sgo1's domain structure and splice variants

The canonical Sgo1 peptide sequence contains two evolutionarily well conserved regions: the N-terminal coiled coil domain and the C-terminal C-box (see Figure 8). As mentioned in the previous chapter, The C-box is required for Sgo1's recruitment to the centromere by directly associating with phosphorylated H2A. The functionally essential recruitment of PP2A is mediated through the N-terminal coiled coil domain. (Tang *et al*, 2006; Xu *et al*, 2009).

The human *SGO1* gene transcript is subject to extensive alternative splicing. According to the Ensembl database (Ensembl number: ENSG00000129810), 13 different mature *SGO1* transcripts exist, which code for seven different proteins. Five of these transcripts, coding for three different proteins (the so-called "B" isoforms), are believed to be the product of aberrant splicing as their products are associated with tumorigenesis (further discussed in chapter 3.3.4). The remaining transcripts and associated proteins are classified into two main categories, depending on their status regarding exon 6: transcripts, which have this exon spliced in, are named "A" and those that lack exon 6 are called "C". For further sub-characterization, the exon 9 status is considered: exon 9-lacking transcripts are referred to as "2" and those including it, are called "1". So in summary, the remaining transcripts code for four different proteins: Sgo1 A1, A2, C1 and C2 (Figure 8). The canonical centromere-associated cohesin-protecting Sgo1 is Sgo1 A1, which contains the peptide encoded by exon 6 but lacks the one encoded by exon 9. The

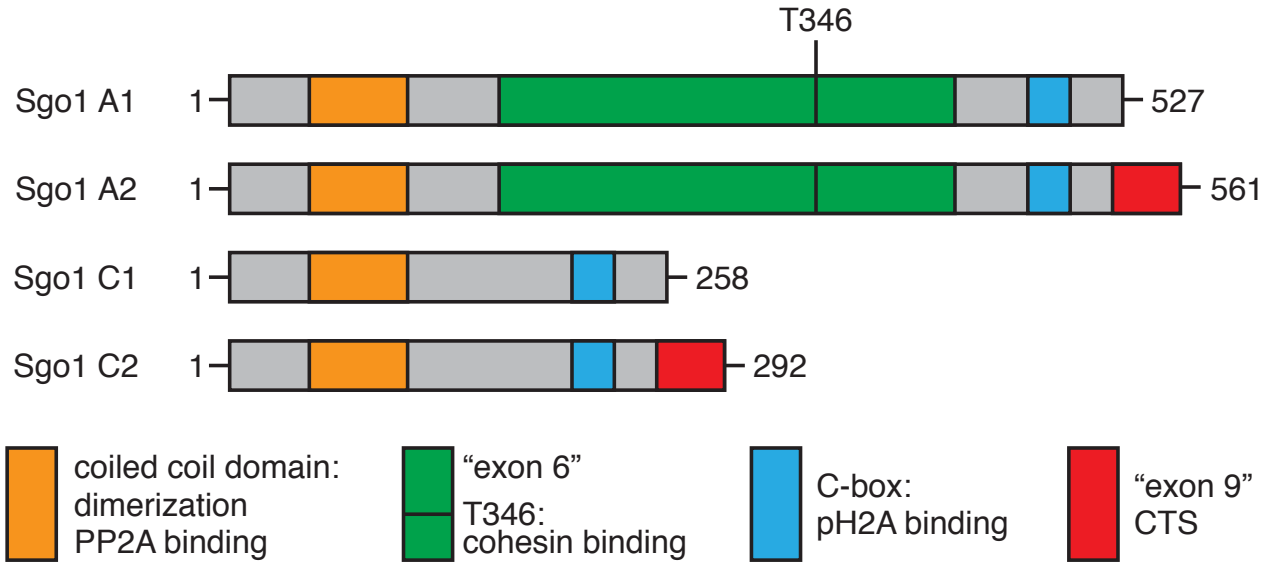

Figure 8 | **Sgo1 splice variants.** Comparison between the main Sgo1 splice variants Sgo1 A1, A2, C1 and C2. Shown are Sgo1's coiled coil domain, which is required for binding of PP2A, as well as its C-box, which facilitates Sgo1 recruitment to the outer kinetochore via association with phosphorylated histone 2 A (pH2A). In addition, the relative size and position of the peptides encoded by exon 6 and exon 9 are depicted. The exon 6-encoded region contains threonine 346 (T346), whose phosphorylation is required for proper binding of Sgo1 to cohesin.

functional role of the other isoforms, however, is far less clear. But fact is that all of them include coiled coil domains and C-box regions, suggesting that they should be able to form basic Sgo1 interactions like PP2A-recruitment and docking to phosphorylated H2A. Importantly, however, only variants including the peptide encoded by exon 6 contain threonine 346, which has been linked to direct association of Sgo1 with cohesin (see chapter 1.6.1 and discussion chapter 3.3.1).

1.7 Aims of this study

1.7.1 Cohesin dynamics in mitosis

The cohesin complex performs a myriad of functions in the eukaryotic cell cycle, which require it to be either stably bound to DNA (e.g. sister chromatid cohesion) or highly dynamic (presumably for most non-canonical functions). In fact, it is widely believed that pools of variable dynamics exist at the same time, the most prominent example probably being the rapid redistribution of cohesin molecules to DNA damage sites during G2 phase in which most of cohesin is stably bound to sister chromatids to keep them tightly cohesed (Ünal *et al*, 2004; Ström *et al*, 2004). Thus, cohesin dynamics, i.e. cohesin loading onto and release from DNA, must be highly regulated in space and time. One of the most

dramatic shifts in cohesin-DNA interaction can be observed in mitosis. Centromeric cohesin must be removed from chromosomes to allow for sister chromatid separation at the metaphase-to-anaphase transition by separase-dependent proteolytic cleavage of cohesin's Scc1 subunit. In vertebrates, however, the bulk of ring molecules leaves chromosome arms already in prophase by a non-proteolytic mechanism, allowing them to be reloaded onto chromatin in the following telophase (Waizenegger *et al*, 2000). How this so-called prophase pathway accomplishes removal of a ring complex embracing its target without proteolytic cleavage has long remained a mystery. To allow DNA to exit the cohesin ring, its removal in prophase should require the ring to open up at (at least) one of its three subunit interaction sites, called "gates", either between Smc3 and Scc1, Scc1 and Smc1, or Smc1 and Smc3 (the hinge). In this study I sought to investigate, whether this theory is valid and if so, which of the three possible gates has to open to let DNA exit the ring structure. I furthermore wanted to address, how cohesin is loaded onto DNA in human telophase. The fact that cohesin's initial loading is already topological (Murayama & Uhlmann, 2014), implies the necessity for gate opening and a study from yeast suggested that opening of the hinge gate situated between Smc1 and Smc3 is required for proper ring loading (Gruber *et al*, 2006). Whether this DNA entry gate is conserved between yeast and human has so far never been clarified.

In order to study the dynamics of cohesin gates, I planned to employ the FRB/FKBP system (Paulmurugan & Gambhir, 2005), which had already been used in a similar context (Gruber *et al*, 2006). FRB (FKBP-rapamycin binding domain of mTOR) and FKBP (FK506 binding protein) are small 11-12 kDa proteins that can be fused to a protein of interest. These two proteins have a very low affinity to each other until the small molecule rapamycin (also FK506) is added (Banaszynski *et al*, 2005). Rapamycin binds to both proteins with opposite surfaces and allows the formation of a very stable ternary complex ($K_D \approx 12$ nM), in which rapamycin is sandwiched between FRB and FKBP (Choi *et al*, 1996; Liang *et al*, 1999; Banaszynski *et al*, 2005). To put the FRB/FKBP system to my advantage, I sought to generate fusion proteins consisting of the integral ring components of cohesin fused to either FRB or FKBP (as exemplified in Figure 11). Addition of rapamycin ought to act as a conditional trigger for ternary complex formation, preventing any cell cycle-regulated dissociation of the two cohesin subunits in question. To study the three gates individually, the gene sequences of pairs of cohesin subunits, each constituting one gate, were to be manipulated accordingly and stably integrated into the genome of a human host cell line (for more details on the method, see chapters 2.1.2, 2.1.3 and

materials and methods). The resulting three human cell lines (each representing one cohesin gate) would then be used in a series of experiments designed to determine, (1) whether the generated fusion proteins are still functional (i.e. proficient in functional cohesin ring assembly), (2) which of the three gates is cohesin's DNA exit gate during prophase and (3) which gate constitutes the ring's entry gate during cohesin loading in telophase.

1.7.2 Cohesin dynamics in S phase

The size of a human replicon far exceeds the average distance between cohesin associated regions (Jackson & Pombo, 1998; Parelho *et al*, 2008; Wendt *et al*, 2008). Together with the fact that cohesin is topologically loaded before S phase (Murayama & Uhlmann, 2014), this introduces a fundamental caveat: how can the replisome bypass cohesin rings while simultaneously depositing the nascent DNA strand inside its lumen? There are three basic mechanisms conceivable: (1) the cohesin ring is removed from DNA and reloaded after the replisome has passed, (2) the replisome passes through the closed ring or (3) the replisome surpasses the closed ring by a different mechanism, which would pose the problem of how the newly synthesized DNA strand ends up inside the ring complex. While there has been extensive research on the topic in recent years, this issue still remains elusive. Capitalizing on the aforementioned doubly stable FRB/FKBP-tagged cohesin subunit cell lines, allowing me to artificially and conditionally close each individual cohesin gate, I sought to investigate, whether dynamics at certain gates are required for proper replication fork progression, and therefore, whether the cohesin ring must dissociate from DNA for replisome bypass. To analyze the processivity of single replication forks, I planned to establish a method, which combines labeling of nascent DNA strands with nucleotide analogs with their subsequent stretching onto a glass surface (Jackson & Pombo, 1998; Terret *et al*, 2009). Immunofluorescence microscopy was then to be used to determine the progression of single replication forks in a given time frame.

1.7.3 Cohesin dynamics at the centrosome and their regulation by Sgo1 splice variants

To allow for proper chromosome bi-orientation in mitosis, it is imperative to coordinate chromosomal and centrosomal events. This coordination is at least partly achieved by the

dual use of cohesin to maintain sister chromatid cohesion as well as centriole engagement until late mitosis. It is quite intuitive to assume that the complex's regulatory framework is also subject to this dual use, and indeed, we and other groups have found that Sgo1 plays a role in protecting centrosomes from premature centriole disengagement in human cells (Wang *et al*, 2006; 2008; Schöckel *et al*, 2011; Yamada *et al*, 2012). Its RNAi-mediated depletion not only causes sister chromatids to separate, but also centrioles to disengage prematurely. While this circumstantial evidence indicates that the prophase pathway might target centrosomal cohesin as well as centromeric, this has never been proven formally. Surprisingly, it was suggested that not the canonical shugoshin (Sgo1 A1), but an alternative splice variant, Sgo1 C2 (also called "sSgo1"), specifically localizes to and functions at the centrosome (Wang *et al*, 2006; 2008). In contrast to Sgo1 A1, C2 lacks the peptide encoded by exon 6 but features the one encoded by exon 9. Which of these two deviations constitutes the molecular determinant of C2's reprogramming remains unclear. In collaboration with my colleague Lisa Mohr, I set out to re-evaluate these findings and extend the analysis to the other relevant shugoshin splice variants, Sgo1 A2 and C1. The genes of these four proteins represent all possible exon 6/exon 9 combinations and, thus, comparing the data gained on their products should clarify, which associated peptide reprograms shugoshin to act as a protector of centriole engagement. Moreover, exploiting the aforementioned stable cell lines allowing conditional cohesin gate closure once again, we sought to determine directly, whether Sgo1's role at the centrosome is conserved, i.e. whether it protects centrosomal cohesin molecules from prophase pathway signaling by recruitment of PP2A.

2. Results

2.1 Cohesin dynamics in mitosis

2.1.1 Establishing experimental setups for the investigation of cohesin dynamics in mitosis

To understand the importance of the prophase pathway for mitotic cohesin localization and, by extension, dynamics, I established a method which allows visualization of chromatin-bound cohesin via immunofluorescence microscopy. Therefore, (control-siRNA-transfected; see below) HeLa L cells were grown on cover slips and ultimately pre-extracted with 0.1% Triton X-100, which penetrates cell and nuclear membranes and leads to extraction of soluble cyto- and nucleoplasmic (but not chromatin-bound) proteins. Thereafter, cells were fixed and (immuno-)stained for DNA (Hoechst 33342), Smc1 (cohesin subunit) and Hec1 (mitosis-specific kinetochore marker). During interphase, cohesin can always be found associated with DNA, but as soon as mitosis is initiated with prophase, an unperturbed prophase pathway removes almost all cohesin from chromatin, which eventually becomes reloaded in telophase (Figure 9 A). Please note that although residual centromeric cohesin cannot be visualized with this method, it remains protected from the prophase pathway, as failure to do so would cause spindle assembly checkpoint (SAC)-mediated mitotic arrest. By transfection of specific siRNAs targeting the mRNA of the essential prophase pathway component Wapl (or GL2/luciferase as a control in Figure 9 A), one can inactivate the pathway due to RNAi-mediated depletion of the protein. Without the prophase pathway, cohesin remains stably associated with chromatin until prometaphase, but is found absent in the following metaphase, most likely due to proteolytic degradation of the ring complex by the action of separase (Figure 9 B). The prophase pathway has no role in cohesin loading, since the complex is reloaded properly in the following telophase. This effect can be reproduced using a different method of prophase pathway-inactivation, namely chemical inhibition of Polo-like kinase 1 (Plk1) by the small molecule BI2536 ("BI"). Addition of BI to pre-synchronized cells shortly before mitosis phenocopies Wapl-depletion, as cohesin remains associated with DNA until prometaphase (Figure 9 C). Please note that Plk1 maintains various functions during the cell cycle and its inhibition leads to a prometaphase arrest among others, due to problems with spindle assembly (Santamaria *et al*, 2011; Paschal *et al*, 2012; Liu *et al*, 2012).

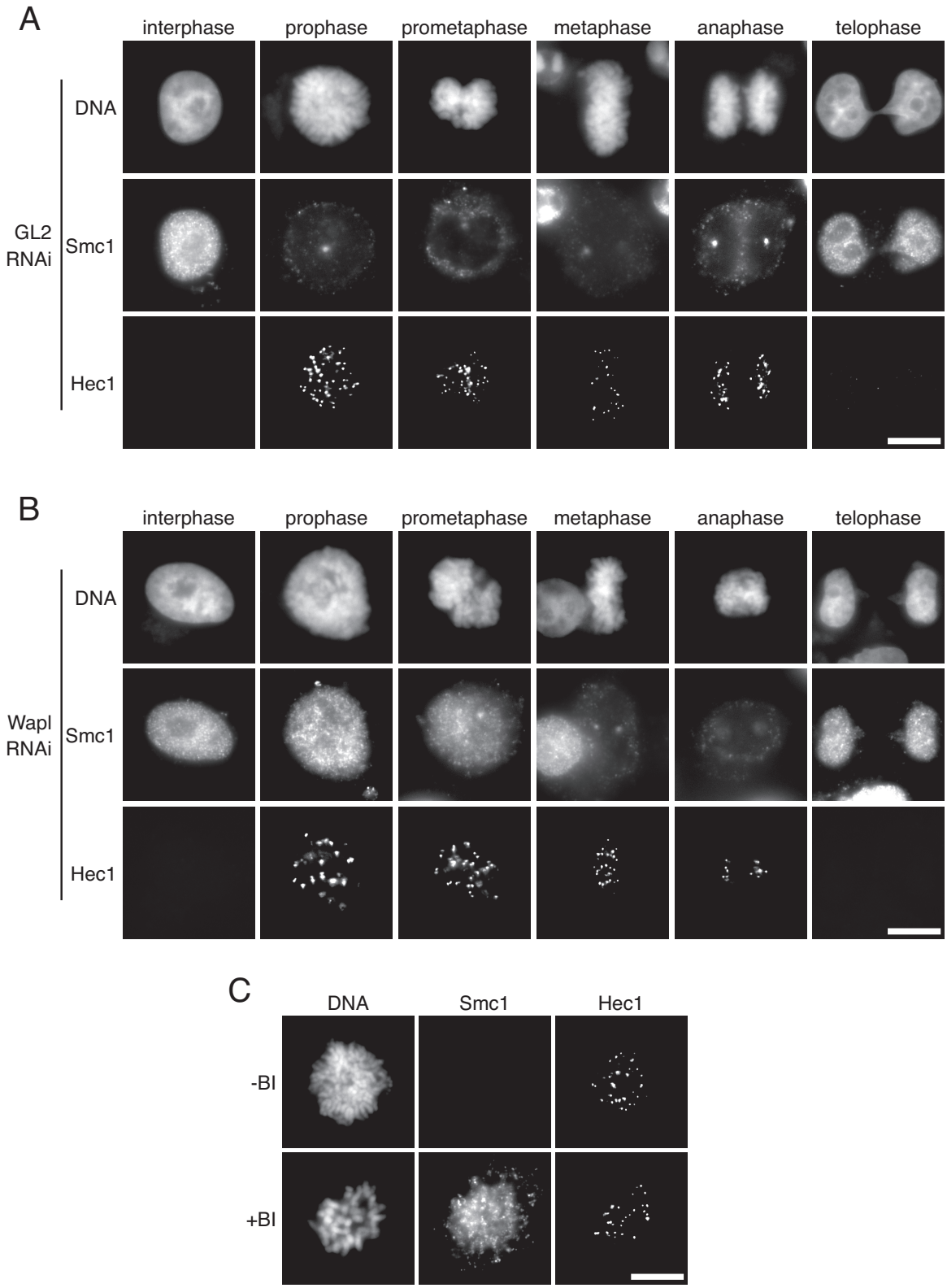

Figure 9 | **Displacement of cohesin from chromatin in early mitosis is dependent on the prophase pathway. (A, B)** The prophase pathway is dependent on Wapl. HeLa L cells were transfected with siRNA targeting the mRNAs of GL2 (luciferase, control; A) or Wapl (B). Two days later cells were pre-extracted and fixed, and their DNA (Hoechst 33342), Hec1 (mitosis-specific kinetochore marker) and Smc1 were (immuno-)stained for fluorescence microscopy. **(C)** The prophase pathway is dependent on Plk1. HeLa cells were synchronized at the G1/S boundary using thymidine. After 16 h they were released from the arrest. 3 h after release 200 nM of Plk1 inhibitor BI2536 ("BI") was added for additional 6 h before cells were pre-extracted and fixed for fluorescence microscopy as described for (A, B). Scale bars = 10 μm.

Cohesin's function is to hold sister chromatids together. Cohesin initially performs this function along the full chromosome axis until only centromeric cohesion is maintained after action of the prophase pathway. To visualize such chromosomes in more detail, I arrested HeLa L cells in prometaphase by the use of the spindle poison nocodazole, which causes depolymerization of microtubules triggering the SAC. Harvested cells were then swelled and fixed to allow spreading of their chromosomes onto a glass slide (see materials and methods). Chromosomes of control-siRNA (GL2/luciferase)-transfected prometaphase-arrested cells feature a typical "butterfly-like" morphology, each displaying four condensed chromosome arms and one centromeric constriction caused by residual cohesin. Disabling removal of arm-cohesin by Wapl RNAi leads to a "zipped" phenotype with condensed chromosomes displaying tight cohesion even at chromosome arms (Figure 10).

These experiments highlight the role of the prophase pathway for the removal of excess cohesin from chromosome arms during mitosis, which ensures typical mitotic chromosome morphology. More importantly for this study, *in situ* immunofluorescence microscopy and chromosome spreading can be utilized to adequately visualize the effects of the prophase pathway on chromosomes.

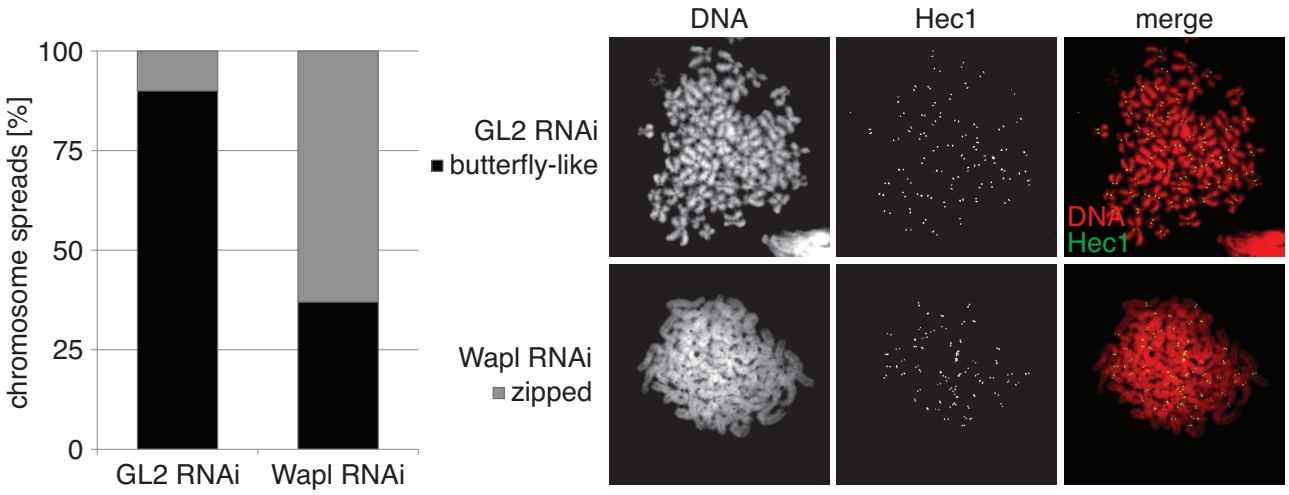

Figure 10 | Inactivation of the prophase pathway results in overcohesed chromosomes. Two days after transfection with *GL2* (luciferase, control) or *WAPL* siRNA, HeLa L cells were arrested in mitosis by treatment with nocodazole for 15 h before being subjected to chromosome spreading. The graph on the left shows the relative number of prometaphase cells with normal ("butterfly-like") or tightly cohesed ("zipped") chromosome morphology (each condition: n = 100) as exemplified on the right. Please note that the experiment on the right was performed differently to allow for additional immunofluorescence staining of the mitotic kinetochore marker Hec1: HeLa L cells were treated as described in Figure 9 A, B and then subjected to chromosome spreading compatible with immunofluorescence staining.

2.1.2 Utilizing the FRB/FKBP system to study cohesin dynamics on chromatin

The integral cohesin ring structure is comprised of the three proteins Scc1, Smc1 and Smc3. These cohesin subunits interact with each other at three positions on the ring, which are called "gates". Smc1 and Smc3 form long intramolecular coiled coils, so that the N- and C-terminal ends join to form a single head domain. The Smc1 and Smc3 head domains are bridged by the α-kleisin subunit Scc1, while the middle regions of the two proteins interact directly at the so called "hinge". As already explained in the introduction, we have various reasons to believe that in prophase, the bulk of cohesin is removed from chromosomes in a non-proteolytic manner. A caveat of this notion is that the ring must be opened at at least one of its three gates, in order to release the sister chromatids. I set out to test this hypothesis by conditionally locking always one gate at a time using the FRB/

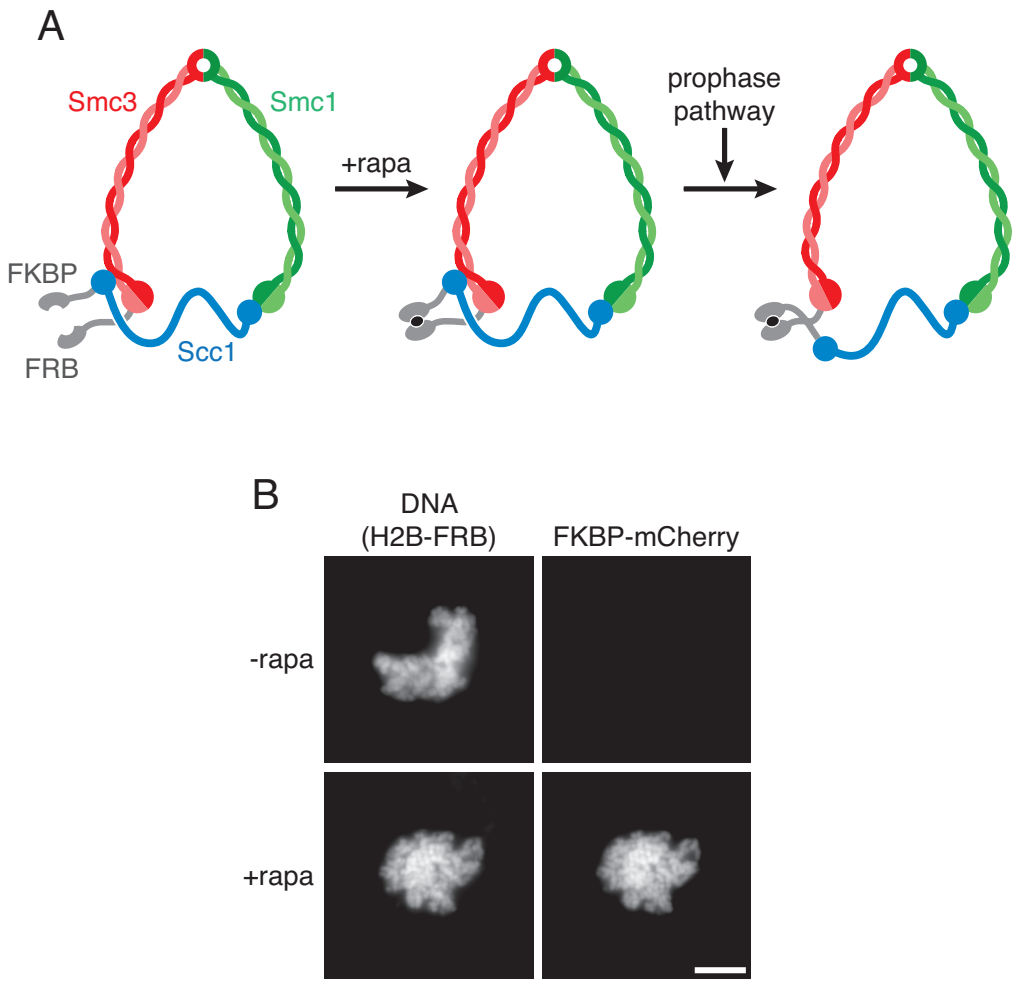

Figure 11 | **Rationale for this study and proof of principle for the FRB/FKBP system. (A)** Rationale for this study as exemplified by rapamycin-mediated locking of the gate constituted by Smc3 and Scc1. If this gate needs to be opened during prophase, cohesin release from chromatin, mediated by the prophase pathway, should be blocked when rapamycin had been added. **(B)** Rapamycin is able to heterodimerize FRB/FKBP-tagged proteins at human chromatin. HEK293T cells were co-transfected with histone 2B-FRB (H2B-FRB) and FKBP-mCherry and arrested in prometaphase in the presence or absence of rapamycin (+/- rapa). Chromatin was isolated, spun onto cover slips and fixed. Scale bar = 10 μm.

FKBP system (see chapter 1.7.1) and subsequently investigating whether shutting a particular gate (i.e. addition of rapamycin) would compromise the prophase pathway (Figure 11 A).

To initially test whether FRB and FKBP can be utilized to dimerize two unrelated proteins at human chromatin *in vivo*, I fused the former C-terminally to Histone 2B (H2B-FRB) and the latter N-terminally to mCherry (FKBP-mCherry). Cells transiently expressing these two fusion proteins were arrested in prometaphase by nocodazole addition and either in the presence or absence of rapamycin, which is supposed to induce heterodimerization. After harvesting, cells were lysed and their genomic DNA isolated and spun onto cover slips for eventual (immuno-)fluorescent staining of DNA (Hoechst 33342) and mCherry. H2B-FRB is incorporated into nucleosomes but FKBP-mCherry remains soluble and is therefore lost during the procedure as long as no rapamycin is present (Figure 11 B). When the small molecule was added, FRB and FKBP were forced to dimerize and, thus, mCherry could be found in the genomic DNA preparation, perfectly colocalizing with chromatin. Therefore, the FRB/FKBP system appears to be suitable to conditionally heterodimerize two proteins at human chromatin *in vivo*.

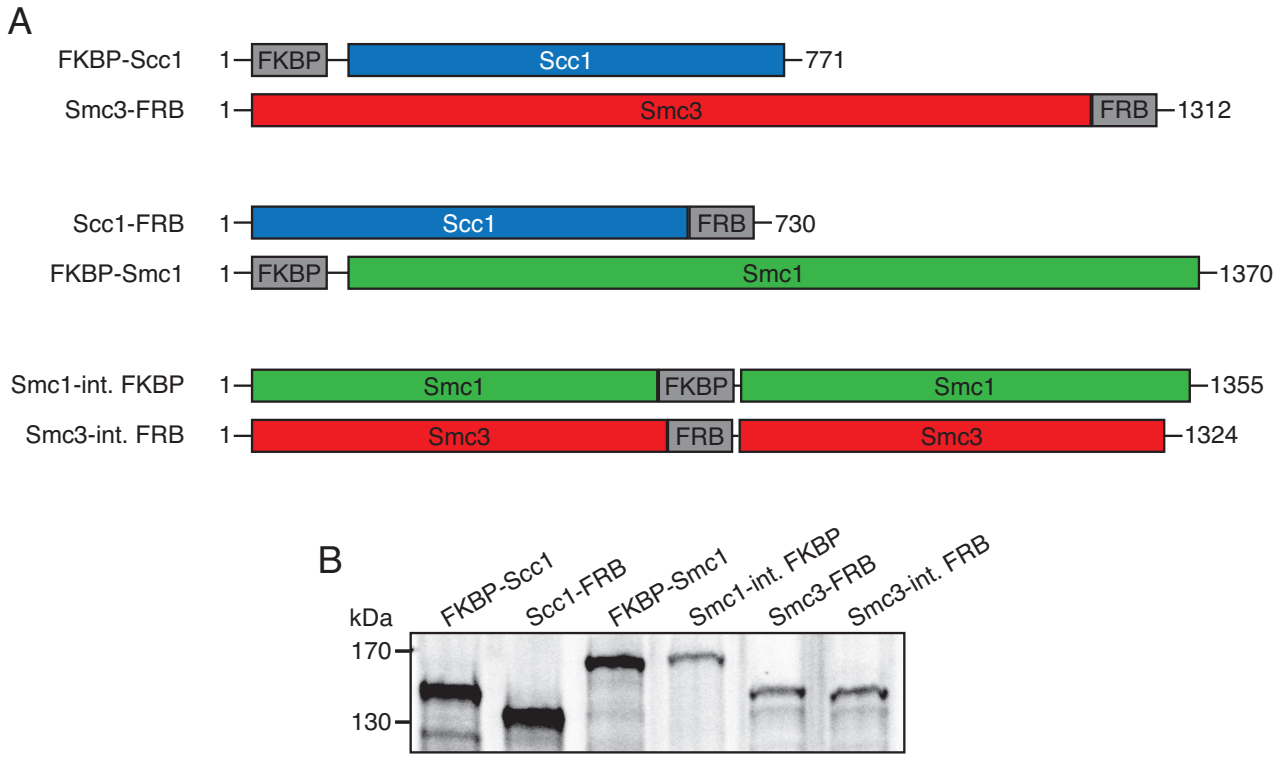

Figure 12 | **Generation of tailored cohesin subunits featuring individually lockable gates. (A)** Cartoon depicting matched pairs of FRB/FKBP-tagged cohesin subunits used in this study. The lines represent linker peptides of 9 (Smc1-internal (int.) FKBP, Smc3-int. FRB) or 29 amino acids (FKBP-Scc1, FKBP-Smc1). **(B)** *in vitro* transcription/translation (IVT/T) from the plasmid constructs bearing the reading frames of the tailored cohesin subunits.

In order to make all cohesin gates individually lockable, FRB/FKBP-tagged versions of Scc1, Smc1 and Smc3 had to be created. To this end, FRB was C-terminally fused to Scc1 and Smc3, and FKBP was N-terminally fused to Scc1 and Smc1. These measures should render the Smc3-Scc1 and the Smc1-Scc1 gates, respectively, lockable by rapamycin addition. In the case of the hinge gate, FRB and FKBP had to be placed into the open reading frames of Smc1 and Smc3, since their interaction surface is located inside the intramolecular coiled-coil (Figure 12 A). All of these plasmid constructs were verified by sequencing and can be successfully transcribed and translated into full-length proteins *in vitro* (Figure 12 B). Please note that for the following *in vivo* studies in human cells, RNAi-mediated depletion of the endogenous cohesin subunits was performed mostly using siRNAs directed against the 5'-untranslated regions (5'-UTRs) of their respective target mRNA. This makes the fusion constructs naturally resistant against those siRNAs, since different UTR regions are expressed from the respective plasmids. Due to poor data on its UTRs, I was unable to find a UTR-directed siRNA for the knockdown of endogenous Smc1. Consequently, an siRNA targeting Smc1's open reading frame was employed. In order to make the two FKBP-tagged Smc1-variants resistant against this siRNA, five silent point mutations were introduced into their gene sequences (therefore, the peptide sequence remained unaltered; for more details, see materials and methods). All further experiments were conducted using siRNA-resistant *SMC1*.

2.1.3 Creating doubly stable cell lines expressing matched pairs of FRB/FKBP-tagged cohesin subunits

Initial tests indicated that simultaneous transfection of two cohesin expression plasmids was not sufficiently efficient to create the required number of cells transiently expressing both transgenes in appreciable amounts. Consequently, I decided to create HEK293 cell lines, which stably, but conditionally, expressed always two FRB/FKBP-tagged cohesin subunits at a time. The method is based on the commercially available Flp-In T-REx system (Invitrogen/Life Technologies), which allows for the integration of one plasmid bearing a gene of interest as well as an FRT-sequence into a FLP-recombinase site in the host's genome. In order to stably integrate a second gene of interest into the host-DNA, a Cre-recombination site (loxP) was additionally inserted into the initial plasmid (carrying the first gene of interest), which can consequently be utilized for a second round of genomic integration of a plasmid by co-expressing Cre-recombinase. Both plasmids carry antibiotic

markers that allow selection and differentiation of singly and doubly stable cells. The target cell line additionally expresses the tetracycline (Tet-)repressor, which allows for tetra- or doxycycline-inducible expression of transgenes, if they are put under control of the Tet-operator sequence as was the case with our cohesin constructs. For more details on creating the doubly stable cell lines, please see the respective section in materials and methods and Figure 40.

The tailored cohesin constructs introduced in Figure 12 A were subcloned into plasmids suitable for stable integration into HEK293 Flp-In Tet-On (carrying a genomic FRT-site and expressing the Tet-repressor) cell lines. I was able to successfully conduct 3 × 2 rounds of genomic integration resulting in three cell lines, expressing FKBP-Scc1 and Smc3-FRB, Scc1-FRB and FKBP-Smc1, or Smc1-internal (int.) FKBP and Smc3-int. FRB in a doxycycline (dox)-inducible fashion, respectively (Figure 13 A). For most of the following experiments, I knocked down the endogenous cohesin subunits by siRNA-mediated RNAi for three days while adding doxycycline to induce the expression of the transgenic proteins. This should lead to sufficient replacement of endogenous cohesin

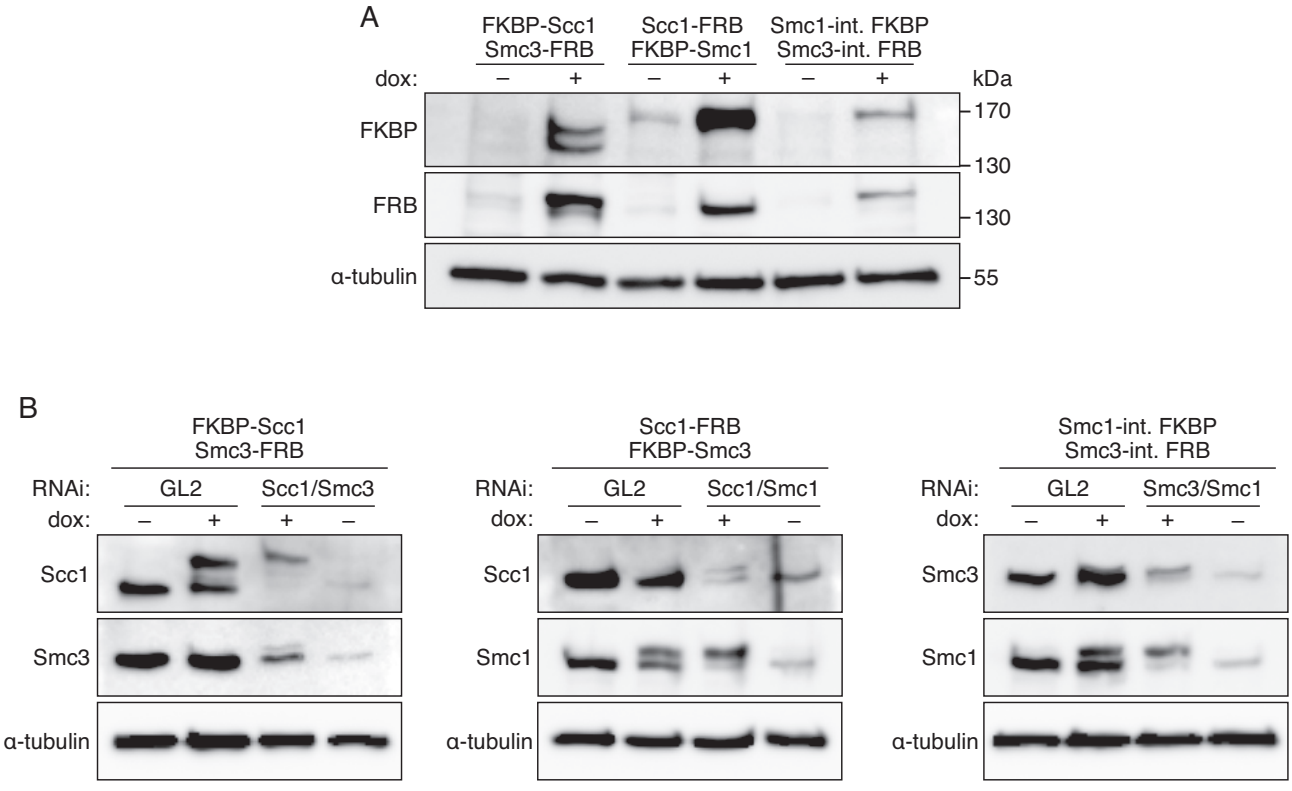

Figure 13 | Generation of doubly stable HEK293 cell lines expressing matched pairs of FRB/FKBP-tagged cohesin subunits. (A) Doubly stable HEK293 cell lines expressing matched pairs of tailored cohesin subunits upon induction with doxycycline (dox). **(B)** Tailored cohesin subunits replace endogenous variants upon 3 days of RNAi-depletion as the main species in the cell. Please note that the levels of C-terminally tagged Smc3 and Scc1 are underrepresented as the respective antibodies are directed against the C-termini.

rings with tailored variants, which would then allow me to investigate the effects of closing an individual gate. To demonstrate the feasibility of this approach, I transfected the three FRB/FKBP-cohesin cell lines with different siRNAs targeting the mRNAs of an individual pair of endogenous cohesin subunits, which were to be replaced by lockable versions (simultaneous dox-addition). Three days after transfection, cells were harvested for Western blot analysis using cohesin antibodies to detect endo- and exogenous species (Figure 13 B). Across all experiments, knockdown efficiencies for the three ring subunits differ slightly with Scc1 being depleted most successfully. In most cases, the slower migrating FRB/FKBP-tagged proteins remain the major species in the cell after three days of endogenous knockdown. Only in the case of Scc1-FRB (Figure 13 B, middle panel), the band intensity of the exogenous species merely matches the endogenous signal and in the case of Smc3-FRB (Figure 13 B, left panel), the designed cohesin subunit seems to be expressed in lower quantities than the wildtype species. However, it has to be taken into account that the employed antibodies targeting either Scc1 or Smc3 were both raised and therefore directed against the C-terminus of their respective antigen and that we have previously observed reduced affinities of these antibodies against C-terminally tagged versions of their targets. Consequently, the actual levels of Scc1-FRB and Smc3-FRB likely appear underrepresented in Western blot analysis. Thus, in summary, using a combination of RNAi and induced transgene expression, it is possible to largely replace endogenous cohesin subunits with tailored variants.

2.1.4 Ability of the FRB/FKBP-tagged cohesin subunits to functionally replace the endogenous variants

All further experiments depend on the ability of the FRB/FKBP-tagged cohesin subunits to functionally replace the endogenous variants at least as long as rapamycin is absent. Therefore, I utilized a co-immunoprecipitation (co-IP) assay to initially test for their retained competence to bind to various endogenous cohesin subunits. The three doubly stable FRB/FKBP cohesin subunit cell lines were transfected with siRNAs in order to individually knock down the endogenous cohesin subunits, which were to be replaced by their respective tailored counterparts (simultaneous doxycycline-addition), for a total of 3 days. 41 hours after transfection, cells were treated with DMSO (-rapa) or rapamycin (+rapa) and 16 hours before harvesting (15 hours after +/-rapa), cells were synchronized in prometaphase by nocodazole addition, which means that most cells had undergone

prophase pathway-mediated cohesin-dissociation from chromatin by the time of cell lysis. This ensures firstly, that most cohesin molecules are soluble and not associated with genomic DNA and secondly, that those cohesin molecules are bound to Wapl. Cells were ultimately harvested, lysed and subjected to IP using an FRB antibody (or unspecific rabbit IgG as a control), targeting specifically the tailored cohesin variants (for details, see materials and methods). Finally, immunoprecipitated proteins were eluted subjected to Western blot analysis, which revealed FRB-tagged cohesin subunits were not only efficiently, but also specifically immunoprecipitated by the FRB antibody, as unspecific IgGs were not proficient in doing so (Figure 14 A). Additionally, in all three cell lines, the

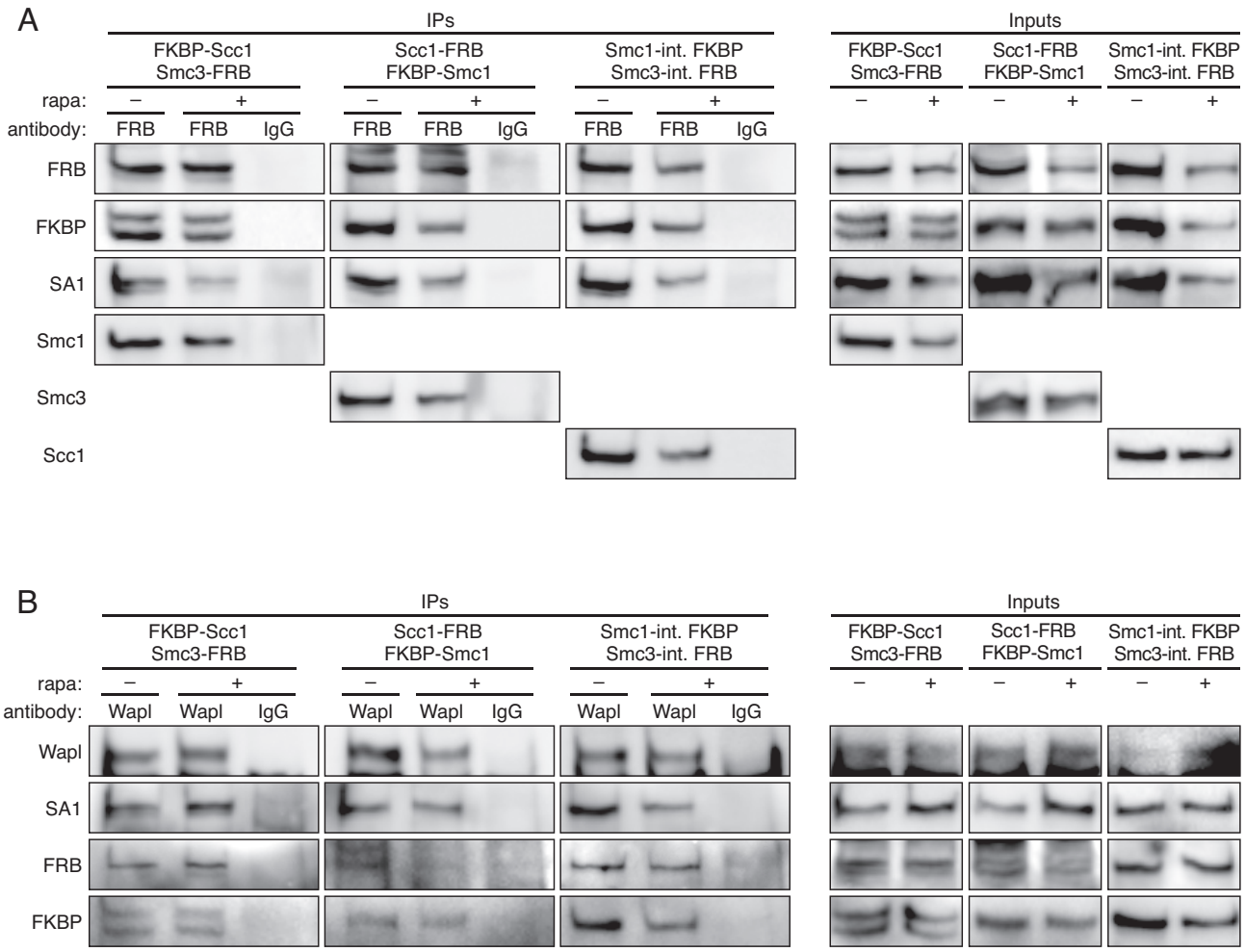

Figure 14 | FRB/FKBP-tagged cohesin variants can be incorporated into a *bona fide* ring complex independent of rapamycin. Doubly stable cell lines were induced by doxycycline (dox) addition and simultaneously transfected with siRNAs directed against the mRNAs of endogenous cohesin subunits that were to be replaced by versions featuring individually lockable gates for 3 days. 41 h after transfection, cells were treated with rapamycin (rapa) or DMSO as a control. 16 h before harvesting, cells were arrested in mitosis by addition of nocodazole. Eventually, cells were lysed and corresponding lysates were cleared by high-speed centrifugation to remove chromatin (Inputs) and ultimately subjected to immunoprecipiation (IPs) experiments using either anti-FRB (A) or anti-Wapl antibodies (B). Unspecific IgG-IP was used as a control. Samples were analyzed by Western blot using the specified antibodies.

FKBP-tagged cohesin subunits were effectively co-immunoprecipitated independently of rapamycin, indicating that wildtype-like interactions between the two altered subunits are still possible. Most importantly however, the two FRB/FKBP-tagged cohesin subunits were able to interact with the individual endogenous third integral ring component as well as the ring-associated SA1 protein, an interaction partner of Scc1. In order to study the prophase pathway using altered cohesin rings, one must make sure that the pathway's key protein Wapl is still interacting with the ring. To this end, I treated the three doubly stable FRB/FKBP cohesin subunit cell lines as described for Figure 14 A, but used a Wapl antibody for the IP (Figure 14 B). Wapl could efficiently and specifically be immunoprecipitated, again judged by comparison with the unspecific IgG controls. More importantly, the FRB/FKBP-tagged cohesin subunits as well as SA1 clearly co-IPed with Wapl, independently of rapamycin.

From the IP experiments, we can now appreciate that the FRB/FKBP-tagged cohesin subunits are most probably incorporated into a proper ring, which can associate with further cohesin subunits, the most critical one being Wapl. But can this designed cohesin ring functionally replace its endogenous counterpart? To answer this question, I sought to test its ability to associate with chromatin in a stable fashion, which requires the ring to be properly, i.e. topologically, loaded onto DNA. The three doubly stable FRB/FKBP cohesin subunit cell lines were largely treated as described for the IP experiments in Figure 14, while omitting mitotic synchronization. After three days of knockdown/expression, cells were harvested and subjected to a simple chromatin isolation procedure yielding a chromatin ("C") and a cytoplasmic supernatant ("SN") fraction, which were ultimately analyzed by Western blot (Figure 15 A). The FRB/FKBP-tagged cohesin subunits were clearly enriched in the chromatin fractions, marked by elevated histone (judged by a Coomassie Brilliant Blue staining of the respective SDS-polyacrylamide gel) and depleted α-tubulin levels compared to the supernatant fractions. Additionally, using immuno-fluorescence microscopy (IFM) on similarly treated cells, I can demonstrate that the FRB-tagged species is present on interphase chromatin of cells that have been pre-extracted (i.e. the species is stably bound to DNA and therefore has been loaded properly; Figure 15 B). It should be noted that the anti-FRB antibody is specific for its target and does not cross-react with DNA as can be appreciated from IFM experiments in Figures 16 and 21, where the antibody does not produce a DNA staining due to cohesin's absence from chromatin. Importantly, in both experiments from Figure 15, the observed chromatin-association remains independent of rapamycin.

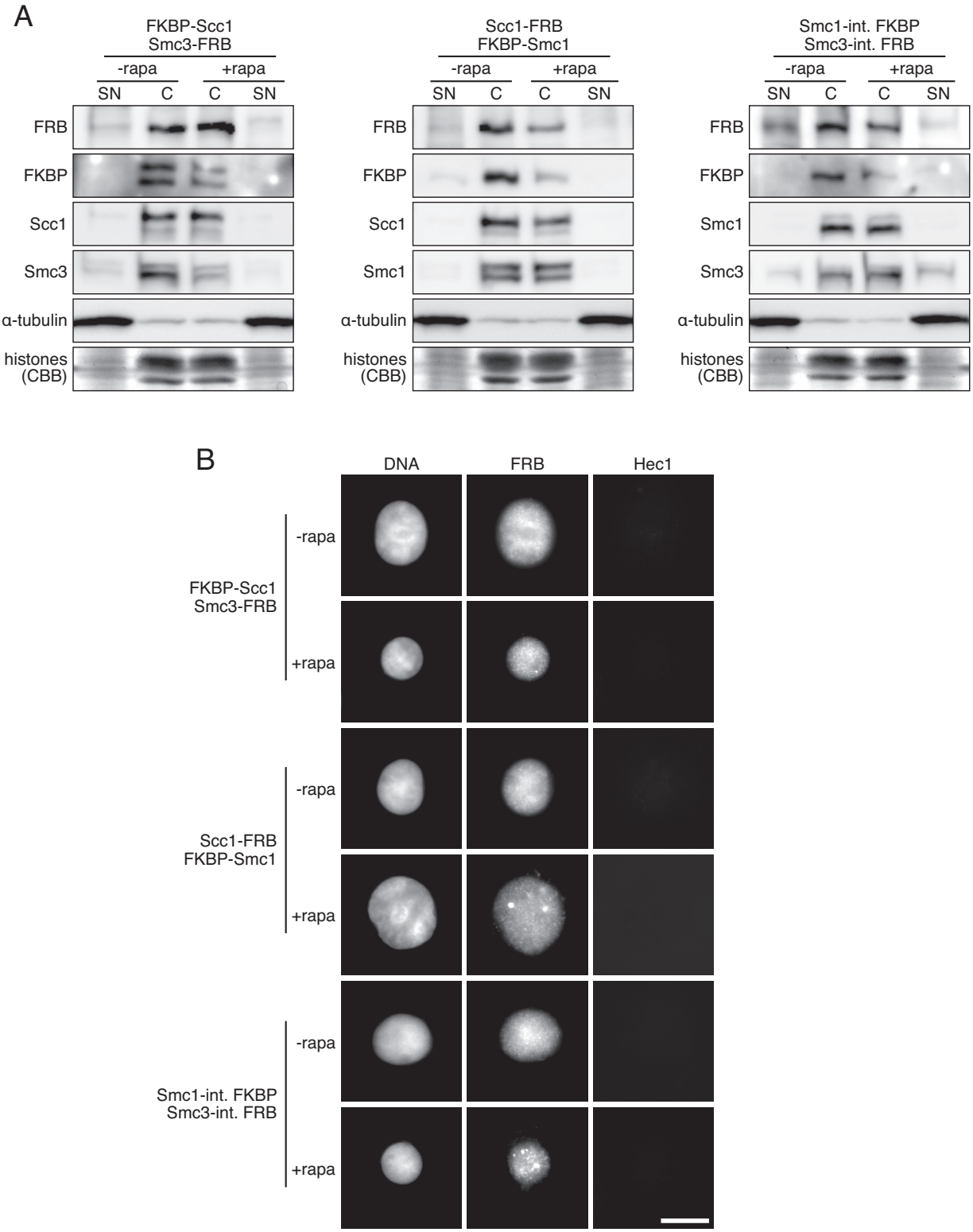

Figure 15 | Tailored cohesin rings can stably associate with DNA *in vivo* independent of rapamycin. **(A)** Doubly stable cohesin cell lines were largely treated as described in Fig. 14 while omitting nocodazole-synchronization. Cell lysates were prepared in the presence of nuclei-permeabilizing detergent and fractionated into soluble supernatant (SN) and pelleting chromatin (C) by centrifugation, both of which were subsequently analyzed by Coomassie Brilliant Blue staining (CBB, for histones) and Western blot using the specified antibodies. **(B)** Depicted are exemplary interphase cells from the experiments shown in Figure 16 B-E that had not yet entered mitosis (marked by the absence of Hec1 staining). Cells were treated as described in Figure 16 A. Before fixation, cells were pre-extracted to clear the cyto- and nucleoplasm from any cohesin not bound to chromatin. Scale bar = 10 μm.

The immunoprecipitation experiments unequivocally demonstrate that the tailored cohesin subunits can be incorporated into a *bona fide* ring complex, which moreover interacts with additional cohesin components, namely SA1 and, most critically, the prophase pathway effector Wapl. Additionally, this ring complex is able to stably associate with DNA as concluded from chromatin isolation and IFM experiments. All of these interactions do neither require, nor are they abrogated by the presence of rapamycin, strongly indicating that addition of the small FRB/FKBP-tags does not impair the cohesin subunit's basic functions.

2.1.5 Determining cohesin's "exit gate"

As already illustrated in Figure 11 A, I predicted that artificially closing cohesin's prophase exit gate before letting the cells pass through early mitosis should result in two readily testable phenotypes: 1) cohesin remains associated with chromatin in early mitosis, which leads to 2) overcohesed chromosomes. To confirm the first prediction and finally determine, which of cohesin's gates has to be opened during prophase to efficiently release the complex from DNA, the three doubly stable FRB/FKBP cohesin subunit cell lines were treated as illustrated in Figure 16 A. In short, the cell lines were grown on cover slips and transfected with siRNA to individually knock down the endogenous cohesin subunits, which were to be replaced by lockable variants whose expression was simultaneously induced by doxycycline addition (total time of knockdown/expression: 3 days). The cells were synchronized at the G1/S-barrier by addition of thymidine. After 16 hours, thymidine was washed out and the cells released for 7 hours before nocodazole was added for additional 7 hours to block the cells in the following prometaphase. Ultimately, the cells were pre-extracted and fixed for immunofluorescence microscopy (IFM). Rapamycin (rapa) was added to independently close the three gates at two different time points. The small molecule was either added together with thymidine ('early') or with nocodazole ('late'). The two time points were intended as controls for each other, since 'early' rapa-addition could have caused problems over the course of the remaining experiment (e.g. after thymidine-release in S phase) and 'late' addition might not have had a sufficiently pronounced effect in the following analyses. Both, early and late rapa-additions (+rapa 'early'; +rapa 'late') were always controlled by adding DMSO to otherwise identically treated cells (-rapa). Fixed cells were (immuno-)stained for DNA (Hoechst 33342), the mitosis-specific kinetochore marker Hec1 and either Smc1 (detects both endo-

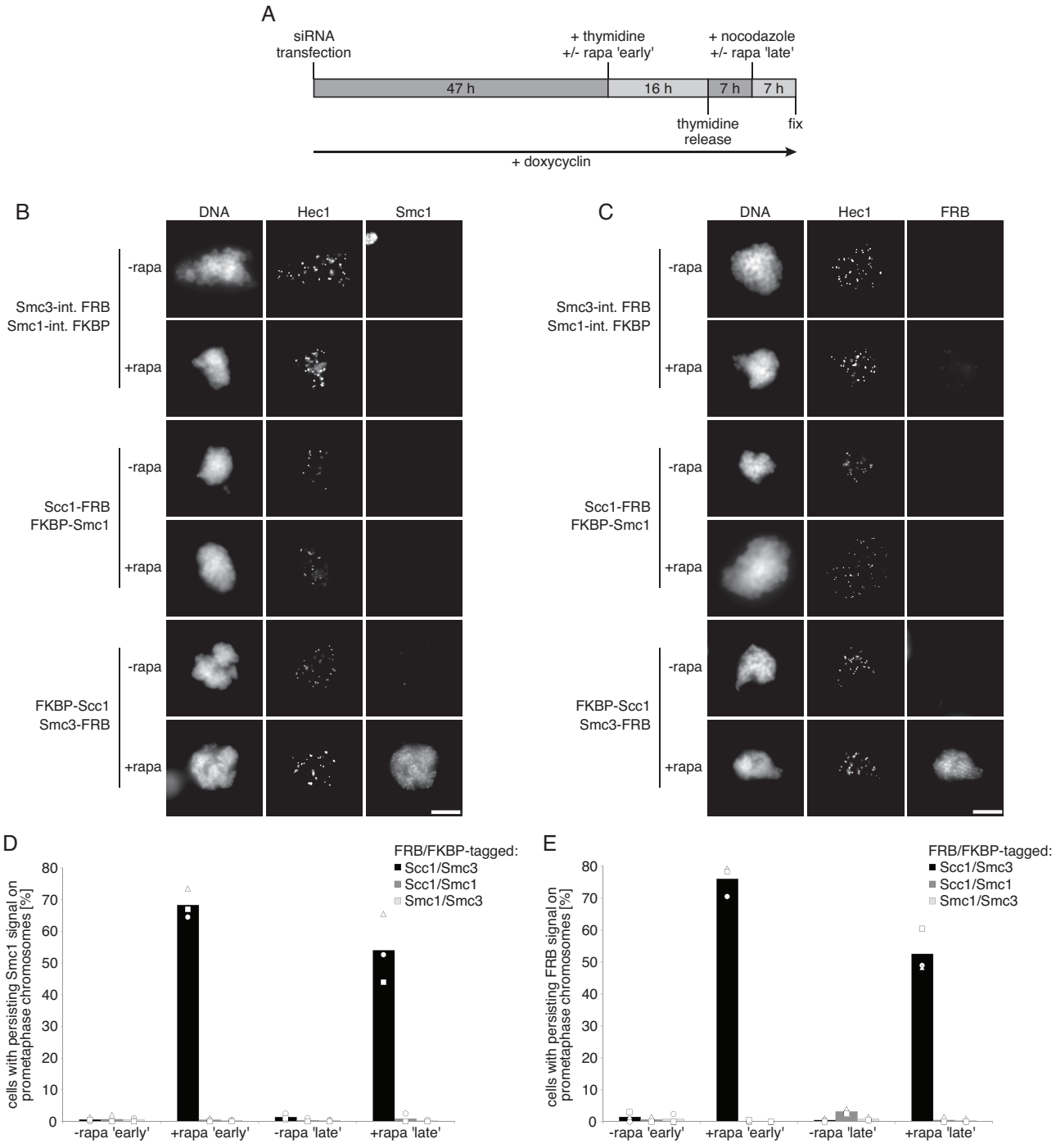

Figure 16 | DNA exits the cohesin ring through the Smc3-Scc1 gate. (A) Assay time line for results shown in (B-E). **(B, C)** Indicated doubly transgenic cell lines were treated as illustrated in (A) and then Hoechst 33342- and immunostained to *in situ*-visualize DNA, Hec1 and Smc1 (B) or FRB (C). Exemplary images are shown. Scale bars = 10 μm. **(D, E)** Quantification of the data shown in (C) and (D), respectively. The relative numbers of cells with prometaphase chromatin positive for Smc1 (E) or FRB (F) are plotted. Circles, triangles and squares correspond to individual data points of three independent reiterations while columns represent means. Data sets of each experiment across all cell lines and conditions are represented by identical shapes. Between 293 and 600 cells were analyzed per column.

and exogenous species; Figure 16 B) or FRB (detects only exogenous cohesin complexes; Figure 16 C). The IFM analysis revealed that in all three cell lines prometaphase-arrested Hec1-positive cells do not show any remaining association of

cohesin with DNA, when rapamycin was absent (Figure 16 B, C; "-rapa"). Rapamycin-dependent closure of the gates constituted by Smc1/Smc3 or Scc1/Smc1, did also not result in prolonged binding of cohesin to chromatin (Figure 16 B, C; "+rapa"). However, cells expressing lockable versions of Scc1 and Smc3 exhibited strong Smc1 and FRB signals on early mitotic chromatin, but only when rapamycin was present (Figure 16 B, C; "FKBP-Scc1, Smc3-FRB", "+rapa"), strongly suggesting that the gate situated between Smc3 and Scc1 constitutes cohesin's DNA exit gate during prophase. These experiments were performed three times for each cell line and condition, and the number of cells with persisting Smc1 (Figure 16 D) or FRB signal (Figure 16 E) in prometaphase was quantified. The quantification confirms that closing the Smc1-Smc3 and Scc1-Smc1 gates by early or late rapa-addition does never lead to extended cohesin-association with chromatin in almost 100% of the respective cells. Strikingly, over 50% of cells expressing FRB/FKBP-tagged Smc3/Scc1 keep cohesin bound to chromatin in early mitosis, when rapamycin is added late, only 7 hours before fixation. The relative number of cells exhibiting this phenotype even increases to around 70% when rapa is added earlier, i.e. 30 hours prior to fixation. Moreover, although I have previously shown that my tailored cohesin variants can interact with endogenous Wapl (Figure 14 B), the question whether the latter is actually functional on those cohesin rings and thus able to drive their release from chromatin in prophase, still remained unanswered. Since we know that the FRB/FKBP-tagged cohesin complexes were efficiently loaded onto DNA in my experiments (the interphase cells shown in Figure 15 B were actually cells from the experiments in Figure 16 that had not yet entered mitosis), the fact that respective early mitotic cells were devoid of any cohesin signal (at least when rapa was absent) clearly indicates that the prophase pathway is functional towards the transgenic complexes.

According to my second prediction, closing cohesin's exit gate should result in overcohesed chromosomes. To test this, the doubly stable cell lines were treated as illustrated in Figure 16 A but ultimately fixed for chromosome spreading. The relative amount of nuclei displaying tightly cohesed ("zipped") chromosomes (as opposed to "butterfly-like" chromosomes; exemplified in the lower panel of Figure 17) were quantified from three independent experiments for each cell line and condition (Figure 17). As expected, only in the FKBP-Scc1/Smc3-FRB-expressing cell line and more importantly, only when rapamycin was present, chromosomes displayed zipped morphology in an appreciable amount of 40-50% of the cases. Again, early rapa-addition increases the number of zipped chromosomes rather than decreasing it, dismissing involvement of

cohesin's exit gate in S phase cohesion establishment. It should be noted that exclusively in the FKBP-Scc1/Smc3-FRB cell line some chromosome spreads exhibited an extreme overcohesion phenotype, which I termed "hyperzipped" (exemplified in Figure 17, lower panel right), featuring long thin DNA threads held together in a very tight fashion.

Summed up, my results unequivocally identify the gate situated between Smc3 and Scc1 as cohesin's exit gate required to be opened by the prophase pathway to release the bulk of the ring complexes from DNA in early mitosis. Artificially shutting the gate using the FRB/FKBP system leads to prolonged association of cohesin with chromatin, which results in overcohesed chromosomes. It is important to mention that identifying the Smc3-Scc1 gate as cohesin's exit gate does not disqualify the other gates from taking on a role during prophase. While the respective cohesin complexes featuring FRB/FKBP-tags can

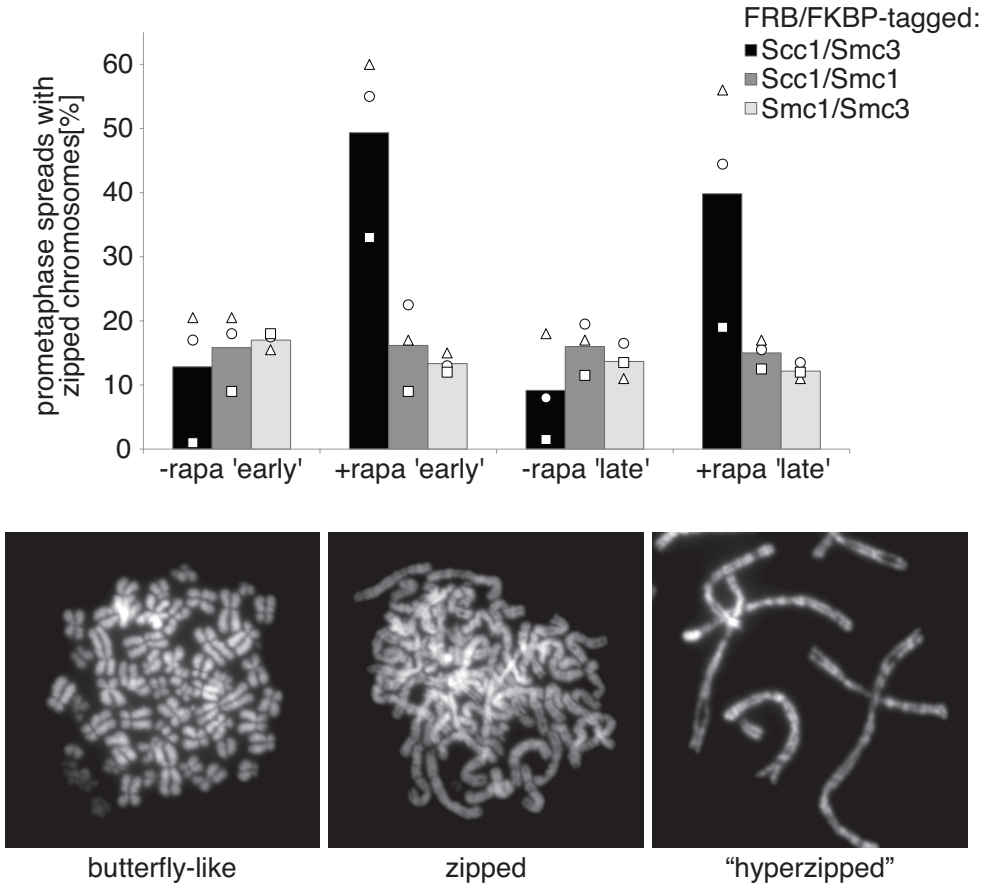

Figure 17 | Artificially closing cohesin's exit gate leads to overcohesed chromosomes. Indicated doubly transgenic cell lines were treated as illustrated in Fig. 16 A and then subjected to chromosome spreading and quantitative assessment of arm cohesion. The relative numbers of cells displaying tightly cohesed ("zipped") prometaphase chromosomes are plotted. Each column represents the mean of three independent data points (represented by circles, triangles and squares) totalling 600 analyzed cells. Corresponding data sets across all cell lines and conditions are identified by identical shapes. Typical examples for butterfly-like and zipped morphologies are shown below. The picture on the right demonstrates an extreme cohesion phenotype termed "hyperzipped".

demonstrably perform in a wildtypic manner, there is no way to infer successful rapamycin-mediated gate-closing from the conducted experiments, since the particular cell lines do not show any phenotypes in the tested scenarios. Therefore, further experiments were necessary to either verify rapamycin's ability to close a particular gate or at least to rule out any involvement during prophase.

2.1.6 Assessing the role of the Scc1-Smc1 gate during prophase

As mentioned above, I cannot exclude any involvement of the Scc1-Smc1 gate during prophase, since functional rapamycin-mediated gate-closing cannot be inferred from the experiments in chapter 2.1.5. To work around this problem, I fused the open reading frame of Smc1 to the one of Scc1 via a small linker oligonucleotide resulting in an in-frame Scc1-Smc1 fusion construct (Figure 18 A). Expressing this construct, while simultaneously depleting endogenous Scc1 and Smc1, should efficiently replace endogenous cohesin by a version featuring a covalently closed Scc1-Smc1 gate (Figure 18 B). Based on this construct, I created a stable HEK293 cell line, which conditionally expresses the Scc1-Smc1 fusion construct upon doxycycline (dox)-addition (Figure 18 C). The Scc1-Smc1 fusion might not be expressed to levels comparable to the endogenous protein(s) (very large proteins can be underrepresented due to decreased blotting efficiency), but already small amounts of cohesin rings stably encompassing sister chromatids would be expected to exert a dominant negative effect. A similar fusion protein has already been shown to be able to functionally replace endogenous Scc1 and Smc1 in yeast (Gruber *et al*, 2006). Nonetheless, to demonstrate the fusion protein's ability to perform in a wildtype-like manner in human cells, it was subjected to the same functionality tests as the other tailored cohesin subunits. To determine, whether the fusion protein can be incorporated into a *bona fide* cohesin ring, I depleted endogenous Scc1 and Smc1 by siRNA-mediated RNAi while simultaneously inducing expression of the Scc1-Smc1 fusion by doxycycline-addition. After three days of knockdown plus induction, cells were harvested for immunoprecipitation (IP). Using Smc3 and Wapl antibodies for IP, I could produce proof that the Scc1-Smc1 fusion protein is proficient in binding to endogenous Smc3, SA1, and most importantly, Wapl (Figure 19 A, B). It is furthermore enriched in the chromatin fraction (marked by high histone and low α-tubulin levels) isolated from similarly treated stable cells (Figure 19 C). From these experiments and from the observation that expression for extended periods of time does not cause any obvious viability-issues, I conclude that the

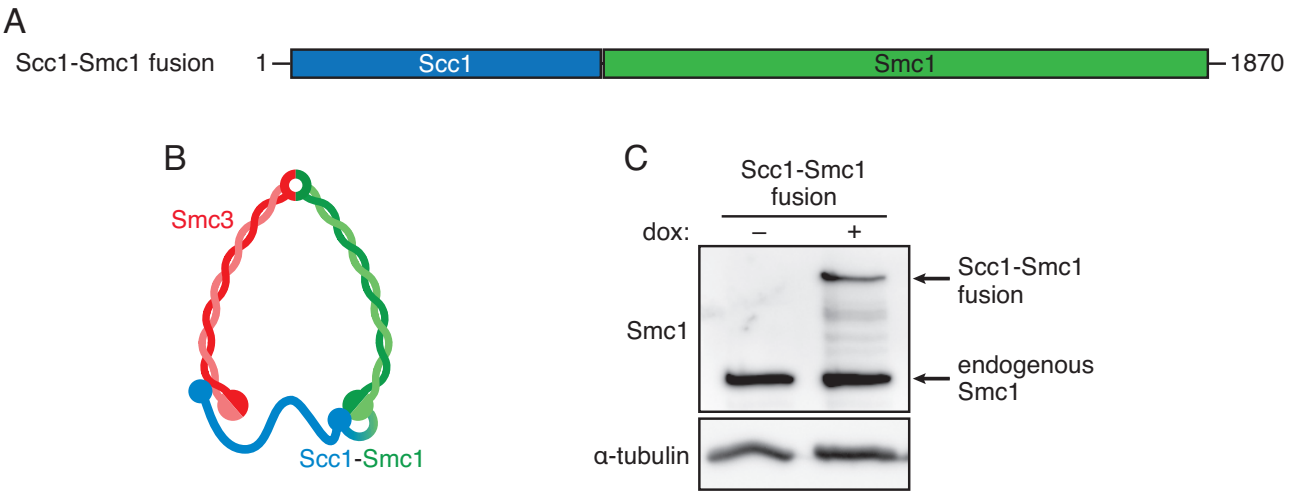

Figure 18 | Generation of a stable cell line expressing an Scc1-Smc1 fusion protein. (A, B) Cartoons depicting the fusion of the peptide sequences of Scc1 and Smc1. **(C)** Doxycycline-inducible expression of the Scc1-Smc1 fusion protein in a stable HEK293 cell line after 2 days of RNAi knockdown of the endogenous protein is shown by a Western blot using an Smc1 antibody.

Scc1-Smc1 fusion protein is able to functionally replace endogenous unlinked Scc1 and Smc1 in a functional manner.

To finally assess the involvement of Scc1-Smc1 gate dynamics in the prophase pathway, I conducted experiments analog to the ones described in chapter 2.1.5. For this, the stable Scc1-Smc1 fusion cell line was largely treated as described in Figure 16 A while omitting any addition of rapamycin. The cells were transfected with siRNAs targeting the mRNAs of endogenous Scc1 and Smc1, and doxycycline was added to induce transgene expression at the same time. Cells were pre-synchronized with thymidine and released into a nocodazole-mediated mitotic arrest before they were ultimately harvested and fixed for immunofluorescence microscopy (IFM; Figure 20 A) or chromosome spreading (Figure 20 B). For IFM, cells were pre-extracted before fixation and eventually (immuno-)stained for DNA (Hoechst 33342), Hec1 and Smc1. Since the Scc1-Smc1 fusion protein did not carry any specific tags I relied on staining with an Smc1 antibody, which detects remaining endogenous as well as inducibly expressed exogenous cohesin. If replacing endogenous cohesin with a version featuring a covalently shut Scc1-Smc1 gate would abrogate cohesin's ability to exit DNA in prophase, a reasonable percentage of cells should exhibit at least slightly elevated levels of cohesin on prometaphase chromatin. This was clearly not the case as in two independent experiments almost 100% of prometaphase cells were devoid of any cohesin staining (Figure 20 A). This result is corroborated by the fact that cells stably expressing an Scc1-Smc1 fusion protein do not exhibit overly cohesed

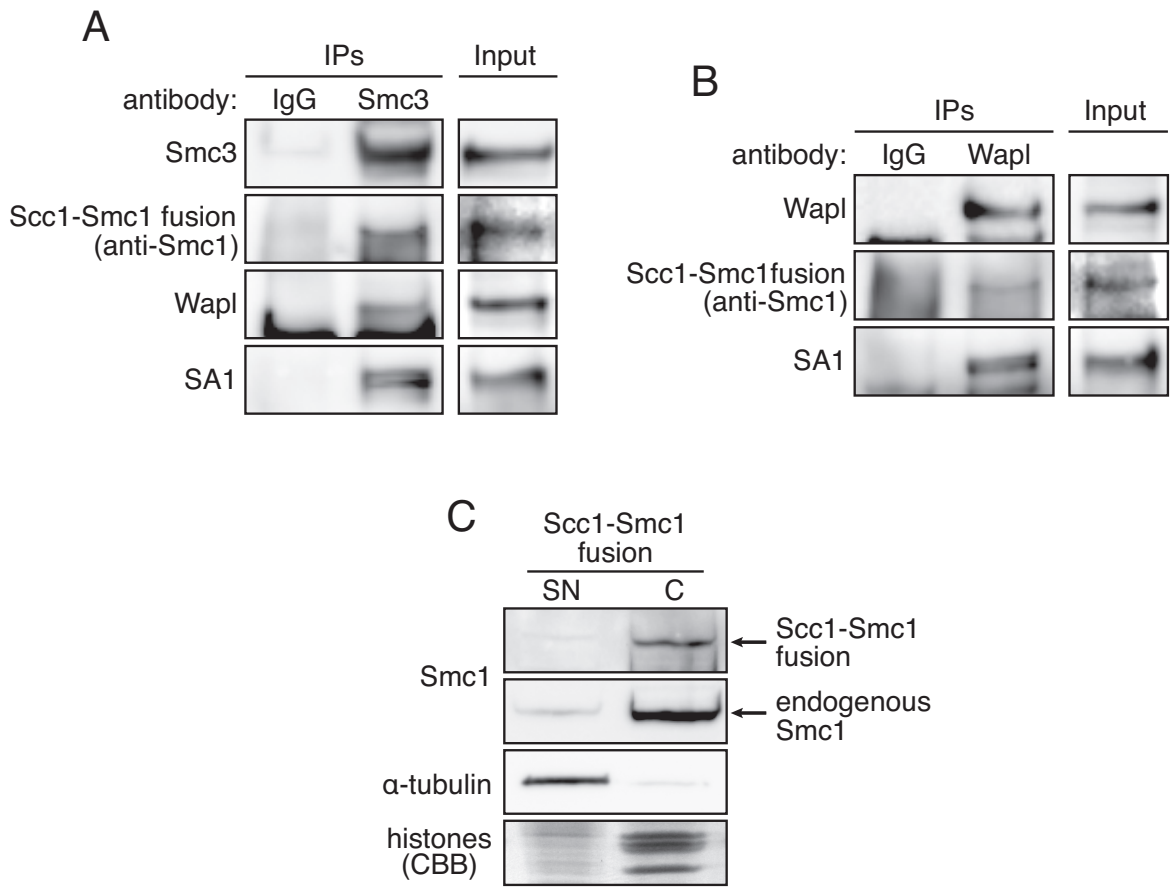

Figure 19 | **The Scc1-Smc1 fusion protein can be incorporated into a *bona fide* ring complex which stably binds to DNA. (A, B)** The stable Scc1-Smc1 fusion cell line was largely treated as desribed in Fig. 6 while omitting rapamycin-addition. Eventually, cells were lyzed and corresponding lysates were cleared by high-speed centrifugation to remove chromatin (Inputs) and ultimately subjected to immunoprecipitation (IPs) experiments using either anti-Smc3 (A) or anti-Wapl antibodies (B). Unspecific IgG-IP was used as a control. Samples were analyzed by Western blot using the specified antibodies. **(C)** The stable Scc1-Smc1 fusion cell line was treated as described in Fig. 15. Cell lysates were prepared in the presence of nuclei-permeabilizing detergent and fractionated into soluble supernatant (SN) and pelleting chromatin (C) by centrifugation, both of which were subsequently analyzed by Coomassie Brilliant Blue staining (CBB, for histones) and Western blot using the specified antibodies.

("zipped") chromosomes (Figure 20 B). Around 95% of the stable cells derived from three independent experiments displayed normal "butterfly-like" chromosome morphology.

In conclusion, I can rule out any involvement of Scc1-Smc1 gate-dynamics for proper function of the prophase pathway with a high degree of certainty. Covalently closing this gate does neither cause elevated cohesin levels on chromatin in prometaphase nor does it result in overly cohesed chromosomes. In concordance with a yeast study (Gruber *et al*, 2006), replacing endogenous cohesin at least partly with the fusion protein does not seem to have any consequence for cell cycle progression or viability in general, despite the fact that any impaired cohesin dynamics were expected to cause dominant negative effects.

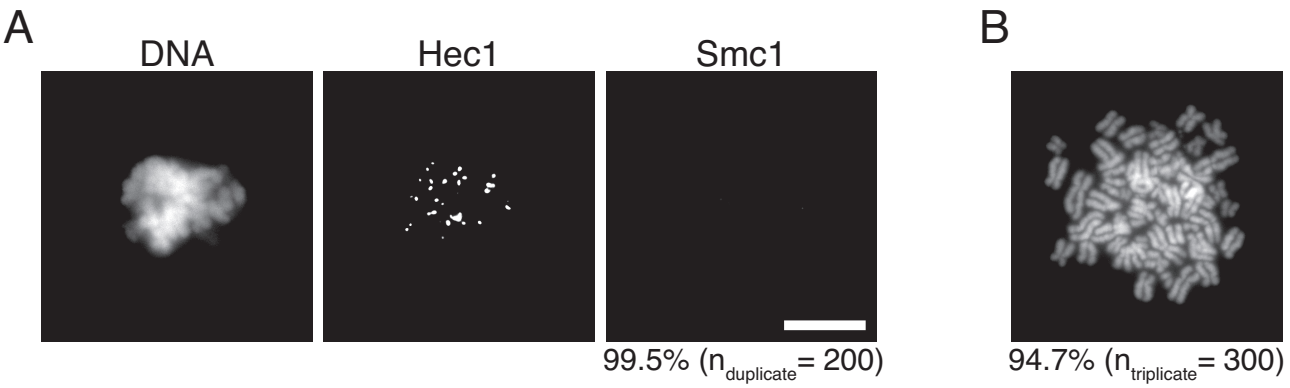

Figure 20 | **DNA does not leave cohesin through the Scc1-Smc1 gate.** The stable Scc1-Smc1 fusion cell line was largely treated as desribed in Fig. 8 A while omitting rapamycin-addition and then analyzed by immunofluorescence microscopy (A) and chromosome spreading (B). **(A)** Averaged over two independent experiments, 99.5% of a total of 200 Hoechst 33342, anti-Hec1, and anti-Smc1 stained cells did not exhibit any signs of Smc1-chromatin association beyond prophase. **(B)** Averaged over three independent experiments, 94.7% of a total of 300 spread nuclei displayed butterfly-like chromosomes. An increase in tightly cohesed ("zipped") chromosomes could not be detected.

2.1.7 Determining cohesin's "entry gate"

It has been shown in yeast that cohesin loading onto DNA requires opening of the Smc1-Smc3 hinge (Gruber *et al*, 2006), but whether this gate's function is conserved in vertebrates remained an unanswered question. I set out to determine, whether the gate constituted by Smc1 and Smc3 has to be opened for proper cohesin loading by artificially closing this gate using the FRB/FKBP system. An observed phenotype would additionally serve as a confirmation for the ability of internally FRB/FKBP-tagged Smc1/Smc3 to dimerize in a rapamycin-dependent fashion, further validating the identity of cohesin's DNA exit gate as determined before (Figure 16). To this end, I treated the doubly stable Smc1-int. FKBP/Smc3-int. FRB cell line as illustrated in Figure 21 A: the cell line was transfected with siRNAs targeting the mRNAs of endogenous Smc1 and Smc3, while doxycycline was added simultaneously to induce transgene expression. The cells were arrested in prometaphase by the use of nocodazole, which means that most cohesin molecules are soluble and ready to be reloaded onto chromatin in the following telophase. Rapamycin (or DMSO as a control) was added 14 hours into the nocodazole-arrest to lock the hinge gates of all chromatin-bound and, more crucially, -unbound cohesin molecules. Two hours later the cells were released from the arrest in the presence of rapamycin (or DMSO) for 2.5 hours before being pre-extracted and fixed for IFM. If the two halves of the hinge gate can in fact be forced to dimerize via the internally inserted FRB/FKBP-tags, and moreover, if cohesin's entry gate is actually conserved between yeast and humans, then

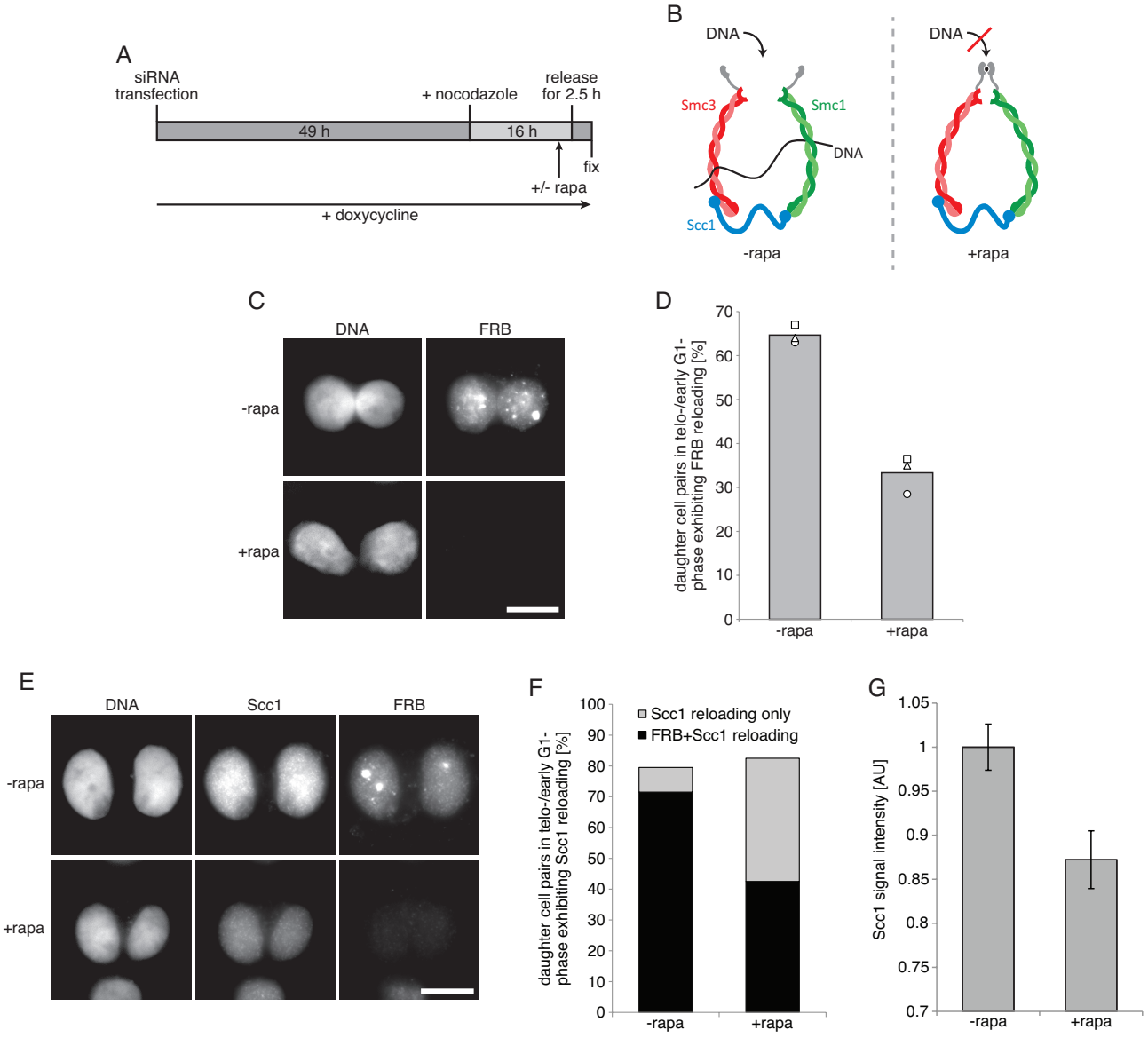

Figure 21 | Cohesin loading requires opening of the Smc1-Smc3 hinge. (A) Assay time line for results shown in (C-F). **(B)** The rationale for the experiments performed in (C-F). If DNA entry into the cohesin ring requires the hinge gate ito open, then rapamycin-addition to the Smc1-int. FKBP/Smc3-int. FRB cell line should cause less cohesin to be reloaded onto DNA in telopphase. For details see text. **(C)** Closing the hinge gate abrogates cohesin-loading onto DNA in the following telophase. Stable HEK293 cells inducibly expressing FKBP-Smc1/Smc3-FRB (hinge) were treated as described in (A). Following pre-extraction, fixation and staining of DNA and FRB, only those cells were analyzed that were still in telophase or formed closely coupled pairs with similar FRB levels. Exemplary images are shown. Scale bar = 10 μm. **(D)** The relative numbers of cell pairs exhibiting FRB staining in telo-/early G1 phase are plotted. Columns correspond to means of three independent experiments with each triplicate totalling 600 cells. Circles, triangles and squares represent data points and identify respective sets from individual experiments. **(E-G)** Cells were treated as described in (A, C) and stained for FRB and endogenous Scc1. Most of the early G1 phase nuclei that lacked an FRB signal could still reload endogenous Scc1 in the presence of Smc1-int. FKBP, Smc3-int. FRB and rapamycin (due to incomplete knockdown of endogenous Smc1/3 and the rapamycin-independent loading of cohesin complexes that retain at least one untagged SMC subunit; E, F). However, the intensities of the Scc1 signals were reduced consistent with the transgenic proteins exerting a dominant-negative effect on cohesin reloading (see text for details; E, G). Scale bar = 10 μm. For each quantification, 100 cells were counted. Columns in (F) show medians and whiskers SEMs.

rapamycin-addition should impair efficient cohesin-reloading onto DNA in telophase, as illustrated in Figure 21 B. After fixation, cells were (immuno-)stained for DNA (Hoechst 33342) and FRB (Figure 21 C). IFM analysis of telophase/early G1 cells revealed that FRB and therefore transgenic cohesin was indeed reloaded onto chromatin less frequently when rapamycin was present. Quantification of three independent experiments demonstrates that closing the Smc1-Smc3 gate results in a distinctively reduced fraction of cells (to around 30%) featuring an FRB signal on chromatin (Figure 21 D). To corroborate these findings, I repeated the experiment and additionally stained post-mitotic cells with an antibody targeting endogenous Scc1, the rationale being that reduced reloading of FRB/FKBP-tagged cohesin subunits should also impair (but not necessarily diminish) reloading of endogenous Scc1 since the α-kleisin is necessary to form a proper ring structure. IFM analysis did, indeed, demonstrate that Scc1-reloading after nocodazole-release is compromised, when the hinge gate is artificially closed by addition of rapamycin (Figure 21 E). Since the knockdown of endogenous Smc1 and -3 is incomplete, it was not expected that Scc1-reloading is completely abrogated, as it can still be incorporated into remaining wildtypic cohesin rings. In accordance with this notion, quantification of the IFM results revealed that, while the total fraction of cells exhibiting Scc1 signals remained stable (Figure 21 F), its signal intensity dropped by around 15% (Figure 21 G). Additionally, supporting the results from Figure 21 C and D, the amount of cells featuring FRB signals were drastically reduced upon rapamycin-addition (Figure 21 F).

The experiments shown in Figure 21 unequivocally identify cohesin's hinge gate, constituted by Smc1 and Smc3, as the ring's DNA entry gate in human cells, nicely complementing published results from yeast (Gruber *et al*, 2006). Artificially closing this gate leads to dramatically reduced reloading of the complex onto DNA during telophase. Additionally, the experiments prove that the FRB/FKBP-tags inserted into Smc1 and Smc3 are actually functional, which lends further credit to the results from chapter 2.1.5, ruling out any involvement of hinge gate-opening for the prophase pathway.

2.2 Cohesin dynamics in S phase

2.2.1 Establishing experimental setups for the investigation of cohesin dynamics in S phase

If cohesin dynamics are required for proper DNA replication, then individually closing one or more of cohesin's subunit interaction sites should compromise replication fork progression (Figure 22 A). To be able to test this, I established a DNA fiber assay, which allows stretching of single DNA fibers onto standard microscopy glass slides. After fixation

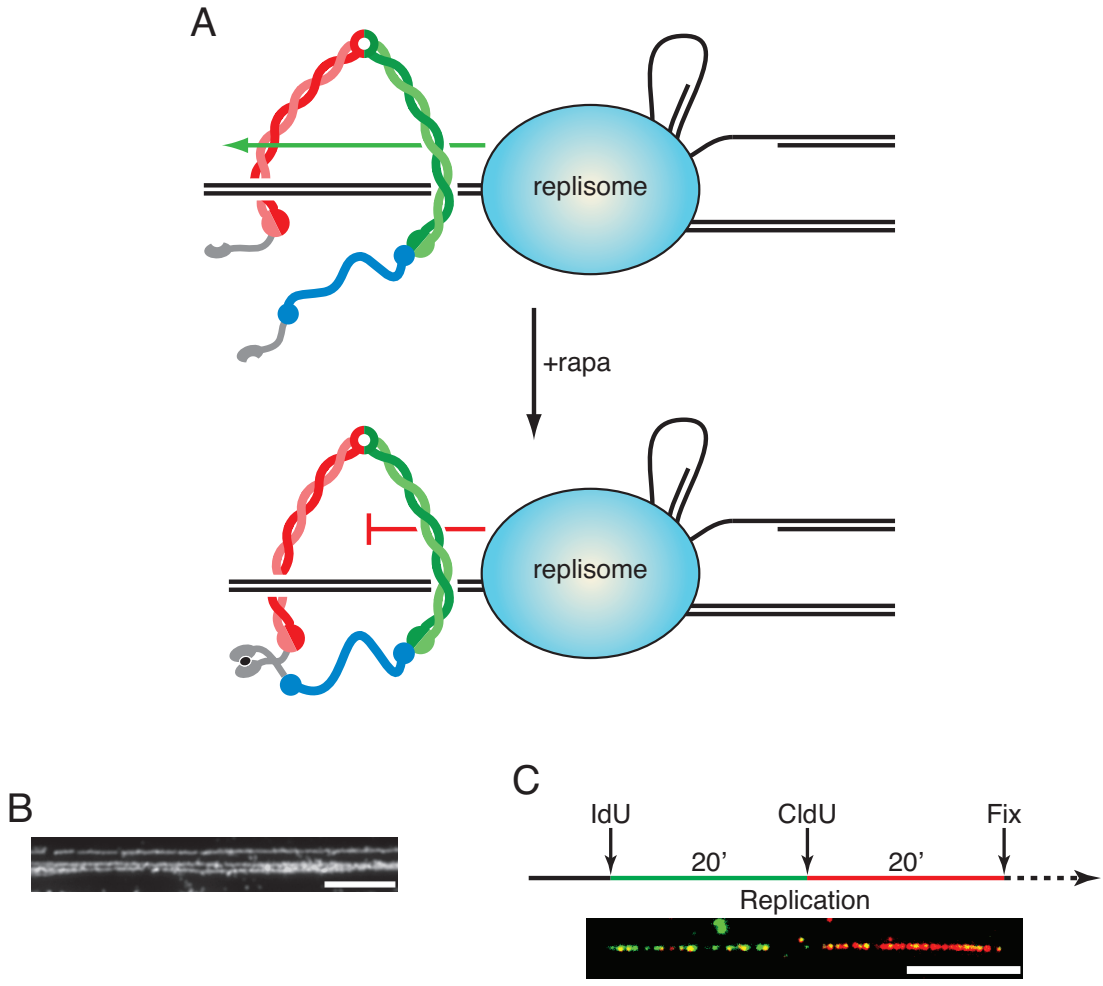

Figure 22 | Establishment of an IdU-CldU pulse chase fiber assay for the investigation of cohesin dynamics during DNA replication. (A) Rationale for our study as exemplified by rapamycin (rapa)-mediated locking of the gate constituted by Smc3 and Scc1. If this gate has to be opened to allow the replisome to efficiently process and replicate DNA, then rapamycin-induced ectopic closure of the gate should block DNA replication. **(B)** Establishment of the fiber assay. HEK293 cells were lysed and their genomic DNA stretched onto glass slides as described in the materials and methods section. Denatured DNA fibers were visualized by immunofluorescence microscopy using an anti-ssDNA antibody. Scale bar = 5 μm. **(C)** Establishment of the IdU-CldU pulse chase. Cartoon above shows assay time line. HEK293 cells were pulse labeled with 50 μM IdU for 20 min and then with 50 μM CldU for additional 20 min. Thereafter, cells were lysed and fixed for a DNA fiber assay. IdU and CldU were detected by immunofluorescence microscopy using two anti-BrdU antibodies, each cross-reacting with either IdU or CldU. Scale bar = 10 μm.

and denaturation, the nucleotides are accessible for antibodies and can now be stained for immunofluorescence microscopy (Figure 22 B). To follow replication fork progression on these fibers, newly replicated DNA had to be labeled *in vivo*, which is typically done by incorporation of nucleotide analogs such as 5-bromo-2'-deoxyuridine (BrdU). The problem with these experiments is that, in addition to single replication forks, also con- and diverging pairs of forks are identically labeled and cannot be discerned in the analysis. To overcome this limitation, one can pulse-label replication forks with two different nucleotide analogs in a consecutive fashion; staining these two analogs differently then allows discrimination between single and pairs of replication forks. For my studies, I first pulse-labeled nascent DNA fibers by supplementing cells with 50 μM 5-iodo-2'-deoxyuridine (IdU) for 20 minutes, followed by 50 μM 5-chloro-2'-deoxyuridine (CldU) for the same time frame before they were fixed for the DNA fiber assay (Figure 22 C). IdU- and CldU-labeled regions were differently stained using two antibodies from different species. To analyze single replication forks, only those fibers were considered that switch their labeling from IdU (green) to CldU (red) exactly once (Figure 22 C).

Cohesin dynamics have previously been implicated in proper replication fork progression. So has it been shown that expression of a non-acetylatable Smc3 mutant dramatically reduces the velocity of replication forks (Terret *et al*, 2009), a fact, which I decided to exploit to validate my newly established assay. Therefore, I created a C-terminally FRB-tagged Smc3 variant, in which two adjacent lysine residues had been mutated to alanine (K105A, K106A; "Smc3^{AA}"). HEK293T cells were transfected with siRNAs targeting the mRNA of endogenous Smc3 and constructs for the expression of either wildtype ("WT") or acetylation-mutant ("AA") Smc3-FRB (Figure 23 A). After two days of knockdown and expression, cells were IdU-CldU pulse-labeled and subsequently harvested for DNA fiber assays. IFM analysis revealed strongly reduced IdU-CldU fiber lengths ("tracks") when the acetylation-mutant Smc3^{AA} is expressed (Figure 23 B). Quantification of two independent experiments corroborates this impression, as expression of Smc3^{AA} reduced IdU-CldU track lengths by over 50% (Figure 23 C), an amount consistent with previously published data (Terret *et al*, 2009). To give this method further credibility, I tested an additional prediction made by the Jallepalli group: depletion of the cohesin destabilizer Wapl should rescue reduced replication fork velocity in Smc3^{AA}-expressing cells. To test this, I essentially repeated the experiment from Figure 23 A-C but simultaneously RNAi-depleted either GL2 (luciferase, control) or Wapl (Figure 23 D). Indeed, while expression of an acetylation-mutant Smc3 again reduced IdU-CldU tracks

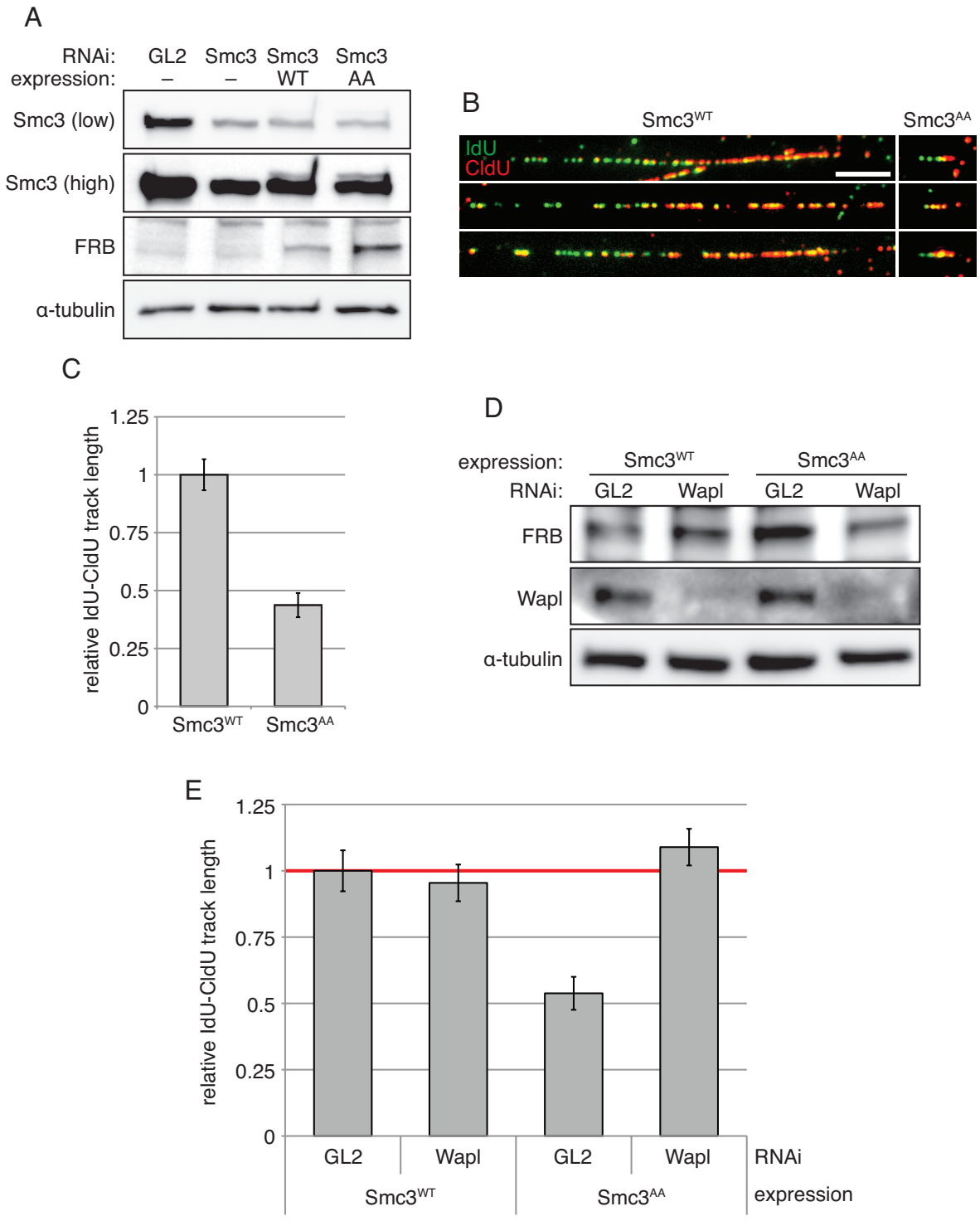

Figure 23 | The IdU-CldU pulse chase fiber assay can be used to study replication fork progression. **(A-C)** Expression of a non-acetylatable Smc3 mutant (K105A, K106A; "Smc3^{AA}") leads to decreased replication fork progression. HEK293T cells were transfected with siRNA targeting the mRNAs of either GL2 (luciferase, control) or endogenous Smc3. Simultaneously, cells were transfected with plasmids coding for C-terminally FRB-tagged versions of either wildtype Smc3 ("WT") or its non-acetylatable AA-mutant. After two days, cells were subjected to an IdU-CldU pulse chase and subsequently harvested for a DNA fiber assay. **(A)** Successful knockdown of endogenous Smc3 and expression of Smc3^{WT}-FRB and Smc3^{AA}-FRB was demonstrated by Western blot analysis. Please note that the amount of exogenous protein is underrepresented in the anti-Smc3 blot since the used antibody is directed against the C-terminus and shows decreased affinity towards C-terminally tagged targets. **(B)** Expression of Smc3^{AA}-FRB causes dramatically decreased replication fork velocities. Scale bar = 5 μm. **(C)** Quantification of the IdU-CldU pulse

Figure 23 (cont.) | chase fiber assay shows the relative length of IdU-CldU-labeled DNA fibers ("tracks") in Smc3^{AA}-FRB-expressing cells compared to cells expressing the wild type version (set to 1). Each column displays the median length of 100 tracks derived from two independent experiments. Whiskers represent SEM. **(D, E)** Wapl knockdown rescues the Smc3^{AA} phenotype. HEK293T cells were largely treated as described in (A-C). All samples were transfected with siRNA targeting *SMC3*. Simultaneously, cells were transfected with siRNA targeting either *GL2* (luciferase, control) or *WAPL*, and plasmids coding for either Smc3^{WT}-FRB or Smc3^{AA}-FRB. **(D)** Western blot demonstrates successful knockdown of Wapl and the expression of the Smc3 variants. **(E)** Quantification of the IdU-CldU pulse chase fiber assay shows the relative length of IdU-CldU-labeled DNA fibers ("tracks") in Smc3^{AA}-FRB-expressing cells compared to cells expressing the wild type version. Also compared are the effects of the Wapl-knockdown for each Smc3 variant. All track lengths are quantified relative to Smc3^{WT}-FRB expressing cells without Wapl knockdown (set to 1). Each column displays the median length of 100 tracks derived from two independent experiments. Whiskers represent SEM.

lengths in two independent experiments by about 50%, simultaneous depletion of Wapl fully rescued this phenotype (Figure 23 E). From this, I conclude the IdU-CldU pulse chase DNA fiber assay to be suitable to investigate the effects of cohesin dynamics on replication fork progression.

Replisome processivity phenotypes observed on single replication forks do not necessarily translate to global replication, since healthy cells are able to counteract such issues (at least to a certain extent) by firing dormant replication origins (reviewed in Blow *et al*, 2011). To evaluate, whether this is also the case, when replication fork progression is compromised due to impaired cohesin dynamics, I sought to analyze global replication using flow cytometry. The method is based on labeling DNA that is being replicated with yet another nucleotide analog, called 5-ethynyl-2'-deoxyuridine (EdU). EdU has an advantage over the other analogs in that it can be stained chemically using a fluorophore-coupled azide (for details, see materials and methods). Cells that have been incubated with EdU are harvested, fixed and then incubated with a reaction cocktail including the fluorophore-coupled (in this case Alexa Fluor 488) azide. After this, total DNA is co-stained using the intercalating agent propidium iodide (PI). Measuring the PI fluorescence for each individual cell using a flow cytometer gives an overview over the amount of cells in a population currently undergoing certain cell cycle stages (Figure 24 A). Since the PI and Alexa Fluor 488 emission spectra are quite different, both their values can be measured at the same time and plotted in a single graph, which allows a simple visual interpretation of global replication in a given cell population (Figure 24 B). Expectedly, cells treated as described for the experiments in Figure 23 do not differ in global EdU incorporation, independent of whether they express Smc3^{WT} or non-acetylatable Smc3^{AA}, confirming that

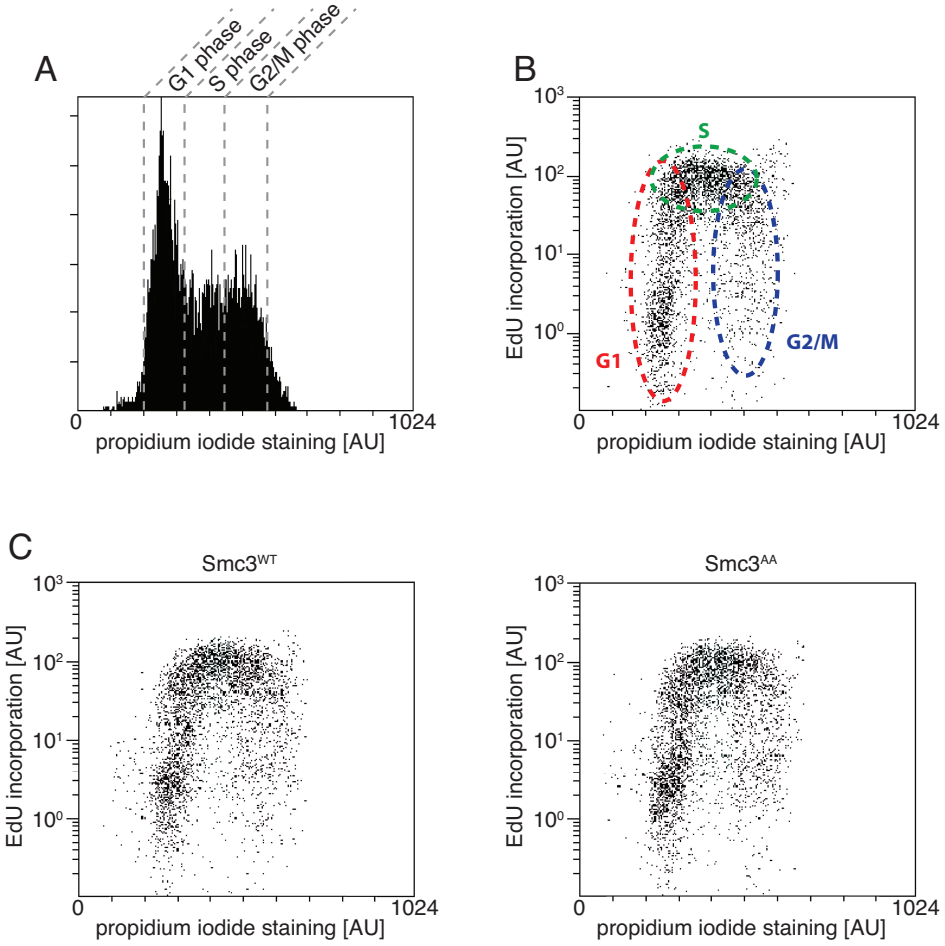

Figure 24 | Global replication appears normal in cells with perturbed cohesin dynamics. (A, B) Unsynchronized HEK293T cells were pulse labeled with 10 μM EdU for 90 min and then harvested for propidium iodide staining of total DNA and EdU detection with an Alexa Fluor 488-coupled azide covalently binding to the nucleotide analog (for details, see materials and methods). **(A)** Typical cell cycle profile of an unsynchronized cell population judged by propidium iodide-stained total DNA content of each individual cell. Cells that are in G1-, S- or G2/M-phase can be discriminated. **(B)** Plotting EdU incorporation against propidium iodide staining gives a more precise overview on global replication. G1- (red) and G2/M-phase (blue) can be clearly distinguished from S phase (green). **(C)** Reduced progression of single replication forks due to perturbed cohesin dynamics caused by expression of Smc3^{AA} does not translate to reduced global replication. HEK293T cells were treated as described in Fig. 23 A-C, but after two days of knockdown/ expression, cells were EdU pulse labeled and stained as described for (A, B).

reduced progression of single replication forks due to impaired cohesin dynamics do not cause global replication deficiency (Figure 24 C).

From my initial experiments, I conclude that I am able to adequately measure replication fidelity on single replication forks using an IdU-CldU pulse chase in combination with a DNA fiber assay. I validated this assay reproducing published phenotypes associated with impaired cohesin dynamics. It is certainly an interesting question, why blocking cohesin acetylation, typically associated with stable cohesin-DNA interaction, reduces replisome progression and even more so, why depletion of Wapl does rescue this

phenotype. While we don't exactly know the answers yet, I will touch upon these efects in the discussion (see chapter 3.2.1). Finally, it is important to mention that these phenotypes do not translate to global cellular replication, since otherwise unperturbed cells are demonstrably able to counteract processivity phenotypes on single replication forks by dormant origin firing. As a consequence, all further experiments will employ DNA fiber assays, when it comes to assessing replication phenotypes upon cohesin-gate closure.

2.2.2 Assessing the role of cohesin dynamics for replication

The first question I wanted to address was whether opening of a cohesin gate during S phase is required for proper replication fork progression. To this end, the doubly stable FRB/FKBP cohesin subunit cell lines were transfected with siRNAs targeting individual mRNAs giving rise to cohesin subunits, which were to be replaced by tailored versions. Simultaneously, transgene expression was induced by doxycycline (dox)-addition. After three days, cells were pulse-labeled first with IdU, then with CldU (20 minutes each). Rapamycin (rapa) was not added until addition of IdU to study the effects of compromised cohesin dynamics in S phase directly. Please note that the cell lines were not (pre-)synchronized, as this is not necessary because only DNA of replicating cells (i.e. cells in S phase) is labeled and can afterwards be identified in the analysis. After labeling, cells were harvested for Western blot analysis (Figure 25 A) and DNA fiber assays (Figure 25 B). Although replacement of endogenous cohesin subunits with FRB/FKBP-tagged versions proved to be quite efficient (Figure 25 A), rapamycin-addition during replication did not cause altered replication fork dynamics in neither of the three cell lines (Figure 25 B). This impression was confirmed by quantification of two independent experiments (Figure 25 C).

I have previously demonstrated that the IdU-CldU pulse chase DNA fiber assay can adequately reflect replication fork progression and, furthermore, that rapamycin can efficiently close at least the DNA entry and exit gates of FRB/FKBP-tagged cohesin rings. Thus, I must conclude that, in fact, DNA replication does not require cohesin gate opening during S phase. But how can this result be reconciled with the fact that defective replication fork progression can be demonstrably induced by other means of compromising cohesin dynamics, namely expression of non-acetylatable Smc3 ($Smc3^{AA}$; see Figure 23)? This apparent discrepancy might lie in the fact that cohesin dynamics are abrogated with very precise timing using the FRB/FKBP system, while $Smc3^{AA}$ is expressed over the

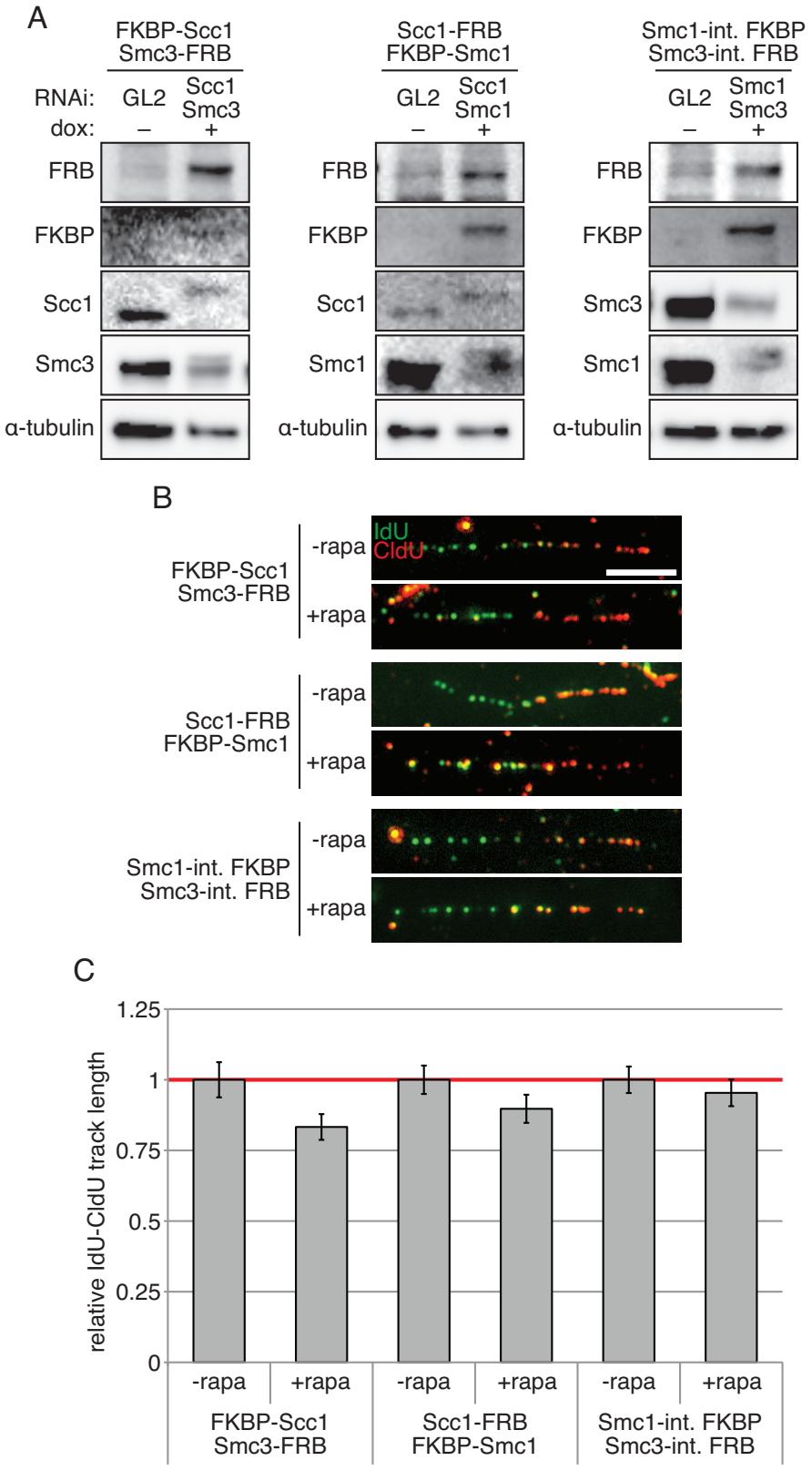

Figure 25 | Disturbance of cohesin dynamics in G1 phase negatively affects replication fork progression in the subsequent S phase. Doubly transgenic FRB/FKBP-tagged cohesin subunit cell lines were induced by doxycycline (dox) addition and transfected with siRNAs targeting the mRNAs of either GL2 (luciferase, control) or a pair of cohesin subunits which were to be replaced by transgenic FRB/FKBP-tagged counterparts. After three days, cells were subjected to an IdU-CldU pulse chase, while adding rapamycin (+rapa) or DMSO (-rapa) simultaneously with IdU. After the pulse chase, cells were harvested for a DNA fiber assay. **(A)** Western blot demonstrates successful knockdown of endogenous cohesin subunits and the

Figure 25 (cont.) | doxycycline (dox)-inducible expression of the FRB/FKBP-tagged variants. Please note that the low FKBP-signal observed for the FKBP-Scc1/Smc3-FRB cell line is due to high dilution of the sample but successful expression can also be appreciated from the Scc1 blot. **(B)** Immunofluorescence-microscopic analysis of the DNA fiber assay shows no reduction of replication fork progression when individual cohesin gates are closed during the pulse chase. Scale bar = 5 μm. **(C)** Quantification of the IdU-CldU pulse chase fiber assay shows the relative length of IdU-CldU-labeled DNA fibers ("tracks") in FRB/FKBP-tagged cohesin subunits expressing cells that have been induced to close their respective gates (+rapa) during replication compared to tracks from cells with unperturbed gates (-rapa; set to 1). Each column displays the median length of 100 tracks derived from two independent experiments. Whiskers represent SEM.

course of the entire experiment. This means that, while ring gate-opening during S phase might not be required for proper replication fork progression, cohesin dynamics before S phase might very well be. Since mammalian cohesin is loaded onto DNA in telophase, the observed issues most probably manifest in G1 phase. In fact, cohesin has been proven to be very dynamic in this phase, which has been associated with non-canonical cohesin-functions including gene regulation and organization of chromatin structure (Gerlich *et al*, 2006; Tedeschi *et al*, 2013; Merkenschlager & Odom, 2013). To investigate whether proper pre-S phase cohesin dynamics contribute to normal replication fork progression, I repeated the experiment from Figure 25 but added rapamycin nine hours before IdU-CldU pulse labeling, i.e. at a time, when cells that will appear in the analysis, are most probably in G1 phase. All three doubly stable cell lines expressing FRB/FKBP-tagged cohesin subunits as replacement for their RNAi-depleted endogenous counterparts (Figure 26 A), exhibited normal replication fork velocities as long as no rapamycin was present (Figure 26 B). Strikingly, when either cohesin's entry or exit gate was forced shut by rapamycin-addition, replication fork velocity dramatically decreased, while a constitutively closed Scc1-Smc1 gate did, again, not give rise to any phenotype. Quantification of two independent experiments revealed that fork progression dropped by about 75% compared to the -rapa-controls in both cases (Figure 26 C), arguing that proper cohesin dynamics in G1 phase are indeed essential for efficient replication fork progression.

Similar to earlier experiments, one must exclude any involvement of putative Scc1-Smc1 gate dynamics for replication, since the absence of any phenotype could be explained by the respective FRB/FKBP-tags failing to dimerize. Therefore, the HEK293 cell line stably expressing an Scc1-Smc1 fusion protein featuring a covalently closed gate (see also chapter 2.1.6) was transfected with siRNAs targeting the mRNAs of either *GL2* (luciferase, control) or *SCC1* and *SMC1*. At the same time, ethanol (control) was added to the GL2-knockdown cells (these cells retain endogenous cohesin), while doxycycline was

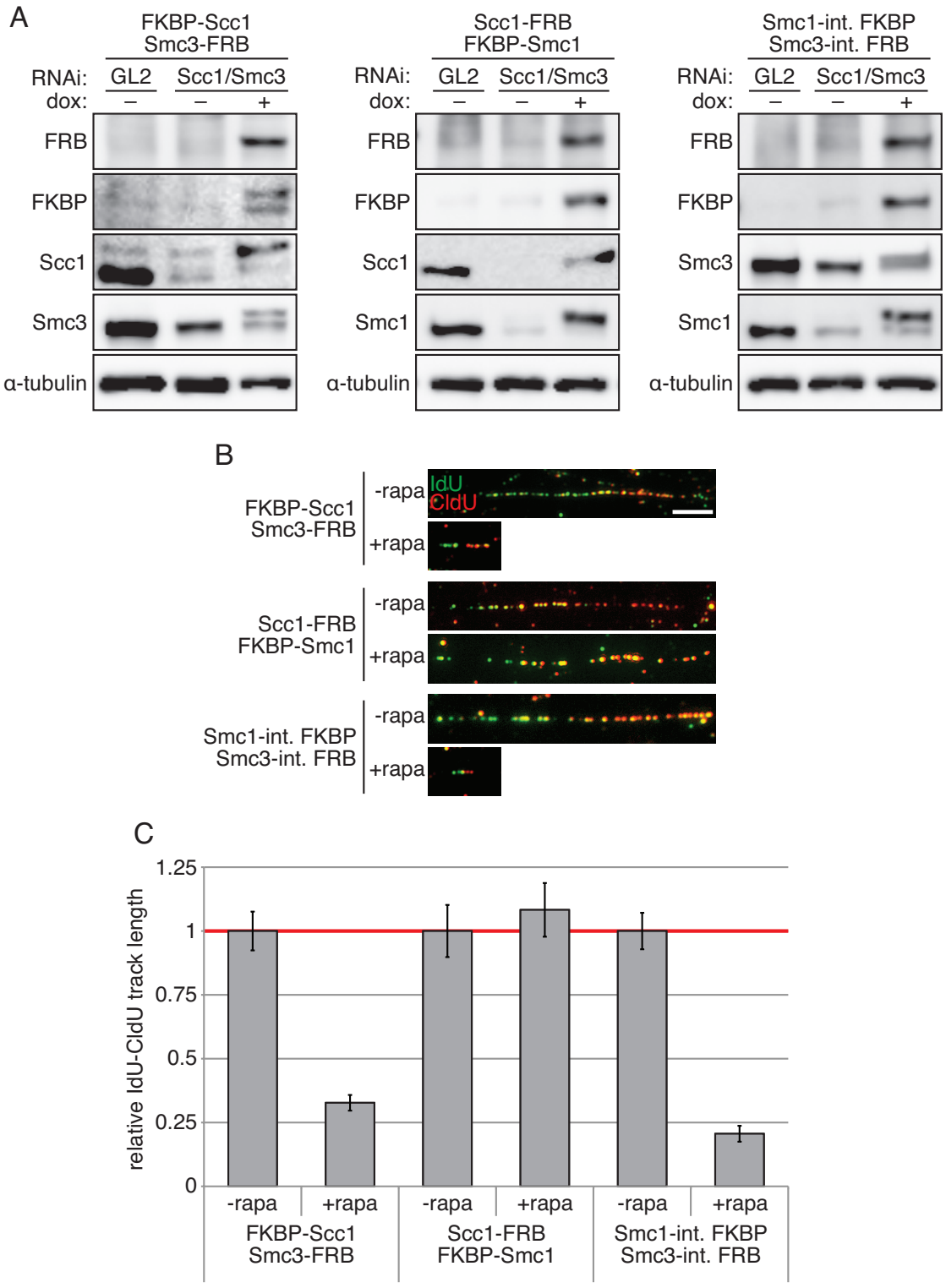

Figure 26 | Disturbance of cohesin dynamics in G1 affects replication fork progression in the subsequent S phase. Doubly transgenic FRB/FKBP-tagged cohesin subunit cell lines were induced by doxycycline (dox) addition and transfected with siRNAs targeting the mRNAs of either GL2 (luciferase, control) or a pair of cohesin subunits which were to be replaced by transgenic FRB/FKBP-tagged counterparts. After three days, cells were subjected to an IdU-CldU pulse chase, while rapamycin (+rapa) or DMSO (-rapa) was added 9 h before that (i.e. in G1 phase). After the pulse chase, cells were harvested for a DNA fiber assay. **(A)** Western blot demonstrates successful knockdown of endogenous cohesin subunits and the doxycycline (dox)-inducible expression of the FRB/FKBP-tagged variants. **(B)** Immunofluorescence-microscopic analysis of the DNA fiber assay shows a dramatic reduction of replication fork progression when

Figure 26 (cont.) | individual cohesin gates are closed during the preceeding G1 phase. Scale bar = 5 μm. **(C)** Quantification of the IdU-CldU pulse chase fiber assay shows the relative length of IdU-CldU-labeled DNA fibers ("tracks") in FRB/FKBP-tagged cohesin subunits expressing cells that have been induced to close their respective gates (+rapa) during G1 phase compared to tracks from cells with unperturbed gates (-rapa; set to 1). Each column displays the median length of 100 tracks derived from two independent experiments. Whiskers represent SEM.

added to the Scc1 and Smc1-depleted cells to induce expression of the fusion protein (Figure 27 A). After three days the cells were IdU-CldU pulse-labeled and subsequently harvested for DNA fiber assays. The rationale was that if Scc1-Smc1 gate-dynamics are important for replication, then it should cause a phenotype in the IdU-CldU pulse-chase DNA fiber assay, independent of whether these dynamics are required during S phase directly or earlier in G1. Consistent with the previous experiments, expression of an Scc1-Smc1 fusion protein does not cause a pronounced phenotype associated with replication forks progression, as judged from two independent experiments (Figure 27 B).

In summary, proper replication fork progression does not seem to require opening of any cohesin gate during S phase, despite my initial experiments (see Figure 23) strongly indicating a connection between cohesin dynamics and replication. However, further investigations revealed that proper cohesin dynamics in the preceding G1 phase are

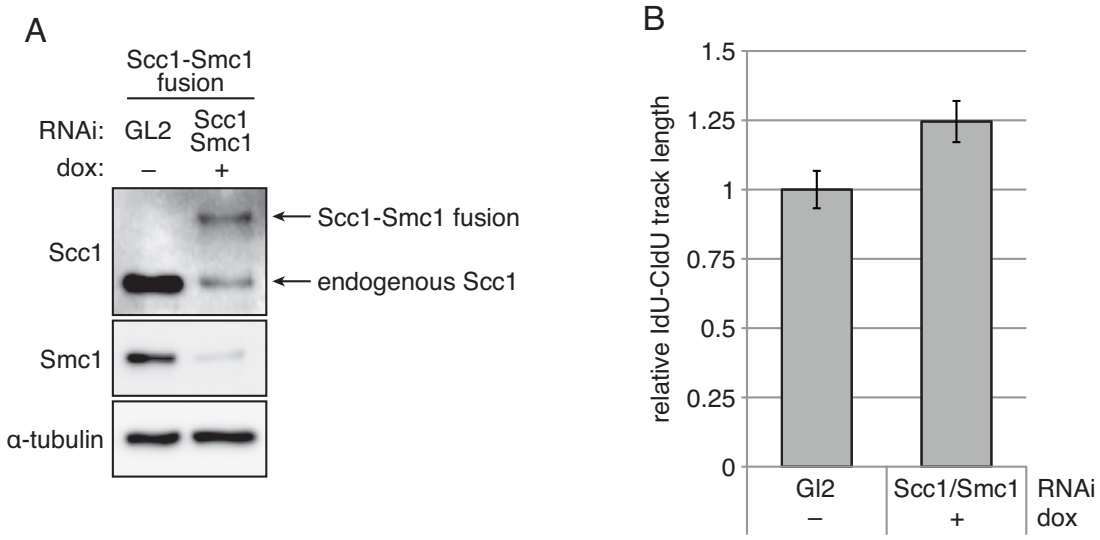

Figure 27 | **Replication fork progression does not require opening of cohesin's Scc1-Smc1 gate.** The stable Scc1-Smc1 fusion cell line was largely treated as desribed in Figure 25 while omitting rapamycin-addition and then analyzed by immunofluorescence microscopy of IdU-CldU pulse labeled DNA fibers. **(A)** The Western blot shows the knockdown of Scc1/Smc1 as well as the expression of the Scc1-Smc1 fusion protein. **(B)** Quantification of the IdU-CldU pulse chase fiber assay shows the relative length of IdU-CldU labeled DNA fibers ("tracks") in cells whose endogenous Scc1 and Smc1 have been largely replaced by the Scc1-Smc1 fusion protein (Scc1/Smc1 RNAi, +dox) compared to tracks from cells featuring endogenous Scc1 and Smc1 (GL2 RNAi, -dox). Each column displays the median length of 100 tracks derived from two independent experiments. Whiskers represent SEM.

indeed integral for unperturbed replication fork movement: artificially closing the Smc3-Scc1 gate (exit gate) or the Smc1-Smc3 gate (entry gate) both results in dramatically reduced replication fork progression. Similar to earlier experiments, the Scc1-Smc1 gate does not seem to perform any function implicated with DNA synthesis during or before S phase.

2.2.3 Further investigations on replication fork progression defects caused by compromised pre-S phase cohesin dynamics

Since cohesin's entry and exit gate are part of two diametrically opposite pathways, it is difficult to fathom why disabling either gate would cause the same replication phenotype. Moreover, that these phenotypes can only be prompted by altered cohesin dynamics in the preceding G1 phase seems counter-intuitive. So how does cohesin gate closure in G1 phase cause phenotypes in S phase hours later? As already mentioned, cohesin is very dynamic in G1. These dynamics involve cohesin to repeatedly exit from and reload onto DNA, most likely utilizing its exit and entry gates. Under this presumption, compromising either gate's function should cause altered levels of cohesin on DNA, which could effect future cell cycle stages. More precisely, artificially closing its exit gate (Smc3-Scc1) should cause elevated levels of cohesin on DNA, while closing its entry gate (Smc1-Smc3) is supposed to cause cohesin's abundance on chromatin to decrease. To test this prediction, I established a method allowing me to specifically assess cohesin levels on chromatin of S phase cells. Therefore, I modified the EdU incorporation assay, which I previously used for flow cytometric analyses (see Figure 24), to be suitable for fluorescence microscopy, in order to visually identify cells actively undergoing replication at the time of fixation (Figure 28 A). I ultimately ended up with a protocol allowing me to pre-extract EdU-labeled cells (so remaining signals originate from stably chromatin-bound proteins) followed by combined chemical and immunofluorescent staining of EdU and cohesin (via Smc1), respectively (Figure 28 B). To put my hypothesis to a test, I repeated the experiment from Figure 26, whose conditions (essentially rapamycin-addition during G1 phase) led to the pronounced effects on replication fork progression. IdU and CldU were replaced by EdU and cells were ultimately harvested for Western blot analysis (Figure 29 A) and combined EdU staining and immunofluorescent labeling of transgenic (FRB-tagged) cohesin (Figure 29 B). The microscopic data unequivocally demonstrates that the abundance of FRB-tagged cohesin on chromatin is, indeed, substantially higher when cohesin's exit gate

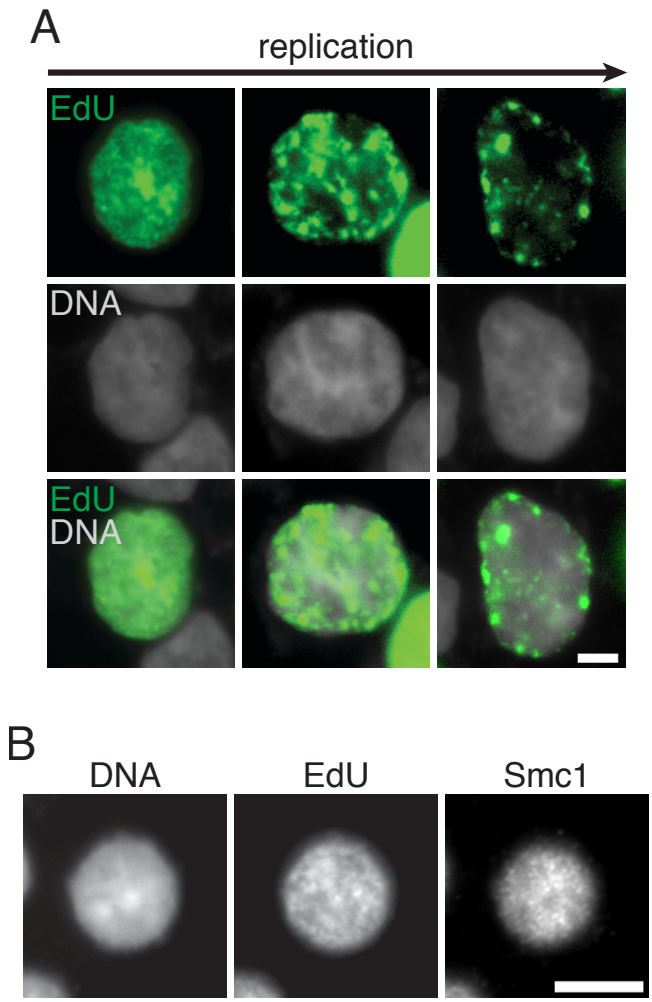

Figure 28 | **Establishment of immunofluorescence microscopy-based identification of S phase cells.** **(A)** EdU incorporation can be used to identify S phase cells in fluorescence microscopy. Unsynchronized HEK293T cells growing on cover slips were EdU pulse labeled for 90 min. Thereafter, cells were fixed before EdU was detected with an Alexa Fluor 488-coupled azide covalently binding to the nucleotide analog using a protocol optimized for fluorescence microscopy (for details, see materials and methods). Sequential stages of replication can be discriminated. Scale bar = 5 μm. **(B)** EdU labling and detection is compatible with pre-extraction and immunofluorescent labeling of additional nuclear targets. Cells were treated as described in (A) and then pre-extracted using a nuclei-permeabilizing detergent removing all soluble (not DNA-bound) proteins from the cyto- and nucleoplasm before being fixed. Using a modified EdU detection protocol (see materials and methods) allowed for additional immunofluorescent staining of Smc1. Scale bar = 10 μm.

(Smc3-Scc1) is kept shut by rapamycin-addition in the preceding G1 phase. Artificially closing the ring's entry gate (Smc1-Smc3) causes a reduction of chromatin-bound cohesin, as predicted earlier. Consistent with the absence of any phenotype in the DNA fiber analysis, the levels of the Scc1-FRB/FKBP-Smc1-containing cohesin complex on chromatin are not affected by rapamycin. Quantification of the observed fluorescence intensities, each normalized to the respective -rapa-control of the cell line, reflects the visual interpretation of the IFM data (Figure 29 C). Similar data was obtained by staining for total Smc1 (data not shown). The differences in the extent of cohesin level increase/

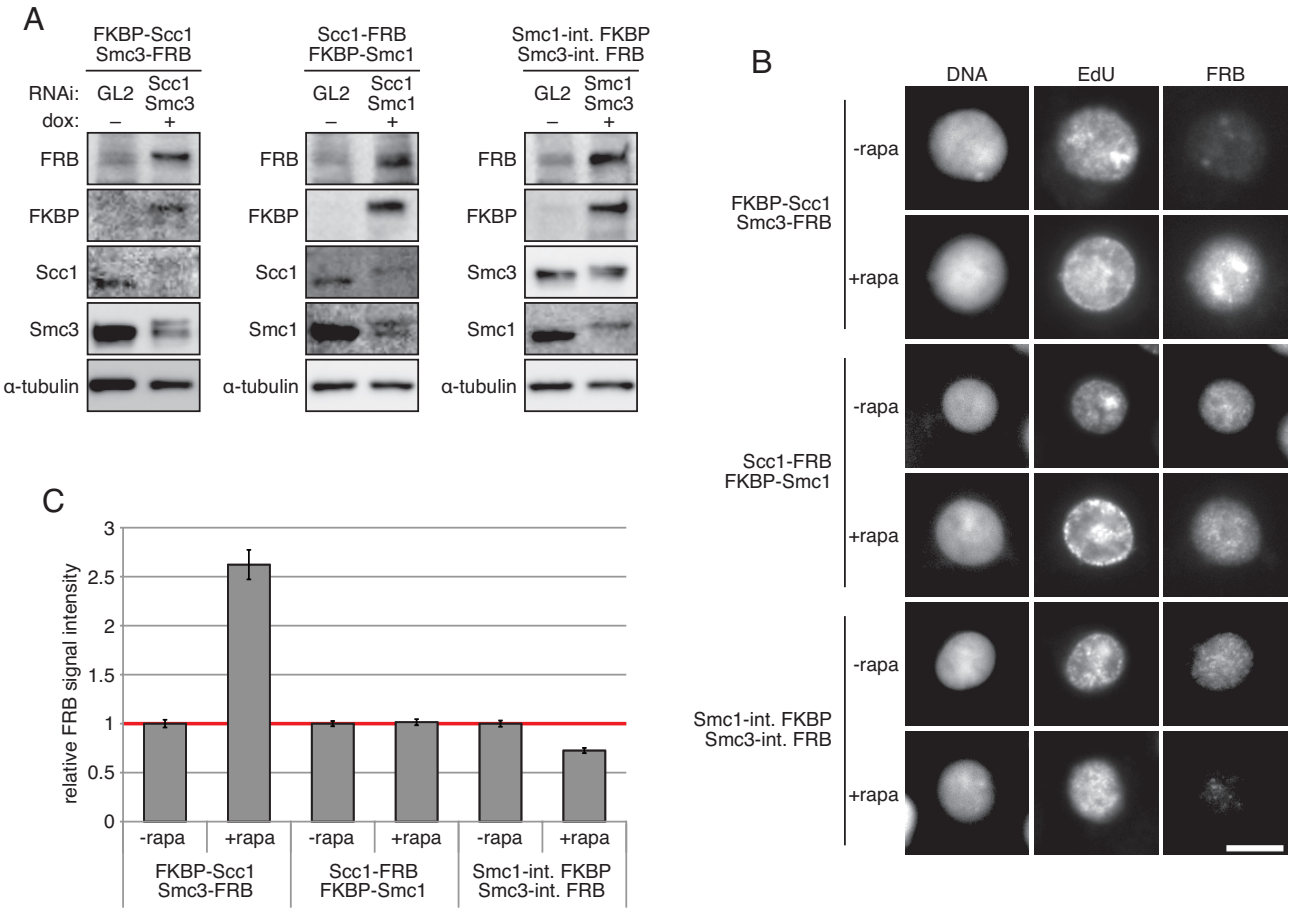

Figure 29 | Perturbed cohesin dynamics during G1 phase lead to improper cohesin levels in the following S phase. Doubly transgenic FRB/FKBP-tagged cohesin subunit cell lines were treated as described in Figure 26, while IdU/CldU incorporation was replaced by EdU. The cells were ultimately pre-extracted and fixed for EdU detection with combined immunofluorescence microscopy. **(A)** Western blot demonstrates successful knockdown of endogenous cohesin subunits and the doxycycline (dox)-inducible expression of the FRB/FKBP-tagged variants. **(B)** Immunofluorescence microscopy of the doubly transgenic cell lines shows dramatic differences in cohesin levels on chromatin, when the ring's exit or entry gates are artificially closed. Only cells that had a uniform EdU staining and were therefore believed to be in similar stages of S phase were used for analysis. Exogenous cohesin was specifically stained by using an anti-FRB antibody. Scale bar = 10 μm. **(C)** Quantification of the relative FRB signal intensity in cells with closed cohesin gates (+rapa) compared to cells with unperturbed gates (-rapa; set to 1). Each column represents the median of the FRB signal intensities of 50 EdU co-labeled cells. Whiskers represent SEM.

decrease observed between the cell lines are probably caused by endogenous subunits being more efficiently replaced in the exit gate than those in the entry gate cell line, owing to the fact that Scc1 is typically depleted more effectively than Smc1.

As already mentioned, it is widely believed that interphase cohesin dynamics rely on the same mechanisms of cohesin release from and reloading onto DNA in pro- and telophase, respectively. Proper cohesin levels on interphase chromatin, for example, have been shown to be dependent on the presence of Wapl (Kueng *et al*, 2006). We know that Wapl depletion is functionally equal to exit gate closure, at least in mitosis, as cohesin's

association with chromatin is prolonged into prometaphase in both respective experiments (compare Figures 9 and 16). Based on these facts, I predicted that 1) since Wapl depletion and exit gate closure should be functionally equal, combining these two conditions should cause no additional phenotype in S phase and 2) depletion of Wapl and artificially closing cohesin's entry gate should have opposing effects, therefore combining these two conditions should rescue the replication phenotype observed upon entry gate closure alone. To test these predictions, I repeated the experiment from Figure 26, which displayed dramatically reduced replication fork progression upon artificial entry or exit gate closure in G1 phase, but additionally transfected the three cell lines with siRNAs targeting the mRNA of Wapl at the beginning of the experiment. Western blot analysis confirmed efficient replacement of endogenous cohesin by tailored versions as well as successful depletion of Wapl (Figure 30 A). As predicted, quantification of two independent DNA fiber assays demonstrated that Wapl depletion has no additional effect on replication fork progression (Figure 30 B), compared to artificial exit gate closure alone (compare Figure 26). Unexpectedly however, IdU-CldU track length was reduced by only 50% (Figure 30 B) as compared to around 70% (Figure 26 C). This apparent discrepancy might just reflect normal experimental variation but could also be attributable to an interesting replication phenotype that has been previously associated with Wapl depletion (Terret *et al*, 2009; further discussed in chapter 3.2.1). My second prediction stated that Wapl depletion should rescue the replication phenotype caused by artificially closing cohesin's entry gate (Smc1-Smc3). Indeed, this prediction is completely fulfilled, as judged by quantification of the respective IdU-CldU track lengths.

In conclusion, I have successfully demonstrated that artificially closing cohesin's entry gate (constituted by Smc1 and Smc3) in G1 phase causes reduced levels of cohesin on chromatin due to compromised DNA loading. Furthermore, I could show that closing cohesin's exit gate (constituted by Smc3 and Scc1) results in highly elevated abundance of cohesin on chromatin. These results complement previous findings of various groups and directly demonstrate that G1 cohesin dynamics rely on the same mechanisms as those observed in pro- and telophase, including the essential role of Wapl. As I previously mentioned, these ring dynamics are tightly controlled and most probably serve various purposes and I have demonstrated one of these purposes to be proper replication fork progression.

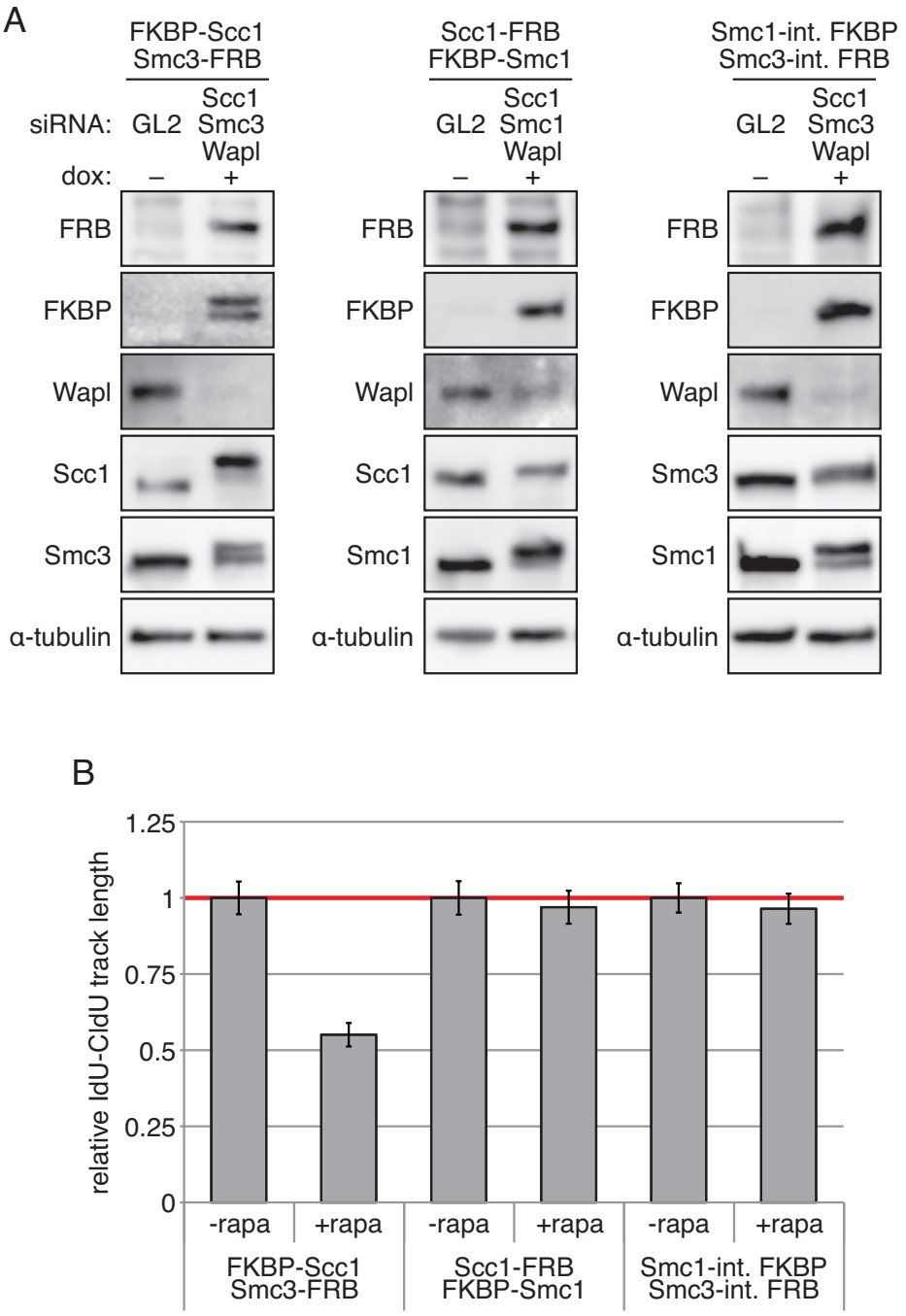

Figure 30 | Wapl knockdown restores reduced replication fork velocities upon entry gate closure in G1 to normal levels. Cells were treated as described in Fig. 26 but were additionally transfected with siRNA targeting Wapl. **(A)** Western blot demonstrates successful knockdown of endogenous cohesin subunits including Wapl and the doxycycline (dox)-inducible expression of the FRB/FKBP-tagged variants. **(B)** Quantification of an IdU-CldU pulse chase fiber assay shows the relative length of IdU-CldU-labeled DNA fibers ("tracks") in FRB/FKBP-tagged cohesin subunits expressing cells that have been induced to close their respective gates (+rapa) during G1 phase compared to tracks from cells with unperturbed gates (-rapa; set to 1). Each column displays the median length of 100 tracks derived from two independent experiments. Whiskers represent SEM.

2.3 Cohesin dynamics at the centrosome and their regulation by Sgo1 splice variants

2.3.1 Differently spliced Sgo1 variants perform different cellular functions

Depleting Sgo1 in human cells causes two main phenotypes, premature sister chromatid separation and precocious centriole disengagement, consistent with roles for Sgo1 at the chromosomes as well as the centrosomes (Wang *et al*, 2008; Schöckel *et al*, 2011). Interestingly, it has been suggested that these two functions are, in fact, performed by two different mRNA splice variants of Sgo1. So has it been demonstrated that the canonical Sgo1 isoform Sgo1 A1 localizes to and functions on centromeres, while a shorter Sgo1 variant called Sgo1 C2 (formerly sSgo1) performs its functions at the centrosomes (Wang *et al*, 2006; 2008). The transcripts of Sgo1 A1 and C2 are quite different in their exon composition as the latter lacks a peptide encoded by the relatively large exon 6 but, in contrast to Sgo1 A1, retains a short peptide encoded by exon 9. It was proposed that the lack of the exon 6-encoded peptide renders Sgo1 from a protector of centromeric to a protector of centrosomal cohesin. Since involvement of the exon 9-encoded peptide has never been empirically disproven, we decided to investigate this instance to gain further insights into the exact nature of Sgo1's change of function. Therefore, our group created plasmid constructs harboring the open reading frames of the four main Sgo1 splice variants Sgo1 A1, A2, C1 and C2 (Figure 8). We first wanted to determine, whereto these differently spliced Sgo1 isoforms would localize. Therefore, based on the constructs illustrated in Figure 8, stably transgenic HEK293 cell lines were created that conditionally expressed one of the various Sgo1 isoforms each with an N-terminal Myc_6-tag. After 24 hours of induction with doxycycline (dox), endogenous Sgo1 was depleted by transfecting the cells with siRNAs directed against the UTRs of its target's mRNA (which makes our other UTR-containing constructs naturally resistant against this treatment). The cells, which were grown on cover slips, were pre-extracted and fixed for (immuno-)fluorescence microscopy, staining DNA (Hoechst 33342) and Myc (Sgo1). As markers for the cellular structures known to recruit Sgo1, centrosomes were co-stained using an anti-centrin2 antibody, while centromeres were marked by an anti-CREST staining (Figure 31). Analysis of the microscopy data confirmed that canonical Sgo1 A1 colocalized with centromeric CREST-staining, while the shorter Sgo1 C2 was clearly associated with the centrosomal centrin2-marker. Strikingly, Sgo1 C1, which is characterized by lacking both peptides encoded by exon 6 (similar to Sgo1 C2) and exon 9 (as in Sgo1 A1), localized to the

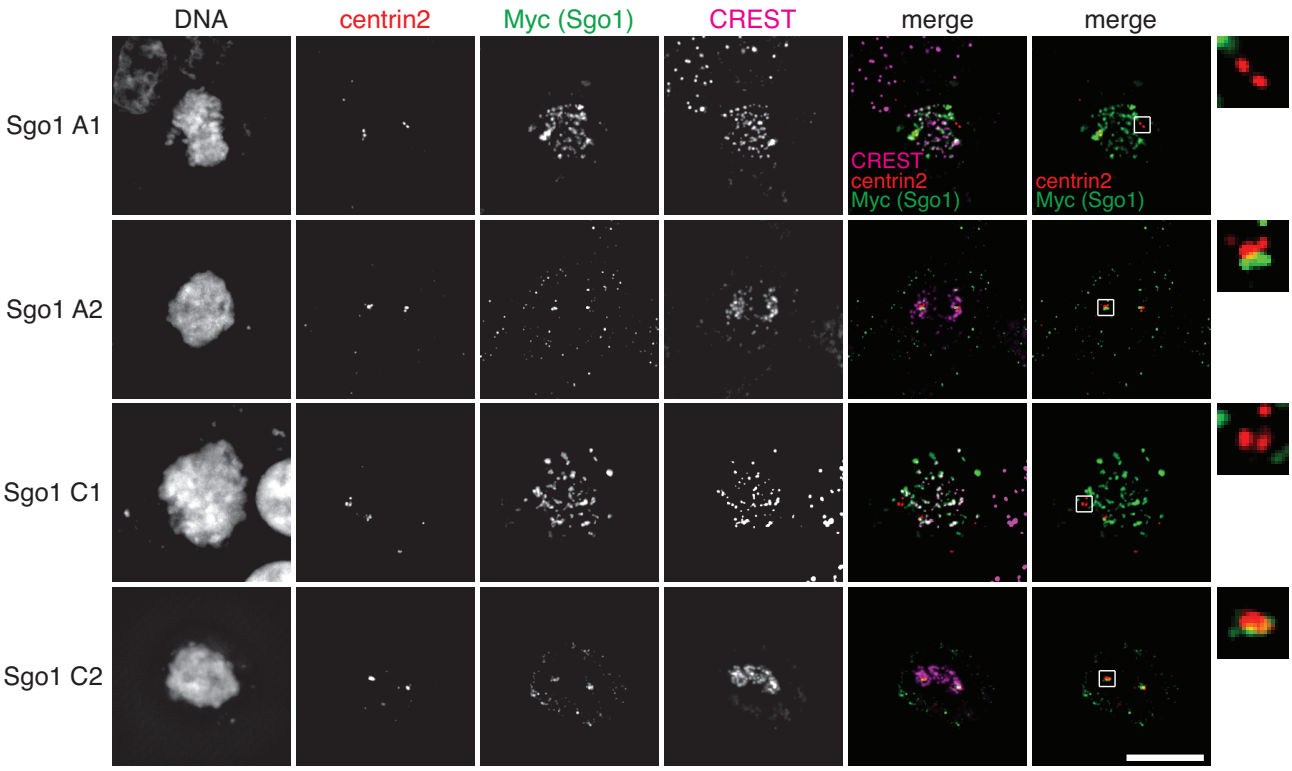

Figure 31 | Alternatively spliced Sgo1 variants locate to either the centromere or the centrosome in a mutually exclusive manner. Sgo1 isoforms containing the peptide encoded by exon 9 localize to the centrosomes (all "2" isoforms), while all Sgo1 variants devoid of this peptide do not (all "1" isoforms). Stable HEK293 cell lines harboring the ORFs of the various N-terminally Myc_6-tagged Sgo1 isoforms were induced by doxycycline addition to allow expression of the transgenes for 48 h. 24 h before harvesting, cells were transfected with siRNA targeting endogenous Sgo1. Cells were CSK pre-extracted (see materials and methods) and fixed for (immuno-)fluorescence microscopy using Hoechst 33342 as a DNA marker and indicated antibodies to stain for centrin2 (centrosome marker), Myc (Sgo1 isoforms) and CREST (centromere marker). Scale bar = 10 μm. Indicated centrosomes were magnified by 500%.

centromeres. Moreover, Sgo1 A2, which is very similar to Sgo1 A1 with the exception of additionally featuring the small C-terminal exon 9-encoded peptide (only 40 aa), loses its centromeric association in favor of a centrosomal one. From these experiments, we must conclude that it is not the lack of "exon 6" but the presence of the peptide encoded by exon 9, which drives centrosomal localization of Sgo1. Due to these results we have named the region encoded by exon 9, the "centrosomal targeting signal of Sgo1" or in short "CTS". Further analyses from our group have shown that function (almost) always follows localization, as the centromeric Sgo1 A1 is exclusively able to rescue premature sister chromatid separation upon siRNA-mediated depletion of endogenous Sgo1, whereas all centrosomal Sgo1 isoforms ("2" isoforms) are only proficient in rescuing premature centriole disengagement in the same scenario (Mohr *et al*, 2015). The only exception from this rule is the minimal variant Sgo1 C1, which lacks both peptides encoded by exons 6 and 9: Despite its centromeric localization, it is deficient in rescuing

associated (or any other) phenotypes. On the contrary, its overexpression leads to dominant-negative effects (Mohr *et al*, 2015).

There are generally two options for how the CTS might confer centrosomal localization: 1) It might act indirectly, e.g. by changing the protein's tertiary structure, thereby increasing Sgo1's affinity towards centrosomes or 2) directly by functioning as a centrosomal localization signal itself, e.g. by binding to a centrosomal target. If the latter is true, than transferring the CTS to an unrelated protein should drive its localization to the centrosomes. To test this prediction, I transfected a construct harboring the mCherry marker protein N-terminally fused to the last 40 amino acids of Sgo1 A2 (aa521-561; "mCherry-CTS"), into HEK293T and HeLa L cells. After 30 hours of expression, cells were pre-extracted, fixed and ultimately (immuno-)stained for DNA (Hoechst 33342), γ-tubulin (centrosomal marker) and mCherry (Figure 32 A). IFM analysis revealed that the CTS efficiently drives mCherry-localization to the centrosomes in both HEK293T and HeLa L cells, unambiguously establishing the exon 9-encoded peptide as a transferable centrosomal localization signal. Further analysis of the CTS peptide sequence uncovered a short but conserved patch of amino acids, which proved to be quintessential for competent centrosomal localization: Mutating only three of Sgo1 A2's amino acids 535-ILY-537 to alanines (CTS^{AAA}) completely abrogates mCherry-CTS localization to centrosomes (Figure 32 A). More impressively, inserting the AAA-mutation into full length Sgo1 A2 (Sgo1 $A2^{AAA}$) not only abrogates its centromeric localization but reverts Sgo1 A2 into a Sgo1 A1-like centromere-associated protein as judged by co-localization with CREST (Figure 32 B). Even more strikingly, Sgo1 $A2^{AAA}$ appears to be functionally reprogrammed as the mutant loses its ability to suppress premature centriole disengagement upon depletion of endogenous Sgo1 but instead gains the function as a protector of sister chromatid separation (Mohr *et al*, 2015).

My experiments unambiguously identified the peptide encoded by exon 9 of respective Sgo1 transcripts as the centrosomal targeting signal of Sgo1 (CTS). These results contradict the previously published notion of centrosomal localization being conferred by the absence of the exon 6-encoded peptide (Wang *et al*, 2008; see discussion chapter 3.3.1 for more details). The CTS constitutes a transferable centrosome localization signal suggesting it to directly interact with a centrosomal target. In fact, mutation of only three consecutive amino acids in the exon 9-encoded peptide to alanines completely diminishes centrosomal localization of mCherry-CTS^{AAA} and full-length Sgo1 $A2^{AAA}$. These localization data are complemented by functional studies, confirming that

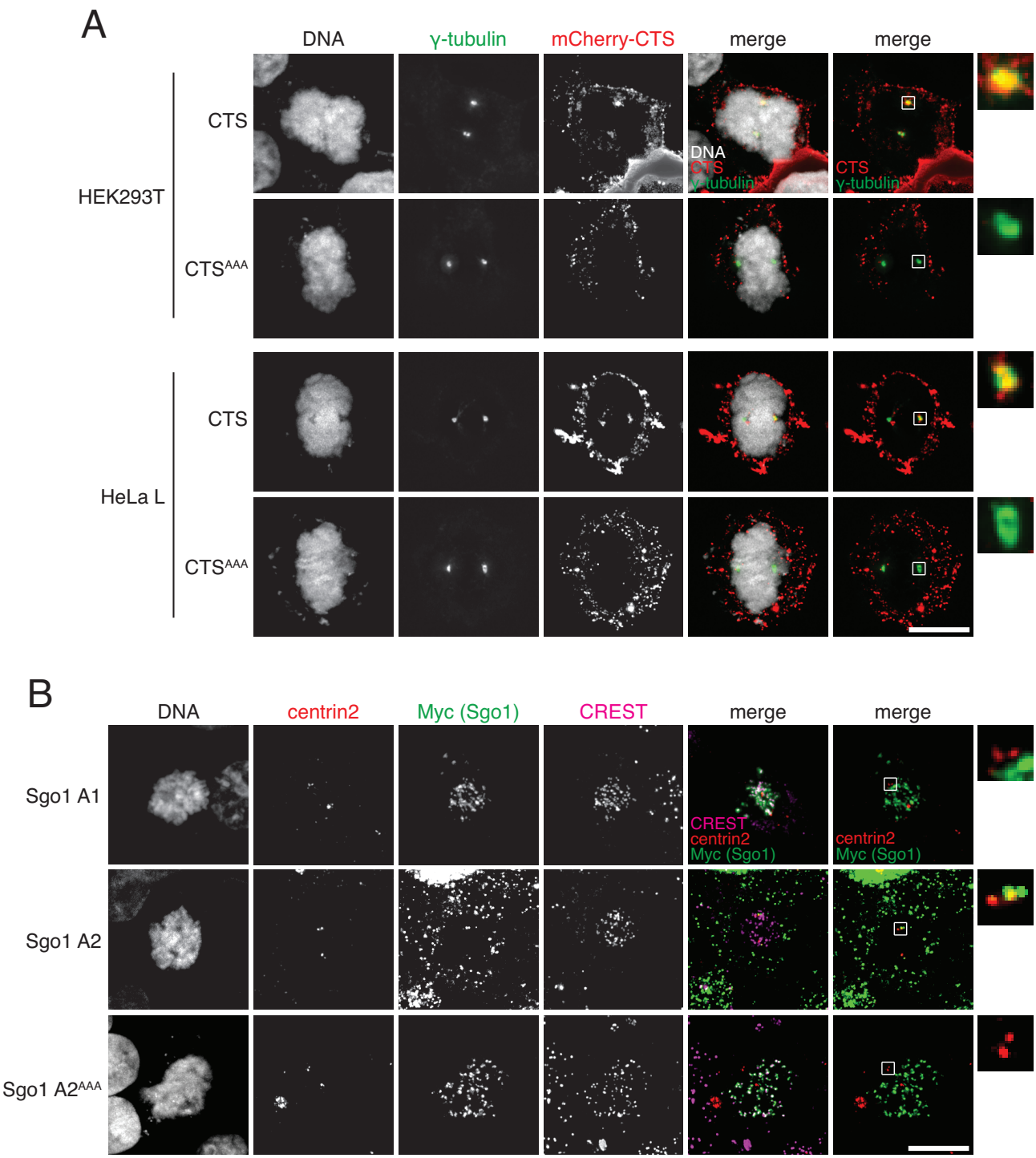

Figure 32 | The C-terminal 40 amino acids encoded by exon 9 ("CTS") are sufficient to mediate centrosomal localization in mammalian cells. (A) The C-terminal 40 amino acids of Sgo1 A2 ("CTS") and a mutant version thereof (535-ILY-537 to 535-AAA-537; "CTS^{AAA}") were C-terminally fused to mCherry and transfected into HEK293T and HeLa L cells. After 30 h expression, cells were CSK pre-extracted and fixed for (immuno-)fluorescence microscopy using Hoechst 33342 as a DNA marker and indicated antibodies to stain for γ-tubulin (centrosome marker) and mCherry (mCherry-CTS or mCherry-CTS^{AAA}). **(B)** Mutation of only three amino acids (ILY to AAA) in the exon 9 encoded peptide of Sgo1 A2 (Sgo1 A2^{AAA}) is sufficient to abrogate Shugoshin's binding to the centrosome. Stable HEK293 cell lines harboring the ORFs of the indicated N-terminally Myc$_6$-tagged Sgo1 isoforms were treated and analyzed as described in Fig. 23 B. Scale bars = 10 μm. Indicated centrosomes were magnified by 500%.

centrosomal Sgo1 isoforms exclusively protect centriole engagement, while centromeric Sgo1 A1 is selectively functional on the level of sister chromatid cohesion (Mohr *et al*, 2015).

2.3.2 The role of the prophase pathway on centrosomes

Does Sgo1 protect centriole disengagement by protecting cohesin? If this prediction were true, one should be able to prevent centriole disengagement in response to Sgo1 knockdown, by ectopically closing cohesin's exit gate (Smc3-Scc1). Therefore, I treated the doubly stable FRB/FKBP-tagged cohesin subunit cell lines, allowing ectopic closure of all three cohesin gates individually, as outlined in Figure 33 A. The three cell lines were transfected with siRNAs targeting the mRNAs of two cohesin subunits, which were to be replaced by transgenic ones. At the same time, doxycycline was added to induce transgene expression. The cells were synchronized at the G1/S barrier by addition of thymidine for 31.5 hours. Six hours before releasing the cells from the thymidine arrest, *SGO1*-siRNAs were transfected. The cells were then allowed to traverse through S phase before taxol was added, which stabilizes microtubules and causes cells to arrest in the following prometaphase due to activation of the tension-sensitive branch of the mitotic checkpoint. At the same time, rapamycin or DMSO (control) was added for a total of 13 hours before cells were harvested and split for three different analyses: A Western blot was to ensure that endogenous cohesin was efficiently replaced by FRB/FKBP-tagged variants (Figure 33 B), chromosome spreads demonstrated the effects of Sgo1-depletion and ectopic cohesin gate closure on sister chromatids (Figure 33 C), and IFM analysis of isolated centrosomes documented the effects on centrioles (Figure 33 D). As already explained above, depletion of Sgo1 causes sister chromatids to separate prematurely, which is evident by chromosomes spreading into single chromatid threads (Figure 33 C, upper panel left). Typically, around 80% of nuclei exhibit a "separated" phenotype under these conditions. Abrogating prophase pathway-dependent opening of cohesin's Smc3-Scc1 exit gate by rapamycin-addition, rescued the Sgo1-depletion phenotype by over 50% (phenotype shifts from "separated" to "cohesed"; Figure 33 C, upper panel right) in three independent experiments (Figure 33 C, graph). This result further substantiates the role of cohesin's Smc3-Scc1 gate in the prophase pathway on chromosomes. To analyze centriole disengagement in the same experiment, centrosomes were isolated from harvested cells by spinning them onto cover slips. Centrioles were immunofluorescently

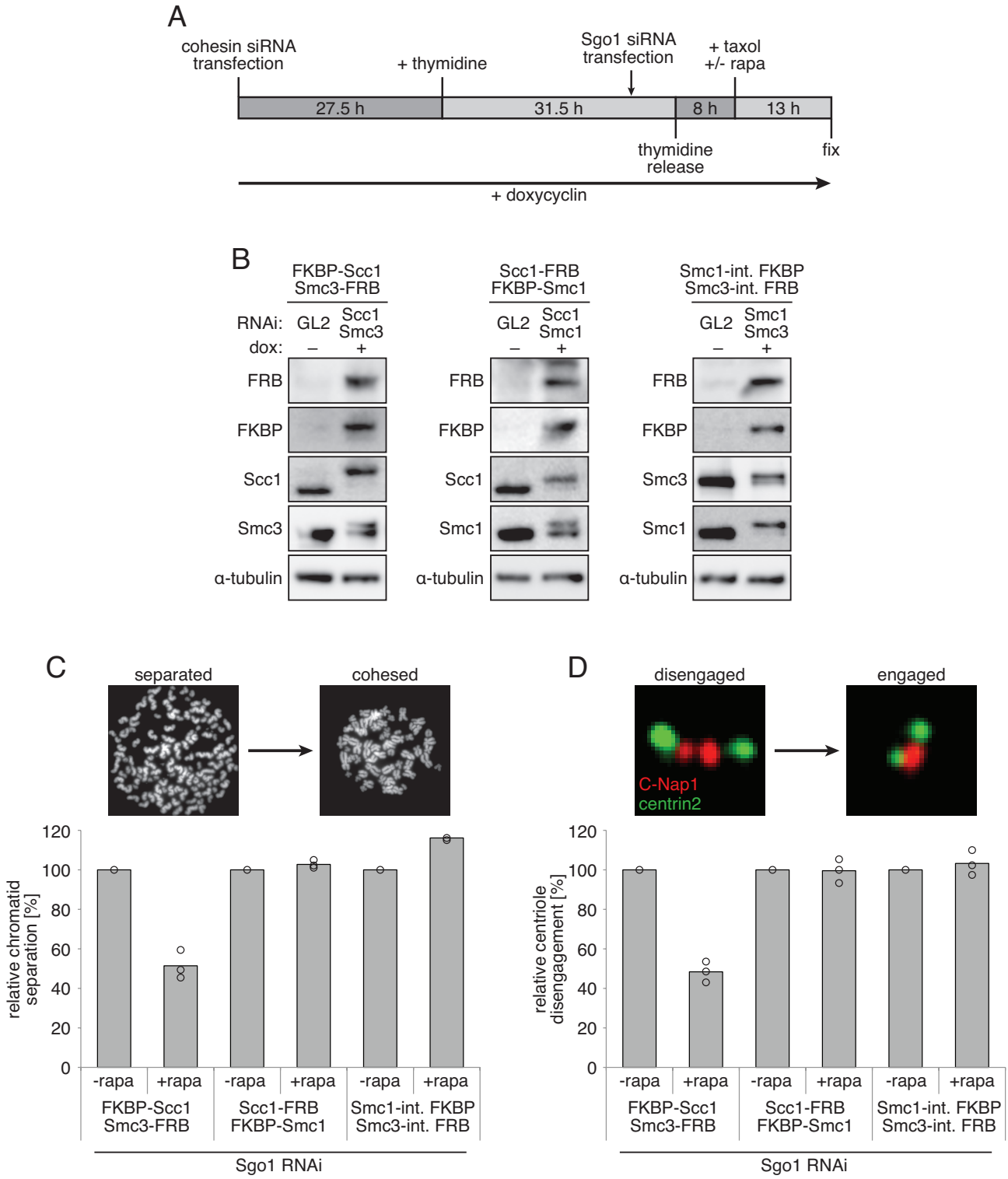

Figure 33 | Sgo1 counteracts centriole disengagement by protecting centrosomal cohesin from the prophase pathway. (A) Assay time line for results shown in (B-D). **(B-C)** Indicated doubly transgenic cell lines were treated as illustrated in (A) then subjected to chromosome spreading (C) and centrosome isolation (D). **(B)** Western blot demonstrates successful knockdown of endogenous cohesin subunits and the doxycycline (dox)-inducible expression of the FRB/FKBP-tagged variants. **(C)** Chromosomes were spread and stained with Hoechst 33342. Graph depicts the relative number of chromosome spreads displaying precocious sister chromatid separation (single chromatid threads as opposed to the typical butterfly-like morphology) normalized to the -rapa control of each cell line. Exemplary images are shown above. Each column represents the mean of three independent experiments totalling 300 analyzed cells. **(D)** Isolated

Figure 33 (cont.) | centrosomes were immunostained to visualize C-Nap1 (proximal centriole marker; red) and Centrin2 (distal centriole marker; green). Graph depicts the relative number of isolated centrosomes displaying precocious centriole disengagement (indicated by two green centrin2 dots and two red C-Nap1 dots as opposed to only one red C-Nap1 dot) normalized to the -rapa control of each cell line. Exemplary images are shown above. Each column represents the mean of three independent experiments totalling ≥300 analyzed centrosomes. Note: Centrosome isolation and quantification was performed by Lisa Mohr, University of Bayreuth, Germany.

stained for C-Nap1 (proximal centriole marker) and centrin2 (distal centriole marker) allowing us to easily discern disengaged centrioles displaying one C-Nap1 and one centrin2 dot per centriole from engaged centrioles, which are more tightly coordinated causing the C-Nap1-foci to fuse into one dot while still retaining two centrin2 signals (Figure 33 D, upper panels; red: C-Nap1, green: centrin2). Sgo1-depletion causes centriole disengagement to a similar extent as sister chromatid separation. Strikingly, only when cohesin's exit gate is artificially closed by rapamycin-addition, centriole disengagement is rescued by over 50% compared to the control in three independent experiments, causing the amount of disengaged centrioles (one red and two green dots) to decrease (Figure 33 D, graph). Similar to the situation on chromosomes, artificially closing either Scc1-Smc1 or Smc1-Smc3 gate does not cause any rescue of the Sgo1-depletion phenotype on centrosomes.

As with earlier experiments, the results from Figure 33 do not display any phenotype associated with artificially closing the Scc1-Smc1 gate. Therefore, I once again had to exclude any involvement of this gate by repeating the experiment using my cell line stably expressing the Scc1-Smc1 fusion protein (see also chapter 2.1.6), whose gate is covalently closed. Cells were treated as described in Figure 33 A (while omitting rapamycin-addition), and ultimately harvested and split for Western blot analysis (Figure 34 A), chromosome spreading (Figure 34 B), and IFM on isolated centrosomes (Figure 34 C). Despite effective knockdown of endogenous Scc1 and Smc1, and their replacement by the fusion protein (Figure 34 A), the degree of chromatid separation (Figure 34 B) and centriole disengagement (Figure 34 C) did not change significantly when compared to the individual -rapa-controls of the Scc1-FRB/FKBP-Smc1 cell line from the experiment shown in Figure 33. These results are consistent with the Scc1-Smc1 gate not assuming any role in the prophase pathway. Please note that, as this was a joint project, centrosome isolation and quantification shown in Figures 33 and 34 were performed by Lisa Mohr, University of Bayreuth, Germany.

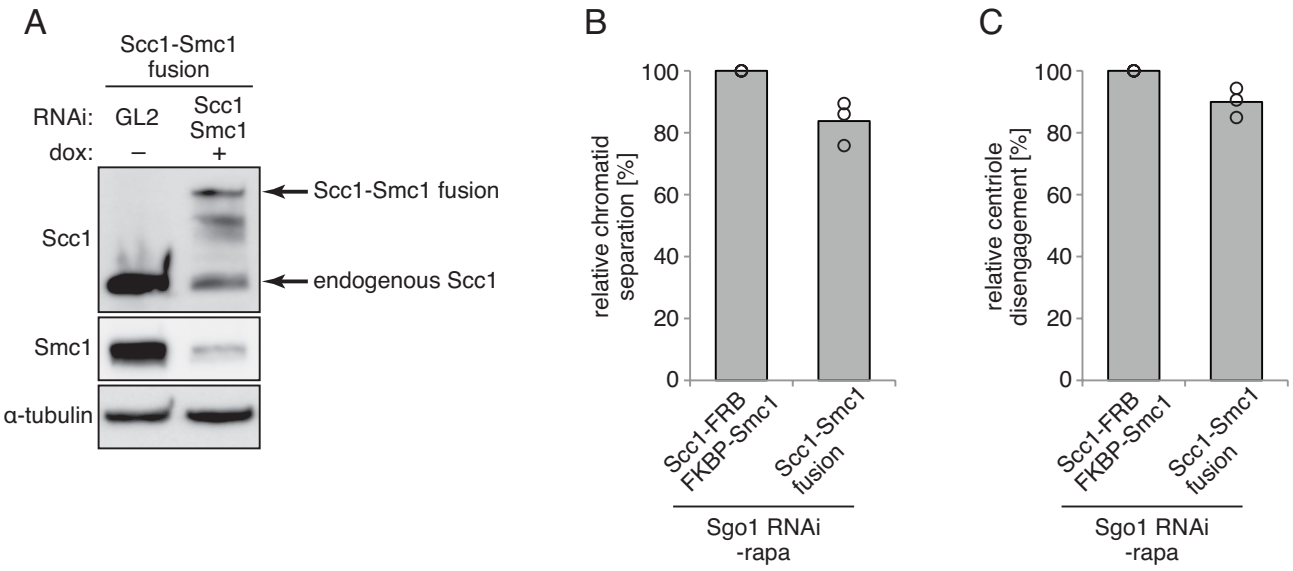

Figure 34 | **Opening of the Scc1-Smc1 gate is not required to release cohesin from centrosomes.** The stable Scc1-Smc1 fusion cell line was largely treated as desribed in Fig. 33 A while omitting rapamycin-addition and then analyzed by chromosome spreading (B) and centrosome isolation (C). **(A)** Western blot demonstrates successful knockdown of endogenous cohesin subunits and the doxycycline (dox)-inducible expression of the Scc1-Smc1 fusion protein. **(B)** Chromosomes were spread and stained with Hoechst 33342. Graph depicts the total number of chromosome spreads displaying cohesed sister chromatid (butterfly-like morphology as opposed to single chromatid threads) compared to the -rapa control of the Scc1-FRB/FKBP-Smc1 cell line from the experiment shown in Fig. 33 C. Each column represents the mean of three independent experiments totalling 300 analyzed cells. **(C)** Isolated centrosomes were immunostained to visualize C-Nap1 (proximal centriole marker; red) and centrin2 (distal centriole marker; green). Graph depicts the total number of isolated centrosomes displaying engaged centrioles (indicated by two green centrin2 dots and one red γ-tubulin dot as opposed to two red C-Nap1 dots) compared to the the -rapa control of the Scc1-FRB/FKBP-Smc1 cell line from the experiment shown in Fig. 33 D. Each column represents the mean of three independent experiments totalling ≥300 analyzed centrosomes. Note: centrosome isolation and quantification was performed by Lisa Mohr, University of Bayreuth, Germany.

I have previously shown that closing cohesin's exit gate during G1 phase causes a massive increase of the ring molecule binding to chromatin (see Figure 29). If this was also the case in the experiment in Figure 33, one could argue the observed effect to be just an artifact caused by excessive cohesin abundance on chromatin "overloading" the prophase pathway, e.g. by titrating out Wapl. It should be noted that in this experiment rapamycin was added during G2 phase, i.e. in a phase of low cohesin dynamics. Therefore, cohesin is not expected to be unproportionally loaded onto DNA. However, to exclude the small possibility of the observed effects for cohesin's exit gate to be coincidentally caused by altered cohesin dynamics upon gate-closure, I repeated the experiment from Figure 33 using the doubly stable exit gate cell line. I reasoned that if the detected rescue was just an artifact and not directly associated with the phenotype caused by Sgo1 depletion, then background centriole disengagement observed without Sgo1

depletion should already be "rescued" to a certain extent. Furthermore, to demonstrate that completely abrogating cohesin dynamics over the course of the whole experiment has no influence on baseline centriole disengagement, I additionally transfected cells with siRNAs targeting the mRNA of either GL2 (luciferase, control) or Wapl at the beginning of the experiment. Western blot analysis confirmed proper transgene expression and efficient Wapl knockdown (Figure 35 A). Background centriole disengagement, quantified from isolated and C-Nap1/centrin2-stained centrosomes, was set to 100% to visualize even small changes. Quantification of two independent experiments confirmed that rapamycin-mediated exit gate closure in G2 phase does not cause any differences in baseline centriole disengagement compared to the -rapa-control (Figure 35 B). Completely abrogating proper cohesin dynamics by Wapl-depletion over the course of the entire experiment did also not alleviate background disengagement, even when combined with exit gate closure (Figure 35 B, "+rapa").

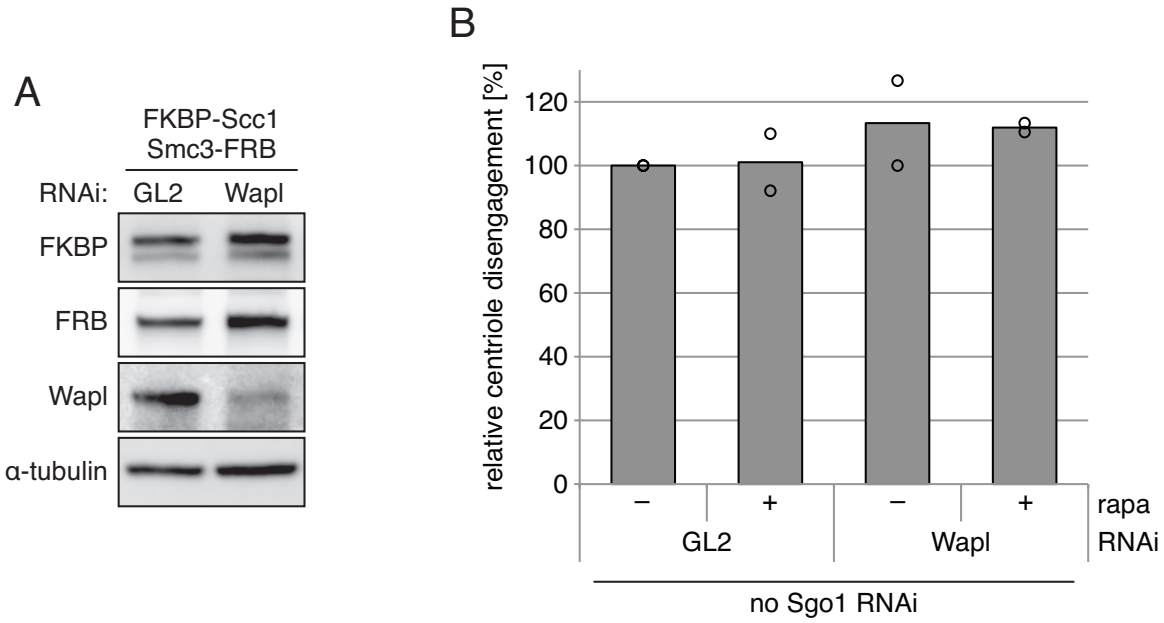

Figure 35 | Observed effects on centriole disengagement are not due to generally perturbed cohesin dynamics. A HEK293 cell line stably expressing FKBP-Scc1/Smc3-FRB (exit gate) was treated as described in Fig. 25 A with two exceptions: Sgo1 depletion was ommitted but cells were additionally transfected with siRNAs targeting either GL2 (luciferase, control) or Wapl at the beginning of the experiment. Cells were ultimately lysed for centrosome isolation. **(A)** Western blot demonstrates successful knockdown of Wapl and expression of the FRB/FKBP-tagged cohesin subunits. **(B)** Isolated centrosomes were immunostained to visualize C-Nap1 (proximal centriole marker; red) and centrin2 (distal centriole marker; green). Graph depicts the relative number of isolated centrosomes displaying (precocious) centriole disengagement (indicated by two green centrin2 dots and two red C-Nap1 dots as opposed to only one red C-Nap1 dot) normalized to the the -rapa control of each RNAi condition (GL2 vs. Wapl). Each column represents the mean of two independent experiments totalling 200 analyzed centrosomes.

The experiment shown in Figure 33 (in combination with the controls shown in Figures 34 and 35) confirms Sgo1's protective role towards centromeric cohesin against the action of the prophase pathway. More impressively, it demonstrates for the first time that the prophase pathway is mechanistically conserved on centrosomes in that it also here triggers opening cohesin's canonical exit gate constituted by Smc3 and Scc1. Moreover, Sgo1 can be explicitly linked to the protection of centrosomal cohesin from the prophase pathway further consolidating the role of cohesin dynamics and their regulation in the coordination of the chromo- and centrosome cycle.

2.3.3 Cohesin loading onto centrosomes

Prompted by the large number of parallels between the chromosome and centrosome cycle, we decided to ask whether the mechanism conferring cohesin-loading, i.e. opening of cohesin's Smc1-Smc3 entry gate, might also be conserved at centrosomes. To test this, I treated the three doubly stable FRB/FKBP-cohesin cell lines as illustrated in Figure 36 A. Endogenous cohesin subunits were replaced by FRB/FKBP-tagged variants as before and corresponding cells were arrested in prometaphase by nocodazole-addition. This means that most of the cell's cohesin molecules had been released from chromatin (and possibly also centrosomes) by the prophase pathway and should hence be soluble and ready to be reloaded. Two hours before releasing the cells from the nocodazole arrest, rapamycin (or DMSO as a control) was added to individually close the cohesin gates, compromising proper cohesin-reloading onto DNA (see Figure 21) and conceivably also onto centrosomes upon entry gate-closure. Eight hours after release from nocodazole, taxol was added to ultimately trap cells in the next mitosis. After harvesting, the cells were split for three different analyses including Western blot (Figure 36 B), chromosome spreading (Figure 36 C), and centrosome isolation with subsequent IFM (Figure 36 D). Western blot analysis confirmed proper knockdown and transgene expression (Figure 36 B). Quantification of the chromosome spreads derived from three independent experiments revealed some interesting results. First, exit gate closure greatly reduced the amount of chromatid separation found in the control (Figure 36 C). However, one should note that this experiment was not conducted under Sgo1 knockdown conditions, meaning that all observed premature sister chromatid separation represents the quite low background separation, which typically peaks at around 20%. Therefore, as the control was set to 100%, the +rapa-effect seen for the exit gate cell line might appear exaggerated.

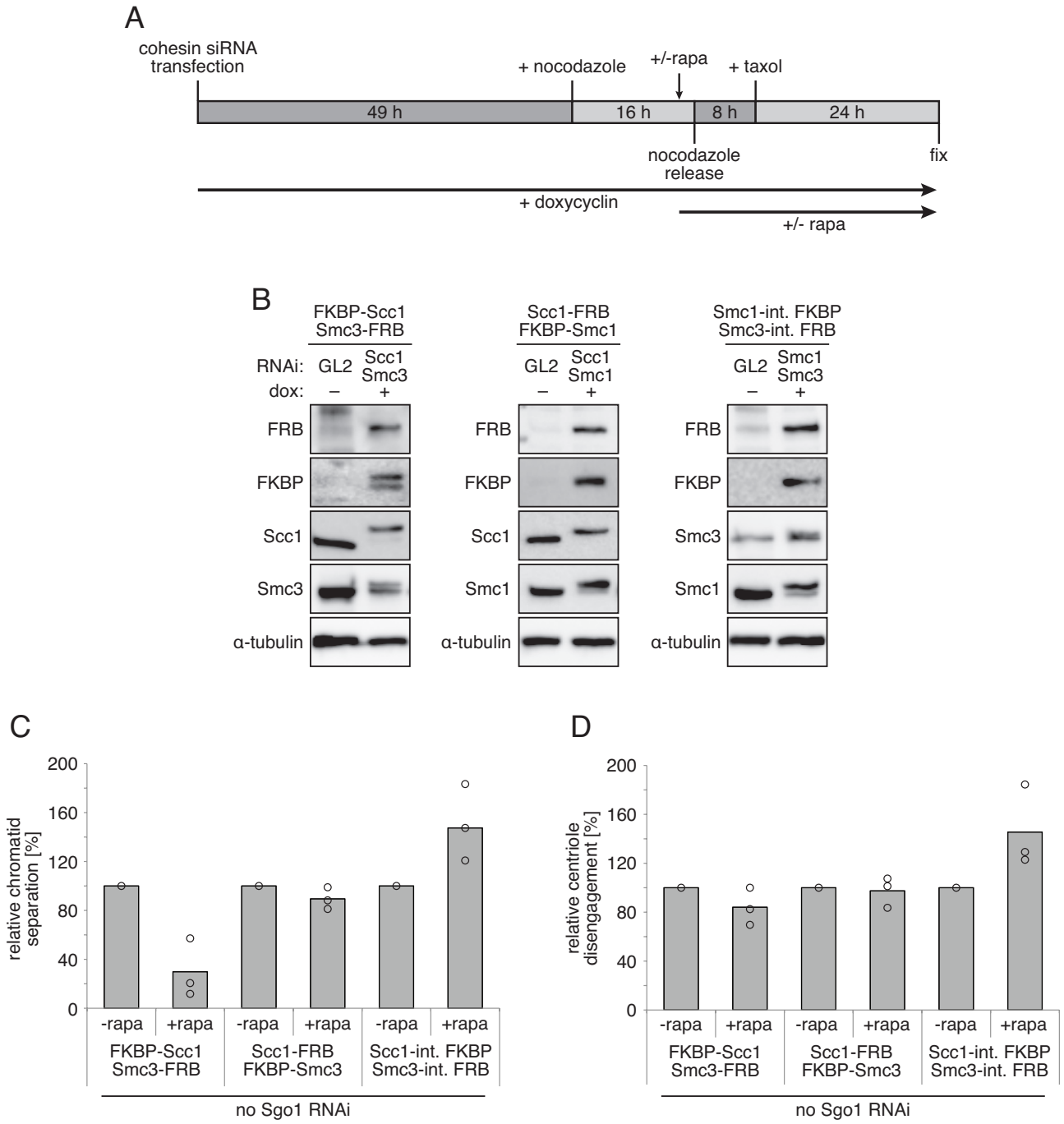

Figure 36 | Centrosomal cohesin loading might require opening of the Smc1-Smc3 hinge. (A) Assay time line for results shown in (B-D). **(B-D)** Indicated doubly transgenic cell lines were treated as illustrated in (A) then subjected to chromosome spreading (C) and centrosome isolation (D). **(B)** Western blot demonstrates successful knockdown of endogenous cohesin subunits and the doxycycline (dox)-inducible expression of the FRB/FKBP-tagged variants. **(C)** Chromosomes were spread and stained with Hoechst 33342. Graph depicts the relative number of chromosome spreads displaying (precocious) sister chromatid separation (single chromatid threads as opposed to the typical butterfly-like morphology) normalized to the the -rapa control of each cell line. Each column represents the mean of three independent experiments totalling 300 analyzed cells. **(D)** Isolated centrosomes were immunostained to visualize C-Nap1 (proximal centriole marker; red) and centrin2 (distal centriole marker; green). Graph depicts the relative number of isolated centrosomes displaying (precocious) centriole disengagement (indicated by two green centrin2 dots and two red C-Nap1 dots as opposed to only one red C-Nap1 dot) as well as single centrioles (indicated by one green centrin2 dot associated with one red C-Nap1 dot; counted as 0.5 centrosomes) normalized to the

Figure 36 (cont.) | -rapa control of each cell line. Each column represents the mean of three independent experiments totalling ≥300 analyzed centrosomes. Note: centrosome isolation and quantification was performed by Lisa Mohr, University of Bayreuth, Germany.

Nonetheless, a positive effect of exit gate closure on sister chromatid cohesion is absolutely conceivable as adding rapamycin this early should cause highly elevated cohesin-abundance on chromatin (compare also Figure 29). Even more interestingly, ectopically closing cohesin's DNA entry gate, situated between Smc1 and Smc3, causes increased levels (over 45% higher than in the control) of untimely sister chromatid separation in the following mitosis. This result is likely a reflection of reduced cohesin-binding to chromosomes upon rapamycin-addition and thereby further corroborates the results from Figure 21. Centriole disengagement on isolated centrosomes immuno-fluorescently stained for C-Nap1 and centrin2 was quantified from three individual experiments (Figure 36 D). Background centriole disengagement, which is typically around 30% in unperturbed (not Sgo1-depleted) cells, was set to 100%. Although a tendency towards reduced centriole disengagement might be perceived, the effects of artificially closing centrosomal cohesin's exit gate (Smc3-Scc1) were not as pronounced as on chromosomes. But it has to be stressed that such an effect is not necessarily expected, as we are looking at background centriole disengagement in this case. To alleviate these occurrences of disengagement, a plethora of requirements would have to be met, such as the requirement for centrosomes to actually have the capacity to recruit more cohesin molecules in the first place. The results suggest that these requirements were fulfilled on chromosomes as chromosomal cohesin is demonstrably highly dynamic (at least in G1 phase) and its maximum loading capacity is not easily exhausted (see also Figures 15 and 16). Thorough microscopical examination of the centrosomes isolated from the Smc1-int. FKBP/Smc3-int. FRB (entry gate) cell line uncovered an interesting behavior. Ectopically shutting cohesin's entry gate appeared to produce an unusually large amount of untethered centrioles, marked by only one red C-Nap1 and one green centrin2 focus in close proximity. Albeit typically in low numbers, these single centrioles can be found in every centrosome preparation but are believed to be merely a product of mechanical forces acting on centrosomes during isolation. Routinely, untethered centrioles are ignored while assessing centriole engagement but in this case we were prompted to specifically quantify this putative effect. Indeed, while the other two cell lines exhibited even a slightly decreased amount of untethered centrioles upon rapamycin-addition, artificially closing the Smc1-Smc3 gate significantly augmented these occurrences by nearly 34% (Lisa Mohr,

University of Bayreuth, Germany; unpublished data). These results led us to believe that loss of centriole tethering might be part of the phenotype associated with entry gate-closure and that it should therefore be included in the assessment of centriole (dis-)engagement. To keep the effects simple and, more importantly, as comparable to our previous analyses as possible, we decided to quantify centriole disengagement as usual but include untethered single centrioles by counting them as one half (0.5) disengaged centrosome. Of course, all samples from all cell lines were quantified accordingly to also keep their internal comparability maximal. In this analysis, the effects on centriole engagement upon rapamycin-addition closely mirrored the effects seen on DNA (Figure 36 D): ectopically closing the Smc1-Smc3 gate before allowing the cells to reload cohesin caused an appreciable increase in centriole disengagement in the following mitosis by over 45% compared to the control, as would be expected if opening of the Smc1-Smc3 gate conferred centrosomal cohesin-loading. Please note that, as this was a joint project, centrosome isolation and quantification shown in Figure 36 were performed by Lisa Mohr, University of Bayreuth, Germany.

Summed up, the results from Figure 36 strongly corroborate my previous findings identifying cohesin's DNA exit gate to be situated between Smc3 and Scc1 and its DNA entry gate to be constituted by Smc1 and Smc3 (see Figures 16, 17 and 21). Especially the cohesin reloading experiments, which identified cohesin's entry gate solely via compromised *in situ* localization upon gate-closure (Figure 21), are nicely complemented by the functional data from Figure 36 C. Moreover, the data from Figure 36 D strongly support the hypothesis of cohesin's loading/entry gate being conserved between chromo- and centrosomes. Interestingly, ectopic Smc1-Smc3 gate-closure seems to cause problems with proper centriole tethering. However, since I cannot satisfactorily discern whether centriole disengagement causes the tethering-phenotype or *vice versa*, I consider this question to remain open until these concerns have been addressed (see also discussion chapter 3.3.3).

2.3.4 The centrosomal role of Sgo1 is recruitment of PP2A

The protective nature of Sgo1 towards centromeric cohesin lies in its ability to recruit protein phosphatase 2A (PP2A; Kitajima *et al*, 2006). Since the roles and functions of both cohesin and Sgo1 appear to be conserved at centrosomes, we assumed Sgo1's centrosomal function to be intimately linked to PP2A as well. In accordance with this

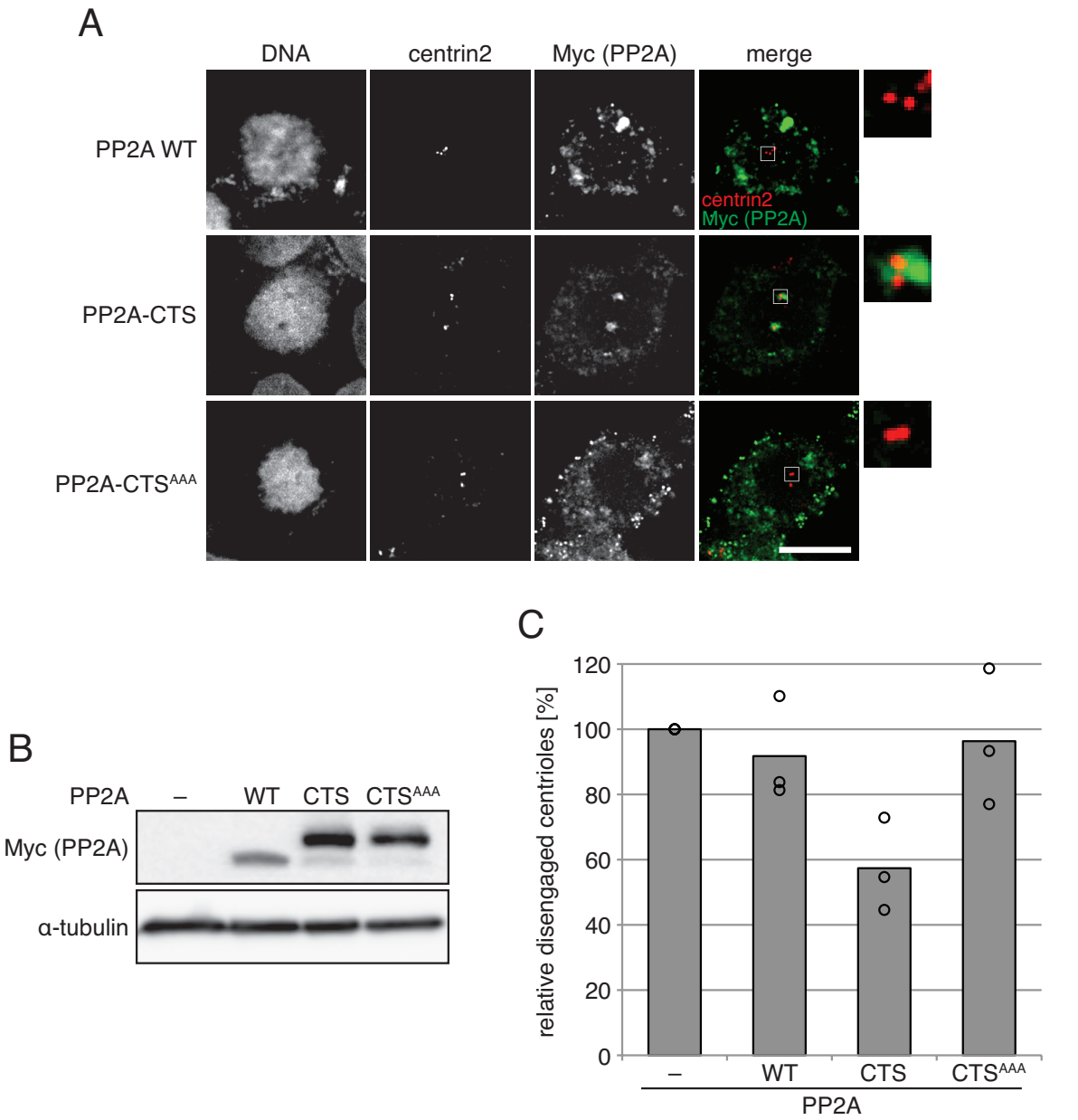

Figure 37 | **Sgo1 protects centrosomal cohesin by recruitment of PP2A. (A)** PP2A-CTS is artificially recruited to centrosomes in a Sgo1-depletion background. HEK293T cells were transfected with plasmids coding for either N-terminally Myc_6-tagged wildtype PP2A ("WT"), Myc_6-PP2A N-terminally fused to the CTS of Sgo1 A2 ("CTS") or in a fusion with the non-functional CTS^{AAA} (535-ILY-537 to 535-AAA-537; "CTS^{AAA}"). Cells were allowed to express these proteins for 48 h. 24 h before harvesting, cells were additionally transfected with siRNAs targeting Sgo1's mRNA. After harvesting, cells were CSK-preextracted and fixed for (immuno-)fluorescence microscopy using Hoechst 33342 as a DNA marker and indicated antibodies to stain for centrin2 (centrosome marker) and Myc (PP2A). Scale bars = 10 μm. Indicated centrosomes were magnified by 500%. **(B, C)** HEK293T cells were largely treated as described in Fig. 33. Instead of siRNAs targeting cohesin subunits, cells were transfected with the plasmids described for (A). Thymidine was added 28.5 h after transfection and washed out 30.5 h thereafter. **(B)** The various Myc_6-PP2A fusion proteins were expressed at similar levels during the experiment as judged by Western blot using an anti-Myc antibody. **(C)** Artificially targeting PP2A to the centrosomes rescues centriole disengagement caused by Sgo1-depletion. Graph depicts the relative number of isolated centrosomes displaying precocious centriole disengagement (indicated by two green centrin2 dots and two red C-Nap1 dots as opposed to only one red C-Nap1 dot) for each condition normalized to the the control (Sgo1 knockdown; mock transfection). Each column represents the mean of three independent experiments totalling 300 analyzed centrosomes.

notion, PP2A localizes to human centrosomes in a Sgo1-dependent manner (Mohr *et al*, 2015). If PP2A was indeed the protector of cohesin on centrosomes, than artificially recruiting the phosphatase to centrosomes should suppress premature centriole disengagement upon depletion of Sgo1. PP2A is a quite promiscuous enzyme, which, in addition to its core subunits PP2A-C (catalytic) and PP2A-A (scaffold), requires specificity-conferring regulatory ("B") subunits to bind its targets correctly. The subunit PP2A-B' is specific for the its function in protecting untimely ring-opening on chromosomes (Kitajima *et al*, 2006) and is therefore the most promising candidate to act accordingly on centrosomes. For these experiments, I created several eukaryotic plasmids to express N-terminally Myc_6-tagged PP2A-B' (from here on simply "PP2A") in fusion with wildtype CTS, the non-functional CTS^{AAA}, or without a C-terminal extension ("WT"). IFM experiments on HEK293T cells confirmed successful recruitment of transiently expressed Myc_6-PP2A-CTS (but not -PP2A-CTS^{AAA} or -PP2A-WT) to centrosomes in a Sgo1-depletion background (Figure 37 A). To ultimately test PP2A's ability to protect centrosomal cohesin, I largely treated HEK293T cells as illustrated in Figure 33 A. Instead of cohesin siRNAs, I transiently transfected the cells with either buffer ("-", control) or the aforementioned plasmids. As indicated, cells were thymidine-pre-synchronized and transfected with siRNAs targeting Sgo1's mRNA, which, by extension, not only strips endogenous (as well as exogenously expressed wildtypic) PP2A from centrosomes (Mohr *et al*, 2015 and Figure 37 A) but also causes premature centriole disengagement due to centrosomal cohesin becoming sensitive towards the prophase pathway (this study). Cells were released from thymidine and re-arrested in the following prometaphase using taxol before being harvested and split for Western blot analysis (Figure 37 B) and centrosome isolation/ IFM (Figure 37 C). Transient expression of the various Myc_6-tagged PP2A constructs appeared to be quite uniform over three independent experiments (representative blot in Figure 37 B). Quantification of relative centriole disengagement, judged by isolated and C-Nap1/centrin2-stained centrosomes, did not disclose a large effect of ectopic PP2A WT-expression compared to the buffer control (Figure 37 C). Strikingly, however, expression of centrosome-directed PP2A-CTS rescued centriole engagement in absence of Sgo1 to 60% of the control. In contrast, PP2A-CTS^{AAA}, which is centrosome-binding-deficient, causes no such effect, keeping the level of disengagement high.

Confirming our last prediction concerning the tight coordination of chromosome- and centrosome-cycles, the experiment in Figure 37 revealed that the actual effector protecting centrosomal cohesin is, analogously to the situation at the centromere, protein

phosphatase 2A. It's centrosomal association is lost upon Sgo1-depletion but ectopically recruiting it back bypasses the requirement for Sgo1 to protect centriole disengagement.

3. Discussion

3.1 Cohesin dynamics in mitosis

3.1.1 DNA enters and exits the cohesin ring through different gates

From my experiments using the FRB/FKBP system in human cells to systematically shut all three cohesin gates individually, I can conclude that DNA enters and exits the cohesin ring structure through different gates (see model Figure 38). Blocking the Smc3-Scc1 gate from opening (by rapamycin addition) exclusively caused cohesin to remain associated with chromatin beyond prophase, while control cells (without rapamycin addition), expressing the same tailored cohesin subunits, were able to remove the complex via prophase pathway signaling (Figure 16). Those retained cohesin rings were functional, as they caused chromosome arms to remain tightly cohesed in the same assay (Figure 17). On top of that, artificially closing this gate rescued premature sister chromatid separation upon Sgo1-depletion to a considerable extent, consistent with this treatment abrogating the prophase pathway and therefore the need for cohesin protection by Sgo1 (Figure 33). On the other hand, artificially closing the hinge gate constituted by Smc1 and Smc3 had no effect on cohesin release in prophase but impaired its ability to reload onto chromatin in the following telophase (Figure 21). Even more strikingly, these reduced amounts of cohesin on chromatin were insufficient to maintain proper sister chromatid cohesion in the following mitosis (Figure 36).

Previous experiments in yeast had already suggested a role in hinge gate opening during cohesin loading (Gruber *et al*, 2006), but conservation in humans had never been described until this study. At first glance, utilization of the Smc1-Smc3 gate seems unintuitive, because this notion introduces two major caveats. First, cohesin loading requires ATP hydrolysis by cohesin's own head domains at the other end of the coiled coil located over 40 nm away (Weitzer *et al*, 2003; Arumugam *et al*, 2003; Hu *et al*, 2011; Ladurner *et al*, 2014). But how the produced energy can be transferred to the hinge domain still remains a mystery. Initial suggestions included a conformational change, which would span the length of the coiled coil(s). However, data from yeast implied a more immediate way of energy transfer, as it was shown that Smc head and hinge domains might be able to form direct contacts as judged by fluorescence resonance energy transfer (FRET; Mc Intyre *et al*, 2007). Since the authors of this study were able exclude FRET

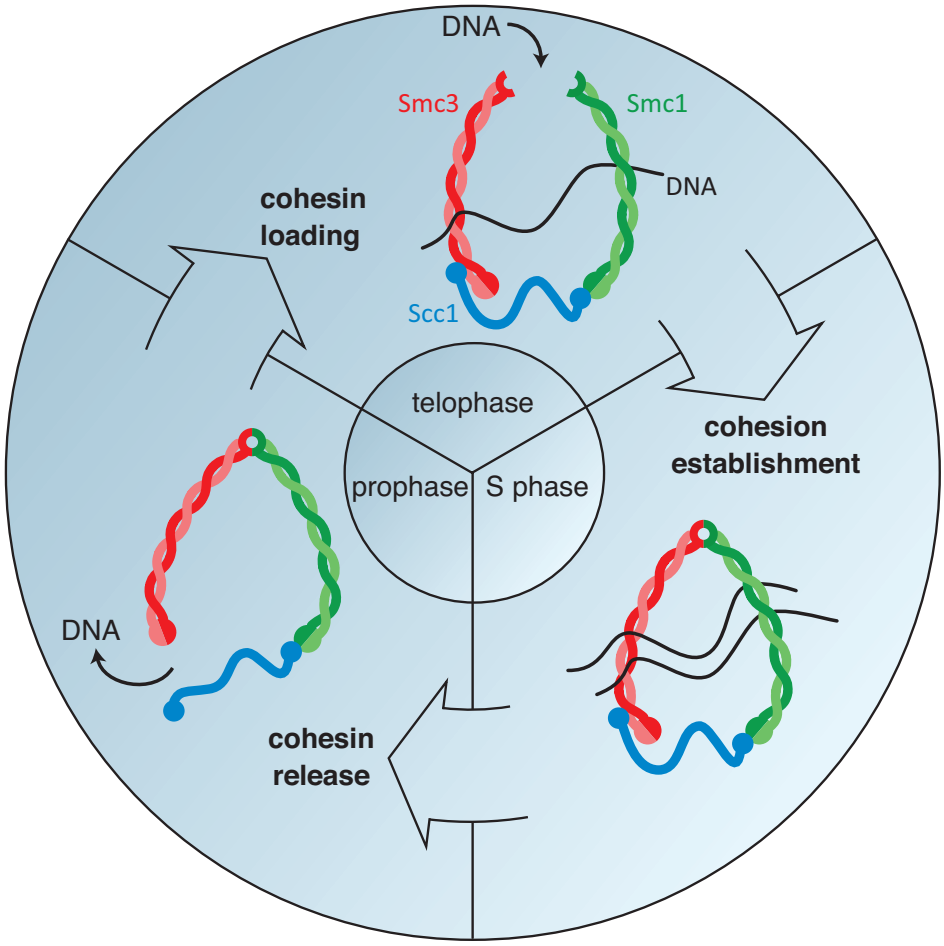

Figure 38 | **Model depicting cohesin's entry and exit gate.** Cohesin's DNA entry gate during telophase is situated between Smc1 and Smc3 (hinge). Cohesin's DNA exit gate during prophase is situated between Smc3 and Scc1. For more details, see text.

between two separate cohesin complexes, one must assume an intramolecular interaction, which would require the ring structure to collapse to a substantial degree. And indeed, under this assumption, the expected stress on the usually quite rigid coiled coils might be alleviated by a readily observable "kink" in cohesin's coiled coils (Anderson *et al*, 2002; Huis In 't Veld *et al*, 2014). The second major caveat lies in the tight association between Smc1 and Smc3, whose dissociation constant (K_D) has been reported to be in the low nanomolar range (Haering *et al*, 2002; Kurze *et al*, 2011). Thus, the energy produced from hydrolyzing one ATP molecule might not suffice to open up the hinge for cohesin loading onto chromatin. The solution to this problem might lie in the physical properties of the hinge domain itself. The Smc1/Smc3 interaction surface actually consists of two smaller surfaces, which interact to form a pseudo-symmetric toroid structure (Haering *et al*, 2002; Kurze *et al*, 2011; compare also Figure 4). If the process of hinge opening would initially only require dissociation at one of the two interaction sites, the energy-demand would be dramatically decreased (the expected K_D would lie well in the micromolar range; Gruber *et*

al, 2006). Because of structural similarities to the PCNA ring complex (whose chromatin-loading had been studied earlier; Barsky & Venclovas, 2005), it has been suggested that upon opening of one interaction surface, an out-of-plane twisting motion could allow a DNA double strand to enter the (otherwise too small) lumen of the half-open toroid by interacting with its positively charged surface (Gruber *et al*, 2006; Kurze *et al*, 2011). Thus, the twisting motion might facilitate the establishment of extensive electrostatic interactions between the helical DNA and the inner hinge surface which would provide additional energy for the opening of the second Smc1/Smc3 interface. Strikingly, a crystal structure of the Smc hinge from the maritime prokaryote *T. maritima* displayed a twisted half-open morphology, further supporting this hypothesis (Haering *et al*, 2002; Gruber *et al*, 2006). In addition, this proposed sequential opening of the two hinge-halves might also contribute to the unidirectionality of DNA entry into the cohesin ring (see also next chapter).

While it had been hypothesized before that the Smc3-Scc1 gate might perform the function of an exit gate (Nasmyth, 2011), this suggestion was merely based on circumstantial evidence such as the physical proximity to the site of cohesin-stabilizing acetylations on Smc3's head domain (Zhang *et al*, 2008; Ünal *et al*, 2008; Rolef Ben-Shahar *et al*, 2008; Sutani *et al*, 2009; Rowland *et al*, 2009; Nishiyama *et al*, 2010; Gligoris *et al*, 2014). This study provides the first unequivocal proof that the gate constituted by Smc3 and Scc1 does indeed open up during prophase to allow chromosome arms to exit the cohesin ring. Strikingly, this mechanism not only applies to early mitotic human cells but is also employed to mediate cohesin dynamics in interphase of *S. cerevisiae* (which does not have a prophase pathway, at least in a canonical sense; see also chapter 3.1.3) as well as in *Drosophila* salivary glands and is therefore conserved from yeast to man (Chan *et al*, 2012; Eichinger *et al*, 2013).

Ultimately, it should be noted that artificially closing the Scc1-Smc1 did not cause any phenotype in all corresponding experiments (this includes experiments from chapters 2.2 and 2.3). As already thoroughly discussed in chapter 2.1.6, this might either mean that opening of this gate is not involved in any of the mechanisms investigated in this study, or it might indicate a methodical problem. As a workaround to this caveat, all experiments in question were repeated using a cell line stably expressing an in-frame fusion construct of Scc1 and Smc1 (see Figure 18), in which the gate is covalently closed (see Figures 20, 27, 34 and 37). Together, all of these experiments confirmed that opening of the Scc1-Smc1 gate is not required for the investigated cohesin dynamics during M and G1/S phase.

3.1.2 Cohesin – a molecular turnstile

The usage of different gates for DNA entry and exit into and from the cohesin ring allows chromosomes to pass through cohesin only in one direction. This unidirectionality is maintained by the use of different protein complexes exclusively involved in either cohesin loading (kollerin: Scc2 and -4) or release (releasin: Pds5 and Wapl; Nasmyth, 2011). Collectively, these systems allow the exquisite regulation of cohesin dynamics during the cell cycle. For example, the releasin complex is fully activated during prophase, while most if not all kollerin is released from chromatin during that time (at least in higher eukaryotes; Gillespie & Hirano, 2004; Nasmyth, 2011). Kollerin reassociation with chromatin in late mitosis then triggers proper G1 phase cohesin dynamics, marked by constant release and reloading of the ring complex, which is probably required for non-canonical cohesin functions (see introduction chapter 1.4.7) as well as proper DNA replication in the following S phase (this study). Especially in the light of cohesin's non-canonical capacities, which are believed to be a leading cause for the development of cohesinopathies and even cancer, it will be of particular significance to further extend our knowledge of cohesin's regulatory framework.

3.1.3 The role of the prophase pathway

In yeast, all cohesin dissociation in mitosis relies on the action of separase, despite the fact that most prophase pathway components, as for example Wapl (Rad61 in *S. cerevisiae*) and Pds5, are present and have a role in the dynamic association of cohesin with sister chromatids, albeit only in interphase (Uhlmann *et al*, 1999; Hartman *et al*, 2000; Panizza *et al*, 2000; Kueng *et al*, 2006). Interestingly, also in human cells, all cohesin can be processed by separase when the prophase pathway is disabled (see Figure 9 B) but nonetheless, it is still deliberately activated in early mitosis by phosphorylation of SA2 and sororin (Hauf *et al*, 2005; Nishiyama *et al*, 2010). In fact, lower eukaryotes do not even seem to possess an obvious sororin ortholog. So why have metazoans evolved such a unique pathway?

The emergence of a non-destructive mechanism for dissociating the bulk of cohesin from chromosome arms might simply be explained by an energetic advantage, since the whole complex can be recycled as Scc1 remains unspoiled and does not have to be resynthesized. The fact that artificially closing cohesin's entry gate after prophase reduces the amount of reloaded cohesin in telophase/G1 phase (Figure 21) strongly supports this

theory. Similarly, compromising the prophase pathway in mouse embryonic fibroblasts increases the amount of Scc1-cleavage by separase (separase preferably cleaves chromatin-bound cohesin; Sun *et al*, 2009), which, again, impairs reloading (Tedeschi *et al*, 2013). Interestingly, the N-terminal cleavage fragment of Scc1 has even been shown to be highly toxic to budding yeast, and is therefore immediately degraded by the proteasome upon anaphase onset (Rao *et al*, 2001). This fragment is believed to act dominant-negatively on ring complex re-formation, which further supports the model of the prophase pathway as part of a cohesin recycling mechanism. Such a mechanism might also provide an explanation for the faster reassociation of cohesin with chromatin in telophase of higher eukaryotes as opposed to late G1 phase in yeast. Another reason for the intentional loss of arm cohesion might involve cohesin's role in chromatin organization (Hadjur *et al*, 2009; Nativio *et al*, 2009; Hou *et al*, 2010; Kagey *et al*, 2010; Seitan *et al*, 2011; 2013; Sofueva *et al*, 2013; Gosalia *et al*, 2014), which could be important during early mitosis as a mechanism complementing chromosome condensation as had already been suggested by data from yeast and human (Heidinger-Pauli *et al*, 2010; Lopez-Serra *et al*, 2013; Tedeschi *et al*, 2013). Additionally, the prophase pathway might contribute to correct timing of chromatid separation and the following processes involved in mitotic exit. It has been long known that separase plays an important role in inhibiting Cdk1-cyclin B1 activity following initiation of sister chromatid separation, allowing for proper cytokinesis (Gorr *et al*, 2005; Hellmuth *et al*, 2015b). Engaging separase into cleavage of the entire chromatin-bound cohesin fraction, while the kinetics of downstream pathways remain constant, might jeopardize the temporal cascade which leads to mitotic exit. In this scenario, the absence of a prophase pathway in yeast could simply be rationalized by its smaller genome size. My experiments, however, imply that separase activity in early anaphase can compensate for impaired cohesin dissociation from chromosome arms in prophase, although it should be noted that I cannot exclude any longterm issues that might only arise after several cell divisions. In fact, it has just been shown recently that specifically the prolonged depletion of Wapl, causes chromatid segregation defects (Haarhuis *et al*, 2013). Interestingly, these defects could be tied to cohesin's functions in Aurora B localization at the centromere (important for the correction of erroneous microtubule-kinetochore attachments) and in sister chromatid decatenation (Wang *et al*, 2010; Haarhuis *et al*, 2013). Thus, the prophase pathway in humans is essentially required to ensure the fidelity of chromosome separation.

3.2 Cohesin dynamics in S phase

3.2.1 The intricate bond between pre-S phase cohesin dynamics and DNA replication

In this thesis, I could demonstrate that pre-S phase cohesin dynamics influence DNA replication on a single replication fork level to an extensive degree. More specifically, blocking the cell's ability to continuously load and release ring complexes onto and from chromatin in G1 phase causes a dramatic decrease in replication fork processivity in the following S phase (Figure 26). These results perfectly tie into our current understanding of how human cells guarantee the correct sequence of events between cohesin loading in telophase and cohesion establishment in S phase.

As already outlined in the introduction, cohesin, whose loading onto DNA initiates in late mitosis, remains very dynamic during G1, being constantly released from and reloaded onto chromatin (see chapter 1.4.4). However, the cell must ultimately ensure that cohesin is topologically embracing the chromatids before it is being stabilized in order to properly establish cohesion during S phase. According to the prevailing model, this is accomplished by kollerin (Scc2 and -4) stimulating cohesin's ATPase activity upon mediating its initial transient (non-topological) association with DNA (Ladurner *et al*, 2014). Subsequent topological loading via hinge-opening is then required to make Smc3 susceptible for Eco1-mediated acetylation, which in turn facilitates Wapl-displacement by sororin during S phase (Nishiyama *et al*, 2010; Ladurner *et al*, 2014). Thus, pre-S phase cohesin dynamics, or more precisely, cohesin's pre-S phase loading status can have a significant impact on co-replicative cohesion establishment. My data now takes this notion one step further by suggesting that proper replication fork progression requires precisely balanced cohesin levels on chromatin (which are established in G1 phase) during S phase. Artificially closing cohesin's exit gate (Smc3-Scc1) during G1 phase causes elevated cohesin levels, while closing the ring's entry gate (Smc1-Smc3) results in reduced amounts of cohesin on replicating DNA (Figure 29). Strikingly, despite the fact that these two gates are not only locally but also functionally on different sides of the ring complex, individually manipulating either one coincides with the same phenotype of dramatically reduced replication fork velocities (Figure 26). How can this be explained?

First of all, since global replication levels appear to be normal (Figure 24), it is safe to assume that perturbed cohesin levels do not trigger a full checkpoint response but rather cause firing of dormant origins to counteract replisome stalling (reviewed in Blow *et*

al, 2011). Therefore, the effects observed on single replication forks must represent a specific functional interaction between the replication machinery and the ring complex *in cis*. While the detrimental effect of excessive cohesin might simply be explained by the complex acting as a physical "roadblock" for the replisome, this would still not explain the replication defects detected in cells with reduced chromosomal cohesin levels. Since we know that cohesin's loading status is tied to events in S phase via Smc3 acetylation (see above), Eco1 seems like a more plausible connection between cohesin dynamics and replication. And in accordance with this concept, the acetyl transferase was shown to promote cohesion establishment (Skibbens *et al*, 1999; Tóth *et al*, 1999) as well as to genetically and physically associate with the replisome component PCNA (Skibbens *et al*, 1999; Moldovan *et al*, 2006; see also introduction chapter 1.4.4 and Figure 2). More crucially, this link is also functionally relevant, as failure to acetylate Smc3 (which stabilizes cohesin on chromatin) causes problems with DNA replication (Figure 23 and Terret *et al*, 2009) and *vice versa* (Rolef Ben-Shahar *et al*, 2008). This notion is further corroborated by the fact that a temperature-sensitive *eco1* yeast mutant shows synthetic lethality in combination with a deletion-mutant of Ctf18, which is part of the alternative PCNA-loader complex RFC^{Ctf18} (Skibbens *et al*, 1999). In humans, deletion of another RFC^{Ctf18} component, namely DCC1, causes reduced Smc3 acetylation and phenocopies the detrimental effects of non-acetylatable Smc3 or ESCO1/-2 depletion on replication fork progression (Terret *et al*, 2009). In their sum, these results are consistent with a model in which RFC^{Ctf18}-loaded PCNA recruits Eco1, which, by acetylating Smc3, acts as a transducer, directly or indirectly relaying cohesin's loading status to the replisome. If this hypothesis holds true, then superabundance of cohesin on chromatin might simply oversaturate the acetylation capacity of Eco1, causing replisome stalling. The effects of reduced chromosomal cohesin levels on the other hand could then only be explained by the existence of a feedback mechanism, which ensures that cohesion is established as the second sister chromatid is synthesized. This hypothesis is supported by the fact that Wapl-depletion can rescue replication fork velocities exclusively in cells harboring cohesin rings with artificially closed DNA entry gates (Figure 30), as this is expected to counteract reduced cohesin levels on chromatin. Interestingly, RNAi-mediated reduction of Wapl levels also rescued replication fork processivity in $Smc3^{AA}$-expressing cells (Figure 23 and Terret *et al*, 2009). This effect would be easily explained by non-acetylatable Smc3 ($Smc3^{AA}$) also causing reduced cohesin levels on chromatin. And since Smc3-acetylation is generally associated with sororin-recruitment and therefore the ring's stability on DNA

(Schmitz *et al*, 2007; Nishiyama *et al*, 2010), a non-acetylatable mutant would indeed be expected to be less associated with chromatin. However, this is most likely not the case as reducing Smc3-acetylation by depletion of ESCO1 or -2 does not give rise to perturbed cohesin levels on S phase chromatin (Nishiyama *et al*, 2010). It is also particularly the Wapl knockdown data from Figures 23 and 30, which calls the theory of excess cohesin causing replisome stalling into question, since depletion of the complex's destabilizer does not cause any phenotype on its own, despite it being expected to increase chromatin-cohesin levels (see above). Therefore, it might make sense, if the proposed feedback mechanism for co-replicative cohesion establishment would not sense the presence of cohesin *per se* but actually provide information on sororin's binding status to the ring complex, which would indicate stabilization. If such a mechanism would sense stability-conferring sororin-association with cohesin (which at least partly depends on Smc3-acetylation), then the absence of Wapl (which competitively binds to the same cohesin binding site as sororin) might abrogate the need for acetylation, explaining the positive effect of Wapl on the replisome in my and other studies (Figures 23, 30 and Terret *et al*, 2009; Nishiyama *et al*, 2010). However, since it has been shown that in the absence of Wapl, sororin is dispensable for sister chromatid cohesion (Nishiyama *et al*, 2010), the cohesin-stabilizer is an unlikely candidate for this task. This leaves only Wapl itself. The putative feedback mechanism could sense the absence of Wapl, whose dissociation is indirectly triggered by Smc3 acetylation. As had already been suggested by Terret and coworkers, the presence of Wapl (or more specifically, releasin consisting of Pds5 and Wapl) might cause the cohesin ring to assume a conformation that is not permissible for replisome passage through the ring, since Pds5 has been shown to establish extensive contacts not only with Scc1 but also with the hinge-region (Mc Intyre *et al*, 2007; Terret *et al*, 2009). This hypothesis is intriguing as it not only elegantly combines the earlier proposed "roadblock" mechanism (without necessarily requiring excessive cohesin conditions on chromatin) with a feedback mechanism sensing acetylation-dependent releasin displacement, but more importantly, also fits well with the Wapl-knockdown data in this study, possibly even including the slight alleviating effect on replication fork velocity upon artificial exit gate closure (Figure 30). However, these theories remain highly speculative and additional studies are necessary to further elucidate the exact mechanisms that tie replisome progression to cohesion establishment.

3.2.2 DNA replication does not require cohesin dynamics during S phase

As already outlined in the introduction (chapter 1.7.2), there are several hypotheses regarding the mechanism by which the replisome surpasses the (topologically loaded) cohesin ring and they all come with their respective set of predictions. The most discussed mechanisms, however, group into two general categories: those that require the cohesin ring to open up (at least) one of its gates and those that do not. By capitalizing on the already established doubly stable FRB/FKBP-tagged cohesin subunit cell lines, I was able to show that despite the fact that perturbed cohesin dynamics in G1 phase causes dramatic effects on replication fork progression in the following S phase (see above), ring gate opening during S phase itself does not seem to be a requirement for DNA replication (Figure 25). While I cannot fully exclude this apparent lack of phenotype being due to slow rapamycin diffusion and/or binding kinetics (rapamycin was added 40 min before fixation), data from yeast deems this concern unfounded as efficient FRB/FKBP dimerization of nuclear proteins was reported to occur in under three minutes upon rapamycin-addition (Haruki *et al*, 2008). Although it has been suggested that the replisome might simply push closed cohesin rings along DNA, this mode of action would pose the problem of how the newly synthesized DNA is deposited inside the ring's lumen, which, according to the ring embrace model (see chapter 1.4.1) is a fundamental prerequisite for sister chromatid cohesion. Thus, my data most strongly implies that the replisome is able to pass through the closed cohesin ring.

In fact, the literature provides extensive evidence in support for this hypothesis. Cohesin is not only topologically loaded before S phase *in vitro* (Murayama & Uhlmann, 2014), its stable (non-transient) association with DNA is even required for co-replicative cohesion establishment *in vivo* (Ladurner *et al*, 2014). Moreover, these preloaded ring complexes most likely represent the cohesive species, since Scc2-dependent cohesin reloading after the G1/S transition is not required for proper chromatid cohesion in yeast (Lengronne *et al*, 2006). However, it should be mentioned that kollerin-independent loading cannot be excluded from the data of this study. On a more general note, the replisome must be designed to deal with DNA-associated proteins on a large scale. And indeed, the replication machinery does exhibit substantial plasticity in this regard: So can the SV40 large T antigen (a helicase), for example, easily bypass bulky adducts that remain stably bound to DNA (Yardimci *et al*, 2012). The metazoan replisome can even repair covalent protein-DNA crosslinks in order to continue DNA synthesis (Duxin *et al*, 2014). Besides the myriads of different DNA binding proteins, one very typical protein-

DNA heterocomplex, with which the eukaryotic replisome is confronted in a frequent fashion, is the nucleosome. How the tight association of histone octamers with chromatin is loosened remains enigmatic, but is believed to require so-called histone remodeling proteins associated with the replisome (reviewed in Leman & Noguchi, 2013). Thus, the eukaryotic replisome might employ its inherent capacity to bypass DNA-associated proteins to overcome the cohesin complex without requiring it to open up its ring structure.

The idea of the massive replication machinery passing through a ring complex with an inner diameter of not over 45 nm seems unintuitive at first. However, the globular size of the yeast replisome (without DNA) has been estimated to measure around 15-20 nm in diameter (Bylund & Burgers, 2005), which, even assuming a larger size for the human complex, would indicate feasibility of its passage through cohesin. However, the bulkiest structure of the replisome might not be made up of protein but of DNA: in order to couple leading and lagging strand duplication at one single replication fork, it is believed that the lagging strand must at least transiently form a large loop ("trombone") structure (Sinha *et al*, 1980; see also Figure 2), which would have to be rearranged/collapsed in concert with cohesin passage. And indeed, increasing evidence over the last years has pointed towards a close link between cohesion establishment and lagging strand synthesis. So has it been shown that Ctf4/AND-1 not only tethers Pol α (whose action is repeatedly required on the lagging strand) to the CMG helicase but is also required for proper sister chromatid cohesion in yeast and human (Hanna *et al*, 2001; Lengronne *et al*, 2006; Zhu *et al*, 2007; Gambus *et al*, 2009; Bermudez *et al*, 2010; Fumasoni *et al*, 2015). Even more strikingly, cohesion defects are also observed, when activities of Fen1, a flap endonuclease involved in Okazaki fragment maturation, and Chl1/ChlR1, a lagging-strand specific helicase, are impaired (Farina *et al*, 2008; Rudra & Skibbens, 2012). It has been suggested that PCNA loading and unloading could be a major force behind replisome rearrangement (Bylund & Burgers, 2005). Specifically the unloading of PCNA has been associated with RFC^{Ctf18} activity, which would tie the proposed rearrangement to cohesion establishment (see above). Interestingly, RPA, which protectively coats ssDNA in the lagging strand loop, aids the cohesion-mediating Chl1 helicase (see above) in unwinding DNA (Farina *et al*, 2008) but inhibits RFC^{Ctf18} (Bylund & Burgers, 2005). Taken together, these interdependencies support a model in which decreasing amounts of RPA (which likely correlate directly with ongoing lagging strand synthesis; Mass *et al*, 1998), would activate RFC^{Ctf18}-mediated PCNA-unloading and subsequent replisome rearrangement, leading to collapse of the lagging strand loop, and thereby allowing passage of the

replication machinery through the closed cohesin ring. Of course, further studies have to be conducted to confirm these observations under the light of co-replicative cohesion establishment.

3.2.3 Cohesin dynamics, replication and cancer

Although many studies point towards transcriptional regulation as cohesin's role in cancer development (see introduction chapter 1.4.8), there is an increasing body of evidence drawing a direct line between cohesin mutations and genome instability, which are a hallmark of cancer (Hanahan & Weinberg, 2011). For example, it has been demonstrated that SA2 inactivation can cause aneuploidy in human cancers without altering gene expression (Solomon *et al*, 2011). Even more interestingly, recent studies suggested that tumorigenic phenotypes caused by cohesin defects might arise during replication. So can SA1-deficiency produce aneuploidies and tumors in mice by impairing telomere replication (Remeseiro *et al*, 2012). In another study, the authors demonstrated that induced pRB-deficiency in human cells causes mitotic cohesion failure, which results in genome instability (Manning *et al*, 2014). Intriguingly, those cohesion deficiencies were revealed to manifest much earlier, during S phase, where respective cells exhibited replication defects and DNA damage. But even more strikingly, all observed defects, including those on sister chromatid cohesion and DNA replication, could be completely suppressed by artificially enhancing cohesion via Wapl RNAi, which is compellingly reminiscent of the positive effect of Wapl-depletion on replication fork progression in this thesis (Figures 23 and 30). Together these studies not only further endorse the notion that sister chromatid cohesion is closely linked to DNA replication but also that precise regulation of cohesin dynamics before or during S phase is paramount for chromosome stability and, by extension, tumor suppression.

3.3 Cohesin dynamics at the centrosome and their regulation by Sgo1 splice variants

3.3.1 Humans employ differently spliced Sgo1 variants to maintain centriole engagement instead of sister chromatid separation

I have provided unequivocal evidence that human cells employ different Sgo1 variants (derived from alternatively spliced mRNA), namely Sgo1 A2 and Sgo1 C2, that specifically localize to the centrosomes, while the canonical Sgo1 A1 and the minimal variant Sgo1 C1 can only be found associated with centromeres (Figures 8, 31 and model Figure 39). Crucially, function always follows localization (however, with one exception; see below), meaning that centrosomal Sgo1 variants can only rescue centrosome-associated Sgo1-depletion phenotypes (premature centriole disengagement) but not centromere-associated phenotypes (premature sister chromatid separation) and *vice versa* (Mohr *et al*, 2015). It had been speculated before that a smaller Sgo1 variant (Sgo1 C2) might exert functions at the centrosome, which was attributed to C2's lack of the large exon 6-encoded peptide, when compared to the Sgo1 A1 (Wang *et al*, 2006; 2008). Conversely however, by comparing data on all Sgo1 variants present in human cells, we can undoubtedly prove that Sgo1's determinant for centrosomal localization (this study) and function (Mohr *et al*, 2015) is the small peptide encoded by exon 9 of its gene sequence. Accordingly, we coined this C-terminal stretch of 40 amino acids the "centrosomal targeting signal of Sgo1" or simply CTS.

As already stated before (chapter 1.6.1), centromeric Sgo1 localization/function depends on its initial recruitment by Bub1-phosphorylated histone 2A (via Sgo1's C-box) and subsequent direct binding to cohesin via Cdk1-phosphorylated T346, which is situated in the peptide encoded by exon 6 of the *SGO1* gene (Liu *et al*, 2013b; 2013a). Abrogating Sgo1's C-box does not, however, disrupt Sgo1-association with DNA *per se*, but causes Sgo1 to mislocalize to chromosome arms, keeping it even proficient in protecting DNA-bound cohesin from the prophase pathway (Liu *et al*, 2013a). Strikingly, a T346 mutant retains its centromeric localization (which apparently requires initial recruitment via H2A) but fails to rescue premature chromatid separation upon Sgo1-depletion, which strongly suggests that Sgo1's ability to directly bind to cohesin is crucial for its function (Liu *et al*, 2013b; 2013a). This sufficiently explains why Sgo1 C1 (which lacks the T346-containing exon 6-encoded peptide) is unable to rescue the chromosomal phenotype in our

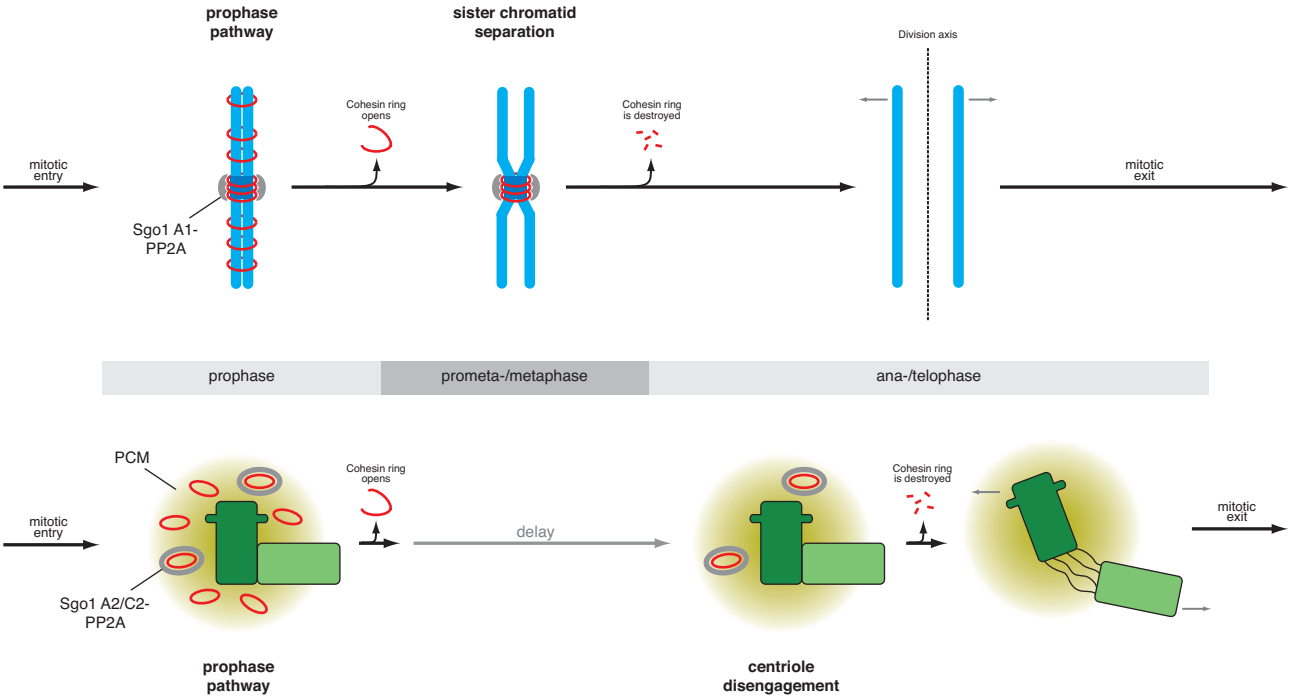

Figure 39 | Comparison of major chromosomal and centrosomal events in mitosis. When cells enter mitosis cohesin is present all along the chromosomes and most likely localizes to the centrosomal PCM. Early in prophase, cohesin is removed from chromosome arms and likely in parts from the PCM. A small fraction at the centromeres/PCMs is protected from prophase pathway signaling by specific Sgo1 splice variants. Sgo1 A1 protects centromeric cohesin, while Sgo1 A2 and C2 only act on centrosomal cohesin. In late mitosis separase is activated, which cleaves the cohesin ring at centromeres as well as in the PCM (albeit, with some delay), which ultimately leads to sister chromatid separation and centriole disengagement. For more details, see text.

experiments (Mohr *et al*, 2015) despite its unperturbed localization to the centromeres (Figure 31).

According to my results, Sgo1's centrosomal targeting depends on the CTS. Since both centrosomal isoforms retain their C-box (see also Figure 8), the CTS must incorporate both pro-centrosomal as well as anti-centromeric properties. How can the small CTS fulfill these requirements? For once, the CTS and the C-box might directly interact, which could give rise to a model, in which the CTS would mask the C-box for phosphorylated H2A. However, such an interaction could never be confirmed in a yeast-2-hybrid approach (Lisa Mohr, University of Bayreuth, Germany; unpublished data). We can furthermore exclude that the CTS acts as a nuclear export sequence, since chemical inhibition of global nuclear export did not produce cause centrosomal Sgo1 variants to accumulate in the nucleus (Lisa Mohr, University of Bayreuth, Germany; unpublished data). Therefore, the presence of the CTS might either cause a drastic change of Sgo1's three-dimensional structure leading to allosteric inactivation of the C-box, and/or the affinity of respective Sgo1 variants to their centrosomal target might simply exceed that to

their centromeric one (phosphorylated H2A). In any case, the facts that the CTS is functionally transferable, and that mutating only three consecutive amino acids (ILY) causes it to lose its targeting-ability (Figure 32), strongly argues in favor of the peptide having a direct binding partner at the centrosome, which we have not identified so far.

3.3.2 Sgo1 A2 and C2 protect centrosomal cohesin from prophase pathway signaling by recruitment of PP2A

In late mitosis, separase-dependent cleavage of centromere- and centrosome-associated cohesin triggers sister chromatid separation and (with some delay) centriole disengagement (Gregson *et al*, 2001; Tsou & Stearns, 2006; Wong & Blobel, 2008; Kong *et al*, 2009; Tsou *et al*, 2009; Nakamura *et al*, 2009; Schöckel *et al*, 2011 and Figure 39). But RNAi-mediated depletion of all Sgo1 isoforms causes these two processes to occur prematurely (Figure 33). However, artificially closing cohesin's Smc3-Scc1 gate and thereby abrogating the prophase pathway rescues both chromosomal and centrosomal phenotypes to a considerable extent. This result not only gives further credence to this gate's identity as cohesin's DNA exit gate during prophase (chapters 2.1 and 3.1), but even more crucially, establishes centrosomal cohesin as a prophase pathway-target and appropriate Sgo1 isoforms as protectors of the ring complex from said pathway. Moreover, Sgo1 not only recruits PP2A to the centrosomes (Mohr *et al*, 2015), but the phosphatase even seems to be the actual effector in centrosomal cohesin protection, since artificially localizing the phosphatase to centrosomes (by fusing it to the CTS) partially suppresses centriole disengagement upon Sgo1 depletion (Figure 37).

Since the only other centromere-associated Sgo1 splice variant, Sgo1 C1, is not functional, the canonical Sgo1 A1 is the only isoform that protects centromeric cohesin. In contrast, proper rescue of centriole disengagement requires simultaneous action of both centrosome-associated isoforms, Sgo1 A2 and C2 (Mohr *et al*, 2015). Such an additive effect is typically explained by separate pathways working towards the same outcome, which, by extension, would imply a second Sgo1-protected target at the centrosomes involved in centriole engagement. There is, in fact, a second protein known, which has been ascribed such an involvement: pericentrin (PCNT; also kendrin). Interestingly, in the case of PCNT, it is again its proteolysis, which triggers centriole disengagement and even more strikingly, this proteolysis is again mediated by separase (Matsuo *et al*, 2012; Lee & Rhee, 2012; Pagan *et al*, 2015). So there are two separase targets at the centrosome,

cohesin and PCNT, whose separate and/or simultaneous cleavage results in centriole disengagement (Philip Kahlen, University of Bayreuth, Germany; unpublished data). Centrosomal cohesin is furthermore a target of the prophase pathway, whose action must be locally counteracted by a centrosomal Sgo1 isoform. In this scenario, this isoform would expected to be Sgo1 A2, since it retains the T346-containing exon 6-encoded peptide, which is required for direct binding to cohesin (Liu *et al*, 2013b). Again, our data implies a second Sgo1 target at the centrosome and although there is no substantial evidence for this, it would now be tempting to assume Sgo1 C2's centrosomal target to be PCNT. But what would this Sgo1 isoform protect PCNT from? The prophase pathway would be an obvious, albeit unlikely, candidate, because of the very specific interactions of prophase pathway components with the cohesin ring complex. Another possibility might be inferred by taking a cue from Sgo1's meiotic counterpart, Sgo2. Sgo2-PP2A's mode of cohesin-protection is quite different as it dephosphorylates the meiotic Scc1 homolog Rec8, whose phosphorylation is dependent on Plk1 (Lee & Amon, 2003; Kitajima *et al*, 2006; Riedel *et al*, 2006). Since in meiosis α-kleisin phosphorylation is indispensable for bivalent separation, Sgo2-PP2A acts as a direct inhibitor of separase-dependent cleavage of cohesin. One could hypothesize mitotic Sgo1 C2-PP2A to act similarly, protecting pericentrin from premature separase-cleavage. This hypothesis is supported by preliminary data indicating that Plk1-dependent phosphory-lation of PCNT is required for its separase-dependent proteolysis (Philip Kahlen, University of Bayreuth, Germany; unpublished data). Even if these predictions were accurate, they could still not explain, why the mitotic cell would employ two shugoshin-protected pathways to maintain centriole engagement. The answer may lie in the fact that centriole disengagement happens later in mitosis (ana-/telophase; Kuriyama & Borisy, 1981) than sister chromatid separation, despite the regulation of both mechanisms being seemingly coordinated by the dual use of cohesin, the prophase pathway, and separase (see also Figure 39). In fact, it has even been suggested recently that separase is locally activated at the centrosomes ahead of its activation at the chromosomes (Agircan & Schiebel, 2014), which could theoretically cause centrioles to disengage even prior to chromatid separation, were we to assume that Sgo1 only acts against the prophase pathway. If this result was true, then one would have to infer the existence of a mechanism dampening or even delaying separase activity at the centrosomes during metaphase-to-anaphase transition. However, according to my results, a role for centrosomal Sgo1 as a direct antagonist for separase seems unlikely, because my experiments were performed with cells, which were arrested in prometaphase, i.e. at a

time when separase is still inactive. Thus, the protease's activity cannot have caused the observed phenotypes upon Sgo1-depletion. In addition, the delayed timing of centriole disengagement can be more easily explained by recent results that suggested that some residual separase can be re-inhibited by cyclin B1 after metaphase-to-anaphase transition, which might reserve some of its activity for later processes (Hellmuth *et al*, 2015b). It should be noted that artificial recruitment of PP2A to centrosomes solely via the CTS, already rescued centriole engagement in the absence of Sgo1 to a great extent (Figure 37). Therefore, Sgo1 A2's and C2's combined function might simply be to accumulate enough phosphatase at the centrosomes, regardless of any precise sub-localization.

3.3.3 Cohesin loading onto centrosomes

Since many cohesin functions appear to be conserved between chromo- and centrosomes, we asked whether even cohesin loading onto centrosomes might have similar requirements. These experiments nicely confirmed the results from Figure 21 and strengthen the hinge's identity as cohesin's DNA entry gate (Figure 36). Even more so, while my initial characterization was purely based on localization data, the results from Figure 36 provide additional information over function, as impaired cohesin reloading caused premature sister chromatid separation in the following mitosis to a considerable extent. The results on centrosomal loading of cohesin paint a similar picture: only when the Smc1-Smc3 gate was forced to stay shut before reloading, centrioles exhibited increased disengagement in the following mitosis. However, this phenotype became only apparent, when completely untethered centrioles (that do not appear to have a second centriole in the vicinity) were included in the quantification. These are typically present in very low numbers in our analyses and are likely a result of physical forces on centrosomes during the isolation procedure. In this case however, artificially closing cohesin's hinge gate (and only this) caused a marked increase of untethered centrioles, strongly suggesting a role for cohesin in centriole tethering for example by recruiting involved proteins. However, this seems not to be the case as judged by the unimpaired recruitment of rootletin (part of the tethering network; Bahe *et al*, 2005) in rapamycin-treated Smc1-int. FKBP/Smc3-int. FRB cells (data not shown). Thus, since I cannot fully exclude any experimental artifact, I consider this question to remain unanswered until cohesin's putative role in centriole tethering can be addressed.

From all that we know about cohesin's association with centrosomes, it remains uncertain, however, whether opening of the cohesin ring is an expected requirement for its centrosomal loading. Preliminary data from immuno-electron microscopical studies ongoing in our group (Michaela Rogowski, University of Bayreuth, Germany; unpublished data) as well as our microscopical observations of immunofluorescently labeled cohesin with respect to known proximal or distal centrosome markers (Mohr *et al*, 2015), indicate that cohesin is most likely associated with the PCM (see also Figure 39). Therefore, the ring complex is not expected to be an actual topological linker between centrioles, calling the requirement for ring opening to load cohesin onto centrosomes into question. Interestingly, PCNT, whose cleavage by separase is also involved in centriole disengagement (see above), is not only also associated with the PCM but is moreover believed to play a main role for its structural integrity, rather than to physically connect the two centrioles (Haren *et al*, 2009; Lee & Rhee, 2011; Fu & Glover, 2012; Mennella *et al*, 2012; Lawo *et al*, 2012). So, taking all of these data into account, how do cohesin and/or PCNT mediate centriole engagement, and furthermore, how is this affected by their proteolysis in late mitosis? While we do not know the definite answers to these questions, we propose that both, PCNT and cohesin, play a role in PCM integrity. As a result of separase-mediated cleavage of both proteins (PCNT and Scc1), the PCM's gel-like structure is lost, which causes the centrioles to passively (and/or by cytoskeletal pulling forces) drift apart; A mechanism reminiscent of the transition of F-actin networks from an gel-like to a soluble state by the action of actin-severing proteins (reviewed in Silacci *et al*, 2004). This model for centriole disengagement is supported by recent data from *Caenorhabditis elegans*, which are consistent with centrioles remaining engaged by being embedded into the PCM rather than by a physical linker (Cabral *et al*, 2013). More importantly, ultimate disengagement was reported to be caused by cytoskeletal forces acting on centrioles upon PCM breakdown. It is important to note, however, that this does not negate the requirement for separase in this process at least in (male) meiosis of *C. elegans* (Schvarzstein *et al*, 2013; Cabral *et al*, 2013).

3.3.4 The advantages (and disadvantages) of using different Sgo1 splice variants

The CTS of human Sgo1 is a peculiar peptide as it manages to effectively reprogram human Sgo1 from a protector of centromeric cohesin to one of centrosomal cohesin (and possibly other factors; see chapter 3.3.2) with only being 40 amino acids long. Even more

interestingly, CTS-like sequences can only be found in Sgo1 orthologs of higher primates like gibbons and orangutans and therefore are a quite recent invention of evolution (Mohr *et al*, 2015). However, this does not mean that non-primates do not need Sgo1 function at the centrosomes but rather that this CTS-dependent division of labor seems to be a unique requirement for cognitive life. For example, murine Sgo1 does not contain a CTS-like sequence but localizes to and functions on both centromeres and centrosomes in unison (Mohr *et al*, 2015). Whether cohesin-based mechanisms are required for centriole (dis-)engagement in other (centrosome harboring) organisms, however, remains unclear. So has it been shown that cohesin cleavage is dispensable for centriole disengagement in flies. In *C. elegans* meiosis on the other hand, Rec8-containing cohesin has been reported to maintain centriole engagement until its separase-dependent cleavage (Oliveira & Nasmyth, 2013; Schvarzstein *et al*, 2013).

At first glance, the dual use of the cohesion regulation machinery seems to imply that the processes on chromosomes and centrosomes need to be tightly coordinated during mitotic exit (and they likely do). However, the development of distinct Sgo1 splicing mechanisms in higher primates to utilize specific isoforms for each task, points towards an evolutionary advantage associated with uncoupling these functions. One of the more prominent reasons why chromatid separation and centriole disengagement might have to be uncoupled is their timing difference in late mitosis. As already mentioned, centriole disengagement happens after sister chromatid separation (Kuriyama & Borisy, 1981) despite the fact that both processes are triggered by separase activation in late mitosis (see also Figure 39). It is easily conceivable that different isoforms exist to allow for more differentiated (timely) regulation of these processes (see chapter 3.3.2). Another obvious event in most eukaryotic organisms' life cycle, in which chromo- and centrosomal cycles have to be uncoupled, is male meiosis. Here, chromosomes undergo two rounds of separation, while skipping DNA replication in between. Centrosomes on the other hand, are duplicated between meiosis I and II (Cunha-Ferreira *et al*, 2009). However, despite these differences, it is still separase, which acts on both chromosomal and centrosomal cohesin. Interestingly, data from *C. elegans* show that at the end of meiosis II centrioles do not become disengaged due to protection of Rec8 against separase-cleavage by the functional analogs of mammalian Sgo2 (Schvarzstein *et al*, 2013). Inactivation of these analogs (or overexpression of a separase mutant that hyperaccumulates at centrosomes) causes premature centriole disengagement in those spermatocytes, ultimately leading to an elevated number of zygotes harboring supernumerary centrosomes after fertilization. In

humans, a specialized shugoshin-PP2A complex might be utilized to protect centriole engagement from separase activity in late meiosis II, while sister chromatid separation can progress. This is consistent with the fact that mature human sperm centrosomes are seemingly devoid of any phosphorylations, as they cannot be bound by a pan-phosphoepitope antibody, unless they had been preincubated with meiotic extract from frog oocytes (Simerly *et al*, 1999).

Alternative splicing always harbors the risk for splicing errors and in rare cases, erroneous products can have harmful effects in the cell. For Sgo1, there are some abnormal splicing products known, of which one, Sgo1 B1, has been found to be associated with the development and drug resistance of non-small cell lung cancer (Matsuura *et al*, 2013). Interestingly, Sgo1 B1 is similar to Sgo1 C1 (Sgo1 B1 retains a small fragment of the exon 6-encoded peptide), which in our hands behaves in a dominant-negative manner upon overexpression (Mohr *et al*, 2015). Strikingly, Sgo1-haploinsufficient mice exhibit enhanced colonic tumorigenesis accompanied by chromosomal instabilities as well as impaired centrosome dynamics, strongly suggesting a direct link between Sgo1's centrosomal function and cancer development (Yamada *et al*, 2012).

4. Materials and Methods

4.1 Materials

4.1.1 Hard- and software

This work was written on a MacBook Pro 15" Early 2011 ("MacBookPro8,2"; Apple, Cupertino, CA, USA) running "MacOS X" version 10.10.3 (Apple, Cupertino, CA, USA) and using the text editing software "Pages '09" version 4.3 (Apple, Cupertino, CA, USA). Image processing was performed with "Photoshop CS4" version 11.0 and "Photoshop CS6 Extended" version 13.0.6 (Adobe Systems, San Jose, CA, USA). To analyze microscopic images, ImageJ64 (http://imagej.nih.gov/ij) was used, sometimes in conjunction with the "Bio-Formats" plugin (http://openmicroscopy.org/info/bio-formats) to open certain microscopy formats. For the generation of figures, "Illustrator CS4" version 14.0 and "Illustrator CS6" version 16.0.4 (Adobe Systems, San Jose, CA, USA) were used. Analysis of nucleic acid and protein sequences was performed using "Lasergene" versions 8.0.3 and 11.0.0 (DNASTAR, WI, USA). "Papers 3" version 3.2.2 (Mekentosj, Dordrecht, The Netherlands) was used as bibliography software. Literature and database searches were done using online tools provided by the National Center for Biotechnology Information (NCBI, http://www.ncbi.nlm.nih.gov/) and the European Bioinformatics Institute/Wellcome Trust Sanger Institute (EBI/WTSI, http://www.ensembl.org). Chemiluminiscence signals from Western Blots were detected using an "LAS-4000" system and corresponding software (FUJIFILM Europe, Düsseldorf, Germany). Radioactively labeled proteins from coupled *in vitro* transcription/translation were analyzed using the "FLA-7000" system and corresponding software (FUJIFILM Europe, Düsseldorf, Germany). Immunofluorescence microscopy was performed on an "Axio Imager A1" microscope (Zeiss, Jena, Germany) fitted with a "Pursuit" CCD camera (SPOT Imaging solutions, Sterling Heights MI, USA), an "Axioplan 2" microscope fitted with an "AxioCam MRm" CCD camera (Zeiss, Jena, Germany) or a "DMI6000 B" microscope (Leica Microsystems, Wetzlar, Germany). Centrifuges were supplied from Beckman Coulter (Krefeld, Germany), Eppendorf (Hamburg, Germany), Heraeus/Thermo Fisher Scientific (Bonn, Germany). Cell culture clean benches were from Kojair (Vught, Netherlands) and incubators from Heracell/ Thermo Fisher Scientific (Bonn, Germany). Precision pipettes were provided by Eppendorf (Hamburg, Germany) and Gilson (Limburg-Offheim, Germany).

4.1.2 Chemicals and reagents

All chemicals were of analytical grade and, unless otherwise noted, purchased from Abcam (Cambridge, UK), AppliChem (Darmstadt, Germany), BD Biosciences (Heidelberg, Germany), Carl Roth (Karlsruhe, Germany), Fermentas/Fisher Scientific (Schwerte, Germany), GE Healthcare (Munich, Germany), Grüssing GmbH (Filsum, Germany), Invitrogen/Life Technologies (Darmstadt, Germany), Merck (Darmstadt, Germany), Millipore/Merck (Schwalbach, Germany), New England Biosciences (NEB; Frankfurt a.M., Germany), Pierce/Thermo Fisher Scientific (Bonn, Germany), Roche Diagnostics (Mannheim, Germany), Serva (Heidelberg, Germany), Sigma-Aldrich (Munich, Germany) and VWR (Darmstadt, Germany). Deionized water was further filtered by a GenPure water purifier (TKA, Niederelbert, Germany) and subsequently autoclaved to obtain "ddH_2O".

4.1.3 DNA oligonucleotides

The following DNA oligonucleotides were used as primers for PCR reactions (for cloning) or sequencing (Microsynth/Seqlab, Göttingen, Germany). They were synthesized to order by MWG Biotech/Eurofins Genomics (Ebersberg, Germany), Metabion (Planegg/ Steinkirchen, Germany) and Sigma-Aldrich (Munich, Germany).

name	sequence (5'->3')
5'Nhe1_FKBP	ATAGGCTAGCGCAGGATCCATGGGAGTGCAGGT
5'Nhe1_FRB	ATAGGCTAGCGCAGGATCCATGATCCTCTGGCA
Bu_hSmc1_3'A	GGCGCGCCCTACTGCTCATTGGGGTTGG
Bu_hSMC1_ 3'BamHI	CATGGATCCTGCGCTAGCC
Bu_hSMC1_3'NheI	TTGGCTAGCTCACTCTCCAGC
Bu_hSMC1_5'F	ATAGGCCGGCCCATGGGGTTCCTGAAACTGATTG
Bu_hSMC1_5'SacI	ATGGAGCTCCTGTGGGCAAG
Bu_hSMC1_NheI/SphI_down	GATGAGGCTAGCGGCGCATGCAAACTCCGGGAGCTGAAGGG
Bu_hSMC1_NheI/SphI_up	GTTTGCATGCGCCGCTAGCCTCATCTGTAGGCTTCACCTCC
Bu_hSMC1_seq1	GGTACAGCTGCAGCTCTTTAAG
Bu_hSMC1_seq2	CGCATCGACCGCCAGGAGAG
Bu_hSMC1_seq3	CATTCAGAGCCGAGAGAGGG
Bu_hSmc1_Seq4	CTCCTTCAGTTCATCCTCCAC
Bu_hSMC1_siResist_down	AACGAAAGAAGGTGGAAACGGAGGCCAAGATCAAGCAAAAGCTG
Bu_hSMC1_siResist_up	CCTCCGTTTCCACCTTCTTTCGTTCTTCCAGATCCAGACGG
Bu_hSmc1hinge_ fwd	GCGAGATCTAGCCGCCAGCAGC

name	sequence (5'->3')
Bu_hSmc1hinge_ rev	AGAGCGGCCGCTTATTTCAACTTGTCTACTGCTTT
Bu_hSMC3_NheI/XmaI_down	CCTGAAGCTAGCGGCCCCGGGACCAATGATGCTATTCCTATGATC
Bu_hSMC3_NheI/XmaI_up	TGGTCCCGGGGCCGCTAGCTTCAGGATAGGCTGTATCCC
Bu_hSMC3_seq1	CTCAGCAGGATGCAAGAGATAAAA
Bu_hSMC3_seq2	GATCAGAAGAGAGTAGATGCACT
Bu_hSmc3AA_3'AscI_Stop	GGCGCGCCTTAACCATGTGTGGTATCATCTTCTAC
Bu_hSmc3AA_5'FseI	ATCAGGCCGGCCAATC
Bu_hSmc3AA_down	GTTATTGGTGCCGCAGCGGATCAGTATTTCTTAGACAAGAAG
Bu_hSmc3AA_up	CTGATCCGCTGCGGCACCAATAACTCTTCGAAG
Bu_hSmc3hinge_fwd	AGGCAATTGATGAAGCAACAACTTCTTAGAG
Bu_hSmc3hinge_rev	CGCGGTACCTTATTCTGCTTTTCTAACATCTTTTT
Bu_Linker_5'XhoI	ATACTCGAGATAACAATGGCCGGGCTCCCGCCC
CS2_for	CGCCATTCTGCCTGGGGAC
CS2_rev	TCTGGATCTACGTAATACGAC
FKBP_3'Sph1	TTCAGCATGCGGGAGCCCGGCCATTGTTATTTTC
FKBP-for	CATCCCACCACATGCCACTCT
FKBP-linker_3'FA	AGAGGCGCGCCCTCGAGAGG
FKBP-linker_5'B	ATACCAACCGGATGGATGGGAGTGCAGGTGGAAAC
FRB_3'M	ATAACGCGTTCACTTTGAGATTCGTCGGAACACAT
FRB_5'FA	TCAGGCCGGCCGTTTAAACG
FRB_3'Xma1	TTACTACCCGGGAGCCCGGCCGTTGTTGTTCT
FRB_rev	GTACAAACGAGATGCCTCTTCCA
hSmc3.seq1	GTAACCCCTATCTAACTCTTCTTGACGCTT
hSmc3.seq3	GCTATCATGGTATTGTAATGAATAAC
MO_hSMC3_3'A	AATGGCGCGCCTTAACCATGTGTGGTATCATC
MO_hSMC3_5'F	AATGGCCGGCCCATGTACATAAAGCAGGTGATTAT
pcDNA_FAfor_OS	CCTGGAGACGCCATCCAC
pcDNA_FArev_OS	GCACGGGGGAGGGGCAAA

4.1.4 RNA oligonucleotides (siRNAs)

The following table lists all small interfering (si)RNAs, which were used in this study to knock down proteins in mammalian cells via RNA interference (RNAi; Elbashir *et al*, 2001). All siRNAs are 21mers consisting of 19 target specific nucleotides with an additional 5' dTdT-overhang (not included in the table).

name	sequence (5'->3')
BM_GL2-luc	CGUACGCGGAAUACUUCGA
BM_hSgo1	CAGUAGACCCUGCUCAGAA
LM_Sgo1	GAUGACAGCUCCAGAAAUU
siSgo1_5'UTR	GAUAGCUGUUGCAGAAGUA
siSmc1_ORF_1	GGAAGAAAGUAGAGACAGA
hSmc3(3'UTRI)	UGGGAGAUGUAUAUAGUAA
siRNAhScc13UTR1	ACUCAGACUUCAGUGUAUA
siRNAhScc13UTR2	AGGACAGACUGAUGGGAAA
siRNA_SMC3_3UTR_2	UGUCAUGUUUGUACUGAUA
siWapl_1	CGGACUACCCUUAGCACAA
siWapl_2	GGUUAAGUGUCCCUCUAAU

4.1.5 Plasmids

The following table contains plasmids from the Stemmann laboratory plasmid collection, which were used in the course of this work. The MCS of each vector has been replaced by single *Fse*I- and an *Asc*I-sites, which were used for transgene insertion and rapid subcloning.

plasmid identifier	insert	tag(s)	backbone	origin
pIC-Cre	Cre recombinase	–	pUC-9	Addgene, Cambridge, MA, USA
pMO1511	hPP2A-B'α	N-Myc6-	pCS2	Michael Orth
pAG1786	FLP recombinase	–	pCS2	Amelie Gutsmiedel
pBM2644	hSgo1 A1 (siResist)	N-Myc6-	pcDNA5/FRT/TO	Bernd Mayer
pBM2645	hSgo1 A2 (siResist)	N-Myc6-	pcDNA5/FRT/TO	Bernd Mayer
pBM2646	hSgo1 C2 (siResist)	N-Myc6-	pcDNA5/FRT/TO	Bernd Mayer
pJB2683	hScc1	N-FKBP-linker-	pCS2	this study
pJB2684	hScc1	-FRB-C	pCS2	this study
pJB2685	hSmc1	N-FKBP-linker-	pCS2	this study
pJB2686	hSmc1	internal FKBP	pCS2	this study
pJB2687	hSmc3	-FRB-C	pCS2	this study
pJB2688	hSmc3	internal FRB	pCS2	this study
pBM2740	hSgo1 C1 (siResist)	N-Myc6-	pcDNA5/FRT/TO	Bernd Mayer
pJB2790	hScc1	N-FKBP-linker-	pcDNAL/FRT/TO	this study
pJB2791	hScc1	-FRB-C	pcDNAL/FRT/TO	this study
pJB2792	hSmc1 (siResist)	N-FKBP-linker-	pcDNA5/loxP/TO	this study

plasmid identifier	insert	tag(s)	backbone	origin
pJB2793	hSmc1 (siResist)	internal FKBP	pcDNA5/loxP/TO	this study
pJB2794	hSmc3	-FRB-C	pcDNA5/loxP/TO	this study
pJB2795	hSmc3	internal FRB	pcDNAL/FRT/TO	this study
pDK2889	hSgo1 $A2^{AAA}$ (siResist)	N-Myc6-	pcDNA5/FRT/TO	Dorothea Karalus
pJB2897	hScc1-hSmc1 fusion	–	pcDNAL/FRT/TO	this study
pLM3012	hSgo1 A2 C-terminus (CTS)	N-mCherry-	pCS2	Lisa Mohr
pJB3027	$hSmc3^{AA}$	-FRB-C	pCS2	this study
pLM3066	hSgo1 A2 C-$terminus^{AAA}$ (CTS^{AAA})	N-mCherry-	pCS2	Lisa Mohr
pJB3319	hPP2A-B'α-linker-CTS	N-Myc6-	pCS2	this study
pJB3323	hPP2A-B'α-linker-CTS^{AAA}	N-Myc6-	pCS2	this study

4.1.6 Antibodies

The following table contains informations to all antibodies used in this study.

target protein	species	clonality	dilution/ concentration	origin
BrdU (crossreactive towards CldU)	rat	monoclonal	IFM: 1:100	Abcam, ab6326
BrdU (crossreactive towards IdU)	mouse	monoclonal	IFM: 1:100	BD Biosciences, 347580
Centrin2	rabbit	polyclonal	IFM: 1:5000	self-made (Schöckel *et al*, 2011), affinity purified
CREST	human	polyclonal	IFM: 1:2000	Immunovision, hct-0100
C-Nap1	guinea pig	polyclonal	IFM: 1:2500	self-made (Schöckel *et al*, 2011), affinity purified
FKBP12	mouse	monoclonal	WB: 1:1000 - 1:500 IFM: 1:500	Abcam, ab58072
FRB	rabbit	polyclonal	WB: 0.34-1.41 μg/ml IFM: 2.82 μg/ml IP: 10 μg/2 × 10^7 cells	self-made, raised against the bacterially expressed full-length protein (Coring System Diagnostics), affinity purified
Hec1	mouse	monoclonal	IFM: 1:500	Genetex, 70268
mCherry	rabbit	polyclonal	IF: 1:3000	kindly provided by Stefan Heidmann, affinity purified

target protein	species	clonality	dilution/ concentration	origin
Myc	mouse	monoclonal	WB: 1:2000 IFM: 1:1500	Millipore, clone 4A6, 05-724
Pds5A	rabbit	polyclonal	WB: 1:1000	kindly provided by Susannah Rankin, affinity purified
SA1	rabbit	polyclonal	WB: 3.5 μg/ml	kindly provided by Susannah Rankin, raised against the C-terminal 199 aa of *Xenopus* SA1, affinity purified
Scc1	rabbit	polyclonal	WB: 1:1000	self-made (Stemmann *et al*, 2001), serum; only used for initial experiments
Scc1	mouse	monoclonal	WB: 1:1000 IFM: 1:500	Millipore, 05-908
Smc1	rabbit	polyclonal	WB: 1:4000 IFM: 1:500	Bethyl Laboratories, A300-055A
Smc3	rabbit	polyclonal	WB: 1:1000	self-made (Schöckel *et al*, 2011), affinity purified; only used for initial experiments
Smc3	rabbit	polyclonal	WB: 1 μg/ml IP: 10 μg/2 × 10^7 cells	kindly provided by Susannah Rankin, raised against the C-terminal 180 aa of *Xenopus* Smc3, affinity purified
ssDNA	mouse	monoclonal	IFM: 1:300	Millipore, MAB3034
α-tubulin	mouse	monoclonal	WB: 1:200	Developmental Studies Hybridoma Bank, clone 12G10, self-made hybridoma supernatant
Wapl	rabbit	polyclonal	WB: 1.3 μg/ml IP: 5 μg/2 × 10^7 cells	kindly provided by Susannah Rankin, raised against the C-terminus of *Xenopus* Wapl, affinity purified
Wapl	mouse	monoclonal	WB: 1:5 (hybridoma supernatant) or 2 μg/ml (affinity purified)	self-made, clone D9, raised against the bacterially expressed N-terminal 88 aa of human Wapl

As secondary antibodies in WB experiments, polyclonal goat anti-mouse-IgG and anti-rabbit-IgG from Sigma-Aldrich (Munich, Germany), all conjugated to horseradish peroxidase, were used (1:20,000). For IFM (all 1:500, unless otherwise noted), goat anti-mouse- and -rabbit-IgG (Life technologies), fused to either AlexaFluor 488 or Cy3, were used. In addition, goat anti-guinea pig-IgG, fused to Cy3 (Jackson Immunoresearch Laboratories, Westgrove, PA, USA) as well as goat anti-human-IgG fused to Cy5 (Bethyl Laboratories, Montgomery, TX, USA), have been used.

4.2 Microbiological methods

4.2.1 Strains

The *E. coli* XL1-Blue strain was used for molecular cloning and plasmid production:

*E. coli sup*E44 *hsd*R17 *rec*A1 *gyr*A46 *thi rel*A1 *lac*$^-$ *F'*[*pro*AB$^+$ *lac*I^q Δ(*lacZ*)M15 Tn*10*(*tet*^{r})] (Stratagene/Agilent Technologies, Santa Clara, CA, USA)

4.2.2 Media

LB medium:
1% (w/v) tryptone
0.5% (w/v) yeast extract
1% (w/v) NaCl

LB agar:
LB medium + 1.5% (w/v) agar

4.2.3 Cultivation of *E. coli*

E. coli strains were grown in LB medium at 37°C in a rotator at ca. 200 rpm. LB agar plates were incubated at 37°C. For selection of transformed bacteria 100 µg/ml ampicillin (final concentration) was added to the medium/agar. Culture densities were determined by measuring the optical density at a wavelength of 600 nm (OD_{600}).

4.2.4 Preparation of chemically competent *E. coli* XL1-Blue

Tbf1 buffer:
30 mM KAc
50 mM $MnCl_2$
100 mM KCl
15% (v/v) glycerol
pH 5.8

Tbf2 buffer:
10 mM MOPS-NaOH
75 mM $CaCl_2$
10 mM KCl
15% (v/v) glycerol
pH 7.0

SOB medium:
2% (w/v) tryptone
0.5% (w/v) yeast extract
0.5% (w/v) NaCl
2.5 mM KCl
pH 7.0

300 ml SOB medium was inoculated with 4 ml of an overnight culture of *E. coli* XL1-Blue with an OD_{600} of 0.5. The culture flask was chilled on ice for 15 min before cells were harvested by centrifugation (4°C, 3000 g, 15 min). All following steps were performed

using prechilled (4°C) and sterile vessels and solutions. Bacteria were resuspended in 90 ml Tbf1 buffer and incubated on ice for 15 min. After additional centrifugation (4°C, 1500 g, 15 min), bacteria were resuspended in Tbf2 buffer and incubated on ice for 5 min. This suspension then was aliquoted, snap-frozen and stored at -80°C.

4.2.5 Transformation of *E. coli* XL1-Blue

Frozen, chemically competent *E. coli* XL1-Blue were thawed on ice. 5 µl of a ligation mix 0.5-1 µl of plasmid DNA (typically 0.25-1 µg) was added to 40 µl bacterial suspension and incubated on ice for 20 min. The cells were then heat shocked at 42°C for 45 s and subsequently put on ice for 2 min. 400 µl LB medium without antibiotics was added to the transformation mix, which was then incubated at 37°C for 1 h on a shaker to allow for the resistance gene to be expressed before the cells were plated onto LB-ampicillin agar plates and incubated overnight at 37°C. Since Ampicillin-selection does not necessarily require this pre-incubation, oftentimes 400 µl LB medium with 100 µg/ml ampicillin was added to the transformation mix, which was then immediately plated onto LB-ampicillin agar plates and incubated overnight at 37°C.

4.3 Molecular biological methods

4.3.1 Isolation of plasmid DNA from *E. coli* XL1-Blue

Depending on the amount of plasmid DNA needed, different kit-based plasmid isolation methods were used. Therefore, 2-300 ml LB-ampicillin medium were typically inoculated from a single colony of transformed *E. coli* XL1-Blue. Occasionally, if a fresh plasmid preparation of an existing plasmid had to be generated, the bacterial culture was directly inoculated using the transformation mix (thereby omitting the over night incubation of the LB-agar plate). The next day, the bacteria were harvested. Alkaline lysis and DNA purification via silica or anion exchange columns was done using plasmid preparation kits from Fermentas/Thermo Scientific (Schwerte, Germany), Macherey-Nagel (Düren, Germany), and QIAGEN (Hilden, Germany) according to the manufacturer's instructions.

4.3.2 Determination of DNA concentrations in solutions

DNA concentrations in solutions were determined by measuring the optical density at a wavelength of 260 nm (OD_{260}) using an ND-1000 spectrophotometer (Peqlab, Erlangen, Germany). An $OD_{260}=1$ corresponds to 50 μg/ml double-stranded DNA.

4.3.3 Restriction digestion of DNA

Site-specific endonucleases were obtained from NEB (Frankfurt a.M., Germany) and used to digest DNA according to the manufacturer's instructions. For digestion of 1 μg DNA 1 - 4 units of the respective endonucleases and the appropriate buffer were used. Samples were typically incubated at 37°C (some endonucleases need higher temperatures) for 1-1.5 h. When a DNA fragment/plasmid had to be digested by two different endonucleases, this was usually performed in one single reaction using a buffer suitable for both enzymes. If this was not possible, due to different buffer or temperature requirements, two different digestion reactions were applied, while exchanging buffers and enzymes between the two incubations via "PCR purification" (for details see 4.3.9).

4.3.4 Polymerase chain reaction (PCR)

PCR was utilized to amplify specific DNA fragments or whole genes using plasmids or commercially available human cDNA (Clontech, Mountain View, CA, USA) as templates. DNA was multiplied *in vitro* by a DNA polymerase ("Phusion", Finnzymes/NEB, Frankfurt a.M., Germany; "Pfu", self-made) using specific DNA oligonucleotides (see 4.1.3) flanking the desired amplificate's region as primers. A typical PCR reaction was prepared as follows:

10 μl 5× HF buffer/GC buffer (supplied with Phusion polymerase)
1 μl 10 mM deoxynucleotide triphosphate mix (dNTPs)
0.25 μl 0.1 mM primer forward
0.25 μl 0.1 mM primer reverse
0.5-3 μl template
0.5 μl Phusion polymerase
ddH_2O to 50 μl

PCR reactions were performed in a thermocycler ("TC-512" and "TC-312", Techne, Stone, UK), which allows repetitive heating and cooling of the samples to denature DNA into single strands (Pfu: 95°C; Phusion: 98°C), anneal the primers to these single strands

(50-69°C) and ultimately polymerize a new DNA strand from dNTPs at the optimal temperature for the DNA polymerase (72°C). Annealing temperatures were typically determined by rounding up the individual melting temperatures (T_M) of the primers to the next full degree Celsius (if the primers had different T_Ms the lower one was applied; for Pfu polymerase reactions, annealing temperatures were: T_M + 5°C). T_Ms are mainly dependent on the length and the base composition of the primer and was calculated as "Davis, Botstein, Roth" temperature using the sequence analysis tool "EditSeq" (DNASTAR, WI, USA). A typical thermocycler program for the Phusion polymerase was as follows:

step	temperature [°C]	time [s]	repeats
initial denaturation	98	30	
denaturation	98	10	
annealing	50-69	30	× 5-30
polymerization	72	15-30/kb	
final polymerization	72	300-600	

Generally, the number of polymerization cycles was kept as low as possible to minimize sequence errors. Oftentimes, PCR reactions were used to add specific restriction sites to the 5'- and 3'-ends of a DNA fragment. Therefore, the 5'-ends of the sequence-specific oligonucleotide primers were extended by the respective endonuclease recognition sequences, that consequently did not anneal to the amplification target. Hence, only the fraction of the oligonucleotide correctly aligning to the template was used to calculate the annealing temperature. In these cases, to increase fidelity and accumulate full length fragments (containing the restriction sites), two subsequent polymerization cycles featuring different annealing temperatures were employed: The first cycle used the primer-specific annealing temperature excluding the restriction sites, the second one included them in the calculation. Thereby, annealing temperature was increased during the reaction which increases its stringency. In all instances, in which the calculated annealing temperature exceeded 69°C, the annealing step of the thermocycling program was omitted and replaced by a slightly longer polymerization step. To confirm successful PCR, and to purify the amplificate, the reaction mix was subjected to agarose gel electrophoresis and subsequent gel extraction (see 4.3.8 and 4.3.9). For following ligation reactions (see 4.3.6), the restriction sites had to be cleaved by the respective endonucleases to generate suitable overhangs.

4.3.5 Mutagenesis PCR

Classical mutagenesis PCR was used to insert new restriction sites into the ORFs of Smc1 and -3 (for the later insertion of FKBP or FRB, respectively), to make Smc1 resistant against siRNA mediated RNAi, and to generate the $Smc3^{AA}$ mutant. This method involved three independent PCR reactions: The first two PCR reactions were used to amplify the ORF 5' and 3' of the region to be mutated. The respective inner primers (which anneal to the region to be modified) either introduced altered nucleotides (which accordingly feature short mismatches with the target DNA) to specifically change the ORF's sequence or featured additional sequences (such as restriction sites) attached to their 5'-end to generate insertions. In any case, the inner primers were designed to overlap and (in this overlapping region) perfectly align to each other to allow later fusion of the two PCR products. The outer primers annealed to the 5'- and 3'-ends of the gene and also included restriction sites at their 5'-ends for final insertion into a suitable vector. The two resulting amplificates were purified via gel extraction (see 4.3.9) and mixed for a third PCR using only the outer primers. Since the two fragments overlap, they can prime each other to be completed to a double strand by the DNA polymerase in the reaction. The outer primers were then used to amplify the full length polynucleotide, which now featured the point mutation/insertion and could be ligated into a new vector via standard methods (see 4.3.6).

4.3.6 DNA ligation

T4 DNA ligase buffer:
50 mM Tris-HCl, pH 7.5
10 mM $MgCl_2$
1 mM ATP
10 mM DTT

A DNA ligation reaction was used to insert DNA fragments derived from PCR reactions or restriction digestion of plasmids into a different vector. A typical 10 µl ligation reaction consisted of 1 µl vector, 7.5 µl DNA fragment, 1 µl T4 DNA ligase buffer and 0.5 µl T4 DNA ligase (self-made in the lab). Ligation reactions were carried out for 1 h at RT or overnight at 14-15°C. For efficient ligation, some reactions required larger amounts of T4 DNA ligase or different vector/fragment ratios. 5 µl of a ligation reaction mix was directly

transformed into *E. coli* XL1-Blue to amplify and eventually purify the successfully ligated plasmid (see 4.2.5 and 4.3.9)

4.3.7 5'-dephosphorylation of vectors

To minimize religation of vectors with themselves, they were subjected to a reaction, in which the 5'-situated phosphate groups (which are paramount for successful ligation of this end) are removed by a phosphatase. Therefore, restriction digested plasmids were supplemented with 5 U/μg antarctic phosphatase (NEB; Frankfurt a.M., Germany) and the appropriate buffer according to the manufacturer's instructions and incubated for 1 h at 37°C.

4.3.8 Separation and analysis of DNA fragments by agarose gel electrophoresis

10× TPE buffer:	*6× DNA loading buffer:*
0.5 M Tris	50% (v/v) glycerol
1.3% (v/v) H_3PO_4	0.1 M EDTA
20 mM EDTA	0.02% (w/v) xylene cyanol
	0.02% (w/v) bromophenol blue
	0.02% (w/v) SDS

For analysis of DNA fragments the respective solutions were complemented with DNA loading buffer (to 1×) and loaded onto gels containing 1% (w/v) agarose and 0.5 μg/ml ethidium bromide (a fluorescent dye, that intercalates into DNA) in TPE buffer. The gels were run at 100 - 120 V in an electrophoresis chamber containing TPE buffer for 30 - 45 min. The gels were then analyzed with a UV transilluminator (324 nm; Syngene, Cambridge, UK). Fragment size was estimated using the standard size marker "O'Gene Ruler 1 kb" (Fermentas, St. Leon-Rot, Germany) or a self-made standard made from *Eco*RI-restriction digestion of SPP1 bacteriophage DNA.

4.3.9 Reisolation of DNA from reaction mixes

Two methods were employed to reisolate DNA from reaction mixes. The first one is agarose gel electrophoresis (see 4.3.8) and subsequent gel extraction. The advantage of this method is that one can visually verify not only the existence but also the size of the DNA fragment/vector of interest. Since gel electrophoresis allows to separate differently

sized DNA fragments, gel extraction is ideally suited to retrieve a specific polynucleotide from a more or less complex mixture (such as a vector and an excised insert, for example). For this, the DNA band corresponding to the desired fragment was excised from the gel using a clean scalpel to be subsequently purified using a gel purification kit from Fermentas/Thermo Scientific (Schwerte, Germany), Macherey-Nagel (Düren, Germany) or QIAGEN (Hilden, Germany) according to the manufacturer's instructions.

The second method for DNA reisolation is the so-called "PCR purification", which retrieves all polynucleotides from a reaction mix while removing proteins, oligonucleotides (such as primers) and buffer components. PCR purification was, again, kit-based and performed as instructed by the manufacturer (Fermentas/Thermo Scientific, Schwerte, Germany; Macherey-Nagel, Düren, Germany; QIAGEN, Hilden, Germany).

4.3.10 DNA sequencing

0.5-1 μg plasmid DNA was supplemented with 20 pmol of a sequencing primer. Sequencing services were provided from Microsynth/Seqlab (Göttingen, Germany).

4.4 Protein biochemical methods

4.4.1 Determination of protein concentrations in solutions

Protein concentrations in solutions were determined by measurement of the optical density at wavelength of 280 nm (OD_{280}) with the ND-1000 spectrophotometer (Peqlab, Erlangen). An $OD_{280}=1$ corresponds to 1 mg/ml protein.

4.4.2 Separation of proteins by denaturing SDS polyacrylamide gel electrophoresis (SDS-PAGE)

17% resolving gel (37.5 ml):
14 ml 1 M Tris-HCl, pH 8.8
21.3 ml 30% acryl amide-bisacryl amide (37.5:1)
2 ml 2.5 M sucrose
20 μl 20% SDS
160 μl 10% ammonium persulfate (APS)
11 μl TEMED

1× Laemmli running buffer:
25 mM Tris
192 mM Glycine
0.1% (w/v) SDS

8% resolving gel (35 ml):
13.1 ml 1 M Tris-HCl, pH 8.8
9.3 ml 30% acryl amide-bisacryl amide (37.5:1)
12.4 ml ddH_2O
20 µl 20% SDS
160 µl 10% ammonium persulfate (APS)
11 µl TEMED

7% stacking gel (32.5 ml):
4.1 ml 1 M Tris-HCl, pH 6.8
7.6 ml 30% acryl amide-bisacryl amide (37.5:1)
20.6 ml ddH_2O
20 µl 20% SDS
160 µl 10% ammonium persulfate (APS)
11 µl TEMED

4× SDS sample buffer:
40% (v/v) glycerol
250 mM Tris-HCl, pH 6.8
8% (w/v) SDS
0.04% (w/v) bromophenol blue
2 M beta-mercaptoethanol

Samples were complemented with SDS sample buffer (to 1×) and denatured at 95°C for 5 to 10 min prior to loading onto self-poured 8-17% gradient SDS gels. Gels were run at 120-140 V (~25 mA/gel) in wet chambers containing 1× Laemmli buffer for 75-90 min. Protein masses were estimated using the PageRuler Prestained Protein Ladder (Thermo Scientific, Schwerte, Germany)

4.4.3 Immunoblotting (Western Blot)

Blotting buffer:
25 mM Tris
192 mM Glycine
0.01% (w/v) SDS
15% (w/v) methanol

TBS/T:
25 mM Tris/HCl, pH 7.5
137 mM NaCl
2.6 mM KCl
0.05% (v/v) Tween-20

10x PBS:
1.37 M NaCl
27 mM KCl
80 mM Na_2HPO_4
14 mM KH_2PO_4
pH 7.4

For the purpose of immunoblotting, proteins were, after separation by SDS-PAGE (see 4.4.2), electrophoretically transferred to polyvinylidene fluoride (PVDF) membranes (Serva, Heidelberg, Germany). This was done using the semi-dry blotting procedure. For

this the protein gel and the membrane were assembled in a sandwich with extra thick blot paper (BioRAD, Munich, Germany) on each side. The sandwich components were preincubated in blotting buffer with an additional preincubation of the PVDF membrane in 100% methanol (this makes the membrane accessible for the aqueous blotting buffer). Blotting was performed in a semi-dry blotter (Peqlab, Erlangen, Germany; BioRAD, Munich, Germany) at 13 V and 120 mA/gel for 1.5 h.

All incubation steps from here on were performed on a shaker. After blotting, the membrane was blocked for ≥45 min in 5% (w/v) dry milk in 1× PBS. The membrane was subsequently washed 3 times for 10 min in TBS/T before incubation with primary antibody (overnight, 4°C). Primary antibodies were typically diluted in 1× Roti-Block (Carl Roth, Karlsruhe, Germany) supplemented with 0.02% (v/v) NaN_3 and were recollected and reused until a clear reduction in signal strength was detected. Some primary antibodies required to be always freshly diluted for each blot or were only available in very small quantities, which did not allow for large dilution volumes. Such antibodies were diluted in 1× PBS/3% BSA and the respective (parts of) blots were placed between to thin sheets of clear polypropylene in a wet chamber to allow proper immersion in the small dilution volumes. After washing (3 times for 10 min in TBS/T), followed incubation with HRP conjugated secondary antibody diluted (1:20,000) in 5% (w/v) dry milk in 1× PBS for 1 h at RT. The membrane was then washed 3 to 4 times briefly and then additionally for at least 1 h and 5 buffer changes with TBS/T. Detection was based on electrochemiluminescence (ECL) and carried out according to the ECL solution's manufacturer ("HRP Juice", PJK, Kleinblittersdorf, Germany; "ECL Ultra", Lumigen, Southfield, MI, USA) using an "LAS-4000" detection system (FUJIFILM Europe, Düsseldorf, Germany).

4.4.4 Coomassie staining

To prepare the staining solution 80 g $(NH_4)_2SO_4$ were dissolved in 765.2 ml ddH_2O. 112.9 ml 85% phosphoric acid were added. 800 mg Coomassie Brilliant Blue G250 (Sigma-Aldrich, Munich, Germany) were dissolved in 16 ml ddH_2O and subsequently added to the solution while stirring.

For staining, protein gels were incubated over night in 80% (v/v) staining solution + 20% (v/v) methanol on a shaker. Excess staining was removed by washing the gel for ≥1 h in ddH_2O, while changing the wash at least 5 times.

4.4.5 Generation and purification of anti-FRB and -Wapl antibodies

His_6-$SUMO_1$-tagged full length FRB-domain (aa 2021-2113, T2098L) of mTOR (NCBI reference number: NM_004958) and the His_6-$SUMO_3$-tagged N-terminal 88 amino acids of human Wapl (NCBI reference number: NM_015045) were bacterially expressed from pET28-based vectors, purified via ion metal affinity chromatography (IMAC), and then used to either immunize rabbits (FRB; Coring System Diagnostix, Gernsheim a. Rhein, Germany) or mice (Wapl). Mouse lymphocytes were harvested, fused with myeloma cells to generate hybridoma cells and ultimately cloned to yield monoclonal antibodies using standard molecular biological methods (carried out by Klaus Ersfeld and Markus Schuster, University Bayreuth, Germany).

In order to purify the antibodies, the respective bacterially expressed target proteins were immobilized on HiTrap NHS-activated HP columns according to the manufacturer's instructions (GE Healthcare, Freiburg, Germany). Final bleed serum (FRB) or hybridoma supernatant (Wapl, clone D9) was then allowed to cycle through the columns for purification using a P1 circular pump. The desired antibodies were eluted from the column according to the manual and eventually dialyzed against 1× PBS/50% (v/v) glycerol for storage (anti-Wapl antibody purification carried out by Markus Schuster).

4.4.6 Immunoprecipitation (IP)

All washing/centrifugation steps were performed at 4°C and 200 g for 1.5 min. All buffers and solutions were pre-chilled and supplemented with a protease inhibitor cocktail (Roche Diagnostics, Mannheim, Germany).

60 μl Protein G sepharose bead slurry ("Protein G Sepharose 4 Fast Flow", GE Healthcare, Freiburg, Germany) were washed twice with 0.5 to 1 ml, and eventually resuspended in 60 μl 1× PBS/3% (w/v) BSA/0.02% (v/v) NaN_3. 5 to 10 μg antibody was added to the bead suspension. The coupling was performed over night at 4°C on a rotator. The antibody-coupled beads were then washed twice with LP2 buffer (see 4.5.8) before they were added to the cell extract. IP was performed over night at 4°C on a rotator. The next day, the beads were washed 6 times in 0.5 to 1 ml LP2 buffer. The proteins were eluted by boiling up the beads in 2× SDS sample buffer (see 4.4.2) for up to 10 min. The resulting beads-eluate suspension was subsequently transferred to "Mobicol" filter

columns (MoBiTec, Göttingen, Germany), on which the beads can be separated from the eluate by centrifugation.

4.4.7 Centrosome isolation

LP2:*
LP2 buffer (see 4.5.8)
1 µg/ml nocodazole
20 µg/ml DNase I

5× BRB80:
2 M PIPES/KOH, pH 6.8
25 mM $MgCl_2$
25 mM EGTA

sucrose cushion:
1× BRB80
20 mM EDTA
0.01% (w/v) Triton X-100
40% (w/v) sucrose

For the isolation of centrosomes, cells were harvested from a ∅ 10 cm cell culture dish per sample using a standard harvesting protocol (see 4.5.8). From the 10 ml cell suspension 0.5 - 1 ml were transferred to a 1.5 ml tube in order to generate a Western blot sample (see 4.4.3). When chromosome spreads of the same sample were to be prepared, additional 1.5 ml were taken from each individual cell suspension and transferred to a 15 ml conical tube (for the chromosome spreading protocol, see 4.5.15). Residual cells were washed once with 1× PBS (300 g, 2 min, RT) and resuspended in LP2* buffer. After lysing the cells with a dounce homogenizer (see 4.5.8), the suspension was further incubated for 20 min on ice. The lysate was centrifuged for 10 min at 3800 g and 4°C to clear it from cell debris. During these incubation and centrifugation steps, a 13 mm round cover slip (Marienfeld, Lauda-Königshofen, Germany) was cleaned by submersing it in 98% ethanol and wiping it off with "Kimtech Science Precision Wipes" (Kimberly-Clark, Roswell, GA, USA). The clean cover slip was placed into a 15 ml COREX round bottom glass tube on top of an appropriate adapter and ultimately submersed in 3.5 ml sucrose cushion. After centrifugation of the lysate, the supernatant (containing the centrosomes) was immediately transferred on top of the sucrose cushion in the COREX tube. The latter was than centrifuged for 25 min at 13.000 g and 4°C in a swing-out rotor featuring a rubber adapter (Corning Life Sciences, Corning, NY, USA) to fit the glass tube. After retrieving the cover slip, it was placed in methanol, prechilled to -20°C, to fix the centrosomes over night at -20°C. The next day, the cover slip was prepared and stained for IFM according to the protocol in chapter 4.5.18. To reduce unspecific binding of the antibodies, the cover slip

was blocked for 2 h. The centrioles were stained using a C-Nap1 antibody as a proximal and a centrin2 antibody as distal marker, which allowed for proper assessment of the centrioles' engagement status (see 4.1.6 for details on the antibodies). Primary antibody incubation was carried out for 2 h. After incubation with secondary antibodies, centrosomes were washed 5 times before the cover slips were mounted onto glass slides (Marienfeld, Lauda-Königshofen, Germany). Isolated centrosomes were microscoped using either an "Axio Imager A1" microscope (Zeiss, Jena, Germany) fitted with a "Pursuit" CCD camera (SPOT Imaging solutions, Sterling Heights MI, USA) and corresponding software or an "Axioplan 2" microscope fitted with an "AxioCam MRm" CCD camera (Zeiss, Jena, Germany) and corresponding software.

4.4.8 Coupled *in vitro* transcription/translation (IVT/T)

Especially when the generation of constructs required more complex cloning strategies (as for example the generation of internally tagged cohesin subunits), I used *in vitro* transcription/translation (IVT/T) as a first test to see, whether a newly generated plasmid allowed the expression of the full-length protein. Wheat germ extract- and SP6 polymerase-based IVT/T was performed using the "TNT SP6 Coupled Wheat Germ Extract System" (Promega, Mannheim, Germany) according to the manufacturer's instructions, except that the suggested 50 µl reaction volume was linearly downscaled to 5 µl. For each reaction ~200-400 ng of plasmid were used and the expressed protein was radioactively labeled by addition of [^{35}S]-labeled methionine. The reaction mix was incubated for 90 min at 30°C. The reaction was stopped by addition of 10 µl 2× SDS sample buffer and boiling up the sample at 95°C for 5-10 min. 7 µl of this sample was subjected to SDS-PAGE (see 4.4.2). After electrophoresis, the gel was fixed in 40% (v/v) methanol/10% (v/v) acetic acid for 30 min under gentle agitation. After washing the gel in ddH_2O for 10 min, it was placed on a wet sheet of blotting paper (Whatman/GE Healthcare, Freiburg, Germany) and subsequently dried for 1 h at 80°C on a "Model 483" vacuum drier (BioRAD, Munich, Germany). The dried gel was then placed into a developing cassette and covered with an imaging plate (FUJIFILM Europe, Düsseldorf, Germany). After 3 h of exposure, the imaging plate was analyzed using the "FLA-7000" system and corresponding software (FUJIFILM Europe, Düsseldorf, Germany).

4.5 Cell biological methods

4.5.1 Basic mammalian cell lines

Depending on the experiment, different mammalian cell types were used, namely:

HEK293T: human embryonic kidney cells, that were transformed with sheared adenovirus sequences and contain the SV40 large T antigen.

HEK293 Flp-In: human embryonic kidney cells, that contain a genomically inserted FRT recombination site to allow for FLP recombinase-mediated transgene insertion. Furthermore, the cells stably express the tetracycline repressor, which, in the absence of tetra- or doxycycline, binds to the tetracycline operator sequence to repress expression of subsequent genes. This can be used for tetra- or doxycycline-induced transgene expression (Life technologies, Darmstadt, Germany).

HeLa L: human cervix carcinoma cell line.

4.5.2 (Doubly) stable mammalian cell lines

The following table contains information to all employed mammalian cell lines, which have the coding sequence of one (single stable) or two (doubly stable) genes of interest stably integrated into their genome. All cells were created as described in 4.5.10 and are based on the HEK293 Flp-In cell line (see 4.5.1). The name of each cell line is derived from the number(s) of the plasmid(s) (compare 4.1.5) used for the transfection. Sometimes the name is followed with a point and a number denoting a specific clone used for the experiments.

name	expressed protein 1	expressed protein 2	origin
2644	Myc_6-Sgo1 A1 (siResist)	–	Laura Schöckel, University of Bayreuth
2645	Myc_6-Sgo1 A2 (siResist)	–	Laura Schöckel, University of Bayreuth
2646	Myc_6-Sgo1 C2 (siResist)	–	Laura Schöckel, University of Bayreuth
2740	Myc_6-Sgo1 C1 (siResist)	–	Lisa Mohr, University of Bayreuth
2790.4 + 2794.3	FKBP-linker-Scc1	Smc3-FRB	this study
2791.6 + 2792.2	Scc1-FRB	FKBP-linker-Smc1 (siResist)	this study
2795.7 + 2793.7	Smc3-int. FRB	Smc1-int. FKBP	this study

name	expressed protein 1	expressed protein 2	origin
2889	Myc_6-Sgo1 $A2^{AAA}$ (siResist)	–	Lisa Mohr, University of Bayreuth
2897.4	Scc1-Smc1 fusion	–	this study

4.5.3 Cultivation of mammalian cells

Mammalian monolayer cultures were grown in cell culture dishes (Greiner Bio-One, Frickenhausen) using Dulbecco's Modified Eagle Medium (DMEM; Biowest, Nuaillé, France; PAA, Pasching, Austria) supplemented with 9% (v/v) heat inactivated (56°C, 30 min) fetal bovine serum (Biochrom, Berlin, Germany; Biowest, Nuaillé, France, PAA, Pasching, Austria; Sigma-Aldrich, Munich, Germany) and antibiotics (90 U/ml Penicillin, 0.09 mg/ml Streptomycin; PAA, Pasching, Austria or 54.3 mg/l Penicillin, 0.09 mg/ml Streptomycin; Biowest, Nuaillé, France). The dishes were kept at 37°C in a 5% CO_2 atmosphere and split in a ratio of 1:4 to 1:12 twice a week. To do so, the medium was removed and cells were washed once with 1× PBS before they were incubated with ~20 μl/cm^2 trypsin-EDTA (pre-warmed at 37°C; PAA, Pasching, Austria; Sigma-Aldrich, Munich, Germany) for 5 min at 37°C. Trypsinized cells were complemented with fresh medium (pre-warmed at 37°C), washed from the dish's surface, and transferred to 15 or 50 ml conical tubes (Greiner Bio-One, Frickenhausen and SARSTEDT, Nümbrecht, Germany). The cells were then pelleted at 300 g for 2-3 min at RT, resuspended in fresh pre-warmed medium and distributed onto new cell culture dishes.

4.5.4 Storage of mammalian cells

Cells were harvested at around 80-100% confluency by trypsination (see 4.5.3) and, after pelleting, resuspended in 90% (v/v) fetal bovine serum (Biochrom, Berlin, Germany; Biowest, Nuaillé, France, PAA, Pasching, Austria; Sigma-Aldrich, Munich, Germany) + 10% (v/v) DMSO (pre-warmed at 37°C). The suspension was subsequently aliquoted into cryotubes (Nalgene/Thermo Fisher Scientific, Rochester, NY, USA; Greiner Bio-One, Frickenhausen, Germany), which were submersed in isopropanol which allows slow freezing of the cells at -1°C/min at -80°C. After 2-3 days, cryostocks were transferred into a liquid nitrogen tank for long term storage.

For use, cryostocks were thawed rapidly at 37°C, directly pipetted into 10 ml pre-warmed medium in a 50 ml conical tube (Greiner Bio-One, Frickenhausen and SARSTEDT, Nümbrecht, Germany) and pelleted at 300 g for 2 min. Cells were then resuspended in fresh pre-warmed medium and distributed onto a new cell culture dish.

4.5.5 Transfection of HEK293T and HEK293 Flp-In cells

2× HBS (500 ml):
8 g NaCl
0.37 g KCl
106.5 mg Na_2HPO_4
1 g glucose
5 g HEPES
pH 7.05 adjusted with NaOH; sterile-filtered

Cells were transfected at 25-90% confluency with the calcium phosphate method. Shortly before transfection, chloroquine was added to the cells to a final concentration of 25 μM. For the transfection of a ∅ 60 mm dish 4-5 μg plasmid DNA was added to 262.8 μl ddH_2O. The mix was then complemented with 37.2 μl sterile-filtered $CaCl_2$. Then, while vortexing, 300 μl 2× HBS was slowly pipetted into the solution. Eventually, the transfection mix was carefully dripped onto the surface of the medium. The cells were incubated with this transfection mix for 6-15 h before the medium was changed. This method was also used for the transfection of siRNAs into HEK293T and HEK293 Flp-In cells.

4.5.6 Transfection of HeLa L cells

HeLa L cells were transfected at 80-90% confluency using the polyethylenimine (PEI)-based method. For the transfection of one well of a six-well plate, 160 μl serum-free "Opti-MEM Glutamax" medium (Life technologies, Darmstadt, Germany) was supplemented with 2-2.5 μg plasmid DNA and incubated for 5 min. Subsequently, 1 mg/ml PEI was added to the transfection mix, which was then incubated for additional 15 min and ultimately added to the cells. Transfection medium was changed after 15-24 h.

4.5.7 Harvesting of mammalian cells

LP2:
20 mM Tris-HCl, pH 7.6
100 mM NaCl
10 mM NaF
20 mM beta-glycerophosphate
5 mM $MgCl_2$
0.1% (v/v) Triton X-100
5% (v/v) glycerol
1× protease inhibitor cocktail (Roche Diagnostics)

Cells were typically harvested by scraping them from the cell culture dish's surface with a rubber policeman. The cell suspension was then transferred to an appropriate reaction tube, pelleted, and washed once with 1× PBS (300 g, 2-3 min, RT). For the generation of Western blot samples, the cells were resuspended in 1× PBS, supplemented with the appropriate amount of 2× or 4× SDS sample buffer (see 4.4.2) and brought to 95°C for 5-10 min before the samples were frozen at -20°C for storage. For various experiments such as immunoprecipitations, a proper cell lysate was prepared by resuspending pelleted cells in LP2 buffer and incubating this suspension for 10 min on ice. To maximize cell lysis, the suspension was transferred to a dounce homogenizer (Wheaton, Millville, NJ, USA) in which cells were mechanically lysed by 10 strokes with a tightly fitting pestle. The cell lysate was eventually cleared from cell debris by centrifugation (16,100 g, 10-30 min, 4°C).

4.5.8 Synchronization of mammalian cells

To synchronize mammalian cells at the G1/S-transition, thymidine was added to the growth medium at 2 mM. Thymidine blocks replication by triggering a negative feedback loop for the production of deoxycytidine-triphosphate (CTP), therefore depleting this nucleotide. To release cells from a thymidine block they were washed once with 1× PBS, then incubated with fresh medium for 2×15 min and 1×30 min and ultimately either supplemented with fresh medium or, depending on the experiment, split by trypsination (see 4.5.3).

To synchronize mammalian cells in prometaphase, either nocodazole or taxol was added at 200 ng/ml. Both small molecules are spindle toxins but act in slightly different ways: nocodazole depolymerizes microtubules, which triggers the attachment-sensing arm of the SAC, while taxol stabilizes microtubules, so that the spindle can no longer apply tension to

the kinetochores, thus triggering the tension-arm of the SAC. To release cells from a nocodazole arrest, they were washed once with 1× PBS, then incubated with fresh medium for 2×15 min and ultimately supplemented with fresh medium.

4.5.9 Generation of (doubly) stable HEK293 Flp-In cell lines

To generate a stable HEK293 Flp-In cell line (for a list of all used stable cell lines, see 4.5.2), the cells were co-transfected with a plasmid containing the gene of interest (under control of a tetracycline operator sequence), a suitable selection marker and an FRT-site (which allows recombination into the FLP-site in the host's genome, see Figure 40), and a plasmid expressing the FLP recombinase (pAG1786). Therefore, a 145 mm cell culture dish was transfected with 3 μg of the integration plasmid (bearing a hygromycin B resistance marker) and 30 μg of the FLP recombinase expression plasmid, using the calcium phosphate method (see 4.5.5). 48 h after transfection, the cells were put under selection (150 μg/ml hygromycin B; PAA), which kills off cells, in which no integration event had taken place. After 2-3 weeks, cell colonies became visible, which were individually trypsinized using small glass rings that were put around single colonies. The clones were transferred into single wells of a multi-well cell culture dish and allowed to grow under selection until they could be test-induced to verify expression of the transgene. The insertion plasmids I used for the first round of stable genomic integration had been modified to feature an additional loxP recombination site, which can be utilized by the Cre recombinase for a second round of genomic insertion (see materials and methods, Figure 40). So, to generate a doubly stable cell line, a single stable cell line was co-transfected with yet another insertion plasmid containing a second gene of interest (again, under control of a tetracycline operator sequence), a suitable unique selection marker and a loxP-site (which allowed recombination into the loxP-site from the first genomic integration), and a plasmid expressing the Cre recombinase (pIC-Cre). Transfection, selection and cloning of doubly stable cell lines is similar to the generation of single stable cell line. For the second round of transfection, a 145 mm cell culture dish containing single stable cells was transfected with 24 μg of the plasmid to be integrated (bearing a Neomycin resistance cassette) and 8 μg of the Cre recombinase expression construct. Doubly stable cell lines were selected with 270 μg/ml G418 (Gibco/Life Technologies, Darmstadt, Germany) and cloned as described above. Stocks of doubly stable cell lines in culture were always kept under G418-selection (single stable cell lines: hygromycin B-

selection). Cells undergoing an experiment, were not kept under selection to ease the stress under experimental conditions.

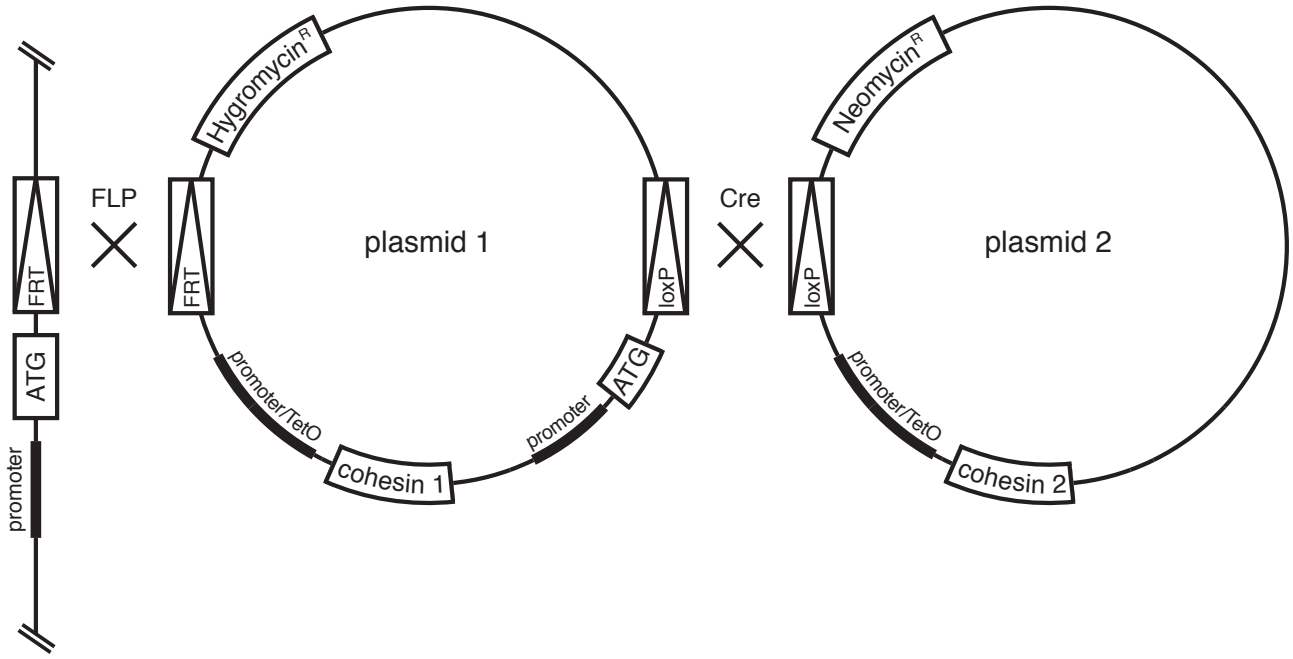

Figure 40 | **Generation of (doubly) stable HEK293 cell lines.** Cartoon depicts two rounds of plasmid integrations into the host cell's genome (on the left) for the generation of doubly stable HEK293 cell lines. ATG: start codon, FRT: FLP recognition target, loxP: Cre recognition target, TetO: tetracycline operator sequence, R: resistance. For more details see text.

4.5.10 Induction of transgene expression in (doubly) stable cell lines

All transgenes that were stably integrated into HEK293 Flp-In cell lines were under the control of a tetracycline operator. Since these cells stably express the tetracyclin repressor, the transgenes cannot be expressed until tetra- or doxycycline is added to the medium. All doubly stable cohesin subunit cell lines, as well as the cell line expressing Scc1-Smc1 fusion protein, were induced with 50 ng/ml doxycycline. Single stable Sgo1 isoform expressing cell lines were induced with 0.5 μg/ml doxycycline.

4.5.11 IdU/CldU pulse chase DNA fiber assay

spreading buffer:
200 mM Tris/HCl, pH 7.4
0.5% (v/v) SDS
50 mM EDTA

To pulse-label the replicated DNA in the S phase population of unsynchronized (omitting pre-synchronizing decreases the amount of labeled DNA fibers on the slides, which is integral for efficient analysis) HEK293T or HEK293 Flp-In cell lines growing on a 6 cm dish, we exchanged the growth medium by a medium supplemented with 50 μM 5-iodo-2'-deoxyuridine (IdU). After 20 min the medium was again immediately replaced by medium containing 50 μM 5-chloro-2'-deoxyuridine (CldU). After additional 20 min of labeling, the cells were harvested (see 4.5.8) and resuspended in ice-cold 1× PBS at ~1×10^6 cells/ml (Western Blot samples were taken at this stage). 2 μl of this cell suspension was spotted on top of a glass slide (Marienfeld, Lauda-Königshofen, Germany), which had been pre-cleaned with 70% ethanol. Cells were lysed by addition of 10 μl spreading buffer and incubation for 6 min. After lysis, the glass slides were tilted at ~15° to allow the drop to run down the length of the slide. The DNA fibers properly align at the liquid/air barrier during this step. The samples were allowed to dry in this position before they were fixed with methanol/acetic acid (3:1) for 2 min. The slides were rinsed shortly by dipping them into a 50 ml conical tube filled with ddH_2O. All following washing steps were performed in this manner using 1× PBS. The slides were dried at least overnight at 4°C. DNA fibers were then denatured by incubation in 2.5 M HCl for 30 min. After 3 washes the samples were immunostained using a standard protocol (see 4.5.18), except that all steps were carried out on the glass slide. Primary and secondary antibodies were diluted in 100 μl blocking solution each to allow proper submersion of the whole slide. IdU was stained with a mouse anti-BrdU antibody (1:100; BD Biosciences, 347580, Heidelberg, Germany), which shows cross-reactivity towards IdU but not to CldU. The latter was co-stained using a rat anti-BrdU antibody (1:100; Abcam, ab6326, Cambridge, UK), which cross-reacts with CldU but not with IdU. Secondary antibodies were used at a dilution of 1:350. The samples were mounted using 24×60 mm cover slips (VWR, Darmstadt, Germany), covering the whole sample. DNA fibers were microscoped on an "Axio Imager A1" microscope (Zeiss, Jena, Germany) fitted with a "Pursuit" CCD camera (SPOT Imaging solutions, Sterling Heights MI, USA) and corresponding software. For each sample 50 DNA fiber tracks were photographed and ultimately measured using ImageJ64 (http://imagej.nih.gov/ij).

4.5.12 Chromatin isolation for Western blot

buffer A:
10 mM HEPES/KOH, pH 7.9
10 mM KCl
1.5 mM $MgCl_2$
0.34 M sucrose
10% (v/v) glycerol
1 mM DTT
1× protease inhibitor cocktail (Roche Diagnostics)

buffer B:
3 mM EDTA/NaOH (pH 8.0)
0.2 mM EGTA/KOH (pH 8.0)
1.5 mM $MgCl_2$
1 mM DTT
1× protease inhibitor cocktail (Roche Diagnostics)

Mammalian cells were harvested from one well of a six-well cell culture dish as described in 4.5.8. After washing, the cells were resuspended in 100 µl buffer A before they were supplemented with Triton X-100 to 0.1% (0.5 µl of a 20% (w/v) Triton X-100 solution). All following centrifugation steps were carried out at 4°C. After 8 min incubation on ice, the chromatin-enriched fraction was spun down at 1300 g for 5 min. The supernatant (cytosolic fraction) was aspirated and kept on ice, while the chromatin pellet was further washed once with 100 µl buffer A (1300 g, 5 min) before being resuspended in 100 µl buffer B. While the chromatin fraction was allowed to incubate for 30 min on ice, the cytosolic fraction was cleared at 16,100 g for 10 min. The cleared supernatant was then transferred to a new 1.5 ml tube, supplemented with 40 µl 4× SDS sample buffer (see 4.4.2) and boiled up at 95°C for ≥5 min. After incubation, the pellet was washed twice with 100 µl buffer B (1700 g, 5 min), resuspended in 100 µl buffer B and ultimately supplemented with 40 µl 4× SDS sample buffer before being boiled up.

4.5.13 Chromatin isolation for immunofluorescence microscopy

1× PME:
5 mM PIPES/NaOH, pH 7.2
5 mM NaCl
5 mM $MgCl_2$
1 mM EGTA

LSS:
1× PME
1% (v/v) thiodiethylene glycol
0.9 M sucrose
0.2% (w/v) digitonin

PME lysis buffer:
1× PME
1% (v/v) thiodiethylene glycol
10 µg/ml cytochalasin B
0.2% (w/v) digitonin
1× protease inhibitor cocktail
(Roche Diagnostics)

At least 500,000 cells were harvested (see 4.5.8) and swelled in 1 ml 1× PME for 5 min at RT. This swelling step was repeated once (300 g, 2 min, RT). Cells were then spun down (300 g, 2 min, RT), resuspended in PME lysis buffer, and incubated for 5 min on ice. A poly-L-lysine-coated cover slip (see 4.5.17) was placed onto a suitable adapter in a COREX round bottom glass tube and submersed in 3 ml LSS. The lysate was carefully transferred onto the LSS cushion and then centrifuged at 2900 g and 4°C for 30 min. After retrieving the cover slip, it was placed on a sheet of parafilm in a wet chamber. For all subsequent steps, 50 µl of the respective solutions were added to the cover slip at RT. The cover slip was washed once with 1× PBS and then fixed with 4% para-formaldehyde (PFA) in PBS for 15 min. After an additional PBS-wash, the fixing reaction was quenched by 50 mM NH_4Cl in PBS for 5 min. The DNA was washed once again with 1× PBS before it was stained with 1 µg/ml Hoechst 33342 in PBS for ≥20 min. After two PBS-washes the cover slip was mounted onto a glass slide as described in 4.5.18.

4.5.14 Chromosome spreads

hypotonic medium:
40% (v/v) serum-free medium
60% (v/v) ddH_2O
5 mM $MgCl_2$
500 ng/ml nocodazole

About 500,000 prometaphase-arrested mammalian cells were harvested (see 4.5.8) and resuspended in 250 µl hypotonic medium at RT (Unless otherwise noted, all following steps are carried out at RT). After 3 min incubation each, another 250 µl and eventually 2 ml hypotonic medium were added to the cell suspension by zestful pipetting (without pipetting up and down). After an additional incubation for 5 min, swollen cells were gently pelleted at 100 g for 5 min. Pelleted cells were resuspended in 20 µl hypotonic medium before being fixed by addition of 250 µl methanol/acetic acid (3:1; again, without pipetting

up and down). In rapid succession, further 250 µl and ultimately 2 ml fixative were added, followed by a ≥30 min incubation time. For further dehydration, the fixed cells were washed twice with 1 ml fixative each (300 g, 4 min) before being ultimately resuspended in up to 250 µl methanol/acetic acid solution. The samples were stored at -20°C. For chromosome spreading, a glass slide (Marienfeld, Lauda-Königshofen, Germany) was placed on a metal block which had been put on ice. The glass slide was allowed to fog up before 7.5 µl of the ice cold cell suspension was dropped onto it. As the fixative spreads radially across the slide, the chromosomes are spread with it. The sample was then dried on 60°C metal block, which had been covered with a wet tissue. After drying, the chromosomes were stained by 1 µg/ml Hoechst33342 in 1× PBS for 10 min at RT. This was followed by two PBS- and one ddH_2O-wash. The chromosome spreads were mounted using square 22 mm cover slips (Marienfeld, Lauda-Königshofen, Germany).

4.5.15 Chromosome spreads for additional immunostaining

hypotonic buffer I:	*hypotonic buffer II:*
30 mM Tris/HCl, pH 8.2	100 mM sucrose
50 mM sucrose	400 ng/ml nocodazole
17 mM sodium citrate	
400 ng/ml nocodazole	

About 500,000 prometaphase-arrested mammalian cells were harvested (see 4.5.8) and resuspended in 250 µl hypotonic buffer I at RT (all following steps are carried out at RT). Another 250 µl, and eventually 2 ml hypotonic medium were added to the cell suspension by zestful pipetting (without pipetting up and down). After incubation for 7 min, swollen cells were pelleted at 300 g for 3 min and resuspended in up to 250 µl hypotonic buffer II. 10 µl of this suspension were immediately transferred onto a corner of a square 22 mm cover slip (Marienfeld, Lauda-Königshofen, Germany), which had been dipped into fixative (1% (w/v) para-formaldehyde, 5 mM sodium borate, 0.15% (w/v) Triton X-100). The solution was immediately dispersed on the cover slip by continuous tilting. The cover slip was allowed to dry in a partially opened wet chamber. Thereafter, it was washed with 1× PBS before being blocked with 1× PBS/3% (w/v) BSA/0.01% (w/v) Triton X-100 for 1 h. Immunostaining was performed as described in chapter 4.5.18 with following exceptions: Antibodies were diluted in 1× PBS/3% (w/v) BSA/0.01% (w/v) Triton X-100 and for chromatin staining 5 µg/ml of Hoechst33342 were used.

4.5.16 Preparation of poly-L-lysine coated cover slips

All mammalian cells used in this study only grow properly when they can adhere to a suitable surface. Cells that were to be analyzed by IFM were split into cell culture dishes in which cover slips had been placed, so that they would adhere to and grow on them. Since pure glass is not an optimal substrate for cell adherence, I added a more suitable poly-L-lysine coating to the cover slips. Therefore, 100 - 200 round 13 mm cover slips (Marienfeld, Lauda-Königshofen, Germany) were incubated in 100 ml 0.01% (w/v) poly-L-lysine solution (Sigma Aldrich, Munich, Germany) for ≥1 h at RT, while being kept in motion by a horizontal shaker. The cover slips were washed 10 times with ddH_2O to get rid of unbound poly-amino acids before they were incubated with 100% ethanol for ≥1 h at RT. Under sterile conditions, the cover slips were individually placed inside a 145 mm cell culture dish, standing upright by leaning them against the side of the dish until they were properly dried.

4.5.17 Immunofluorescence microscopy (IFM)

CSK buffer:
10 mM PIPES/NaOH, pH 7.0
100 mM NaCl
300 mM sucrose
3 mM $MgCl_2$

mounting medium:
20 mM Tris/HCl, pH 8.0
2,33% (w/v) diazabicyclo-[2,2,2]-octane
78 % (v/v) glycerol

Typically, cells were grown on round 13 mm cover slips (Marienfeld, Lauda-Königshofen, Germany), which had been placed into the wells of a six-well cell culture dish. All treatments up until and including incubation in blocking solution, were performed by slowly pipetting 1.5 - 2 ml of each solution into all sample-containing wells of the six-well dish at RT. Between all steps, the cover slips were washed once with 1× PBS. To get rid of soluble proteins, which can cause background issues, the cells were pre-extracted by addition of 1× PBS/0.1% (w/v) Triton X-100 for 3 min before they were fixed by addition of 1× PBS/4% (w/v) para-formaldehyde for 15 min. The fixing reaction was quenched by the addition of 1× PBS/50 mM NH_4Cl for 5 min. The cells were further permeabilized by an additional incubation with 1× PBS/0.1% (w/v) Triton X-100 for 5 min. This was followed by blocking the samples with 1× PBS/3% (w/v) BSA/0.02% NaN_3 for ≥2 h at RT or overnight at 4°C. For the actual immunostaining, the cover slips were transferred to a sheet of parafilm in a wet chamber, and submersed in 50 μl/slip primary antibodies diluted in blocking solution.

After 1 h incubation and 3 PBS-washes, the samples were incubated with secondary antibodies, diluted in blocking solution, for an additional hour. After 2 washes with 1× PBS, the samples were incubated with 1 µg/ml Hoechst33342 in 1× PBS for 10 min to stain chromatin. After additional 3 PBS-washes, the cover slips were mounted onto glass slides (Marienfeld, Lauda-Königshofen, Germany) using 3 µl mounting medium. Differently sized cover slips required different amounts of mounting medium: square 22 mm cover slips (used for chromosome spreads; see 4.5.15) were mounted with 7.5 µl and large 24 × 60 mm cover slips (used for DNA fiber assays; see 4.5.12) were mounted with 22.5 µl mounting medium.

For proper staining of centrosomes *in situ*, a specific pre-extraction method had to be employed. The cover slips were first washed with CSK buffer, then incubated with CSK buffer supplemented with 0.1% (w/v) Triton X-100, and again washed with CSK buffer alone. For fixation, the cover slips were submersed in -20°C methanol and incubated for ≥2 h at -20°C. After a short PBS-wash, fixed cells were permeabilized by incubation with 1× PBS/0.1% (w/v) Triton X-100 for 5 min, then again washed with 1× PBS before being submersed in blocking solution. All steps following blocking, were as described above. *In situ* centrosomes were visualized using a "DMI6000 B" microscope with the corresponding LAS AF software (Leica Microsystems, Wetzlar, Germany). Photographs were subjected to blind deconvolution (5 iterations; performed with LAS AF, Leica Microsystems, Wetzlar, Germany) and depict a maximum projection of the relevant parts of each z-stack ("Max. intensity"-projection performed with ImageJ64, http://imagej.nih.gov/ij)

EdU labeled cells (see 4.5.19) that were grown on cover slips were treated in two different ways, depending on whether the cells had to be co-immunostained. For all following incubations, the samples were protected from light. When only EdU labeling was to be visualized, the cover slips were washed once with 1× PBS and once again with 1× PBS/ 1% (w/v) BSA before they were fixed by addition of the fixative supplied with the kit for 15 min. The samples were subsequently washed twice with 1× PBS/1% (w/v) BSA and then incubated in the supplied wash reagent for 15 min. During this time, 50 µl/sample of the Click-iT reaction cocktail was prepared. Please note that the amounts of the individual cocktail components described in the original kit-protocol were downscaled for the incubation of the cover slips. The Click-iT reaction was performed for 40 min at RT. The samples were washed once with wash reagent, then incubated with 1 µg/ml Hoechst33342 in 1× PBS for 10 min to stain total DNA. Cover slips were mounted onto glass slides after two additional washes with wash reagent. For co-immunostaining of

EdU-labeled cells, the samples were pre-extracted, fixed and blocked as described in the first paragraph of this section, then washed once with 1× PBS/1% (w/v) BSA before being incubated with the supplied wash reagent for 15 min. Click-iT reaction was performed as described above. Thereafter, the cover slips were washed twice with the wash reagent and once with 1× PBS. The following immunostaining and eventual mounting for microscopy was, again, conducted as described above.

4.5.18 EdU-labeling of replicating cells

To identify S phase cells in IFM or flow cytometry, replicated DNA was labeled using the nucleotide analog 5-ethynyl-2'-deoxyuridine (EdU). EdU labeling and detection was done using the "Click-iT EdU Alexa Fluor 488 Flow Cytometry Assay Kit" from Invitrogen/Life Technologies (Darmstadt, Germany). Therefore, 10 μM EdU was added to an unsynchronized population of HEK293T cells for 40 (IFM) or 90 min (flow cytometry) before they were harvested. For further details on the detection of EdU, please see the respective chapters regarding IFM (4.5.18) and flow cytometry (4.5.19)

4.5.19 Flow cytometry

EdU-labeled cells (see 4.5.19) were prepared for flow cytometry according to the kit's manufacturer's standard protocol with two exceptions: first, cells were incubated with the Click-iT reaction cocktail for 40 min and second, to allow co-staining of the cells' whole DNA content, they were washed once with 3 ml and then resuspended in 1 ml of the supplied wash reagent. The suspension was then supplemented with 0.2 mg/ml RNase I and 20 μg/ml propidium iodide (a fluorophore, which intercalates into DNA) and incubated for ≥30 min at RT before they were passed through a cell strainer and immediately analyzed with an "FC-500" flow cytometer (Beckman Coulter, Krefeld, Germany). The corresponding software was used to gate for single cells and carefully discriminate between the Alexa Fluor emission signal at 519 nm and the propidium idodide emission signal at 617 nm.

References

Abe S, Nagasaka K, Hirayama Y, Kozuka-Hata H, Oyama M, Aoyagi Y, Obuse C & Hirota T (2011) The initial phase of chromosome condensation requires Cdk1-mediated phosphorylation of the CAP-D3 subunit of condensin II. *Genes Dev* **25:** 863–874

Agircan FG & Schiebel E (2014) Sensors at centrosomes reveal determinants of local separase activity. *PLoS Genet* **10:** e1004672

Anderson DE, Losada A, Erickson HP & Hirano T (2002) Condensin and cohesin display different arm conformations with characteristic hinge angles. *J Cell Biol* **156:** 419–424

Andrews PD, Ovechkina Y, Morrice N, Wagenbach M, Duncan K, Wordeman L & Swedlow JR (2004) Aurora B regulates MCAK at the mitotic centromere. *Dev Cell* **6:** 253–268

Araki H, Leem SH, Phongdara A & Sugino A (1995) Dpb11, which interacts with DNA polymerase II(epsilon) in Saccharomyces cerevisiae, has a dual role in S phase progression and at a cell cycle checkpoint. *Proc Natl Acad Sci USA* **92:** 11791–11795

Arumugam P, Gruber S, Tanaka K, Haering CH, Mechtler K & Nasmyth K (2003) ATP hydrolysis is required for cohesin's association with chromosomes. *Curr Biol* **13:** 1941–1953

Bahe S, Stierhof Y-D, Wilkinson CJ, Leiss F & Nigg EA (2005) Rootletin forms centriole-associated filaments and functions in centrosome cohesion. *J Cell Biol* **171:** 27–33

Ball AR, Chen Y-Y & Yokomori K (2014) Mechanisms of cohesin-mediated gene regulation and lessons learned from cohesinopathies. *Biochim Biophys Acta* **1839:** 191–202

Ballabeni A, Melixetian M, Zamponi R, Masiero L, Marinoni F & Helin K (2004) Human geminin promotes pre-RC formation and DNA replication by stabilizing CDT1 in mitosis. *EMBO J* **23:** 3122–3132

Banaszynski LA, Liu CW & Wandless TJ (2005) Characterization of the FKBP.rapamycin.FRB ternary complex. *J Am Chem Soc* **127:** 4715–4721

Barrera JA, Kao L-R, Hammer RE, Seemann J, Fuchs JL & Megraw TL (2010) CDK5RAP2 regulates centriole engagement and cohesion in mice. *Dev Cell* **18:** 913–926

Barsky D & Venclovas C (2005) DNA sliding clamps: just the right twist to load onto DNA. *Curr Biol* **15:** R989–92

Bauerschmidt C, Arrichiello C, Burdak-Rothkamm S, Woodcock M, Hill MA, Stevens DL & Rothkamm K (2010) Cohesin promotes the repair of ionizing radiation-induced DNA double-strand breaks in replicated chromatin. *Nucleic Acids Res* **38:** 477–487

Beauchene NA, Diaz-Martinez LA, Furniss K, Hsu W-S, Tsai H-J, Chamberlain C, Esponda P, Giménez-Abián JF & Clarke DJ (2010) Rad21 is required for

centrosome integrity in human cells independently of its role in chromosome cohesion. *Cell Cycle* **9:** 1774–1780

Beckouët F, Hu B, Roig MB, Sutani T, Komata M, Uluocak P, Katis VL, Shirahige K & Nasmyth K (2010) An Smc3 acetylation cycle is essential for establishment of sister chromatid cohesion. *Mol Cell* **39:** 689–699

Bell SP & Stillman B (1992) ATP-dependent recognition of eukaryotic origins of DNA replication by a multiprotein complex. *Nature* **357:** 128–134

Bermudez VP, Farina A, Tappin I & Hurwitz J (2010) Influence of the human cohesion establishment factor Ctf4/AND-1 on DNA replication. *J Biol Chem* **285:** 9493–9505

Bettencourt-Dias M, Hildebrandt F, Pellman D, Woods G & Godinho SA (2011) Centrosomes and cilia in human disease. *Trends Genet* **27:** 307–315

Blat Y & Kleckner N (1999) Cohesins bind to preferential sites along yeast chromosome III, with differential regulation along arms versus the centric region. *Cell* **98:** 249–259

Blow JJ, Ge XQ & Jackson DA (2011) How dormant origins promote complete genome replication. *Trends Biochem Sci* **36:** 405–414

Boos D, Kuffer C, Lenobel R, Körner R & Stemmann O (2008) Phosphorylation-dependent binding of cyclin B1 to a Cdc6-like domain of human separase. *J Biol Chem* **283:** 816–823

Boos D, Sanchez-Pulido L, Rappas M, Pearl LH, Oliver AW, Ponting CP & Diffley JFX (2011) Regulation of DNA replication through Sld3-Dpb11 interaction is conserved from yeast to humans. *Curr Biol* **21:** 1152–1157

Boos D, Yekezare M & Diffley JFX (2013) Identification of a heteromeric complex that promotes DNA replication origin firing in human cells. *Science* **340:** 981–984

Borges V, Lehane C, Lopez-Serra L, Flynn H, Skehel M, Rolef Ben-Shahar T & Uhlmann F (2010) Hos1 deacetylates Smc3 to close the cohesin acetylation cycle. *Mol Cell* **39:** 677–688

Bravo R, Frank R, Blundell PA & Macdonald-Bravo H (1987) Cyclin/PCNA is the auxiliary protein of DNA polymerase-delta. *Nature* **326:** 515–517

Buonomo SB, Clyne RK, Fuchs J, Loidl J, Uhlmann F & Nasmyth K (2000) Disjunction of homologous chromosomes in meiosis I depends on proteolytic cleavage of the meiotic cohesin Rec8 by separin. *Cell* **103:** 387–398

Bylund GO & Burgers PMJ (2005) Replication protein A-directed unloading of PCNA by the Ctf18 cohesion establishment complex. *Mol Cell Biol* **25:** 5445–5455

Cabral G, Sans SS, Cowan CR & Dammermann A (2013) Multiple Mechanisms Contribute to Centriole Separation in C. elegans. *Curr Biol* **23:** 1380–1387

Cai J, Yao N, Gibbs E, Finkelstein J, Phillips B, O'Donnell M & Hurwitz J (1998) ATP hydrolysis catalyzed by human replication factor C requires participation of multiple subunits. *Proc Natl Acad Sci USA* **95:** 11607–11612

Chan K-L, Roig MB, Hu B, Beckouët F, Metson J & Nasmyth K (2012) Cohesin's DNA exit gate is distinct from its entrance gate and is regulated by acetylation. *Cell* **150:** 961–974

Cheeseman IM, Chappie JS, Wilson-Kubalek EM & Desai A (2006) The conserved KMN network constitutes the core microtubule-binding site of the kinetochore. *Cell* **127:** 983–997

Chen S & Bell SP (2011) CDK prevents Mcm2-7 helicase loading by inhibiting Cdt1 interaction with Orc6. *Genes Dev* **25:** 363–372

Chiang T, Duncan FE, Schindler K, Schultz RM & Lampson MA (2010) Evidence that Weakened Centromere Cohesion Is a Leading Cause of Age-Related Aneuploidy in Oocytes. *Curr Biol* **20:** 1522–1528

Choi J, Chen J, Schreiber SL & Clardy J (1996) Structure of the FKBP12-rapamycin complex interacting with the binding domain of human FRAP. *Science* **273:** 239–242

Cimini D, Wan X, Hirel CB & Salmon ED (2006) Aurora kinase promotes turnover of kinetochore microtubules to reduce chromosome segregation errors. *Curr Biol* **16:** 1711–1718

Ciosk R, Shirayama M, Shevchenko A, Tanaka T, Tóth A & Nasmyth K (2000) Cohesin's binding to chromosomes depends on a separate complex consisting of Scc2 and Scc4 proteins. *Mol Cell* **5:** 243–254

Cocker JH, Piatti S, Santocanale C, Nasmyth K & Diffley JF (1996) An essential role for the Cdc6 protein in forming the pre-replicative complexes of budding yeast. *Nature* **379:** 180–182

Cook JG, Chasse DAD & Nevins JR (2004) The regulated association of Cdt1 with minichromosome maintenance proteins and Cdc6 in mammalian cells. *J Biol Chem* **279:** 9625–9633

Corbett KD, Yip CK, Ee L-S, Walz T, Amon A & Harrison SC (2010) The monopolin complex crosslinks kinetochore components to regulate chromosome-microtubule attachments. *Cell* **142:** 556–567

Costa A, Hood IV & Berger JM (2013) Mechanisms for initiating cellular DNA replication. *Annu Rev Biochem* **82:** 25–54

Coster G, Frigola J, Beuron F, Morris EP & Diffley JFX (2014) Origin licensing requires ATP binding and hydrolysis by the MCM replicative helicase. *Mol Cell* **55:** 666–677

Courtheoux T, Gay G, Gachet Y & Tournier S (2009) Ase1/Prc1-dependent spindle elongation corrects merotely during anaphase in fission yeast. **187:** 399–412

Crasta K, Huang P, Morgan G, Winey M & Surana U (2006) Cdk1 regulates centrosome separation by restraining proteolysis of microtubule-associated proteins. *EMBO J* **25:** 2551–2563

Cunha-Ferreira I, Bento I & Bettencourt-Dias M (2009) From zero to many: control of centriole number in development and disease. *Traffic* **10:** 482–498

Darwiche N, Freeman LA & Strunnikov A (1999) Characterization of the components of the putative mammalian sister chromatid cohesion complex. *Gene* **233:** 39–47

Davis BK (1971) Genetic analysis of a meiotic mutant resulting in precocious sister-centromere separation in Drosophila melanogaster. *Mol Gen Genet* **113:** 251–272

de Antoni A, Pearson CG, Cimini D, Canman JC, Sala V, Nezi L, Mapelli M, Sironi L, Faretta M, Salmon ED & Musacchio A (2005) The Mad1/Mad2 complex as a template for Mad2 activation in the spindle assembly checkpoint. *Curr Biol* **15:** 214–225

Deardorff MA, Bando M, Nakato R, Watrin E, Itoh T, Minamino M, Saitoh K, Komata M, Katou Y, Clark D, Cole KE, De Baere E, Decroos C, Di Donato N, Ernst S, Francey LJ, Gyftodimou Y, Hirashima K, Hullings M, Ishikawa Y, et al (2012a) HDAC8 mutations in Cornelia de Lange syndrome affect the cohesin acetylation cycle. *Nature* **489:** 313–317

Deardorff MA, Kaur M, Yaeger D, Rampuria A, Korolev S, Pie J, Gil-Rodríguez C, Arnedo M, Loeys B, Kline AD, Wilson M, Lillquist K, Siu V, Ramos FJ, Musio A, Jackson LS, Dorsett D & Krantz ID (2007) Mutations in cohesin complex members SMC3 and SMC1A cause a mild variant of cornelia de Lange syndrome with predominant mental retardation. *Am J Hum Genet* **80:** 485–494

Deardorff MA, Wilde JJ, Albrecht M, Dickinson E, Tennstedt S, Braunholz D, Mönnich M, Yan Y, Xu W, Gil-Rodríguez MC, Clark D, Hakonarson H, Halbach S, Michelis LD, Rampuria A, Rossier E, Spranger S, Van Maldergem L, Lynch SA, Gillessen-Kaesbach G, et al (2012b) RAD21 mutations cause a human cohesinopathy. *Am J Hum Genet* **90:** 1014–1027

Desai A & Mitchison TJ (1997) Microtubule polymerization dynamics. *Annu Rev Cell Dev Biol* **13:** 83–117

Diaz-Martinez LA, Beauchene NA, Furniss K, Esponda P, Giménez-Abián JF & Clarke DJ (2010) Cohesin is needed for bipolar mitosis in human cells. *Cell Cycle* **9:** 1764–1773

Dimaki M, Xouri G, Symeonidou I-E, Sirinian C, Nishitani H, Taraviras S & Lygerou Z (2013) Cell cycle-dependent subcellular translocation of the human DNA licensing inhibitor geminin. *J Biol Chem* **288:** 23953–23963

Dobbelaere J, Josué F, Suijkerbuijk S, Baum B, Tapon N & Raff J (2008) A genome-wide RNAi screen to dissect centriole duplication and centrosome maturation in Drosophila. *PLoS Biol* **6:** e224

Dreier MR, Bekier ME & Taylor WR (2011) Regulation of sororin by Cdk1-mediated phosphorylation. *J Cell Sci* **124:** 2976–2987

Drury LS, Perkins G & Diffley JF (1997) The Cdc4/34/53 pathway targets Cdc6p for proteolysis in budding yeast. *EMBO J* **16:** 5966–5976

Duxin JP, Dewar JM, Yardimci H & Walter JC (2014) Repair of a DNA-Protein Crosslink by Replication-Coupled Proteolysis. *Cell* **159:** 346–357

Eichinger CS, Kurze A, Oliveira RA & Nasmyth K (2013) Disengaging the Smc3/kleisin interface releases cohesin from Drosophila chromosomes during interphase and mitosis. *EMBO J* **32:** 656–665

Elbashir SM, Harborth J, Lendeckel W, Yalcin A, Weber K & Tuschl T (2001) Duplexes of 21-nucleotide RNAs mediate RNA interference in cultured mammalian cells. **411:** 494–498

Eng T, Guacci V & Koshland D (2014) ROCC, a conserved region in cohesin's Mcd1 subunit, is essential for the proper regulation of the maintenance of cohesion and establishment of condensation. *Mol Biol Cell* **25:** 2351–2364

Evrin C, Clarke P, Zech J, Lurz R, Sun J, Uhle S, Li H, Stillman B & Speck C (2009) A double-hexameric MCM2-7 complex is loaded onto origin DNA during licensing of eukaryotic DNA replication. *Proc Natl Acad Sci USA* **106:** 20240–20245

Fang G, Zhang D, Yin H, Zheng L, Bi X & Yuan L (2014) Centlein mediates an interaction between C-Nap1 and Cep68 to maintain centrosome cohesion. *J Cell Sci* **127:** 1631–1639

Farina A, Shin J-H, Kim D-H, Bermudez VP, Kelman Z, Seo Y-S & Hurwitz J (2008) Studies with the human cohesin establishment factor, ChlR1. Association of ChlR1 with Ctf18-RFC and Fen1. *J Biol Chem* **283:** 20925–20936

Ferguson RL & Maller JL (2008) Cyclin E-dependent localization of MCM5 regulates centrosome duplication. *J Cell Sci* **121:** 3224–3232

Fernández-Cid A, Riera A, Tognetti S, Herrera MC, Samel S, Evrin C, Winkler C, Gardenal E, Uhle S & Speck C (2013) An ORC/Cdc6/MCM2-7 complex is formed in a multistep reaction to serve as a platform for MCM double-hexamer assembly. *Mol Cell* **50:** 577–588

Friocourt G, Marcorelles P, Saugier-Veber P, Quille M-L, Marret S & Laquerrière A (2011) Role of cytoskeletal abnormalities in the neuropathology and pathophysiology of type I lissencephaly. *Acta Neuropathol.* **121:** 149–170

Fry AM, Mayor T, Meraldi P, Stierhof YD, Tanaka K & Nigg EA (1998) C-Nap1, a novel centrosomal coiled-coil protein and candidate substrate of the cell cycle-regulated protein kinase Nek2. *J Cell Biol* **141:** 1563–1574

Fu J & Glover DM (2012) Structured illumination of the interface between centriole and peri-centriolar material. *Open Biol* **2:** 120104

Fu J, Hagan IM & Glover DM (2015) The centrosome and its duplication cycle. *Cold Spring Harb Perspect Biol* **7:** a015800

Fukuda T, Fukuda N, Agostinho A, Hernández-Hernández A, Kouznetsova A & Hoog C (2014) STAG3-mediated stabilization of REC8 cohesin complexes promotes chromosome synapsis during meiosis. *EMBO J* **33**: 1243–1255

Fumasoni M, Zwicky K, Vanoli F, Lopes M & Branzei D (2015) Error-free DNA damage tolerance and sister chromatid proximity during DNA replication rely on the Polα/ Primase/Ctf4 Complex. *Mol Cell* **57:** 812–823

Funabiki H, Yamano H, Kumada K, Nagao K, Hunt T & Yanagida M (1996) Cut2 proteolysis required for sister-chromatid seperation in fission yeast. *Nature* **381:** 438–441

Furuya K, Takahashi K & Yanagida M (1998) Faithful anaphase is ensured by Mis4, a sister chromatid cohesion molecule required in S phase and not destroyed in G1 phase. *Genes Dev* **12:** 3408–3418

Gambus A, Jones RC, Sanchez-Diaz A, Kanemaki M, van Deursen F, Edmondson RD & Labib K (2006) GINS maintains association of Cdc45 with MCM in replisome progression complexes at eukaryotic DNA replication forks. *Nat Cell Biol* **8:** 358–366

Gambus A, van Deursen F, Polychronopoulos D, Foltman M, Jones RC, Edmondson RD, Calzada A & Labib K (2009) A key role for Ctf4 in coupling the MCM2-7 helicase to DNA polymerase alpha within the eukaryotic replisome. *EMBO J* **28:** 2992–3004

Gandhi R, Gillespie PJ & Hirano T (2006) Human Wapl is a cohesin-binding protein that promotes sister-chromatid resolution in mitotic prophase. *Curr Biol* **16:** 2406–2417

Gautier J, Solomon MJ, Booher RN, Bazan JF & Kirschner MW (1991) cdc25 is a specific tyrosine phosphatase that directly activates p34cdc2. *Cell* **67:** 197–211

Gerlich D, Koch B, Dupeux F, Peters J-M & Ellenberg J (2006) Live-cell imaging reveals a stable cohesin-chromatin interaction after but not before DNA replication. *Curr Biol* **16:** 1571–1578

Gillespie PJ & Hirano T (2004) Scc2 couples replication licensing to sister chromatid cohesion in Xenopus egg extracts. *Curr Biol* **14:** 1598–1603

Giménez-Abián JF, Diaz-Martinez LA, Beauchene NA, Hsu W-S, Tsai H-J & Clarke DJ (2010) Determinants of Rad21 localization at the centrosome in human cells. *Cell Cycle* **9:** 1759–1763

Giménez-Abián JF, Sumara I, Hirota T, Hauf S, Gerlich D, la Torre de C, Ellenberg J & Peters J-M (2004) Regulation of sister chromatid cohesion between chromosome arms. *Curr Biol* **14:** 1187–1193

Gligoris TG, Scheinost JC, Bürmann F, Petela N, Chan K-L, Uluocak P, Beckouët F, Gruber S, Nasmyth K & Löwe J (2014) Closing the cohesin ring: structure and function of its Smc3-kleisin interface. *Science* **346:** 963–967

Glynn EF, Megee PC, Yu H-G, Mistrot C, Ünal E, Koshland DE, DeRisi JL & Gerton JL (2004) Genome-wide mapping of the cohesin complex in the yeast Saccharomyces cerevisiae. *PLoS Biol* **2:** E259

Gordillo M, Vega H, Trainer AH, Hou F, Sakai N, Luque R, Kayserili H, Basaran S, Skovby F, Hennekam RCM, Uzielli MLG, Schnur RE, Manouvrier S, Chang S, Blair E, Hurst JA, Forzano F, Meins M, Simola KOJ, Raas-Rothschild A, et al (2008) The

molecular mechanism underlying Roberts syndrome involves loss of ESCO2 acetyltransferase activity. *Hum Mol Genet* **17:** 2172–2180

Gorr IH, Boos D & Stemmann O (2005) Mutual inhibition of separase and Cdk1 by two-step complex formation. *Mol Cell* **19:** 135–141

Gosalia N, Neems D, Kerschner JL, Kosak ST & Harris A (2014) Architectural proteins CTCF and cohesin have distinct roles in modulating the higher order structure and expression of the CFTR locus. *Nucleic Acids Res* **42:** 9612–9622

Graser S, Stierhof Y-D & Nigg EA (2007) Cep68 and Cep215 (Cdk5rap2) are required for centrosome cohesion. *J Cell Sci* **120:** 4321–4331

Gregan J, Polakova S, Zhang L, Tolić-Nørrelykke IM & Cimini D (2011) Merotelic kinetochore attachment: causes and effects. *Trends Cell Biol* **21:** 374–381

Gregson HC, Schmiesing JA, Kim JS, Kobayashi T, Zhou S & Yokomori K (2001) A potential role for human cohesin in mitotic spindle aster assembly. *J Biol Chem* **276:** 47575–47582

Gruber S, Arumugam P, Katou Y, Kuglitsch D, Helmhart W, Shirahige K & Nasmyth K (2006) Evidence that loading of cohesin onto chromosomes involves opening of its SMC hinge. *Cell* **127:** 523–537

Gruber S, Haering CH & Nasmyth K (2003) Chromosomal cohesin forms a ring. *Cell* **112:** 765–777

Guacci V, Koshland D & Strunnikov A (1997) A direct link between sister chromatid cohesion and chromosome condensation revealed through the analysis of MCD1 in S. cerevisiae. *Cell* **91:** 47–57

Guadagno TM & Newport JW (1996) Cdk2 kinase is required for entry into mitosis as a positive regulator of Cdc2-cyclin B kinase activity. *Cell* **84:** 73–82

Guan J, Ekwurtzel E, Kvist U & Yuan L (2008) Cohesin protein SMC1 is a centrosomal protein. *Biochem Biophys Res Commun* **372:** 761–764

Gudimchuk N, Vitre B, Kim Y, Kiyatkin A, Cleveland DW, Ataullakhanov FI & Grishchuk EL (2013) Kinetochore kinesin CENP-E is a processive bi-directional tracker of dynamic microtubule tips. *Nat Cell Biol* **15:** 1079–1088

Guillou E, Ibarra A, Coulon V, Casado-Vela J, Rico D, Casal I, Schwob E, Losada A & Méndez J (2010) Cohesin organizes chromatin loops at DNA replication factories. *Genes Dev* **24:** 2812–2822

Gutiérrez-Caballero C, Herrán Y, Sánchez-Martín M, Suja JA, Barbero JL, Llano E & Pendás AM (2011) Identification and molecular characterization of the mammalian α-kleisin RAD21L. *Cell Cycle* **10:** 1477–1487

Haarhuis JHI, Elbatsh AMO, van den Broek B, Camps D, Erkan H, Jalink K, Medema RH & Rowland BD (2013) WAPL-mediated removal of cohesin protects against segregation errors and aneuploidy. *Curr Biol* **23:** 2071–2077

Hadjur S, Williams LM, Ryan NK, Cobb BS, Sexton T, Fraser P, Fisher AG & Merkenschlager M (2009) Cohesins form chromosomal cis-interactions at the developmentally regulated IFNG locus. *Nature* **460:** 410–413

Haering CH, Farcas A-M, Arumugam P, Metson J & Nasmyth K (2008) The cohesin ring concatenates sister DNA molecules. *Nature* **454:** 297–301

Haering CH, Löwe J, Hochwagen A & Nasmyth K (2002) Molecular architecture of SMC proteins and the yeast cohesin complex. *Mol Cell* **9:** 773–788

Haering CH, Schoffnegger D, Nishino T, Helmhart W, Nasmyth K & Löwe J (2004) Structure and stability of cohesin's Smc1-kleisin interaction. *Mol Cell* **15:** 951–964

Hanahan D & Weinberg RA (2011) Hallmarks of cancer: the next generation. *Cell* **144:** 646–674

Hanna JS, Kroll ES, Lundblad V & Spencer FA (2001) Saccharomyces cerevisiae CTF18 and CTF4 are required for sister chromatid cohesion. *Mol Cell Biol* **21:** 3144–3158

Hara K, Zheng G, Qu Q, Liu H, Ouyang Z, Chen Z, Tomchick DR & Yu H (2014) Structure of cohesin subcomplex pinpoints direct shugoshin-Wapl antagonism in centromeric cohesion. *Nat Struct Mol Biol* **21:** 864–870

Haren L, Stearns T & Lüders J (2009) Plk1-dependent recruitment of gamma-tubulin complexes to mitotic centrosomes involves multiple PCM components. *PLoS One* **4:** e5976

Harper JW & Elledge SJ (1998) The role of Cdk7 in CAK function, a retro-retrospective. *Genes Dev* **12:** 285–289

Hartman T, Stead K, Koshland D & Guacci V (2000) Pds5p is an essential chromosomal protein required for both sister chromatid cohesion and condensation in Saccharomyces cerevisiae. *J Cell Biol* **151:** 613–626

Haruki H, Nishikawa J & Laemmli UK (2008) The anchor-away technique: Rapid, conditional establishment of yeast mutant phenotypes. *Mol Cell* **31:** 925–932

Hauf S, Roitinger E, Koch B, Dittrich CM, Mechtler K & Peters J-M (2005) Dissociation of cohesin from chromosome arms and loss of arm cohesion during early mitosis depends on phosphorylation of SA2. *PLoS Biol* **3:** e69

He R, Huang N, Bao Y, Zhou H, Teng J & Chen J (2013) LRRC45 is a centrosome linker component required for centrosome cohesion. *Cell Rep* **4:** 1100–1107

Heald R & McKeon F (1990) Mutations of phosphorylation sites in lamin A that prevent nuclear lamina disassembly in mitosis. *Cell* **61:** 579–589

Hedglin M, Perumal SK, Hu Z & Benkovic S (2013) Stepwise assembly of the human replicative polymerase holoenzyme. *Elife* **2:** e00278

Heidinger-Pauli JM, Mert O, Davenport C, Guacci V & Koshland D (2010) Systematic reduction of cohesin differentially affects chromosome segregation, condensation, and DNA repair. *Curr Biol* **20:** 957–963

Hellmuth S, Böttger F, Pan C, Mann M & Stemmann O (2014) PP2A delays APC/C-dependent degradation of separase-associated but not free securin. *EMBO J* **33:** 1134–1147

Hellmuth S, Pöhlmann C, Brown A, Böttger F, Sprinzl M & Stemmann O (2015a) Positive and negative regulation of vertebrate separase by Cdk1-cyclin B1 may explain why securin is dispensable. *J Biol Chem* **290:** 8002–8010

Hellmuth S, Rata S, Brown A, Heidmann S, Novak B & Stemmann O (2015b) Human chromosome segregation involves multi-layered regulation of separase by the peptidyl-prolyl-isomerase pin1. *Mol Cell* **58:** 495–506

Hemerly AS, Prasanth SG, Siddiqui K & Stillman B (2009) Orc1 controls centriole and centrosome copy number in human cells. *Science* **323:** 789–793

Hinchcliffe EH, Li C, Thompson EA, Maller JL & Sluder G (1999) Requirement of Cdk2-cyclin E activity for repeated centrosome reproduction in Xenopus egg extracts. *Science* **283:** 851–854

Hirano T (2005) Condensins: organizing and segregating the genome. *Curr Biol* **15:** R265–75

Hoffmann I, Clarke PR, Marcote MJ, Karsenti E & Draetta G (1993) Phosphorylation and activation of human cdc25-C by cdc2--cyclin B and its involvement in the self-amplification of MPF at mitosis. *EMBO J* **12:** 53–63

Holland AJ & Taylor SS (2006) Cyclin-B1-mediated inhibition of excess separase is required for timely chromosome disjunction. *J Cell Sci* **119:** 3325–3336

Hou C, Dale R & Dean A (2010) Cell type specificity of chromatin organization mediated by CTCF and cohesin. *Proc Natl Acad Sci USA* **107:** 3651–3656

Howell BJ, McEwen BF, Canman JC, Hoffman DB, Farrar EM, Rieder CL & Salmon ED (2001) Cytoplasmic dynein/dynactin drives kinetochore protein transport to the spindle poles and has a role in mitotic spindle checkpoint inactivation. *J Cell Biol* **155:** 1159–1172

Hu B, Itoh T, Mishra A, Katoh Y, Chan K-L, Upcher W, Godlee C, Roig MB, Shirahige K & Nasmyth K (2011) ATP hydrolysis is required for relocating cohesin from sites occupied by its Scc2/4 loading complex. *Curr Biol* **21:** 12–24

Huang CE, Milutinovich M & Koshland D (2005) Rings, bracelet or snaps: fashionable alternatives for Smc complexes. *Philos Trans R Soc Lond, B, Biol Sci* **360:** 537–542

Huang X, Andreu-Vieyra CV, Wang M, Cooney AJ, Matzuk MM & Zhang P (2009) Preimplantation mouse embryos depend on inhibitory phosphorylation of separase to prevent chromosome missegregation. *Mol Cell Biol* **29:** 1498–1505

Huang X, Andreu-Vieyra CV, York JP, Hatcher R, Lu T, Matzuk MM & Zhang P (2008) Inhibitory phosphorylation of separase is essential for genome stability and viability of murine embryonic germ cells. *PLoS Biol* **6:** e15

Huis In 't Veld PJ, Herzog F, Ladurner R, Davidson IF, Piric S, Kreidl E, Bhaskara V, Aebersold R & Peters J-M (2014) Characterization of a DNA exit gate in the human cohesin ring. *Science* **346:** 968–972

Ilves I, Petojevic T, Pesavento JJ & Botchan MR (2010) Activation of the MCM2-7 helicase by association with Cdc45 and GINS proteins. *Mol Cell* **37:** 247–258

Im J-S, Ki S-H, Farina A, Jung D-S, Hurwitz J & Lee J-K (2009) Assembly of the Cdc45-Mcm2-7-GINS complex in human cells requires the Ctf4/And-1, RecQL4, and Mcm10 proteins. *Proc Natl Acad Sci USA* **106:** 15628–15632

Indjeian VB, Stern BM & Murray AW (2005) The centromeric protein Sgo1 is required to sense lack of tension on mitotic chromosomes. *Science* **307:** 130–133

Ishiguro K-I, Kim J, Fujiyama-Nakamura S, Kato S & Watanabe Y (2011) A new meiosis-specific cohesin complex implicated in the cohesin code for homologous pairing. *EMBO reports* **12:** 267–275

Ishiguro K-I, Kim J, Shibuya H, Hernández-Hernández A, Suzuki A, Fukagawa T, Shioi G, Kiyonari H, Li XC, Schimenti J, Hoog C & Watanabe Y (2014) Meiosis-specific cohesin mediates homolog recognition in mouse spermatocytes. *Genes Dev* **28:** 594–607

Ishiguro T, Tanaka K, Sakuno T & Watanabe Y (2010) Shugoshin-PP2A counteracts casein-kinase-1-dependent cleavage of Rec8 by separase. *Nat Cell Biol* **12:** 500–506

Ishikawa H & Marshall WF (2011) Ciliogenesis: building the cell's antenna. *Nat. Rev. Mol. Cell Biol.* **12:** 222–234

Ivanov D & Nasmyth K (2005) A topological interaction between cohesin rings and a circular minichromosome. *Cell* **122:** 849–860

Ivanov D & Nasmyth K (2007) A physical assay for sister chromatid cohesion in vitro. *Mol Cell* **27:** 300–310

Ivanov D, Schleiffer A, Eisenhaber F, Mechtler K, Haering CH & Nasmyth K (2002) Eco1 is a novel acetyltransferase that can acetylate proteins involved in cohesion. *Curr Biol* **12:** 323–328

Izumi T & Maller JL (1993) Elimination of cdc2 phosphorylation sites in the cdc25 phosphatase blocks initiation of M-phase. *Mol Biol Cell* **4:** 1337–1350

Jackson DA & Pombo A (1998) Replicon clusters are stable units of chromosome structure: evidence that nuclear organization contributes to the efficient activation and propagation of S phase in human cells. *J Cell Biol* **140:** 1285–1295

Jones KT (2008) Meiosis in oocytes: predisposition to aneuploidy and its increased incidence with age. *Hum Reprod Update* **14:** 143–158

Kagey MH, Newman JJ, Bilodeau S, Zhan Y, Orlando DA, van Berkum NL, Ebmeier CC, Goossens J, Rahl PB, Levine SS, Taatjes DJ, Dekker J & Young RA (2010)

Mediator and cohesin connect gene expression and chromatin architecture. *Nature* **467:** 430–435

Kamimura Y, Masumoto H, Sugino A & Araki H (1998) Sld2, which interacts with Dpb11 in Saccharomyces cerevisiae, is required for chromosomal DNA replication. *Mol Cell Biol* **18:** 6102–6109

Kamimura Y, Tak YS, Sugino A & Araki H (2001) Sld3, which interacts with Cdc45 (Sld4), functions for chromosomal DNA replication in Saccharomyces cerevisiae. *EMBO J* **20:** 2097–2107

Kanemaki M & Labib K (2006) Distinct roles for Sld3 and GINS during establishment and progression of eukaryotic DNA replication forks. *EMBO J* **25:** 1753–1763

Kapoor TM, Lampson MA, Hergert P, Cameron L, Cimini D, Salmon ED, McEwen BF & Khodjakov A (2006) Chromosomes can congress to the metaphase plate before biorientation. *Science* **311:** 388–391

Katis VL, Gálová M, Rabitsch KP, Gregan J & Nasmyth K (2004) Maintenance of cohesin at centromeres after meiosis I in budding yeast requires a kinetochore-associated protein related to MEI-S332. *Curr Biol* **14:** 560–572

Katis VL, Lipp JJ, Imre R, Bogdanova A, Okaz E, Habermann B, Mechtler K, Nasmyth K & Zachariae W (2010) Rec8 phosphorylation by casein kinase 1 and Cdc7-Dbf4 kinase regulates cohesin cleavage by separase during meiosis. *Dev Cell* **18:** 397–409

Kawashima SA, Tsukahara T, Langegger M, Hauf S, Kitajima TS & Watanabe Y (2007) Shugoshin enables tension-generating attachment of kinetochores by loading Aurora to centromeres. *Genes Dev* **21:** 420–435

Kawashima SA, Yamagishi Y, Honda T, Ishiguro K-I & Watanabe Y (2010) Phosphorylation of H2A by Bub1 prevents chromosomal instability through localizing shugoshin. *Science* **327:** 172–177

Keating P, Rachidi N, Tanaka TU & Stark MJR (2009) Ipl1-dependent phosphorylation of Dam1 is reduced by tension applied on kinetochores. *J Cell Sci* **122:** 4375–4382

Kerrebrock AW, Moore DP, Wu JS & Orr-Weaver TL (1995) Mei-S332, a Drosophila protein required for sister-chromatid cohesion, can localize to meiotic centromere regions. *Cell* **83:** 247–256

Kim J-S, Krasieva TB, LaMorte V, Taylor AMR & Yokomori K (2002) Specific recruitment of human cohesin to laser-induced DNA damage. *J Biol Chem* **277:** 45149–45153

Kim Y, Holland AJ, Lan W & Cleveland DW (2010) Aurora kinases and protein phosphatase 1 mediate chromosome congression through regulation of CENP-E. *Cell* **142:** 444–455

Kirschner M & Mitchison T (1986) Beyond self-assembly: from microtubules to morphogenesis. *Cell* **45:** 329–342

Kitajima TS, Hauf S, Ohsugi M, Yamamoto T & Watanabe Y (2005) Human Bub1 defines the persistent cohesion site along the mitotic chromosome by affecting Shugoshin localization. *Curr Biol* **15:** 353–359

Kitajima TS, Kawashima SA & Watanabe Y (2004) The conserved kinetochore protein shugoshin protects centromeric cohesion during meiosis. *Nature* **427:** 510–517

Kitajima TS, Miyazaki Y, Yamamoto M & Watanabe Y (2003) Rec8 cleavage by separase is required for meiotic nuclear divisions in fission yeast. *EMBO J* **22:** 5643–5653

Kitajima TS, Sakuno T, Ishiguro K-I, Iemura S-I, Natsume T, Kawashima SA & Watanabe Y (2006) Shugoshin collaborates with protein phosphatase 2A to protect cohesin. *Nature* **441:** 46–52

Klein F, Mahr P, Gálová M, Buonomo SB, Michaelis C, Nairz K & Nasmyth K (1999) A central role for cohesins in sister chromatid cohesion, formation of axial elements, and recombination during yeast meiosis. *Cell* **98:** 91–103

Kline AD, Krantz ID, Sommer A, Kliewer M, Jackson LG, Fitzpatrick DR, Levin AV & Selicorni A (2007) Cornelia de Lange syndrome: clinical review, diagnostic and scoring systems, and anticipatory guidance. *Am J Med Genet A* **143A:** 1287–1296

Kline-Smith SL, Khodjakov A, Hergert P & Walczak CE (2004) Depletion of centromeric MCAK leads to chromosome congression and segregation defects due to improper kinetochore attachments. *Mol Biol Cell* **15:** 1146–1159

Knowlton AL, Lan W & Stukenberg PT (2006) Aurora B is enriched at merotelic attachment sites, where it regulates MCAK. *Curr Biol* **16:** 1705–1710

Kong X, Ball AR, Sonoda E, Feng J, Takeda S, Fukagawa T, Yen TJ & Yokomori K (2009) Cohesin associates with spindle poles in a mitosis-specific manner and functions in spindle assembly in vertebrate cells. *Mol Biol Cell* **20:** 1289–1301

Kops GJPL, Weaver BAA & Cleveland DW (2005) On the road to cancer: aneuploidy and the mitotic checkpoint. *Nat Rev Cancer* **5:** 773–785

Koshland D & Hartwell LH (1987) The structure of sister minichromosome DNA before anaphase in Saccharomyces cerevisiae. **238:** 1713–1716

Krantz ID, McCallum J, DeScipio C, Kaur M, Gillis LA, Yaeger D, Jukofsky L, Wasserman N, Bottani A, Morris CA, Nowaczyk MJM, Toriello H, Bamshad MJ, Carey JC, Rappaport E, Kawauchi S, Lander AD, Calof AL, Li H-H, Devoto M, et al (2004) Cornelia de Lange syndrome is caused by mutations in NIPBL, the human homolog of Drosophila melanogaster Nipped-B. *Nat Genet* **36:** 631–635

Krishna TS, Fenyö D, Kong XP, Gary S, Chait BT, Burgers P & Kuriyan J (1994) Crystallization of proliferating cell nuclear antigen (PCNA) from Saccharomyces cerevisiae. *J Mol Biol* **241:** 265–268

Kueng S, Hegemann B, Peters BH, Lipp JJ, Schleiffer A, Mechtler K & Peters J-M (2006) Wapl controls the dynamic association of cohesin with chromatin. *Cell* **127:** 955–967

Kumagai A & Dunphy WG (1992) Regulation of the cdc25 protein during the cell cycle in Xenopus extracts. *Cell* **70:** 139–151

Kumagai A, Shevchenko A, Shevchenko A & Dunphy WG (2011) Direct regulation of Treslin by cyclin-dependent kinase is essential for the onset of DNA replication. *J Cell Biol* **193:** 995–1007

Kuriyama R & Borisy GG (1981) Centriole cycle in Chinese hamster ovary cells as determined by whole-mount electron microscopy. *J Cell Biol* **91:** 814–821

Kurze A, Michie KA, Dixon SE, Mishra A, Itoh T, Khalid S, Strmecki L, Shirahige K, Haering CH, Löwe J & Nasmyth K (2011) A positively charged channel within the Smc1/ Smc3 hinge required for sister chromatid cohesion. *EMBO J* **30:** 364–378

Labib K (2010) How do Cdc7 and cyclin-dependent kinases trigger the initiation of chromosome replication in eukaryotic cells? *Genes Dev* **24:** 1208–1219

Lacey KR, Jackson PK & Stearns T (1999) Cyclin-dependent kinase control of centrosome duplication. *Proc Natl Acad Sci USA* **96:** 2817–2822

Ladurner R, Bhaskara V, Huis In 't Veld PJ, Davidson IF, Kreidl E, Petzold G & Peters J-M (2014) Cohesin's ATPase activity couples cohesin loading onto DNA with Smc3 acetylation. *Curr Biol* **24:** 2228–2237

Lafont AL, Song J & Rankin S (2010) Sororin cooperates with the acetyltransferase Eco2 to ensure DNA replication-dependent sister chromatid cohesion. *Proc Natl Acad Sci USA* **107:** 20364–20369

Laloraya S, Guacci V & Koshland D (2000) Chromosomal addresses of the cohesin component Mcd1p. *J Cell Biol* **151:** 1047–1056

Lampson MA & Cheeseman IM (2011) Sensing centromere tension: Aurora B and the regulation of kinetochore function. *Trends Cell Biol* **21:** 133–140

Lau A, Blitzblau H & Bell SP (2002) Cell-cycle control of the establishment of mating-type silencing in S. cerevisiae. *Genes Dev* **16:** 2935–2945

Lawo S, Hasegan M, Gupta GD & Pelletier L (2012) Subdiffraction imaging of centrosomes reveals higher-order organizational features of pericentriolar material. *Nat Cell Biol* **14:** 1148–1158

Lee BH & Amon A (2003) Role of Polo-like kinase CDC5 in programming meiosis I chromosome segregation. *Science* **300:** 482–486

Lee C, Hong B, Choi JM, Kim Y, Watanabe S, Ishimi Y, Enomoto T, Tada S, Kim Y & Cho Y (2004) Structural basis for inhibition of the replication licensing factor Cdt1 by geminin. *Nature* **430:** 913–917

Lee J & Hirano T (2011) RAD21L, a novel cohesin subunit implicated in linking homologous chromosomes in mammalian meiosis. *J Cell Biol* **192:** 263–276

Lee J, Kitajima TS, Tanno Y, Yoshida K, Morita T, Miyano T, Miyake M & Watanabe Y (2008) Unified mode of centromeric protection by shugoshin in mammalian oocytes and somatic cells. *Nat Cell Biol* **10:** 42–52

Lee K & Rhee K (2011) PLK1 phosphorylation of pericentrin initiates centrosome maturation at the onset of mitosis. *J Cell Biol* **195:** 1093–1101

Lee K & Rhee K (2012) Separase-dependent cleavage of pericentrin B is necessary and sufficient for centriole disengagement during mitosis. *Cell Cycle* **11:** 2476–2485

Lee KY, Bang SW, Yoon SW, Lee S-H, Yoon J-B & Hwang DS (2012) Phosphorylation of ORC2 protein dissociates origin recognition complex from chromatin and replication origins. *J Biol Chem* **287:** 11891–11898

Lei M, Kawasaki Y, Young MR, Kihara M, Sugino A & Tye BK (1997) Mcm2 is a target of regulation by Cdc7-Dbf4 during the initiation of DNA synthesis. *Genes Dev* **11:** 3365–3374

Leman AR & Noguchi E (2013) The replication fork: understanding the eukaryotic replication machinery and the challenges to genome duplication. *Genes (Basel)* **4:** 1–32

Lengronne A, Katou Y, Mori S, Yokobayashi S, Kelly GP, Itoh T, Watanabe Y, Shirahige K & Uhlmann F (2004) Cohesin relocation from sites of chromosomal loading to places of convergent transcription. *Nature* **430:** 573–578

Lengronne A, McIntyre J, Katou Y, Kanoh Y, Hopfner K-P, Shirahige K & Uhlmann F (2006) Establishment of sister chromatid cohesion at the S. cerevisiae replication fork. *Mol Cell* **23:** 787–799

Li X, Zhao Q, Liao R, Sun P & Wu X (2003) The SCF(Skp2) ubiquitin ligase complex interacts with the human replication licensing factor Cdt1 and regulates Cdt1 degradation. *J Biol Chem* **278:** 30854–30858

Liang C, Weinreich M & Stillman B (1995) ORC and Cdc6p interact and determine the frequency of initiation of DNA replication in the genome. *Cell* **81:** 667–676

Liang J, Choi J & Clardy J (1999) Refined structure of the FKBP12-rapamycin-FRB ternary complex at 2.2 A resolution. *Acta Crystallogr D Biol Crystallogr* **55:** 736–744

Lindgren E, Hägg S, Giordano F, Björkegren J & Ström L (2014) Inactivation of the budding yeast cohesin loader Scc2 alters gene expression both globally and in response to a single DNA double strand break. *Cell Cycle* **13:** 3645–3658

Lindqvist A, Rodríguez-Bravo V & Medema RH (2009) The decision to enter mitosis: feedback and redundancy in the mitotic entry network. *J Cell Biol* **185:** 193–202

Liu D, Davydenko O & Lampson MA (2012) Polo-like kinase-1 regulates kinetochore-microtubule dynamics and spindle checkpoint silencing. *J Cell Biol* **198:** 491–499

Liu D, Vader G, Vromans MJM, Lampson MA & Lens SMA (2009a) Sensing chromosome bi-orientation by spatial separation of aurora B kinase from kinetochore substrates. *Science* **323:** 1350–1353

Liu E, Li X, Yan F, Zhao Q & Wu X (2004) Cyclin-dependent kinases phosphorylate human Cdt1 and induce its degradation. *J Biol Chem* **279:** 17283–17288

Liu H, Jia L & Yu H (2013a) Phospho-H2A and cohesin specify distinct tension-regulated Sgo1 pools at kinetochores and inner centromeres. *Curr Biol* **23:** 1927–1933

Liu H, Rankin S & Yu H (2013b) Phosphorylation-enabled binding of SGO1-PP2A to cohesin protects sororin and centromeric cohesion during mitosis. *Nat Cell Biol* **15:** 40–49

Liu J, Zhang Z, Bando M, Itoh T, Deardorff MA, Clark D, Kaur M, Tandy S, Kondoh T, Rappaport E, Spinner NB, Vega H, Jackson LG, Shirahige K & Krantz ID (2009b) Transcriptional dysregulation in NIPBL and cohesin mutant human cells. *PLoS Biol* **7:** e1000119

Lopez-Serra L, Kelly G, Patel H, Stewart A & Uhlmann F (2014) The Scc2-Scc4 complex acts in sister chromatid cohesion and transcriptional regulation by maintaining nucleosome-free regions. *Nat Genet* **46:** 1147–1151

Lopez-Serra L, Lengronne A, Borges V, Kelly G & Uhlmann F (2013) Budding yeast wapl controls sister chromatid cohesion maintenance and chromosome condensation. *Curr Biol* **23:** 64–69

Losada A, Hirano M & Hirano T (1998) Identification of Xenopus SMC protein complexes required for sister chromatid cohesion. *Genes Dev* **12:** 1986–1997

Losada A, Yokochi T & Hirano T (2005) Functional contribution of Pds5 to cohesin-mediated cohesion in human cells and Xenopus egg extracts. *J Cell Sci* **118:** 2133–2141

Lou H, Komata M, Katou Y, Guan Z, Reis CC, Budd M, Shirahige K & Campbell JL (2008) Mrc1 and DNA polymerase epsilon function together in linking DNA replication and the S phase checkpoint. *Mol Cell* **32:** 106–117

Lu F, Lan R, Zhang H, Jiang Q & Zhang C (2009) Geminin is partially localized to the centrosome and plays a role in proper centrosome duplication. *Biol. Cell* **101:** 273–285

Luo X, Tang Z, Rizo J & Yu H (2002) The Mad2 spindle checkpoint protein undergoes similar major conformational changes upon binding to either Mad1 or Cdc20. *Mol Cell* **9:** 59–71

Luo X, Tang Z, Xia G, Wassmann K, Matsumoto T, Rizo J & Yu H (2004) The Mad2 spindle checkpoint protein has two distinct natively folded states. *Nat Struct Mol Biol* **11:** 338–345

Manning AL, Yazinski SA, Nicolay B, Bryll A, Zou L & Dyson NJ (2014) Suppression of Genome Instability in pRB-Deficient Cells by Enhancement of Chromosome Cohesion. *Mol Cell* **53:** 993–1004

Mao Y, Desai A & Cleveland DW (2005) Microtubule capture by CENP-E silences BubR1-dependent mitotic checkpoint signaling. *J Cell Biol* **170:** 873–880

Mapelli M, Filipp FV, Rancati G, Massimiliano L, Nezi L, Stier G, Hagan RS, Confalonieri S, Piatti S, Sattler M & Musacchio A (2006) Determinants of conformational dimerization of Mad2 and its inhibition by p31comet. *EMBO J* **25:** 1273–1284

Mardin BR, Agircan FG, Lange C & Schiebel E (2011) Plk1 Controls the Nek2A-PP1γ Antagonism in Centrosome Disjunction. *Curr Biol* **21:** 1145–1151

Marshall WF (2009) Centriole evolution. *Curr Opin Cell Biol* **21:** 14–19

Marston AL (2015) Shugoshins: Tension-Sensitive Pericentromeric Adaptors Safeguarding Chromosome Segregation. *Mol Cell Biol* **35:** 634–648

Masai H, Matsui E, You Z, Ishimi Y, Tamai K & Arai K (2000) Human Cdc7-related kinase complex. In vitro phosphorylation of MCM by concerted actions of Cdks and Cdc7 and that of a criticial threonine residue of Cdc7 bY Cdks. *J Biol Chem* **275:** 29042–29052

Masai H, Taniyama C, Ogino K, Matsui E, Kakusho N, Matsumoto S, Kim J-M, Ishii A, Tanaka T, Kobayashi T, Tamai K, Ohtani K & Arai K-I (2006) Phosphorylation of MCM4 by Cdc7 kinase facilitates its interaction with Cdc45 on the chromatin. *J Biol Chem* **281:** 39249–39261

Mass G, Nethanel T & Kaufmann G (1998) The middle subunit of replication protein A contacts growing RNA-DNA primers in replicating simian virus 40 chromosomes. *Mol Cell Biol* **18:** 6399–6407

Masumoto H, Muramatsu S, Kamimura Y & Araki H (2002) S-Cdk-dependent phosphorylation of Sld2 essential for chromosomal DNA replication in budding yeast. *Nature* **415:** 651–655

Matsumoto Y, Hayashi K & Nishida E (1999) Cyclin-dependent kinase 2 (Cdk2) is required for centrosome duplication in mammalian cells. *Curr Biol* **9:** 429–432

Matsuo K, Ohsumi K, Iwabuchi M, Kawamata T, Ono Y & Takahashi M (2012) Kendrin is a novel substrate for separase involved in the licensing of centriole duplication. *Curr Biol* **22:** 915–921

Matsuura S, Kahyo T, Shinmura K, Iwaizumi M, Yamada H, Funai K, Kobayashi J, Tanahashi M, Niwa H, Ogawa H, Takahashi T, Inui N, Suda T, Chida K, Watanabe Y & Sugimura H (2013) SGOL1 variant B induces abnormal mitosis and resistance to taxane in non-small cell lung cancers. *Scientific Reports* **3:** 3012

Mayor T, Stierhof YD, Tanaka K, Fry AM & Nigg EA (2000) The centrosomal protein C-Nap1 is required for cell cycle-regulated centrosome cohesion. *J Cell Biol* **151:** 837–846

Mäkiniemi M, Hillukkala T, Tuusa J, Reini K, Vaara M, Huang D, Pospiech H, Majuri I, Westerling T, Mäkelä TP & Syväoja JE (2001) BRCT domain-containing protein TopBP1 functions in DNA replication and damage response. *J Biol Chem* **276:** 30399–30406

Mc Intyre J, Muller EGD, Weitzer S, Snydsman BE, Davis TN & Uhlmann F (2007) In vivo analysis of cohesin architecture using FRET in the budding yeast Saccharomyces cerevisiae. *EMBO J* **26:** 3783–3793

McGarry TJ & Kirschner MW (1998) Geminin, an inhibitor of DNA replication, is degraded during mitosis. *Cell* **93:** 1043–1053

McGowan CH & Russell P (1995) Cell cycle regulation of human WEE1. *EMBO J* **14:** 2166–2175

McGuinness BE, Hirota T, Kudo NR, Peters J-M & Nasmyth K (2005) Shugoshin prevents dissociation of cohesin from centromeres during mitosis in vertebrate cells. *PLoS Biol* **3:** e86

Megee PC, Mistrot C, Guacci V & Koshland D (1999) The centromeric sister chromatid cohesion site directs Mcd1p binding to adjacent sequences. *Mol Cell* **4:** 445–450

Mei J, Huang X & Zhang P (2001) Securin is not required for cellular viability, but is required for normal growth of mouse embryonic fibroblasts. *Curr Biol* **11:** 1197–1201

Melby TE, Ciampaglio CN, Briscoe G & Erickson HP (1998) The symmetrical structure of structural maintenance of chromosomes (SMC) and MukB proteins: long, antiparallel coiled coils, folded at a flexible hinge. *J Cell Biol* **142:** 1595–1604

Mennella V, Keszthelyi B, McDonald KL, Chhun B, Kan F, Rogers GC, Huang B & Agard DA (2012) Subdiffraction-resolution fluorescence microscopy reveals a domain of the centrosome critical for pericentriolar material organization. *Nat Cell Biol* **14:** 1159–1168

Meraldi P, Lukas J, Fry AM, Bartek J & Nigg EA (1999) Centrosome duplication in mammalian somatic cells requires E2F and Cdk2-cyclin A. *Nat Cell Biol* **1:** 88–93

Merkenschlager M & Odom DT (2013) CTCF and cohesin: linking gene regulatory elements with their targets. *Cell* **152:** 1285–1297

Méndez J, Zou-Yang XH, Kim S-Y, Hidaka M, Tansey WP & Stillman B (2002) Human origin recognition complex large subunit is degraded by ubiquitin-mediated proteolysis after initiation of DNA replication. *Mol Cell* **9:** 481–491

Michaelis C, Ciosk R & Nasmyth K (1997) Cohesins: chromosomal proteins that prevent premature separation of sister chromatids. *Cell* **91:** 35–45

Mihaylov IS, Kondo T, Jones L, Ryzhikov S, Tanaka J, Zheng J, Higa LA, Minamino N, Cooley L & Zhang H (2002) Control of DNA replication and chromosome ploidy by geminin and cyclin A. *Mol Cell Biol* **22:** 1868–1880

Milutinovich M, Ünal E, Ward C, Skibbens RV & Koshland D (2007) A multi-step pathway for the establishment of sister chromatid cohesion. *PLoS Genet* **3:** e12

Mirchenko L & Uhlmann F (2010) Sli15(INCENP) dephosphorylation prevents mitotic checkpoint reengagement due to loss of tension at anaphase onset. *Curr Biol* **20:** 1396–1401

Mishiro T, Ishihara K, Hino S, Tsutsumi S, Aburatani H, Shirahige K, Kinoshita Y & Nakao M (2009) Architectural roles of multiple chromatin insulators at the human apolipoprotein gene cluster. *EMBO J* **28:** 1234–1245

Mohr L, Buheitel J, Schöckel L, Karalus D, Mayer B & Stemmann O (2015) An Alternatively Spliced Bifunctional Localization Signal Reprograms Human Shugoshin 1 to Protect Centrosomal Instead of Centromeric Cohesin. *Cell Rep*

Moldovan G-L, Pfander B & Jentsch S (2006) PCNA controls establishment of sister chromatid cohesion during S phase. *Mol Cell* **23:** 723–732

Moldovan G-L, Pfander B & Jentsch S (2007) PCNA, the maestro of the replication fork. *Cell* **129:** 665–679

Moritz M, Braunfeld MB, Sedat JW, Alberts B & Agard DA (1995) Microtubule nucleation by gamma-tubulin-containing rings in the centrosome. *Nature* **378:** 638–640

Mueller PR, Coleman TR, Kumagai A & Dunphy WG (1995) Myt1: a membrane-associated inhibitory kinase that phosphorylates Cdc2 on both threonine-14 and tyrosine-15. **270:** 86–90

Murakami Y & Hurwitz J (1993) Functional interactions between SV40 T antigen and other replication proteins at the replication fork. *J Biol Chem* **268:** 11008–11017

Murayama Y & Uhlmann F (2014) Biochemical reconstitution of topological DNA binding by the cohesin ring. *Nature* **505:** 367–371

Murdoch B, Owen N, Stevense M, Smith H, Nagaoka S, Hassold T, McKay M, Xu H, Fu J, Revenkova E, Jessberger R & Hunt P (2013) Altered cohesin gene dosage affects Mammalian meiotic chromosome structure and behavior. *PLoS Genet* **9:** e1003241

Murrell A, Heeson S & Reik W (2004) Interaction between differentially methylated regions partitions the imprinted genes Igf2 and H19 into parent-specific chromatin loops. *Nat Genet* **36:** 889–893

Nakamura A, Arai H & Fujita N (2009) Centrosomal Aki1 and cohesin function in separase-regulated centriole disengagement. *J Cell Biol* **187:** 607–614

Nasmyth K (2011) Cohesin: a catenase with separate entry and exit gates? *Nat Cell Biol* **13:** 1170–1177

Nativio R, Wendt KS, Ito Y, Huddleston JE, Uribe-Lewis S, Woodfine K, Krueger C, Reik W, Peters J-M & Murrell A (2009) Cohesin is required for higher-order chromatin conformation at the imprinted IGF2-H19 locus. *PLoS Genet* **5:** e1000739

Natsume T, Müller CA, Katou Y, Retkute R, Gierliński M, Araki H, Blow JJ, Shirahige K, Nieduszynski CA & Tanaka TU (2013) Kinetochores coordinate pericentromeric cohesion and early DNA replication by Cdc7-Dbf4 kinase recruitment. *Mol Cell* **50:** 661–674

Nerusheva OO, Galander S, Fernius J, Kelly D & Marston AL (2014) Tension-dependent removal of pericentromeric shugoshin is an indicator of sister chromosome biorientation. *Genes Dev* **28:** 1291–1309

Nethanel T, Reisfeld S, Dinter-Gottlieb G & Kaufmann G (1988) An Okazaki piece of simian virus 40 may be synthesized by ligation of shorter precursor chains. *J Virol* **62:** 2867–2873

Nezi L & Musacchio A (2009) Sister chromatid tension and the spindle assembly checkpoint. *Curr Opin Cell Biol* **21:** 785–795

Nguyen VQ, Co C & Li JJ (2001) Cyclin-dependent kinases prevent DNA re-replication through multiple mechanisms. *Nature* **411:** 1068–1073

Nick McElhinny SA, Gordenin DA, Stith CM, Burgers PMJ & Kunkel TA (2008) Division of labor at the eukaryotic replication fork. *Mol Cell* **30:** 137–144

Nigg EA (2002) Centrosome aberrations: cause or consequence of cancer progression? *Nat Rev Cancer* **2:** 815–825

Nishitani H, Sugimoto N, Roukos V, Nakanishi Y, Saijo M, Obuse C, Tsurimoto T, Nakayama KI, Nakayama K, Fujita M, Lygerou Z & Nishimoto T (2006) Two E3 ubiquitin ligases, SCF-Skp2 and DDB1-Cul4, target human Cdt1 for proteolysis. *EMBO J* **25:** 1126–1136

Nishiyama T, Ladurner R, Schmitz J, Kreidl E, Schleiffer A, Bhaskara V, Bando M, Shirahige K, Hyman AA, Mechtler K & Peters J-M (2010) Sororin mediates sister chromatid cohesion by antagonizing Wapl. *Cell* **143:** 737–749

Nishiyama T, Sykora MM, Huis In 't Veld PJ, Mechtler K & Peters J-M (2013) Aurora B and Cdk1 mediate Wapl activation and release of acetylated cohesin from chromosomes by phosphorylating Sororin. *Proc Natl Acad Sci USA* **110:** 13404–13409

Nitzsche A, Paszkowski-Rogacz M, Matarese F, Janssen-Megens EM, Hubner NC, Schulz H, de Vries I, Ding L, Huebner N, Mann M, Stunnenberg HG & Buchholz F (2011) RAD21 cooperates with pluripotency transcription factors in the maintenance of embryonic stem cell identity. *PLoS One* **6:** e19470

Nougarède R, Seta Della F, Zarzov P & Schwob E (2000) Hierarchy of S phase-promoting factors: yeast Dbf4-Cdc7 kinase requires prior S phase cyclin-dependent kinase activation. *Mol Cell Biol* **20:** 3795–3806

Ocampo-Hafalla, M. T., & Uhlmann, F. (2011). Cohesin loading and sliding. *Journal of Cell Science*, *124*(Pt 5), 685–691.

Okazaki R, Okazaki T, Sakabe K, Sugimoto K & Sugino A (1968) Mechanism of DNA chain growth. I. Possible discontinuity and unusual secondary structure of newly synthesized chains. *Proc Natl Acad Sci USA* **59:** 598–605

Oliveira RA & Nasmyth K (2013) Cohesin cleavage is insufficient for centriole disengagement in Drosophila. *Curr Biol* **23:** R601–3

Oliveira RA, Hamilton RS, Pauli A, Davis I & Nasmyth K (2010) Cohesin cleavage and Cdk inhibition trigger formation of daughter nuclei. **12:** 185–192

Ouyang Z, Zheng G, Song J, Borek DM, Otwinowski Z, Brautigam CA, Tomchick DR, Rankin S & Yu H (2013) Structure of the human cohesin inhibitor Wapl. *Proc Natl Acad Sci USA* **110:** 11355–11360

Pacek M & Walter JC (2004) A requirement for MCM7 and Cdc45 in chromosome unwinding during eukaryotic DNA replication. *EMBO J* **23:** 3667–3676

Pagan JK, Marzio A, Jones MJK, Saraf A, Jallepalli PV, Florens L, Washburn MP & Pagano M (2015) Degradation of Cep68 and PCNT cleavage mediate Cep215 removal from the PCM to allow centriole separation, disengagement and licensing. *Nat Cell Biol* **17:** 31–43

Palframan WJ, Meehl JB, Jaspersen SL, Winey M & Murray AW (2006) Anaphase inactivation of the spindle checkpoint. *Science* **313:** 680–684

Panizza S, Tanaka T, Hochwagen A, Eisenhaber F & Nasmyth K (2000) Pds5 cooperates with cohesin in maintaining sister chromatid cohesion. *Curr Biol* **10:** 1557–1564

Parelho V, Hadjur S, Spivakov M, Leleu M, Sauer S, Gregson HC, Jarmuz A, Canzonetta C, Webster Z, Nesterova T, Cobb BS, Yokomori K, Dillon N, Aragon L, Fisher AG & Merkenschlager M (2008) Cohesins functionally associate with CTCF on mammalian chromosome arms. *Cell* **132:** 422–433

Parker LL, Atherton-Fessler S & Piwnica-Worms H (1992) p107wee1 is a dual-specificity kinase that phosphorylates p34cdc2 on tyrosine 15. *Proc Natl Acad Sci USA* **89:** 2917–2921

Paschal CR, Maciejowski J & Jallepalli PV (2012) A stringent requirement for Plk1 T210 phosphorylation during K-fiber assembly and chromosome congression. *Chromosoma* **121:** 565–572

Paul R, Wollman R, Silkworth WT, Nardi IK, Cimini D & Mogilner A (2009) Computer simulations predict that chromosome movements and rotations accelerate mitotic spindle assembly without compromising accuracy. *Proc Natl Acad Sci USA* **106:** 15708–15713

Paulmurugan R & Gambhir SS (2005) Novel fusion protein approach for efficient high-throughput screening of small molecule-mediating protein-protein interactions in cells and living animals. *Cancer Res* **65:** 7413–7420

Peplowska K, Wallek AU & Storchova Z (2014) Sgo1 regulates both condensin and ipl1/aurora B to promote chromosome biorientation. *PLoS Genet* **10:** e1004411

Petermann E, Helleday T & Caldecott KW (2008) Claspin promotes normal replication fork rates in human cells. *Mol Biol Cell* **19:** 2373–2378

Peters J-M (2006) The anaphase promoting complex/cyclosome: a machine designed to destroy. *Nat. Rev. Mol. Cell Biol.* **7:** 644–656

Peters J-M, Tedeschi A & Schmitz J (2008) The cohesin complex and its roles in chromosome biology. *Genes Dev* **22:** 3089–3114

Petronczki M, Matos J, Mori S, Gregan J, Bogdanova A, Schwickart M, Mechtler K, Shirahige K, Zachariae W & Nasmyth K (2006) Monopolar attachment of sister kinetochores at meiosis I requires casein kinase 1. *Cell* **126:** 1049–1064

Porter ACG & Farr CJ (2004) Topoisomerase II: untangling its contribution at the centromere. *Chromosome Res* **12:** 569–583

Potts PR, Porteus MH & Yu H (2006) Human SMC5/6 complex promotes sister chromatid homologous recombination by recruiting the SMC1/3 cohesin complex to double-strand breaks. *EMBO J* **25:** 3377–3388

Prasanth SG, Prasanth KV, Siddiqui K, Spector DL & Stillman B (2004) Human Orc2 localizes to centrosomes, centromeres and heterochromatin during chromosome inheritance. *EMBO J* **23:** 2651–2663

Prelich G, Tan CK, Kostura M, Mathews MB, So AG, Downey KM & Stillman B (1987) Functional identity of proliferating cell nuclear antigen and a DNA polymerase-delta auxiliary protein. *Nature* **326:** 517–520

Pursell ZF, Isoz I, Lundström E-B, Johansson E & Kunkel TA (2007) Yeast DNA polymerase epsilon participates in leading-strand DNA replication. *Science* **317:** 127–130

Qian YW, Erikson E, Taieb FE & Maller JL (2001) The polo-like kinase Plx1 is required for activation of the phosphatase Cdc25C and cyclin B-Cdc2 in Xenopus oocytes. *Mol Biol Cell* **12:** 1791–1799

Rabitsch KP, Gregan J, Schleiffer A, Javerzat J-P, Eisenhaber F & Nasmyth K (2004) Two fission yeast homologs of Drosophila Mei-S332 are required for chromosome segregation during meiosis I and II. *Curr Biol* **14:** 287–301

Rankin S, Ayad NG & Kirschner MW (2005) Sororin, a substrate of the anaphase-promoting complex, is required for sister chromatid cohesion in vertebrates. *Mol Cell* **18:** 185–200

Rao H, Uhlmann F, Nasmyth K & Varshavsky A (2001) Degradation of a cohesin subunit by the N-end rule pathway is essential for chromosome stability. *Nature* **410:** 955–959

Rape M, Reddy SK & Kirschner MW (2006) The processivity of multiubiquitination by the APC determines the order of substrate degradation. *Cell* **124:** 89–103

Rauch A, Thiel CT, Schindler D, Wick U, Crow YJ, Ekici AB, van Essen AJ, Goecke TO, Al-Gazali L, Chrzanowska KH, Zweier C, Brunner HG, Becker K, Curry CJ, Dallapiccola B, Devriendt K, Dörfler A, Kinning E, Megarbane A, Meinecke P, et al (2008) Mutations in the pericentrin (PCNT) gene cause primordial dwarfism. *Science* **319:** 816–819

Reddy SK, Rape M, Margansky WA & Kirschner MW (2007) Ubiquitination by the anaphase-promoting complex drives spindle checkpoint inactivation. *Nature* **446:** 921–925

Remeseiro S, Cuadrado A, Carretero M, Martínez P, Drosopoulos WC, Cañamero M, Schildkraut CL, Blasco MA & Losada A (2012) Cohesin-SA1 deficiency drives aneuploidy and tumourigenesis in mice due to impaired replication of telomeres. *EMBO J* **31:** 2076–2089

Remus D, Beuron F, Tolun G, Griffith JD, Morris EP & Diffley JFX (2009) Concerted loading of Mcm2-7 double hexamers around DNA during DNA replication origin licensing. *Cell* **139:** 719–730

Revenkova E, Eijpe M, Heyting C, Hodges CA, Hunt PA, Liebe B, Scherthan H & Jessberger R (2004) Cohesin SMC1 beta is required for meiotic chromosome dynamics, sister chromatid cohesion and DNA recombination. *Nat Cell Biol* **6:** 555–562

Rhodes JM, McEwan M & Horsfield JA (2011) Gene regulation by cohesin in cancer: is the ring an unexpected party to proliferation? *Mol Cancer Res* **9:** 1587–1607

Riedel CG, Katis VL, Katou Y, Mori S, Itoh T, Helmhart W, Gálová M, Petronczki M, Gregan J, Cetin B, Mudrak I, Ogris E, Mechtler K, Pelletier L, Buchholz F, Shirahige K & Nasmyth K (2006) Protein phosphatase 2A protects centromeric sister chromatid cohesion during meiosis I. *Nature* **441:** 53–61

Robbins E, Jentzsch G & Micali A (1968) The centriole cycle in synchronized HeLa cells. *J Cell Biol* **36:** 329–339

Rolef Ben-Shahar T, Heeger S, Lehane C, East P, Flynn H, Skehel M & Uhlmann F (2008) Eco1-dependent cohesin acetylation during establishment of sister chromatid cohesion. *Science* **321:** 563–566

Rollins RA, Korom M, Aulner N, Martens A & Dorsett D (2004) Drosophila nipped-B protein supports sister chromatid cohesion and opposes the stromalin/Scc3 cohesion factor to facilitate long-range activation of the cut gene. *Mol Cell Biol* **24:** 3100–3111

Rowland BD, Roig MB, Nishino T, Kurze A, Uluocak P, Mishra A, Beckouët F, Underwood P, Metson J, Imre R, Mechtler K, Katis VL & Nasmyth K (2009) Building sister chromatid cohesion: smc3 acetylation counteracts an antiestablishment activity. *Mol Cell* **33:** 763–774

Rubio ED, Reiss DJ, Welcsh PL, Disteche CM, Filippova GN, Baliga NS, Aebersold R, Ranish JA & Krumm A (2008) CTCF physically links cohesin to chromatin. *Proc Natl Acad Sci USA* **105:** 8309–8314

Ruchaud S, Carmena M & Earnshaw WC (2007) Chromosomal passengers: conducting cell division. *Nat. Rev. Mol. Cell Biol.* **8:** 798–812

Rudra S & Skibbens RV (2012) Sister chromatid cohesion establishment occurs in concert with lagging strand synthesis. *Cell Cycle* **11:** 2114–2121

Saha P, Chen J, Thome KC, Lawlis SJ, Hou ZH, Hendricks M, Parvin JD & Dutta A (1998) Human CDC6/Cdc18 associates with Orc1 and cyclin-cdk and is selectively eliminated from the nucleus at the onset of S phase. *Mol Cell Biol* **18:** 2758–2767

Sakuno T, Tada K & Watanabe Y (2009) Kinetochore geometry defined by cohesion within the centromere. *Nature* **458:** 852–858

Salah SM & Nasmyth K (2000) Destruction of the securin Pds1p occurs at the onset of anaphase during both meiotic divisions in yeast. *Chromosoma* **109:** 27–34

Salic A, Waters JC & Mitchison TJ (2004) Vertebrate shugoshin links sister centromere cohesion and kinetochore microtubule stability in mitosis. *Cell* **118:** 567–578

Santaguida S, Vernieri C, Villa F, Ciliberto A & Musacchio A (2011) Evidence that Aurora B is implicated in spindle checkpoint signalling independently of error correction. *EMBO J* **30:** 1508–1519

Santamaria A, Bin Wang, Elowe S, Malik R, Zhang F, Bauer M, Schmidt A, Silljé HHW, Körner R & Nigg EA (2011) The Plk1-dependent Phosphoproteome of the Early Mitotic Spindle. *Mol Cell Proteomics* **10:** M110.004457–M110.004457

Schaar BT, Chan GK, Maddox P, Salmon ED & Yen TJ (1997) CENP-E function at kinetochores is essential for chromosome alignment. *J Cell Biol* **139:** 1373–1382

Schmitz J, Watrin E, Lenart P, Mechtler K & Peters J-M (2007) Sororin is required for stable binding of cohesin to chromatin and for sister chromatid cohesion in interphase. *Curr Biol* **17:** 630–636

Schöckel L, Möckel M, Mayer B, Boos D & Stemmann O (2011) Cleavage of cohesin rings coordinates the separation of centrioles and chromatids. *Nat Cell Biol* **13:** 966–972

Schurtenberger P, Egelhaaf SU, Hindges R, Maga G, Jónsson ZO, May RP, Glatter O & Hübscher U (1998) The solution structure of functionally active human proliferating cell nuclear antigen determined by small-angle neutron scattering. *J Mol Biol* **275:** 123–132

Schüle B, Oviedo A, Johnston K, Pai S & Francke U (2005) Inactivating mutations in ESCO2 cause SC phocomelia and Roberts syndrome: no phenotype-genotype correlation. *Am J Hum Genet* **77:** 1117–1128

Schvarzstein M, Pattabiraman D, Bembenek JN & Villeneuve AM (2013) Meiotic HORMA domain proteins prevent untimely centriole disengagement during Caenorhabditis elegans spermatocyte meiosis. *Proc Natl Acad Sci USA* **110:** E898–907

Seitan VC, Faure AJ, Zhan Y, McCord RP, Lajoie BR, Ing-Simmons E, Lenhard B, Giorgetti L, Heard E, Fisher AG, Flicek P, Dekker J & Merkenschlager M (2013) Cohesin-based chromatin interactions enable regulated gene expression within preexisting architectural compartments. *Genome Res* **23:** 2066–2077

Seitan VC, Hao B, Tachibana-Konwalski K, Lavagnolli T, Mira-Bontenbal H, Brown KE, Teng G, Carroll T, Terry A, Horan K, Marks H, Adams DJ, Schatz DG, Aragon L, Fisher AG, Krangel MS, Nasmyth K & Merkenschlager M (2011) A role for cohesin in T-cell-receptor rearrangement and thymocyte differentiation. *Nature* **476:** 467–471

Seki T & Diffley JF (2000) Stepwise assembly of initiation proteins at budding yeast replication origins in vitro. *Proc Natl Acad Sci USA* **97:** 14115–14120

Senga T, Sivaprasad U, Zhu W, Park JH, Arias EE, Walter JC & Dutta A (2006) PCNA is a cofactor for Cdt1 degradation by CUL4/DDB1-mediated N-terminal ubiquitination. *J Biol Chem* **281:** 6246–6252

Sengupta A & Cancelas JA (2010) Cancer stem cells: a stride towards cancer cure? *J Cell Physiol* **225:** 7–14

Sheu Y-J & Stillman B (2006) Cdc7-Dbf4 phosphorylates MCM proteins via a docking site-mediated mechanism to promote S phase progression. *Mol Cell* **24:** 101–113

Shintomi K & Hirano T (2009) Releasing cohesin from chromosome arms in early mitosis: opposing actions of Wapl-Pds5 and Sgo1. *Genes Dev* **23:** 2224–2236

Shrestha RL & Draviam VM (2013) Lateral to end-on conversion of chromosome-microtubule attachment requires kinesins CENP-E and MCAK. *Curr Biol* **23:** 1514–1526

Silacci P, Mazzolai L, Gauci C, Stergiopulos N, Yin HL & Hayoz D (2004) Gelsolin superfamily proteins: key regulators of cellular functions. *Cell. Mol. Life Sci.* **61:** 2614–2623

Simerly C, Zoran SS, Payne C, Dominko T, Sutovsky P, Navara CS, Salisbury JL & Schatten G (1999) Biparental inheritance of gamma-tubulin during human fertilization: molecular reconstitution of functional zygotic centrosomes in inseminated human oocytes and in cell-free extracts nucleated by human sperm. *Mol Biol Cell* **10:** 2955–2969

Sinha NK, Morris CF & Alberts BM (1980) Efficient in vitro replication of double-stranded DNA templates by a purified T4 bacteriophage replication system. *J Biol Chem* **255:** 4290–4293

Sironi L, Mapelli M, Knapp S, de Antoni A, Jeang K-T & Musacchio A (2002) Crystal structure of the tetrameric Mad1-Mad2 core complex: implications of a 'safety belt' binding mechanism for the spindle checkpoint. *EMBO J* **21:** 2496–2506

Sjögren C & Nasmyth K (2001) Sister chromatid cohesion is required for postreplicative double-strand break repair in Saccharomyces cerevisiae. *Curr Biol* **11:** 991–995

Skibbens RV, Corson LB, Koshland D & Hieter P (1999) Ctf7p is essential for sister chromatid cohesion and links mitotic chromosome structure to the DNA replication machinery. *Genes Dev* **13:** 307–319

Sofueva S, Yaffe E, Chan W-C, Georgopoulou D, Vietri Rudan M, Mira-Bontenbal H, Pollard SM, Schroth GP, Tanay A & Hadjur S (2013) Cohesin-mediated interactions organize chromosomal domain architecture. *EMBO J* **32:** 3119–3129

Solomon DA, Kim T, Diaz-Martinez LA, Fair J, Elkahloun AG, Harris BT, Toretsky JA, Rosenberg SA, Shukla N, Ladanyi M, Samuels Y, James CD, Yu H, Kim J-S & Waldman T (2011) Mutational inactivation of STAG2 causes aneuploidy in human cancer. *Science* **333:** 1039–1043

Sonnen KF, Schermelleh L, Leonhardt H & Nigg EA (2012) 3D-structured illumination microscopy provides novel insight into architecture of human centrosomes. *Biol Open* **1:** 965–976

Sonoda E, Matsusaka T, Morrison C, Vagnarelli P, Hoshi O, Ushiki T, Nojima K, Fukagawa T, Waizenegger IC, Peters JM, Earnshaw WC & Takeda S (2001) Scc1/Rad21/Mcd1 is required for sister chromatid cohesion and kinetochore function in vertebrate cells. *Dev Cell* **1:** 759–770

Speck C, Chen Z, Li H & Stillman B (2005) ATPase-dependent cooperative binding of ORC and Cdc6 to origin DNA. *Nat Struct Mol Biol* **12:** 965–971

Srivastava S, Landy Schmitt C, Clark B, Kline AD, Specht M & Grados MA (2014) Autism traits in children and adolescents with Cornelia de Lange syndrome. *Am J Med Genet A* **164A:** 1400–1410

St-Pierre J, Douziech M, Bazile F, Pascariu M, Bonneil E, Sauvé V, Ratsima H & D'Amours D (2009) Polo kinase regulates mitotic chromosome condensation by hyperactivation of condensin DNA supercoiling activity. *Mol Cell* **34:** 416–426

Stemmann O, Zou H, Gerber SA, Gygi SP & Kirschner MW (2001) Dual inhibition of sister chromatid separation at metaphase. *Cell* **107:** 715–726

Stinchcomb DT, Struhl K & Davis RW (1979) Isolation and characterisation of a yeast chromosomal replicator. *Nature* **282:** 39–43

Ström L, Karlsson C, Lindroos HB, Wedahl S, Katou Y, Shirahige K & Sjögren C (2007) Postreplicative formation of cohesion is required for repair and induced by a single DNA break. *Science* **317:** 242–245

Ström L, Lindroos HB, Shirahige K & Sjögren C (2004) Postreplicative recruitment of cohesin to double-strand breaks is required for DNA repair. *Mol Cell* **16:** 1003–1015

Sumara I, Vorlaufer E, Stukenberg PT, Kelm O, Redemann N, Nigg EA & Peters J-M (2002) The dissociation of cohesin from chromosomes in prophase is regulated by Polo-like kinase. *Mol Cell* **9:** 515–525

Sun Y, Kucej M, Fan H-Y, Yu H, Sun Q-Y & Zou H (2009) Separase is recruited to mitotic chromosomes to dissolve sister chromatid cohesion in a DNA-dependent manner. *Cell* **137:** 123–132

Sundin O & Varshavsky A (1980) Terminal stages of SV40 DNA replication proceed via multiply intertwined catenated dimers. *Cell* **21:** 103–114

Sutani T, Kawaguchi T, Kanno R, Itoh T & Shirahige K (2009) Budding yeast Wpl1(Rad61)-Pds5 complex counteracts sister chromatid cohesion-establishing reaction. *Curr Biol* **19:** 492–497

Szyjka SJ, Viggiani CJ & Aparicio OM (2005) Mrc1 is required for normal progression of replication forks throughout chromatin in S. cerevisiae. *Mol Cell* **19:** 691–697

Tachibana K-EK, Gonzalez MA, Guarguaglini G, Nigg EA & Laskey RA (2005) Depletion of licensing inhibitor geminin causes centrosome overduplication and mitotic defects. *EMBO reports* **6:** 1052–1057

Tachibana-Konwalski K, Godwin J, Borsos M, Rattani A, Adams DJ & Nasmyth K (2013) Spindle assembly checkpoint of oocytes depends on a kinetochore structure determined by cohesin in meiosis I. *Curr Biol* **23:** 2534–2539

Tak Y-S, Tanaka Y, Endo S, Kamimura Y & Araki H (2006) A CDK-catalysed regulatory phosphorylation for formation of the DNA replication complex Sld2-Dpb11. *EMBO J* **25:** 1987–1996

Takahashi TS, Basu A, Bermudez V, Hurwitz J & Walter JC (2008) Cdc7-Drf1 kinase links chromosome cohesion to the initiation of DNA replication in Xenopus egg extracts. *Genes Dev* **22:** 1894–1905

Takahashi TS, Yiu P, Chou MF, Gygi S & Walter JC (2004) Recruitment of Xenopus Scc2 and cohesin to chromatin requires the pre-replication complex. *Nat Cell Biol* **6:** 991–996

Takeda DY, Parvin JD & Dutta A (2005) Degradation of Cdt1 during S phase is Skp2-independent and is required for efficient progression of mammalian cells through S phase. *J Biol Chem* **280:** 23416–23423

Tanaka S & Diffley JFX (2002) Interdependent nuclear accumulation of budding yeast Cdt1 and Mcm2-7 during G1 phase. *Nat Cell Biol* **4:** 198–207

Tanaka S, Umemori T, Hirai K, Muramatsu S, Kamimura Y & Araki H (2007) CDK-dependent phosphorylation of Sld2 and Sld3 initiates DNA replication in budding yeast. *Nature* **445:** 328–332

Tanaka T, Cosma MP, Wirth K & Nasmyth K (1999) Identification of cohesin association sites at centromeres and along chromosome arms. *Cell* **98:** 847–858

Tang Z, Shu H, Qi W, Mahmood NA, Mumby MC & Yu H (2006) PP2A is required for centromeric localization of Sgo1 and proper chromosome segregation. *Dev Cell* **10:** 575–585

Tang Z, Sun Y, Harley SE, Zou H & Yu H (2004) Human Bub1 protects centromeric sister-chromatid cohesion through Shugoshin during mitosis. *Proc Natl Acad Sci USA* **101:** 18012–18017

Tedeschi A, Wutz G, Huet S, Jaritz M, Wuensche A, Schirghuber E, Davidson IF, Tang W, Cisneros DA, Bhaskara V, Nishiyama T, Vaziri A, Wutz A, Ellenberg J & Peters J-M (2013) Wapl is an essential regulator of chromatin structure and chromosome segregation. *Nature* **501:** 564–568

Terret M-E, Sherwood R, Rahman S, Qin J & Jallepalli PV (2009) Cohesin acetylation speeds the replication fork. *Nature* **462:** 231–234

Thornton GK & Woods CG (2009) Primary microcephaly: do all roads lead to Rome? *Trends Genet* **25:** 501–510

Tomkins D, Hunter A & Roberts M (1979) Cytogenetic findings in Roberts-SC phocomelia syndrome(s). *Am J Med Gen* **4:** 17–26

Tonkin ET, Wang T-J, Lisgo S, Bamshad MJ & Strachan T (2004) NIPBL, encoding a homolog of fungal Scc2-type sister chromatid cohesion proteins and fly Nipped-B, is mutated in Cornelia de Lange syndrome. *Nat Genet* **36:** 636–641

Tóth A, Ciosk R, Uhlmann F, Gálová M, Schleiffer A & Nasmyth K (1999) Yeast cohesin complex requires a conserved protein, Eco1p(Ctf7), to establish cohesion between sister chromatids during DNA replication. *Genes Dev* **13:** 320–333

Tóth A, Rabitsch KP, Gálová M, Schleiffer A, Buonomo SB & Nasmyth K (2000) Functional genomics identifies monopolin: a kinetochore protein required for segregation of homologs during meiosis I. *Cell* **103:** 1155–1168

Tsou M-FB & Stearns T (2006) Mechanism limiting centrosome duplication to once per cell cycle. *Nature* **442:** 947–951

Tsou M-FB, Wang W-J, George KA, Uryu K, Stearns T & Jallepalli PV (2009) Polo kinase and separase regulate the mitotic licensing of centriole duplication in human cells. *Dev Cell* **17:** 344–354

Tsukahara T, Tanno Y & Watanabe Y (2010) Phosphorylation of the CPC by Cdk1 promotes chromosome bi-orientation. *Nature* **467:** 719–723

Tsunematsu T, Takihara Y, Ishimaru N, Pagano M, Takata T & Kudo Y (2013) Aurora-A controls pre-replicative complex assembly and DNA replication by stabilizing geminin in mitosis. *Nat Commun* **4:** 1885

Tsurimoto T & Stillman B (1991a) Replication factors required for SV40 DNA replication in vitro. I. DNA structure-specific recognition of a primer-template junction by eukaryotic DNA polymerases and their accessory proteins. *J Biol Chem* **266:** 1950–1960

Tsurimoto T & Stillman B (1991b) Replication factors required for SV40 DNA replication in vitro. II. Switching of DNA polymerase alpha and delta during initiation of leading and lagging strand synthesis. *J Biol Chem* **266:** 1961–1968

Uhlmann F & Nasmyth K (1998) Cohesion between sister chromatids must be established during DNA replication. *Curr Biol* **8:** 1095–1101

Uhlmann F, Lottspeich F & Nasmyth K (1999) Sister-chromatid separation at anaphase onset is promoted by cleavage of the cohesin subunit Scc1. *Nature* **400:** 37–42

Uhlmann F, Wernic D, Poupart MA, Koonin EV & Nasmyth K (2000) Cleavage of cohesin by the CD clan protease separin triggers anaphase in yeast. *Cell* **103:** 375–386

Ünal E, Arbel-Eden A, Sattler U, Shroff R, Lichten M, Haber JE & Koshland D (2004) DNA damage response pathway uses histone modification to assemble a double-strand break-specific cohesin domain. *Mol Cell* **16:** 991–1002

Ünal E, Heidinger-Pauli JM & Koshland D (2007) DNA double-strand breaks trigger genome-wide sister-chromatid cohesion through Eco1 (Ctf7). *Science* **317:** 245–248

Ünal E, Heidinger-Pauli JM, Kim W, Guacci V, Onn I, Gygi SP & Koshland DE (2008) A molecular determinant for the establishment of sister chromatid cohesion. *Science* **321:** 566–569

Van Den Berg DJ & Franke U (1993) Roberts syndrome: a review of 100 cases and a new rating system for severity. *Am J Med Gen* **47:** 1104–1123

Vanoosthuyse V, Prykhozhij S & Hardwick KG (2007) Shugoshin 2 regulates localization of the chromosomal passenger proteins in fission yeast mitosis. *Mol Biol Cell* **18:** 1657–1669

Vass S, Cotterill S, Valdeolmillos AM, Barbero JL, Lin E, Warren WD & Heck MMS (2003) Depletion of Drad21/Scc1 in Drosophila cells leads to instability of the cohesin complex and disruption of mitotic progression. *Curr Biol* **13:** 208–218

Vázquez-Novelle MD & Petronczki M (2010) Relocation of the Chromosomal Passenger Complex Prevents Mitotic Checkpoint Engagement at Anaphase. *Curr Biol* **20:** 1402–1407

Vázquez-Novelle MD, Sansregret L, Dick AE, Smith CA, Mcainsh AD, Gerlich DW & Petronczki M (2014) Cdk1 inactivation terminates mitotic checkpoint surveillance and stabilizes kinetochore attachments in anaphase. *Curr Biol* **24:** 638–645

Vega H, Waisfisz Q, Gordillo M, Sakai N, Yanagihara I, Yamada M, van Gosliga D, Kayserili H, Xu C, Ozono K, Jabs EW, Inui K & Joenje H (2005) Roberts syndrome is caused by mutations in ESCO2, a human homolog of yeast ECO1 that is essential for the establishment of sister chromatid cohesion. *Nat Genet* **37:** 468–470

Verzijlbergen KF, Nerusheva OO, Kelly D, Kerr A, Clift D, de Lima Alves F, Rappsilber J & Marston AL (2014) Shugoshin biases chromosomes for biorientation through condensin recruitment to the pericentromere. *Elife* **3:** e01374

Vink M, Simonetta M, Transidico P, Ferrari K, Mapelli M, de Antoni A, Massimiliano L, Ciliberto A, Faretta M, Salmon ED & Musacchio A (2006) In vitro FRAP identifies the minimal requirements for Mad2 kinetochore dynamics. *Curr Biol* **16:** 755–766

Waga S & Stillman B (1994) Anatomy of a DNA replication fork revealed by reconstitution of SV40 DNA replication in vitro. *Nature* **369:** 207–212

Waga S & Stillman B (1998) The DNA replication fork in eukaryotic cells. *Annu Rev Biochem* **67:** 721–751

Waizenegger IC, Hauf S, Meinke A & Peters JM (2000) Two distinct pathways remove mammalian cohesin from chromosome arms in prophase and from centromeres in anaphase. *Cell* **103:** 399–410

Wang LH-C, Mayer B, Stemmann O & Nigg EA (2010) Centromere DNA decatenation depends on cohesin removal and is required for mammalian cell division. *J Cell Sci* **123:** 806–813

Wang W-J, Soni RK, Uryu K & Tsou M-FB (2011) The conversion of centrioles to centrosomes: essential coupling of duplication with segregation. *J Cell Biol* **193:** 727–739

Wang X, Yang Y & Dai W (2006) Differential subcellular localizations of two human Sgo1 isoforms: implications in regulation of sister chromatid cohesion and microtubule dynamics. *Cell Cycle* **5:** 635–640

Wang X, Yang Y, Duan Q, Jiang N, Huang Y, Darzynkiewicz Z & Dai W (2008) sSgo1, a major splice variant of Sgo1, functions in centriole cohesion where it is regulated by Plk1. *Dev Cell* **14:** 331–341

Ward GE & Kirschner MW (1990) Identification of cell cycle-regulated phosphorylation sites on nuclear lamin C. *Cell* **61:** 561–577

Watanabe Y & Nurse P (1999) Cohesin Rec8 is required for reductional chromosome segregation at meiosis. *Nature* **400:** 461–464

Watrin E, Schleiffer A, Tanaka K, Eisenhaber F, Nasmyth K & Peters J-M (2006) Human Scc4 is required for cohesin binding to chromatin, sister-chromatid cohesion, and mitotic progression. *Curr Biol* **16:** 863–874

Weinreich M & Stillman B (1999) Cdc7p-Dbf4p kinase binds to chromatin during S phase and is regulated by both the APC and the RAD53 checkpoint pathway. *EMBO J* **18:** 5334–5346

Weitzer S, Lehane C & Uhlmann F (2003) A model for ATP hydrolysis-dependent binding of cohesin to DNA. *Curr Biol* **13:** 1930–1940

Welburn JPI, Vleugel M, Liu D, Yates JR, Lampson MA, Fukagawa T & Cheeseman IM (2010) Aurora B phosphorylates spatially distinct targets to differentially regulate the kinetochore-microtubule interface. *Mol Cell* **38:** 383–392

Wendt KS, Yoshida K, Itoh T, Bando M, Koch B, Schirghuber E, Tsutsumi S, Nagae G, Ishihara K, Mishiro T, Yahata K, Imamoto F, Aburatani H, Nakao M, Imamoto N, Maeshima K, Shirahige K & Peters J-M (2008) Cohesin mediates transcriptional insulation by CCCTC-binding factor. *Nature* **451:** 796–801

Whelan G, Kreidl E, Wutz G, Egner A, Peters J-M & Eichele G (2011) Cohesin acetyltransferase Esco2 is a cell viability factor and is required for cohesion in pericentric heterochromatin. *EMBO J* **31:** 71–82

Winters T, McNicoll F & Jessberger R (2014) Meiotic cohesin STAG3 is required for chromosome axis formation and sister chromatid cohesion. *EMBO J* **33:** 1256–1270

Wittmann T, Hyman A & Desai A (2001) The spindle: a dynamic assembly of microtubules and motors. *Nat Cell Biol* **3:** E28–34

Wohlschlegel JA, Dwyer BT, Dhar SK, Cvetic C, Walter JC & Dutta A (2000) Inhibition of eukaryotic DNA replication by geminin binding to Cdt1. *Science* **290:** 2309–2312

Wollman R, Cytrynbaum EN, Jones JT, Meyer T, Scholey JM & Mogilner A (2005) Efficient chromosome capture requires a bias in the 'search-and-capture' process during mitotic-spindle assembly. *Curr Biol* **15:** 828–832

Wong RW & Blobel G (2008) Cohesin subunit SMC1 associates with mitotic microtubules at the spindle pole. *Proc Natl Acad Sci USA* **105:** 15441–15445

Wood KW, Sakowicz R, Goldstein LS & Cleveland DW (1997) CENP-E is a plus end-directed kinetochore motor required for metaphase chromosome alignment. *Cell* **91:** 357–366

Xiong B, Lu S & Gerton JL (2010) Hos1 is a lysine deacetylase for the smc3 subunit of cohesin. *Curr Biol* **20:** 1660–1665

Xu H, Yan M, Patra J, Natrajan R, Yan Y, Swagemakers S, Tomaszewski JM, Verschoor S, Millar EK, van der Spek P, Reis-Filho JS, Ramsay RG, O'Toole SA, McNeil CM, Sutherland RL, McKay MJ & Fox SB (2011) Enhanced RAD21 cohesin expression confers poor prognosis and resistance to chemotherapy in high grade luminal, basal and HER2 breast cancers. *Breast Cancer Res* **13:** R9

Xu Z, Cetin B, Anger M, Cho US, Helmhart W, Nasmyth K & Xu W (2009) Structure and function of the PP2A-shugoshin interaction. *Mol Cell* **35:** 426–441

Yamada HY, Yao Y, Wang X, Zhang Y, Huang Y, Dai W & Rao CV (2012) Haploinsufficiency of SGO1 results in deregulated centrosome dynamics, enhanced chromosomal instability and colon tumorigenesis. *Cell Cycle* **11:** 479–488

Yamamoto A, Guacci V & Koshland D (1996) Pds1p is required for faithful execution of anaphase in the yeast, Saccharomyces cerevisiae. *J Cell Biol* **133:** 85–97

Yang M, Li B, Tomchick DR, Machius M, Rizo J, Yu H & Luo X (2007) p31comet blocks Mad2 activation through structural mimicry. *Cell* **131:** 744–755

Yardimci H & Walter JC (2014) Prereplication-complex formation: a molecular double take? *Nat Struct Mol Biol* **21:** 20–25

Yardimci H, Wang X, Loveland AB, Tappin I, Rudner DZ, Hurwitz J, van Oijen AM & Walter JC (2012) Bypass of a protein barrier by a replicative DNA helicase. *Nature* **492:** 205–209

Yeeles JTP, Deegan TD, Janska A, Early A & Diffley JFX (2015) Regulated eukaryotic DNA replication origin firing with purified proteins. *Nature* **519:** 431–435

Yokobayashi S & Watanabe Y (2005) The kinetochore protein Moa1 enables cohesion-mediated monopolar attachment at meiosis I. *Cell* **123:** 803–817

Zegerman P & Diffley JFX (2007) Phosphorylation of Sld2 and Sld3 by cyclin-dependent kinases promotes DNA replication in budding yeast. *Nature* **445:** 281–285

Zhang J, Shi X, Li Y, Kim B-J, Jia J, Huang Z, Yang T, Fu X, Jung SY, Wang Y, Zhang P, Kim S-T, Pan X & Qin J (2008) Acetylation of Smc3 by Eco1 is required for S phase sister chromatid cohesion in both human and yeast. *Mol Cell* **31:** 143–151

Zhang X, Chen Q, Feng J, Hou J, Yang F, Liu J, Jiang Q & Zhang C (2009) Sequential phosphorylation of Nedd1 by Cdk1 and Plk1 is required for targeting of the gammaTuRC to the centrosome. *J Cell Sci* **122:** 2240–2251

Zheng Y, Wong ML, Alberts B & Mitchison T (1995) Nucleation of microtubule assembly by a gamma-tubulin-containing ring complex. *Nature* **378:** 578–583

Zhu W, Chen Y & Dutta A (2004) Rereplication by depletion of geminin is seen regardless of p53 status and activates a G2/M checkpoint. *Mol Cell Biol* **24:** 7140–7150

Zhu W, Ukomadu C, Jha S, Senga T, Dhar SK, Wohlschlegel JA, Nutt LK, Kornbluth S & Dutta A (2007) Mcm10 and And-1/CTF4 recruit DNA polymerase alpha to chromatin for initiation of DNA replication. *Genes Dev* **21:** 2288–2299

Zou H, McGarry TJ, Bernal T & Kirschner MW (1999) Identification of a vertebrate sister-chromatid separation inhibitor involved in transformation and tumorigenesis. *Science* **285:** 418–422

Zou L & Stillman B (2000) Assembly of a complex containing Cdc45p, replication protein A, and Mcm2p at replication origins controlled by S phase cyclin-dependent kinases and Cdc7p-Dbf4p kinase. *Mol Cell Biol* **20:** 3086–3096

Zuin J, Franke V, van Ijcken WFJ, van der Sloot A, Krantz ID, van der Reijden MIJA, Nakato R, Lenhard B & Wendt KS (2014) A Cohesin-Independent Role for NIPBL at Promoters Provides Insights in CdLS. *PLoS Genet* **10:** e1004153

Abbreviations

aa	amino acid(s)
APC/C	anaphase-promoting complex/cyclosome
APS	ammonium persulfate
BSA	bovine serum albumine
BrdU	5-bromo-2'-deoxyuridine
CBB	Coomassie Brilliant Blue
Cdc	cell division cycle
Cdk	cyclin-dependent kinase
CdLS	Cornelia de Lange syndrome
CldU	5-chloro-2'-desoxyuridine
CTCF	CCCTC-binding factor
Ctf	chromosome transmission fidelity
CTS	centrosomal targeting signal of Sgo1
DAPI	4',6-diamidino-2-phenylindole
DSB	double-strand break
DTT	dithiothreitol
ECL	electrochemiluminescence
Eco1	establishment of cohesion 1
EDTA	ethylenediaminetetraacetic acid
EdU	5-ethynyl-2'-desoxyuridine
EGTA	ethylene glycol tetraacetic acid
ESCO	establishment of cohesion
FKBP	FK506 binding protein
FRB	FKBP-rapamycin binding domain of mTOR
H2A	histone 2 A
HBS	HEPES buffered saline
HEK	human embryonic kidney
HeLa	Henrietta Lacks (patient from whom cell line is derived)
HEPES	4-(2-hydroxyethyl)-1-piperazineethanesulfonic acid
HRP	horse radish peroxidase

IdU	5-iodo-2'-desoxyuridine
IF	immunofluorescence
IFM	immunofluorescence microscopy
IMAC	ion metal affinity chromatography
IP	immunoprecipitation
MCC	mitotic checkpoint complex
MCS	multiple cloning site
mTOR	mechanistic target of rapamycin
NHS	*N*-Hydroxysuccinimide
ORF	open reading frame
PAGE	polyacrylamide gel electrophoresis
PCM	pericentriolar material
PCNA	proliferative cellular nuclear antigen
PCR	polymerase chain reaction
Pds5	precocious dissociation of sisters
PIPES	piperazine-N,N'-bis(2-ethanesulfonic acid)
Plk1	polo-like kinase 1
Pol	polymerase
PP2A	protein phosphatase 2A
PVDF	polyvinylidene fluoride
RBS	Roberts syndrome
RFC	replication factor C
RNAi	RNA interference
RT	room temperature
SA	stromalin antigen
SAC	spindle assembly checkpoint
Scc	sister chromatid cohesion
SDS	sodium dodecyl sulfate
SEM	standard error of the mean
Sgo	shugoshin
Smc	structural maintenance of chromosomes
siRNA	small interfering RNA

STAG	stromalin antigen
TEMED	Tetramethylethylenediamine
T_M	melting temperature
Tris	tris(hydroxymethyl)aminomethane
Wapl	wings apart-like
WB	Western blot
WT	wild type
X. laevis	*Xenopus laevis*

Publikationsliste

Wesentliche Teile dieser Arbeit wurden in folgenden Publikationen veröffentlicht:

Buheitel J, & Stemmann O (2013) Prophase pathway-dependent removal of cohesin from human chromosomes requires opening of the Smc3-Scc1 gate. *EMBO J*, **32(5)**, 666–676, doi: 10.1038/emboj.2013.7

Mohr L, **Buheitel J**, Schöckel L, Karalus D, Mayer B & Stemmann O (2015) An alternatively spliced bifunctional localization signal reprograms human shugoshin 1 to protect centrosomal instead of centromeric cohesin. *Cell Rep*, doi: 10.1016/j.celrep.2015.08.045

Danksagung

Ich möchte mich zuallererst bei Olaf Stemmann bedanken. Für sein in mich gesetztes Vertrauen, für seine Ideen, für die Unterstützung und die vielen Diskussionen während der letzten Jahre. Er war mit ein Grund, warum ich mich in der Arbeitsgruppe immer wohl gefühlt habe und warum ich nach all dieser Zeit mit gutem Gewissen behaupten kann, ein gut und vollständig ausgebildeter Wissenschaftler zu sein.

Weiterhin gilt mein Dank allen Mitgliedern des Prüfungsausschusses, für ihr Interesse und Ihre Zeit. Ein besonderer Dank geht an die weiteren Mitglieder meines Ph.D. Mentorats Stefan Heidmann und Franz Schmid, deren Meinung ich sehr schätze.

Dank geht auch an alle ehemaligen und aktuellen Mitglieder der Arbeitsgruppe Stemmann, welche mich in dieser Zeit begleitet und unterstützt haben: Franziska Böttger, Andreas Brown, Heike Haase, Doris Heidmann, Petra Helies, Susanne Hellmuth, Markus Hermann, Jutta Hübner, Philip Kahlen, Juliane Karich, Bernd Mayer, Lisa Mohr, Brigitte Neumann, Monika Ohlraun, Michael Orth, Michaela Rogowski, Laura Schöckel, Markus Schuster, Petra Seidler und Peter Wolf. Danke auch an die aktuellen und ehemaligen Mitglieder der Arbeitsgruppen Heidmann und Ersfeld für die fruchtvollen Diskussionen und Ideen aber auch für ihre tatkräftige Unterstützung: Karin Angermann, Sabine Herzog, Brigitte Jaunich, Anna Riemer, Kristina Seel und Evelin Urban. Aber natürlich möchte ich all diesen Personen auch für die schönen Zeiten danken, die wir mit unwissenschaftlichen Dingen wie diversen Grillereignissen oder auch auf bayreuther Traditionsveranstaltungen (z.B. dem Bürgerfest) gemeinsam verbracht haben. Diesen Dank möchte ich auch den Arbeitsgruppen-Chefs Klaus Ersfeld und Stefan Heidmann aussprechen. Insbesondere Stefans legendäre Home-Parties werde ich sehr vermissen!

Ich möchte mich bei allen Bachelor- und Masterstudenten bedanken, die mir unter die Arme gegriffen haben: Brigitte Neumann, Annika Pfeiffer, Theresa Rauschendorfer und Barbara Streibl. Hierbei geht ein besonderer Dank an Valentina Ahl, deren Projekt ich weiterführen durfte.

Ich möchte den diversen Korrekturlesern und -leserinnen danken, die viele Stunden Ihrer Lebenszeit in die Verbesserung dieser Arbeit gesteckt haben: Philip Kahlen, Lisa Mohr, Brigitte Neumann und Peter Wolf.

Ein Dank geht auch an die Freunde und Kollegen außerhalb der Uni Bayreuth, die uns mit Wissen, aber auch mit Reagenzien unterstützt haben, insbesondere Susannah Rankin für das bereitstellen diverser Antikörper.

Danke auch an meine Eltern, die mich die ganzen Jahre über unterstützt haben. Ohne sie stünde ich nicht dort, wo ich jetzt bin.

Zum Schluss möchte ich meiner Freundin Lisa Mohr danken. Ich hätte diesen Weg nicht ohne dich gehen können. Vielen Dank, dass du immer für mich da warst und auch in den stressigsten und frustrierendsten Zeiten immer an meiner Seite standst! Ich freue mich auf unsere gemeinsame Zeit in New York!

(Eidesstattliche) Versicherungen und Erklärungen

(§ 8 S. 2 Nr. 6 PromO)

Hiermit erkläre ich mich damit einverstanden, dass die elektronische Fassung meiner Dissertation unter Wahrung meiner Urheberrechte und des Datenschutzes einer gesonderten Überprüfung hinsichtlich der eigenständigen Anfertigung der Dissertation unterzogen werden kann.

(§ 8 S. 2 Nr. 8 PromO)

Hiermit erkläre ich eidesstattlich, dass ich die Dissertation selbständig verfasst und keine anderen als die von mir angegebenen Quellen und Hilfsmittel benutzt habe.

(§ 8 S. 2 Nr. 9 PromO)

Ich habe die Dissertation nicht bereits zur Erlangung eines akademischen Grades anderweitig eingereicht und habe auch nicht bereits diese oder eine gleichartige Doktorprüfung endgültig nicht bestanden.

(§ 8 S. 2 Nr. 10 PromO)

Hiermit erkläre ich, dass ich keine Hilfe von gewerblichen Promotionsberatern bzw. -vermittlern in Anspruch genommen habe und auch künftig nicht nehmen werde.

…….
Ort, Datum, Unterschrift